UNCERTAINTY MANAGEMENT IN DESIGN OF MULTISCALE SYSTEMS

A Thesis

Presented to

The Academic Faculty

by

Ayan Sinha

In Partial Fulfillment

of the Requirements for the Degree

Master of Science in Mechanical Engineering in the

George W. Woodruff School of Mechanical Engineering

Georgia Institute of Technology

May 2011

UNCERTAINTY MANAGEMENT IN DESIGN OF MULTISCALE SYSTEMS

Approved by:

Dr. Janet K. Allen, Advisor

School of Industrial Engineering

University of Oklahoma

Dr. Farrokh Mistree, Co-Advisor

School of Aerospace and Mechanical Engineering

University of Oklahoma

Dr. Jitesh H. Panchal

School of Mechanical Engineering

Washington State University

Dr. David Rosen

School of Mechanical Engineering

Georgia Institute of Technology

Date Approved: April 4, 2011

ACKNOWLEDGEMENTS

Through my journey as a graduate student at Georgia Tech, I have had the privilege of learning and working with outstanding educators. I want to thank everyone who has made this work a reality. First of all, I thank my advisor Dr. Janet K. Allen for her support and guidance beyond the realms of academia and taking an active interest towards a complete education. She pushed me to perform to the best of my abilities while inspiring and guiding me to stay on the critical path in order to write a good thesis. Her insights and attention to detail helped me realize the qualities of an exemplary researcher. I would like to thank Dr. Farrokh Mistree for making my initiative at Georgia Tech possible. He was instrumental in coordinating the Georgia Tech- IIT Kharagpur collaboration and helped me secure an internship in the Summer of 2008. As a co-advisor he was always open to innovative ideas and gave me valuable opportunities to deliver graduate lectures and seminars which I believe has contributed immensely to my academic acumen. I gained a lot from his insights in academia and his talks inspired me to continue with my doctoral studies and eventually secure an academic position in university. I would also like to thank Dr. Jitesh Panchal for providing me intellectual guidance based on his immense experience on design of multiscale systems and without whose help this thesis would not have been possible. Furthermore, I thank my committee member Dr. David Rosen, who started my realms into design through the CAD course and excited me to pursue original research. I also thank Dr. David McDowell, Dr. C.S. Kumar, and Dr. Dirk Schaefer for their guidance, insights and support through the course of my stay and helping me acquire the necessary competencies in material and product design. For his help with the application of the material models and simulation codes, I owe great thanks to Dr. Sudipto Ghosh. For providing the internship opportunity, I thank Dr. Madhusudan Chakraborty. I am also acknowledge Dr. Haejin Choi, on whose PhD work my research is built. Furthermore, I thank all faculty and students in the Systems Realization Laboratory in Atlanta and fellow colleagues at the Engineering Laboratory in University of Oklahoma for their support in my initiatives. Special thanks go to Mukul Singhee, Anriban Patra, Shreevant Tiwari and Jiten Patel for their friendship and encouragement during

my time at Georgia Tech. I also thank Nilanjan Bera, Dibyajat Mishra, Shaumik Lenka and Mukesh Kumar Singh who ensured the timely development of the simulation models and assisted me in their execution. I thank Matt Marston for use of JAVA DSIDES.

I owe the greatest thanks to my brother for his continuous support and encouragement during the course of my entire studies and being a mentor in rough times and role model. I also am grateful to my mother and father for being the pillars of support throughout my education and giving me the intellectual freedom to pursue my dreams.

Furthermore, I acknowledge the funding sources, which made this thesis possible:

• George Woodruff School of Mechanical Engineering

• NSF EAGER Grant 1042340 (OU)

TABLE OF CONTENTS

LIST OF TABLES

LIST OF FIGURES

LIST OF SYMBOLS

Chapter 2

B	Buoyant weight of the submersible
d	Grain diameter
d_p	Reinforcement size
eff	Efficiency of the battery
g	Gravity
h	Depth of the submersible below water
ID	Inner diameter of the shell
k_y	Strengthening coefficient in the Hall-Petch relation
L	Length of the submersible
OD	Outer diameter of the shell
P	External pressure
T	Semisolid processing temperature
T_{opr}	Endurance time of the submersible
t	Thickness of the shell
W	Weight of the cylindrical shell
x_{Cu}	Volume fraction of Cu
X_{TiB_2}	Volume fraction of TiB_2
Y	Output of a response surface model
β_{ij}	Coefficients in a response surface model
ρ	Density of the composite
ρ_{TiB2}, ρ_{Cu}, ρ_{Al}	Densities of TiB_2, copper and aluminum respectively
ρ_w	Density of water
σ	Overall yield stress incorporating Orowan particle bypass
σ_o	Material constant related to lattice resistance

σ_y	Yield stress calculated from the Hall-Petch relation

Chapter 3

B	Buoyant weight of the submersible
d	Grain diameter
r	Reinforcement size
eff	Efficiency of the battery
g	Gravitational constant
h	Depth of the submersible below water
ID	Inner diameter of the shell
k_y	Strengthening coefficient in the Hall Petch relation
L	Length of the submersible
OD	Outer diameter of the shell
P	External pressure
T_1	Semisolid processing temperature
T_2	Particulate processing temperature
T_{opr}	Endurance time of the submersible
t	Thickness of the shell
W	Weight of the cylindrical shell
x_{Cu}	Volume fraction of Cu
x_{TiB2}	Volume fraction of TiB2
Y	Output of a response surface model
β_{ij}	Coefficients in a response surface model
ρ	Density of the composite
ρ_{TiB2}, ρ_{Cu}, ρ_{Al}	Densities of TiB_2, copper and aluminum respectively
ρ_w	Density of water
σ	Overall yield stress incorporating Orowan particle bypass

σ_o	Material constant related to lattice resistance
σ_y	Yield stress calculated from the Hall-Petch relation
C_{dk}^{i}	Design Capability Index for player i.
d_i^+	Positive Deviation variable for Player i.
d_i^-	Negative Deviation variables for Player i.
ΔX	Variance or Variability of X
%L	Percentage of liquid in semisolid processing
Z	Deviation Function
w_i	Weight of deviation variable in deviation function

Chapter 5

A	Area fraction of hard phase in volume element
B	Buoyant weight of the submersible
C	Cooling rate for semisolid processing
d	Grain diameter
d_p	Reinforcement size
D	Depth of operation
eff	Efficiency of the battery
E_d	Energy density of battery
F_i	Models in multiscale system
g	Gravity
h	Convective heat transfer coefficient for water
ID	Inner diameter of the shell
k	Thermal conductivity for the composite
k_{Al-Cu}	Thermal conductivity of Al-Cu matrix
k_{TiB_2}	Thermal conductivity of TiB_2

K	Thermal conductivity for the submersible equipment
L	Length of the submersible
L_f	Fixed load for the submersible
L_p	Propulsion load for the submersible
n	Number of simulation runs or data points
OD	Outer diameter of the shell
p	Total regression coefficients
q	Heat flow rate
$\dot{q}$	Internal heat generated per unit volume
R^2	R^2 statistic for a regression model
t	Time of simulation run for precipitate modeling
T	Temperature for precipitate modeling
T_{op}	Temperature of operation of the submersible
T_{opr}	Endurance time of the submersible
T_∞	Convective temperature of water
TS_1	Temperature at outer radius of submersible
TS_2	Temperature at inner radius of submersible
T_h	Thickness of the shell
W	Weight of the cylindrical shell
x_{Cu}	Volume fraction of Cu
x_i	Response surface variables
Δx_i	Error in design variables
x_{TiB_2}	Volume fraction of TiB_2
X	Matrix of regression variables
Y	Output of a response surface model

Y_{lower}	Lower statistical confidence interval
$Y_{\max}$	Upper confidence interval
$Y_{\min}$	Lower confidence interval
Y_{upper}	Upper statistical confidence interval
ΔY_{CI}	Statistical confidence interval
ΔY_{IP}	Interval due to variability of input variables
θ_{ij}	Coefficients in a response surface model
ε	Random errors in a response surface model
η	Number of design variables in a response surface model
ρ	Density of the composite
ρ_{TiB2}, ρ_{Cu}, ρ_{Al}	Densities of TiB_2, copper and aluminum respectively
σ	Yield strength

Chapter 6

a_o	Constants
B	Buoyant weight of the submersible
C	Cooling rate for semisolid processing
d	Grain diameter
d_p	Reinforcement size
D	Depth of operation
e_i	Residual errors
eff	Efficiency of the battery
E_d	Energy density of battery
f_i	Models in multiscale system
g	Gravity

h	Convective heat transfer coefficient for water
H_e	Highest exponent of a simulation output parameter
ID	Inner diameter of the shell
IP	System improvement potential
IP'	*Ex-ante* system improvement potential
IP_c	Convergence criterion
IP'_c	*Ex-ante* convergence criterion
IP_i	Improvement potential of a simulation model
IP'_i	*Ex-ante* improvement potential of a simulation model
k	Thermal conductivity for the composite
k_{Al-Cu}	Thermal conductivity of Al-Cu matrix
k_{TiB_2}	Thermal conductivity of TiB_2
K	Thermal conductivity for the submersible equipment
L	Length of the submersible
L_f	Fixed load for the submersible
L_p	Propulsion load for the submersible
m	Total feasible solution sets in a multiscale domain
MSE	Mean square error
MSE'	Predicted mean square error
MSE'_r	Predicted mean square error for r additional runs
n	Number of simulation runs or data points
OD	Outer diameter of the shell
p	Total regression coefficients
q	Heat flow rate
$\dot{q}$	Internal heat generated per unit volume

R^2	R^2 statistic for a regression model
SS_E	Error sum of squares
t_i	Time per simulation run
T	Temperature for precipitate modeling
T_i	Computational time for a simulation model
T_{op}	Temperature of operation of the submersible
T_{opr}	Endurance time of the submersible
T_∞	Convective temperature of water
TS_1	Temperature at outer radius of submersible
TS_2	Temperature at inner radius of submersible
t	Thickness of the shell
W	Weight of the cylindrical shell
W_i	Weight of simulation model
W_{PO}	Weight of performance objective
x_{Cu}	Volume fraction of Cu
x_i	Response surface variables
Δx_i	Error in design variables
x_{TiB_2}	Volume fraction of TiB_2
X	Matrix of regression variables
Y	Output of a response surface model
Y_{lower}	Lower statistical confidence interval
$Y_{\max}$	Upper confidence interval
$Y_{\min}$	Lower confidence interval
Y_{upper}	Upper statistical confidence interval

ΔY_{CI}	Statistical confidence interval
ΔY_{IP}	Interval due to variability of input variables
θ_{ij}	Coefficients in a response surface model
ε	Random errors in a response surface model
κ	Number of design variables in a response surface model
ρ	Density of the composite
ρ_{TiB2}, ρ_{Cu}, ρ_{Al}	Densities of TiB_2, copper and aluminum respectively
σ	Overall yield stress

LIST OF ABBREVIATIONS

IDEM	Inductive Design Exploration Method
cDSP	compromise Decision Support Problem
MPU	Model Parameter Uncertainty
NU	Natural Uncertainty
PU	Propagated Uncertainty
MSU	Model Structure Uncertainty
MMD	Microstructure Mediated Design
HD-EMI	Hyper Dimensional Error Margin Index
EMI	Error Margin Index
DCI	Design Capability Index
IDCE	Inductive Design Constrain Evaluation

SUMMARY

In this thesis, a framework is laid for holistic uncertainty management for simulation-based design of multiscale systems. The work is founded on uncertainty management for microstructure mediated design (MMD) of material and product, which is a representative example of a system over multiple length and time scales, i.e., a multiscale system. The characteristics and challenges for uncertainty management for multiscale systems are introduced context of integrated material and product design. This integrated approach results in different kinds of uncertainty, i.e., natural uncertainty (NU), model parameter uncertainty (MPU), model structure uncertainty (MSU) and propagated uncertainty (PU). We use the Inductive Design Exploration Method to reach feasible sets of robust solutions against MPU, NU and PU. MMD of material and product is performed for the product autonomous underwater vehicle (AUV) employing the material in-situ metal matrix composites using IDEM to identify robust ranged solution sets. The multiscale system results in decision nodes for MSU consideration at hierarchical levels, termed as multilevel design. The effectiveness of using game theory to model strategic interaction between the different levels to facilitate decision making for mitigating MSU in multilevel design is illustrated using the compromise decision support problem (cDSP) technique. Information economics is identified as a research gap to address holistic uncertainty management in simulation-based multiscale systems, i.e., to address the reduction or mitigation of uncertainty considering the current design decision and scope for further simulation model refinement in order to reach better robust solutions. It necessitates development of an improvement potential (IP) metric based on value of information which suggests the scope of improvement in a designer's decision making ability against modeled uncertainty (MPU) in simulation models in multilevel design problem. To address the research gap, the integration of robust design (using IDEM), information economics (using IP) and game theoretic constructs (using cDSP) is proposed. Metamodeling techniques and expected value of information are critically reviewed to facilitate efficient integration. Robust design using IDEM

and cDSP are integrated to improve MMD of material and product and address all four types of uncertainty simultaneously. Further, IDEM, cDSP and IP are integrated to assist system level designers in allocating resources for simulation model refinement in order to satisfy performance and robust process requirements. The approach for managing MPU, MSU, NU and PU while mitigating MPU is presented using the MMD of material and product. The approach presented in this article can be utilized by system level designers for managing all four types of uncertainty and reducing model parameter uncertainty in any multiscale system.

CHAPTER 1

MULTISCALE SYSTEMS: FOUNDATIONS FOR MULTILEVEL DESIGN

Goal: Lay a framework for holistic uncertainty management for simulation-based design of multiscale systems in the context of integrated material and product design.

The motivation for the research work presented in this thesis is to lay a framework for robust design of multiscale systems. The method should facilitate robust design against all modeled uncertainty and its propagation through a design chain while adequately capturing the nondeterministic systems behavior. The research work presented is based on augmenting the Inductive Design Exploration Method (IDEM) developed by Choi in his PhD dissertation specific to integrated multiscale design of material and product [1]. The material is this thesis is a culmination of four research articles developed through the study of multiscale systems over the last 3 years. The first research article on microstructure mediated design appeared in IDETC 2009. In this article IDEM is successfully demonstrated for the microstructure mediated design (MMD) task representative of integrated product and material design in Chapter 2. IDEM provides ranged sets of robust solutions useful for early design space exploration. However, to obtain a single solution, game theoretic protocols are investigated leveraging the compromise decision support problem (cDSP approach). This study appeared in IDETC 2010 and is explained in Chapter 3. Independent investigation of the IDEM and cDSP approach leads us to formulate the research questions and hypothesis in context of MMD in Chapter 4. A fundamental limitation of both these approaches is that though they account for both quantifiable and unquantifiable uncertainty in obtaining single or ranged sets of robust solutions, it does not provide for uncertainty mitigation, i.e., it alleviates uncertainty but does not reduce it. This limitation is incumbent for efficient multiscale systems design where initial design space exploration may lead to feasible solutions but not sufficiently robust solutions and the

uncertainty component in the identified feasible points is high. This necessitates systematically understanding the components of uncertainty and investing computational resources for its mitigation. Hence, the phrase **uncertainty management** has been adopted so as to lay an underlying framework for both alleviating uncertainty as well as mitigating it. IDEM and cDSP are coupled to obtain an improved approach suitable both for management of uncertainty using ranged sets as well as obtaining a single robust solution for the MMD task. The research article developed through this study is under review for publication in Journal of Computer Aided Design and appears in Chapter 5. The developed robust design approach is coupled with constructs from information economics to enable efficient resource allocation for uncertainty mitigation. Specifically, uncertainty is classified into four types and the focus is on reducing one of the three kinds of reducible uncertainty. To achieve this end, metamodeling approaches are used in conjunction with a value of information metric, i.e., the improvement potential metric which quantifies the degree of model parameter uncertainty which is the reducible uncertainty in consideration. The improvement potential metric was initially defined by Panchal in his dissertation to capture the degree of uncertainty and evaluate decisions for further simulation refinement. In this thesis, the improvement potential is extended to correlate it to computational cost and optimization techniques are used to reach a trade-off among the cost functions to evaluate resource allocation. The results achieved are under review for publication in Journal of Mechanical Design and is explained in Chapter 6. The validation square method is used to validate my approaches as well as lay scope for future work on holistic uncertainty management in Chapter 7. Because the chapters essentially are independent research articles, same concepts or constructs may appear in multiple chapters. In this chapter the foundations are built on which the subsequent chapters will be based on. Several sections are leveraged from Choi's and Panchal's dissertation which form the foundational works for my thesis. The reader gets acquainted with the hierarchical nature of multiscale systems in an integrated material and product development approach. The challenges associated in design of multiscale systems are described and stress is laid on modeling and accounting for uncertainty in reaching a robust solution. Multiscale modeling is reviewed in context of Olson's diagram for hierarchical

materials design. Different robust design approaches are classified and discussed and the robust design strategy for design space exploration in multiscale systems, i.e., IDEM is looked at greater detail. A section has been devoted to the organization of work in this thesis.

1.1. Multiscale Simulation-Based Systems

The emergence of computational methods has resulted in systems design methods being driven by increasingly effective simulation tools to realize complex products with smaller development cycle times and increased quality. These simulation models are able to predict the behavior of systems at multiple scales and the natural next step is to use systematically use these models to design systems that are able to predict the overall system behavior by integrating the information generated from the constituent models. Most complex systems are hierarchical in nature with coupling between the system, subsystem and components. As defined in the glossary, hierarchical systems design is a method of systems design simulating performance over multiple levels of a hierarchically partitioned system with the objective of reducing the aggregate time required to reach the desired system level performance. In this thesis, hierarchical systems are described as separate from multiscale systems which are systems simulated over multiple length and time scales, Figure 1.1.

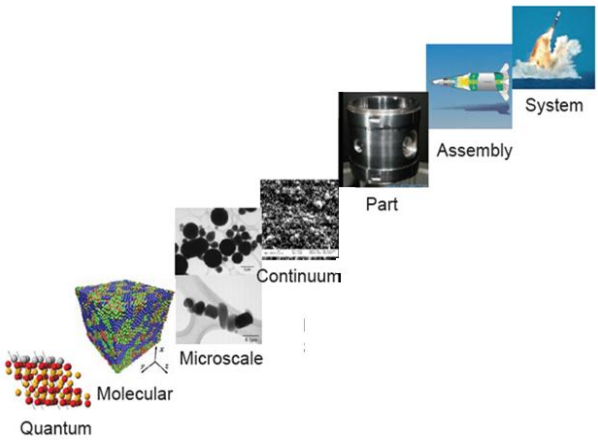

Figure 1.1: A multiscale system[1]

In Figure 1.1, it is seen that the final system level performance is a function of its individual components which in turn depend on the material properties. The material properties can be simulated over different length and time scales ranging from the quantum domain which influences the molecular interactions and results in the microstructure of the material. The microstructure in turn affects continuum behavior and results in constituent mechanical properties. The time scales may vary from the order of few femtoseconds in the quantum domain to the entire life cycle of the system which may be in the order of months or years. As these scales are linked there is interdependency between the system performance and the modeling at these scales and hence these scales are said to be coupled. In hierarchical systems the coupling is primarily between the physical components whereas in multiscale systems coupling may exist within physical phenomena as different scales for the same component[2], i.e., in hierarchical systems coupling exists over the systems, subsystems and individual components at the same scale (horizontal coupling) whereas in multiscale systems, there is an additional element of coupling over the length and time scales for designing the individual components (vertical coupling), Figure 1.2. Hence in multiscale systems, vertical coupling needs to be considered in addition to horizontal coupling to effectively integrate the information from the physical phenomena at the different scales in order to make right decisions and leads to an increased element of complexity.

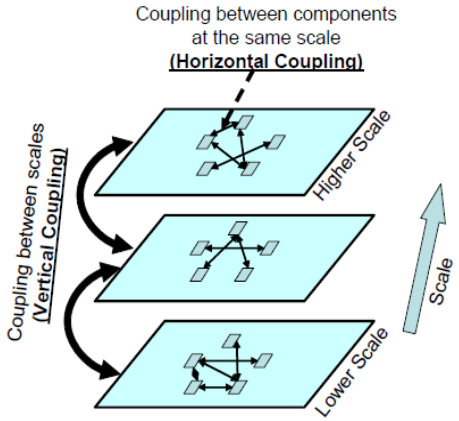

Figure 1.2: Horizontal and vertical coupling in multiscale systems[3]

The advantage of designing system over multiple scales is the increased flexibility of system configuration making it possible to design products with specific performance, not possible by traditional hierarchical systems design. Having defined multiscale systems, we proceed to understanding multiscale systems in the context of integrated material and product design.

1.1.1. Integrated Material and Product Design: A Multiscale Approach

Integrated material and product design refers to designing materials to suit specific multifunctional performance requirements of the product. There is an increasing trend of advancing material systems to satisfy multiple conflicting performance requirements. Integrated material and product design can be viewed as a multiscale system where models at lower scales of the hierarchy are used to provide information for formulating other models on higher scales . To achieve integrated product and material development, Olson developed a materials design hierarchy which partitions the system as a set of deductive mappings from the material processing path, nano-structure and micro-structure, material properties and up to product performance, Figure 1.3. Olson's diagram is central to this thesis and will be referenced in every chapter.

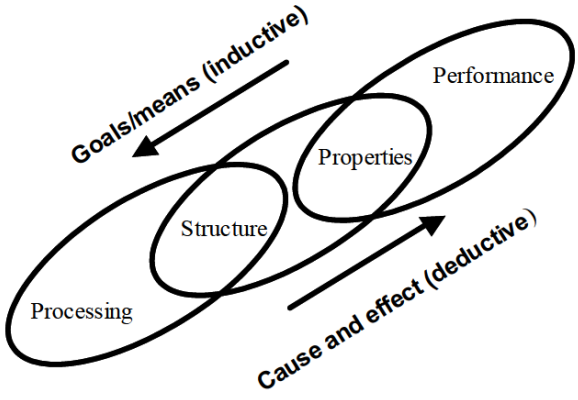

Figure 1.3: Olson's material design hierarchy[4]

It is very difficult to formulate a single model for macroscopic material properties that unifies all of the length scales [5]. Theoretical and solid-state physics can be used on atomistic and molecular

levels to predict the structure and properties of ideal designs. However, such models are computationally expensive to analyze materials with highly heterogeneous microstructures that strongly influence their macroscopic properties. On the other hand, continuum-based models, based on classical continuum theory, are useful for describing properties at a macroscopic scale relevant to many engineering applications; however, they are inappropriate for smaller scale phenomena that require atomistic resolution. Therefore, multiple scale models need to be incorporated to predict precisely a system level product performance considering smaller scale material phenomena[1]. Hence, integrated material and product development can be viewed as a multiscale system. Olson's diagram sets the philosophical foundation for materials design as a set of bottom-up mappings. However, due to the computational expense of modeling at the small scales it becomes critical that a top-down inductive approach assists the deductive mappings for efficient design space exploration. Having looked at multiscale material systems we look at the challenges associated with multiscale modeling of such systems.

1.1.2. Multiscale Modelling for Integrated Material and Product Design

The hierarchy of multiscale computational models incorporated for integrated material and product design is illustrated in Figure 1.4. The length hierarchy extends from Angstroms in the quantum scale to meters in the macroscale while the time hierarchy extends from femto-seconds in the quantum domain to months or years for the entire lifecycle of the product in the macro scale. In the following section, the multiscale models (the boxes in the scale graph) for multifunctional analyses of material and product employed for this research are briefly discussed. This section on multiscale modeling has been leveraged from Choi's disseration[1]

Quantum Mechanics Models

Quantum scale models, the smallest scaled computational model in Figure 1.4, are used to determine the equation of state properties of the individual materials and the likelihood of reaction initiation between reactive components. These ab initio models only require

environmental properties such as pressure and temperature as inputs since the atomic properties are fundamentally derived. The equation of state results are used in the mesoscale discrete particle models to determine the constitutive behavior of the individual components. Evaluation of the transition states and energies that relate to the interaction of reactive components can be processed to determine the likelihood that a reaction will initiate. These probabilities can be used in the mesoscale discrete particle models. Quantum scale models are also used to determine the parameters in potentials used in molecular dynamics models.

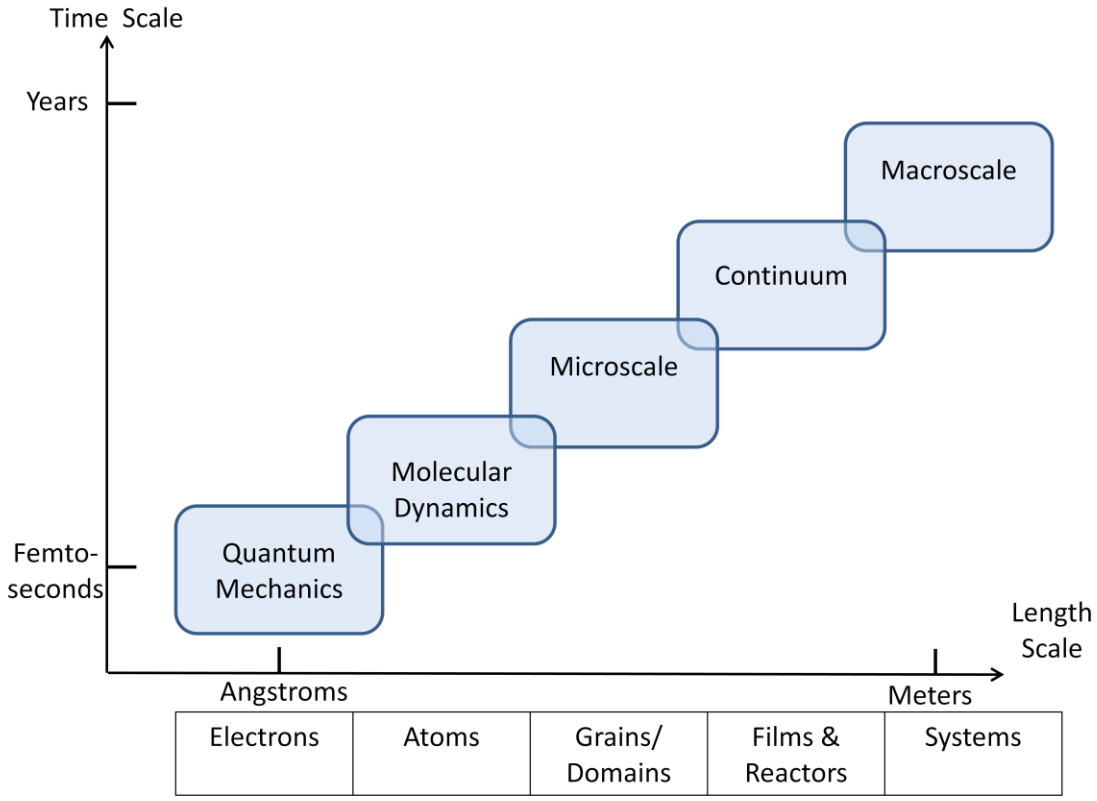

Figure 1.4: Hierarchical materials design[1]

Molecular Dynamics Models

Molecular dynamics (MD) models, the second smallest scaled models in Figure 1.4, can also be used to investigate the equation of state properties and the probability of reaction initiation, but at larger scales. While quantum scale models are limited to tens of atoms, MD models can investigate the interactions of hundreds of thousands to millions of atoms. The MD models can

then be used more effectively to study shock waves through the atoms, size scale effects at reactive component interfaces, and nanoscale domains of the constituents. The MD models can also be compared and verified with quantum scale models. The results of the MD models may be used in the mesoscale discrete particle models.

Mesoscale or Microscale Models

In the microscale model, the third smallest scaled models in Figure 1.4, the constituents are modeled as discrete particles in the nanometer to micron scale range. With a given input, the model estimates reaction initiation and micro-structural information within a volume element measuring in the tens to hundreds of microns in length. The randomly generated morphology is created based on statistical information such as volume fractions, size distributions, and nearest neighbor distributions. The structural information is used in continuum models for property analysis.

Continuum Models

Achieving an accurate continuum model for new materials is important to accurately estimate the property of a material. Structural and reaction information generated from microscale models are interfaced with the continuum model. Experimental data are often required for validating multiscale analysis models at this scale. Constitutive models and reduced order models are implemented at this scale. The reduced order model are used when simulations are infeasible and predicts properties based on the 'rule of mixtures,' in which a mixture's property can be calculated by the weighted average of mixture constituents' properties based on their fractions in a mixture.

Macroscale Models

Macroscale models are used to map between the obtained properties from the microstructure to the performance of the system. Mapping models in the property-performance domain in Olson's diagram are generally well understood and extensive modeling literature exists. Often

they are in the form of an individual or set of ordinary or partial differential equations. Finite element analysis is commonly used for structural modeling in the macroscale domain.

In this section, we introduce the multiscale models for designing material and product as an example of multiscale simulation-based materials design. In the next section, the challenges in the multiscale simulation-based materials design are discussed.

1.1.3. Challenges in Multiscale Modelling for Integrated Product and Material Design

A multiscale model is defined as a model that takes advantage of information from various scales present in the system in order to gain a better understanding of the system while reducing the computational cost. For successful multiscale modeling we must overcome the challenges described in Table 1-1 and discussed in detail in this section. Some of the challenges have been leveraged in part from Panchal's dissertation[3]. Although these challenges are common to all multiscale systems, we describe these in context of integrated product and material design examples.

Table 1.1: Challenges associated with multiscale modeling[3]

a. Balancing the prediction accuracy with computational cost
b. Modelling physical phenomena and interaction between scales
c. Collaborative decision making
d. Collaborative computational infrastructure
e. Managing uncertainty and its propagation
f. The inverse problem

a. Balancing the Prediction Accuracy with Computational Cost

The biggest obstacle hindering design of multiscale systems is the computational cost associated with modeling in the molecular or microscale domain. Ideally, we would

want to use the modeling in the quantum domain to drive the molecular simulations and predict the microstructure using this information. Using the microstructure information and accurate continuum models, the material properties can be predicted which in turn can be mapped to the system performance. Though such a comprehensive analysis of atomistic interactions can give very accurate representations of the true system performance, current computing powers prohibit such an approach. Modeling in the atomistic or molecular domain even under simplified conditions and considering a small number of interactions lead to large computational times, sometimes on order of days to months. A thorough analysis is inefficient especially in the early stages of design. So we sacrifice accuracy for computational efficiency. This translates into using models with lower degrees of freedom which can sufficiently capture the physical phenomena in the material domain and the predictive capabilities of the model are used to generate information fed into models at a higher scale in the material design hierarchy. Accuracy is sacrificed in terms of analyzing discrete points in the design space, screening unimportant variables for modeling the physical phenomena or reducing a 3D analysis into a more tractable 2D analysis. An alternative approach is to use the computational resources in an adaptive fashion by progressively increasing the information content from models which have a greater impact on the overall multiscale system performance and allow targeted refinement. This can be achieved via identifying critical links in the model chain which amplify uncertainty and investing computational resources to increase the level of detail and consequently reduce the uncertainty in the indentified mapping model. The idea is to use the right combination of models and the associated detail in the constituent models so as reach the desired levels of accuracy while ensuring computational efficiency. This approach is also beneficial in terms of evolving design goals and one can tailor the computational resource investment to adjust to new possibilities because of improved simulation model formulation and increased material knowledge with passage of time. This aspect of ensuring computational efficiency and

ensuring targeted refinement of simulation models in multiscale systems is identified as gap for integrated material and product design and addressed in Chapter 6.

b. Modelling Physical Phenomena and Interaction between the Scales

As we saw in our description in the previous section, multiscale systems are coupled between and within the length and time scales as well as between and within the subsystems and components. For example, in the Olson's diagram, coupling exists between the quantum, molecular, microscale and continuum domain and within the individual components and subsystems. These domains or scales are governed by different physical laws and mathematical equations. Though there exists comprehensive literature in macroscale modelling, material modelling in the quantum or molecular scale is still in its infancy. For multiscale modelling, it is also vital to ensure consistent flow of information gathered by simulating the physical phenomena at the different scales. Due to the significant level of complexity in the material modelling, domain experts are entrusted with the task of simulating the mathematical equations or physical laws governing the length and time scales. The models developed by the domain experts are based on varying assumptions and provide different fidelity of insight into the system behavior and hence, must be integrated in a manner so as achieve consistent system level interactions. In summary, multiscale systems represent a special type of complex systems, characterized by multiple components, multiple physics, and multiple scales. The performance of multiscale systems cannot be predicted merely through analysis of subsystems at the different scales but appropriate consideration of interactions as well.

c. Collaborative Decision Making

Design of multiscale systems involves different stakeholders. These may be internal or external stakeholders and the interests of the individual stakeholders must be met. At the internal level, the stakeholders might be the system level designer, the constituent

designer teams, or the employees and at the external level the stakeholders include the society at large, the customers, the government or the creditors. Meeting the minimum level of expectations of all these different stakeholders is a big challenge and entails collaboration between the stakeholders. Additionally, the models developed by the design teams must be linked in a manner that facilitates design space exploration by a collaborative team of experts and as a result reducing the brunt of achieving solution spaces from the system level designer. This strategy contrasts markedly with attempts to design materials using concurrent multiscale modeling. Distributing analysis and synthesis activities also leverages the extensive domain specific knowledge and expertise of various material and product designers who may be specialized according to length and time scales, classes of materials, and domains of functionality. A fundamental role of each domain-specific expert is to make decisions that involve synthesizing and identifying solution alternatives to achieve desirable tradeoffs between sets of conflicting material property goals. However, material subsystems are interdependent, and the individual decisions associated with them rely on information and solutions generated by other decision-makers at other levels of the hierarchy. In the end, preferable *systems-level* solutions are sought, and they are not necessarily obtained by 'optimizing' each subsystem individually. Therefore, it is critical to establish multi-objective *decision protocols* for individual designers as well as standards, tools, and mathematical techniques for *interfacing* and managing individual decisions while facilitating information flow among multiple experts. This aspect of establishing cooperative decision protocols is taken up in detail in Chapter 3 of the thesis using game theoretic constructs to achieve system level performance requirements.

d. Collaborative Computational Infrastructure

In order to realize collaborative decision-making between multidisciplinary material experts, it is critical to establish a computing infrastructure for integrating heterogeneous, distributed software applications and databases in a materials design

process. An effective *computing infrastructure* needs to automate the details of executing and linking various models, freeing a designer to build upon previous model-based developments and to concentrate on higher-level design issues. The computing infrastructure should be easily extensible and platform independent. A computing infrastructure also needs to archive and organize large amounts of data and facilitate real-time data sharing and visualization as well as systematic communication, translation, and search-based retrieval of design information. Tools are needed for on-line collaboration, communication, and project management, and real-time data sharing and archiving. The simulation models may employ various bundled software like MATLAB, ABAQUS, ANSYS or the design team may have its custom code based on C++, JAVA or FORTRAN. The computational infrastructure should enable a seamless interface between these softwares and automatic execution of the design programs. Such infrastructure is not commonplace as is viewed as challenge for multiscale modeling of systems. This has led to a new field of multiscale information science. An alternative approach is to make design space exploration more efficient by using design of computer experiments, approximate metamodeling techniques to create simplified mapping relationships between response variables and responses using the data generated from the computational simulation models. These mapping relationships can be used in lieu of cumbersome and computationally expensive simulation models and can be directly employed in for design space exploration. However mapping models lead to an increased uncertainty component which is discussed in the next section.

e. Managing Uncertainty and its Propagation

Uncertainty in simulation models is categorized as aleatory and epistemic uncertainty. Aleatory uncertainty refers to the uncertainty due to the inherent randomness in the physical processes, whereas epistemic uncertainty refers to the uncertainty due to lack of knowledge about the system, which can be due to lack of information about model parameters and approximations in the model. In order to make appropriate use of

information generated by simulation models, uncertainty quantification plays an important role. Since materials are complex, hierarchical, heterogeneous systems, it is not reasonable or sufficient to adopt a deterministic approach to integrated product and materials design. First, microstructure is inherently random at some scales. Second, parameters of a given model are subject to variation associated with variation of material microstructure from specimen to specimen. Furthermore, uncertainty is associated with model-based predictions for several reasons. Models inevitably incorporate assumptions and approximations that impact the precision and accuracy of predictions. Uncertainty may be magnified when a model is utilized near the limits of its intended domain of applicability and when information propagates through a series of models. Also, to facilitate exploration of a broad design space, approximate or surrogate models may be utilized, but fidelity may be sacrificed for computational efficiency. Experimental data for conditioning or validating approximate or detailed models may be sparse, and they may be affected by measurement errors. Also, variation is associated with the structures and morphologies of realized materials due to variations in processing history and other factors. Often, it is expensive or impossible to remove these sources of variability, but their impact on model predictions and final system performance can be profound. Therefore, systems-level design methods need to account for the many sources of variation and uncertainty. In Section 1.2.3, uncertainties in materials design are discussed in further detail.

f. The Inverse Problem

This challenge is specific to integrated design of material and product. As mentioned previously, multiscale systems are rife with different sources of uncertainty and employing a bottom-up mapping is an idealized approach which may not lead to desired system performance. To overcome this obstacle it is critical to develop infrastructures that employ top-down analysis while being guided by bottom-up simulation models. However, material models are not invertible in the sense that given the output at the

higher level of the material design hierarchy it is not feasible to derive the conditions required in the lower level of the hierarchy. This is because the mapping models are derived using governing equations which are complex sets of partial differential equations and which do not have closed form solutions. This can be viewed as a P not equal NP problem in computational science which states that though the solution can be verified in polynomial time, the solution may or may not be calculated in polynomial time. Quantum computation is an interesting area of research in theoretical computer science and efforts are being made to build quantum computers which overcome this inverse problem, i.e., to be able to find the solution and verify it in polynomial time. However current computing infrastructures do not permit seamless inversion and is viewed as a major obstacle for inductive design space explorations. We will look at how the microstructure mediated approach (MMD) overcomes the inverse problem in Chapter 5.

Having looked at the challenges for multiscale modeling, we proceed to describe how these challenges are overcome through a multilevel design approach through the remainder of the thesis.

1.1.4. Multilevel Design

Multiscale modeling is inherently a bottom-up exercise traversing along the process-structure-property-performance relationships in that order as described in Olson's diagram in Figure 1.3. Although seamless bottom-up mapping is useful from a theoretical or scientific perspective, the uncertainty associated with the modeling and its propagation along the design chain with a compounding of approximations makes it too idealized for materials design and may compromise its viability. Instead we resort to multilevel design where we consider the hierarchy of length and time scales as well as product, assembly and subsystem interfaces with decision nodes, i.e., it employs decision support at the linkages rather seeking automated seamless

connectivity, Figure 1.5. The decision support can be in regards to uncertainty components and its management or in terms of performance measures for optimization. This gives the designer additional flexibility to tailor the design based on the values input at the decision nodes, i.e. , increased design freedom.

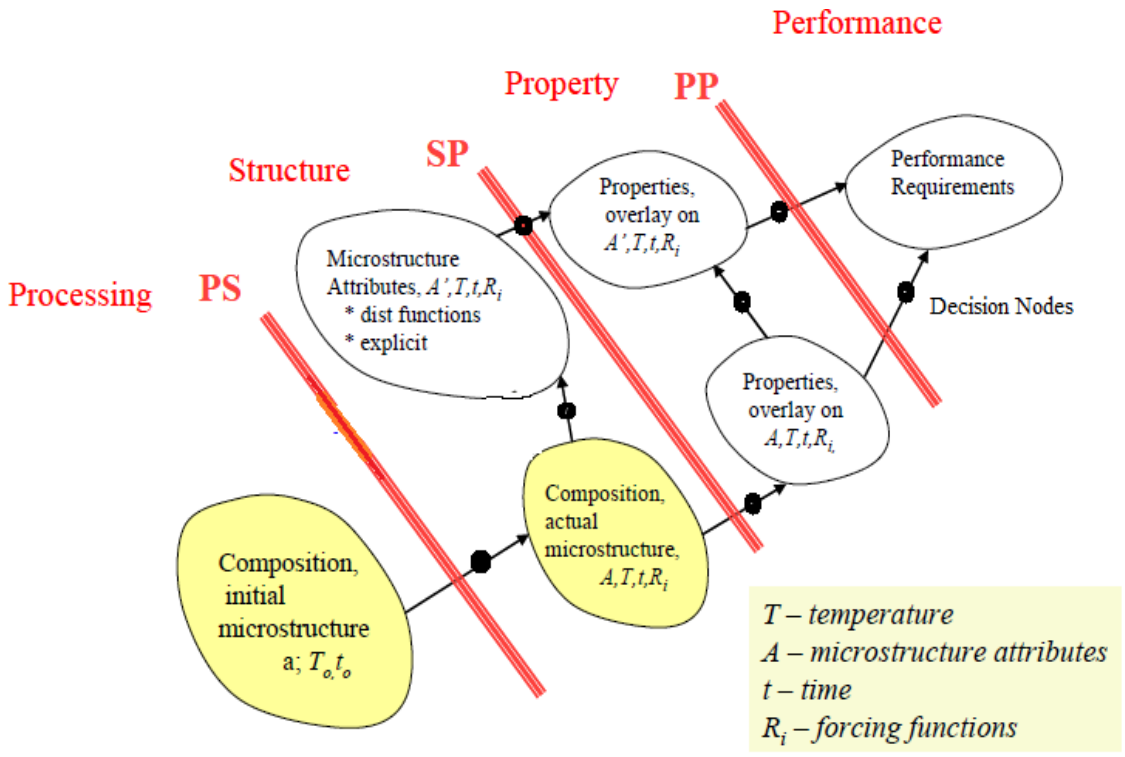

Figure 1.5: Multilevel design

Thus the approach in multilevel design for integrated material and product development is to couple bottom-up simulation mapping models with a top-down assessment of responses using decision support techniques. Thus while multiscale modeling through linking of mapping models achieves predicition of performance, multilevel design focuses on achievement of system level objectives through efficiency in design exploration techniques, i.e., it manages the complexity of the interlinked mapping models while manging uncertainty. Through the remainder of the thesis we will see how multilevel design tackes each of the challenges in multiscale modeling for integrated product and material development. Chapters 2 and 3 lay the foundations for multilevel design approach for integrated product and material design which are analyzed and

further refined in Chapters 5 and 6. Having understood multiscale modeling and multilevel design, we understand how uncertainty can be managed in multiscale systems.

1.2. Uncertainty Management in Multiscale Systems

For managing the sources of uncertainty discussed in the previous section, two primary approaches are available. One approach is reducing the uncertainty itself, and the other is designing a system to be insensitive to uncertainty without reducing or eliminating it, i.e., robust design. The following discussion on management of uncertianty is leveraged from Choi's dissertation.

Reducing or Mitigating Uncertainty

One approach of reducing uncertainty is when the designer has large amounts of data at his disposal. Kennedy and O'Hagan[6] employ a Gaussian Process model (known as kriging in spatial statistics) for fitting simple model data . They assume the model for detailed simulation data is a combination of the fitted simple model, a linear scale term, and error terms. The linear scale is assumed as an unknown constant and error terms are defined in another Gaussian Process model. By adding some detailed simulation results, unknown scale and error terms are estimated for constructing an approximate model of the detailed simulation. Simpson and coauthors[7] extend the kriging metamodeling technique and recommend a guideline for the appropriate use of statistical approximation techniques for multidisciplinary optimization. However in multiscale systems access to large amounts of data translates into a large number of simulation runs and hence becomes computationally expensive. An alternative approach is to adaptively increase the knowledge of the system through improved formulation or stepwise increase in the number of simulation runs to better represent the physical phenomena in the multiscale system. This approach to reducing uncertainty is taken up in Chapter 6 and is termed as uncertainty mitigation in my thesis.

Robust Design

The second approach for managing uncertainty is designing a system to be insensitive to uncertainty without eliminating or reducing its sources in the system; this is called robust design [8-13]. In other words, robust design is used to make the system response insensitive to uncontrollable system input variations, thus improving the quality of a designed product. This is also called parameter design. Parameter design alone does not always leads to sufficiently high quality. Further improvement can be achieved by controlling the source of variation. However, the cost associated with controlling the source's variation may be prohibitively high. A robust design approach can be introduced to design at lower cost by sacrificing the achievement of optimal performance,i.e., identify sub-optimal regions in the design space which are insensitve to variations. Typically, in robust design literature, design parameters are divided into three categories: control factors, noise factors, and responses. Control factors, also known as design variables, are parameters that a designer adjusts. Noise factors are exogenous parameters that affect the performance of a product or process but are not under a designer's control. Responses are performance measures for the product or process. Uncertainty described in Section 1.1.3. reside in system design models, based on which designers make their decision in a scientific manner, with various forms; these are control factors, noise factors, or others, which are discussed in the subsequent section, Section 1.2.1. It is important for designers to identify where the uncertainty sources reside in a system model in order to employ an appropriate uncertainty management method. Thus, robust design is a method for improving the quality of products and processes by reducing their sensitivity to variation, thereby reducing the effects of variability without removing its sources [14,15]. In the following sections, Sections 1.2.1 and 1.2.2, robust design approaches are discussed and sources of uncertainty integrated material and product systems.

1.2.1. Robust Design Approaches

As mentioned, robust design aims to alleviate the consequence of uncertainty without removing the underlying sources. Robust design approaches are classified as:

- Type I- for managing uncertainty in noise factors
- Type II- for managing uncertainty in control factors
- Type III- for managing uncertainty in system models
- IDEM- for managing propagated model chain uncertainty in multiscale systems

Robust design techniques have been developed specifically for each type of uncertainty, Figure 1.6. The distribution functions represent the uncertainty in the control, noise factors or model while its propagation through the design chain may lead to amplification or reduction depending on the connectivity. A thorough explanation of robust design techniques follows.

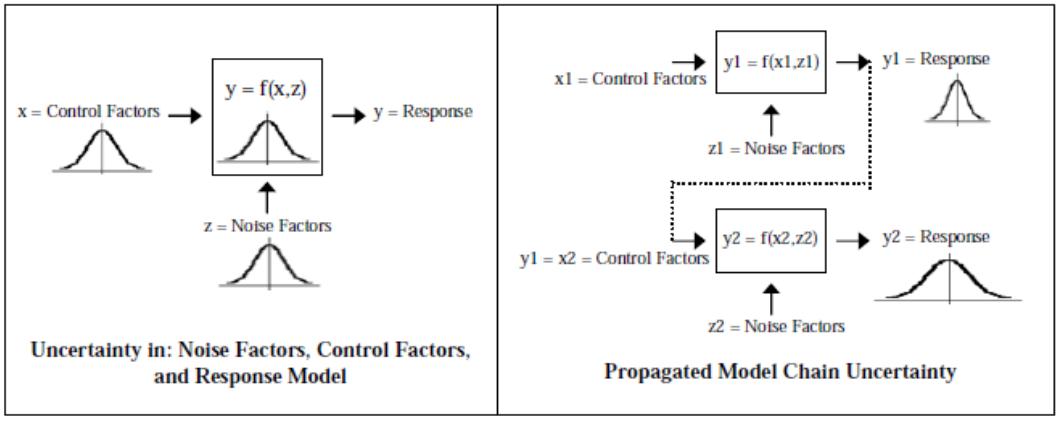

Figure 1.6: Robust design approaches- Type I, II, III and IV[1]

Managing Uncertainty in Uncontrollable Parameters-Type I Robust Design

One of the main forms of uncertainty in a system model is uncertainty in uncontrollable independent system parameters, which are known as "noise factors." Noise factors are in parametric form and may be quantified and characterized as continuous numbers, with or

without probability information. Noise factors are usually given in system models as environmental factors, operating conditions or materials property variances that may be represented as continuous parameters and cannot be controlled by designers. Uncertainty in noise factors can exist as one of the aforementioned uncertainty types; however the most dominant type of uncertainty is variability (natural uncertainty), which can be measured in a statistical way. The degree of uncertainty in noise factors can be decreased by increasing the size of sampling and/or adapting efficient uncertainty analysis methods, leaving only irreducible statistical variability. In order to design a system robust to the uncertainty in noise factors, Type I robust design was proposed by Taguchi [16].

Type I Robust Design: Identify control factor (design variable) values that satisfy a set of performance requirement targets despite variation in noise factors.

Type I robust design is used to design systems that satisfy a set of performance requirement targets despite variations in noise factors which are uncertain, uncontrollable, independent, system parameters. Although Taguchi's robust design principles are advocated widely in both industrial and academic settings, his statistical techniques, including orthogonal arrays and signal-to-noise ratio, have been criticized extensively, and improving the statistical methodology has been an active area of research[17]. During the past two decades, a number of researchers have extended robust design methods for a variety of applications in engineering design[10]

Managing Uncertainty in Controllable Parameters - Type II Robust Design

The second form of uncertainty in a system model is uncertainty in controllable system variables, which are known as "control factors". Similar to noise factors, control factors are also in parametric forms that can be measured and characterized as continuous numbers with or without probability distribution. Control factors are usually derived from the characterized parameters in system models that relate to system performance, including geometric information, mass, amounts of constituents in materials, process control inputs, etc. Designers can determine the means of control factors; however, the deviations of control factors may not be controllable. Therefore, control factors should be characterized in a manner similar to noise

factors. In order to design a system robust to the uncertainty in control factors, Type II robust design was proposed by Chen and coauthors[11].

Type II Robust Design: Identify control factor (design variable) values that satisfy a set of performance requirement targets despite variation in control and noise factors.

Type II robust design is used to design systems that are robust to possible variations in system parameters as a design evolves. In Type II robust design, designers search for means of control factors that satisfy a set of performance requirement targets despite variation in control factors.

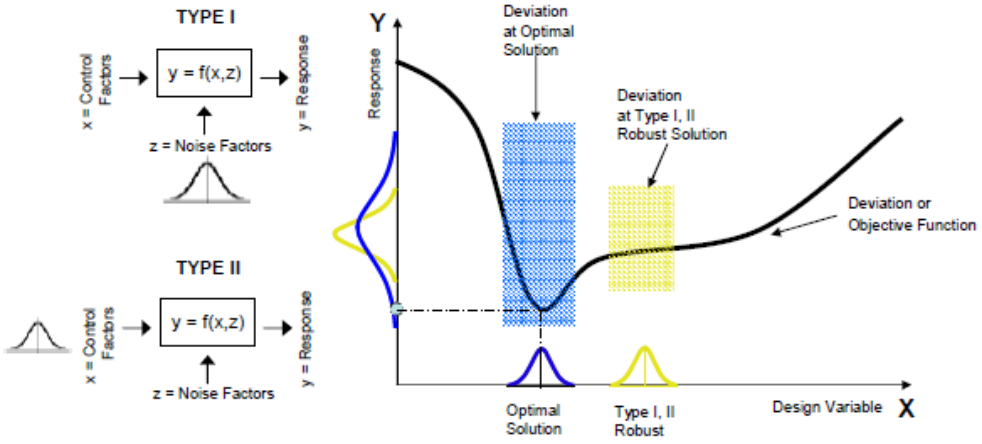

Figure 1.7: Robust design for variations in noise factors and control factors[18]

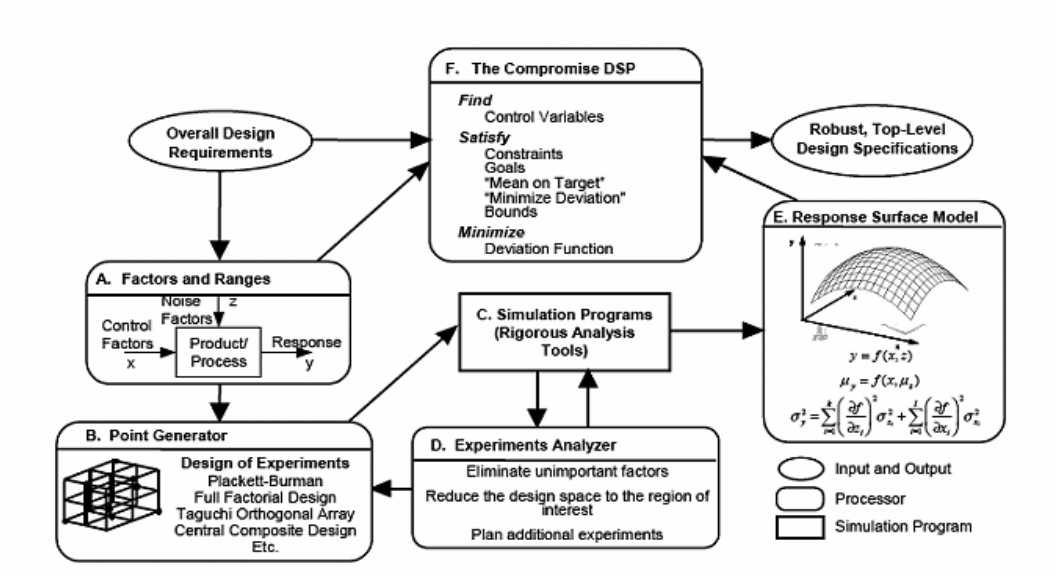

Figure 1.8: Computation infrastructure for RCEM[18]

In Figure 1.7, the optimal design solution is different from the Type I, II robust solution. Optimal solutions may have large components of uncertainty and if uncertainty measures are introduced in the design formulation, one obtains flatter regions in the output response instead of an optimal response. Thus there is a trade-off between optimal system configuration and the uncertainty in the noise and control factors. A method for combining Types I and II robust design in the early stages of product development, namely, the Robust Concept Exploration Method[18] has been developed. RCEM is a domain-independent approach for generating robust, multidisciplinary design solutions. Robust solutions to multifunctional design problems are preference-weighted trade-offs between expected performance and sensitivity of performance due to deviations in design or uncontrollable variables. These solutions are not global optima but most robust within the design space. By strategically employing experiment-based metamodels, some of the computational difficulties of performing probability-based robust design are alleviated. The computational infrastructure for RCEM is shown in Figure 1.8. Briefly, it consists of design of experiments for generating points for running the simulation, analyzing the simulation results and building integrated metamodels followed by trade-off between performance measures and uncertainty components in the compromise decision support problem (cDSP)For detailed discussion of the RCEM framework, refer to Chen, 1997. [18]

Managing Uncertainty in System Models- Type III Robust Design

Tpye III uncertainty is used to design systems that are robust to uncertainty embedded in system functions which may arise due to a combination of limited data and nonparametric system noise (or un-configured system noise). For example, if a nondeterministic system analysis is computationally intensive or experimentally expensive, then the limited data may result in uncertain parameters in metamodels (such as response surface models) of the system response. This is the typical type of uncertainty in materials design that employs computationally intensive models. Another type of uncertainty arises in systems models due to assumptions and idealization during simulation modeling. Thus includes linearization and discretization errors in finite element analysis, errors in computer codes, employment of

uncertain knowledge, and other assumptions due to limited information. The uncertainty embedded in a system model cannot be managed by previous robust design approaches (Type I and II). In order to manage this uncertainty, a new type of robust design approach, called Type III robust design, is proposed. A visual representation of Type III robust design, compared to Type I and Type II robust design, is shown in Figure 1.9. In this figure, an objective function curve is employed to show the differences among the optimal solution, Type I and II robust solution, and Type I, II and III robust solutions. A deviation (or objective) function, which represents the system's response, is illustrated as a solid curve. In addition, two dotted curves are added around the objective function, representing uncertainty limits, which are due to the non-parametric variability, un-configured variability, and model parameter uncertainty as mentioned above. Considering not only the objective function but also the two uncertainty limits, the optimal and Type I and II robust solution have larger performance deviations than the Type I, II, and III robust solution. Type III robust design becomes more important since modern engineering systems are getting more and more complex (or extremely small) and their behaviors are stochastic. For Type III robust design, it is required to build error bounds (uncertainty bounds) in a model in a computationally inexpensive manner. The most accurate way to incorporate the embedded uncertainties as well as the uncertainty in control and noise factors during design exploration is to perform actual simulations using statistical techniques (simulation-based design). In Figure 1.9, a comparisison between Type I, Type I,II and Type I, II, III is illustrated. Type I, II, III acounts for uncertainty in nosie, control and model parameters and the desired solution is obtained a trde-off between performance, flat regions representing robustness against noise and control factors and small error bounds representing robustness against uncertainty in the model response.

Type III Robust Design: Identify adjustable ranges for control factors (design variable), that satisfy a set of performance requirement targets and/or performance requirement ranges and are insensitive to the variability within the model.

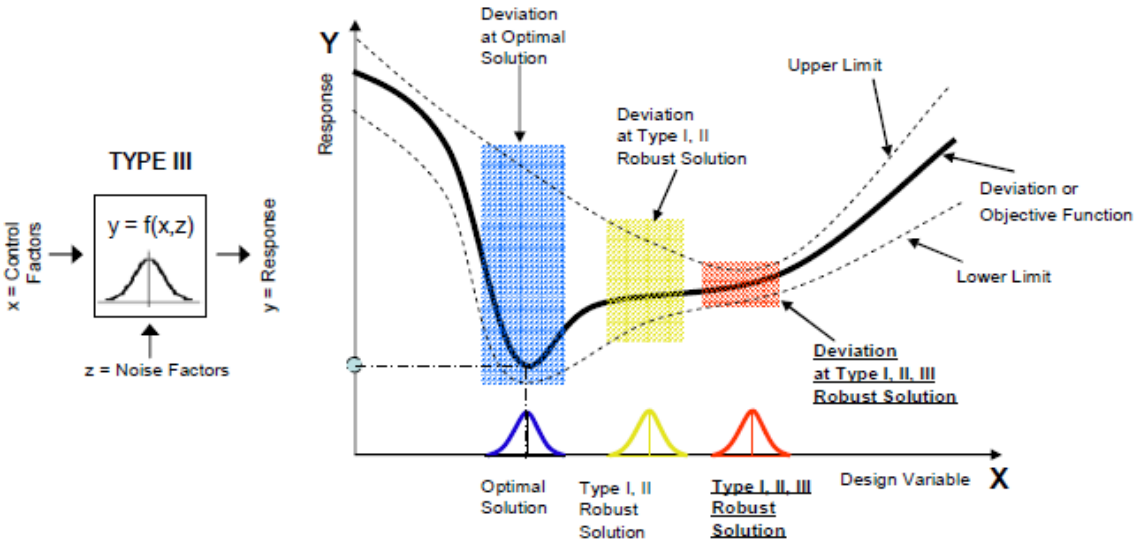

Figure 1.9: Robust design for variations in noise factors, control factors and model response[16]

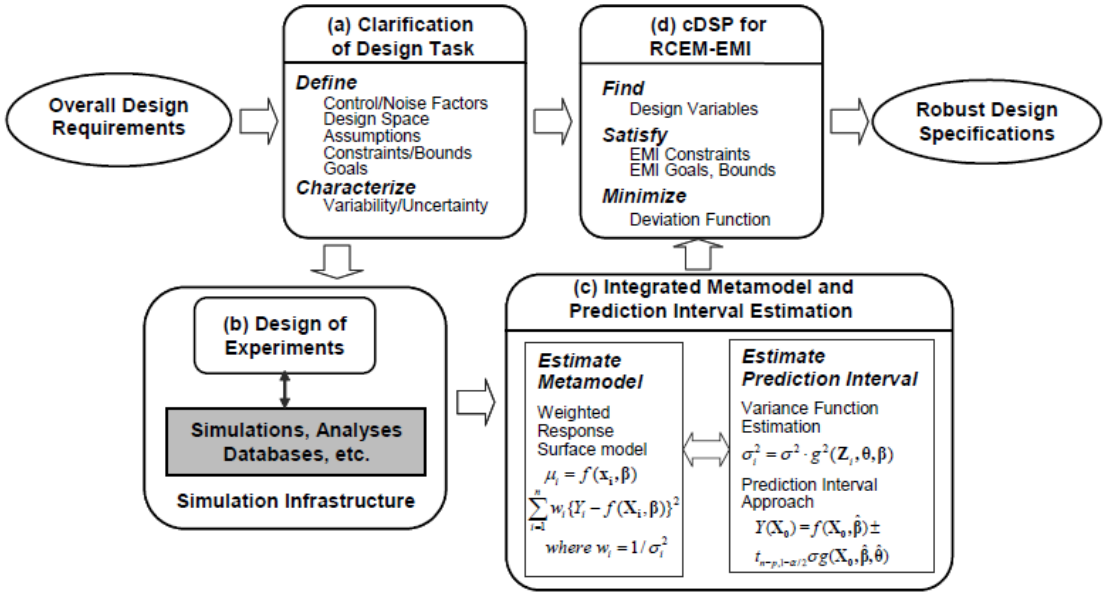

Figure 1.10: Computation infrastructure for RCEM-EMI [16]

The RCEM-EMI (Figure 1.10) construct was introduced by Choi to handle Type III robust design. The RCEM-EMI procedure consists of (a) clarification of the design task, (b) DOE and simulation, (c) integrated metamodel and prediction interval estimation, and (d) design space search using the cDSP for the RCEM-EMI. In the RCEM-EMI, the Error Margin Indices (EMI) are metrics indicating the degree of reliability of a decision that satisfies system constraints and bounds [16]. The design procedure is to find ranged sets of design specifications that meet a range of system

requirements based on the EMIs calculations. Unlike Type I and II robust design, in which only system response variations due to uncertainty from control factors and noise factors are considered, the RCEM includes the response variation due to the variability of the model itself and uncertainty bounds of models into the consideration. For a detailed mathematical understanding of the RCEM-EMI framework, refer to Choi's disseration[1].

The RCEM-EMI framework has its limitation while extending it to the multiscale system analysis. Monte Carlo Simulation is a popular method to measure variations of performance by simulating input variations (uncertainty analysis).Even though this approach could produce accurate results in design exploration, it requires a large number of experiments (more than 10,000 in many cases) for uncertainty analysis even in a single evaluation during a design exploration process. However, most multiscale material performance analyses need intensive computing power (from half an hour to several days for a single simulation run). It is nearly impossible to employ this approach in materials design exploration even if a sampling technique, such as Latin Hypercube sampling, is applied to reduce the number of experiments. Computationally inexpensive uncertainty analysis methods are needed to solve this problem. Hence , IDEM was proposed for managing uncertainty in multiscale systems, discussed next.

Managing Uncertainty in Design Process Chain- Inductive Design Exploration Method (IDEM)

The final type of robust design is for multiscale systems and managing the uncertainty generated in the design and analysis process chain, which, unlike the aforementioned uncertainties in a system model, arises from the complex design and analysis process chain and not from the system model itself. This type of uncertainty is often observed in multidisciplinary uncertain system design problems and includes errors in decisions made by other designers and accumulated errors (propagated uncertainty) by subsequent series of uncertain subsystem models. Typically, complex multidisciplinary system design requires multiple experts to collaborate to make decisions for designing a system. The outputs of other experts' decisions in a subsystem could be input parameters, constraints, or design spaces of other subsystems or systems design. In many cases, multiple subsystem designs even share common design

variables. In these interactions in design activity, a subsystem design error can be propagated to another subsystem or system.Additionally, complex systems design tends to employ multiple analyses and simulations in a series to predict system responses.

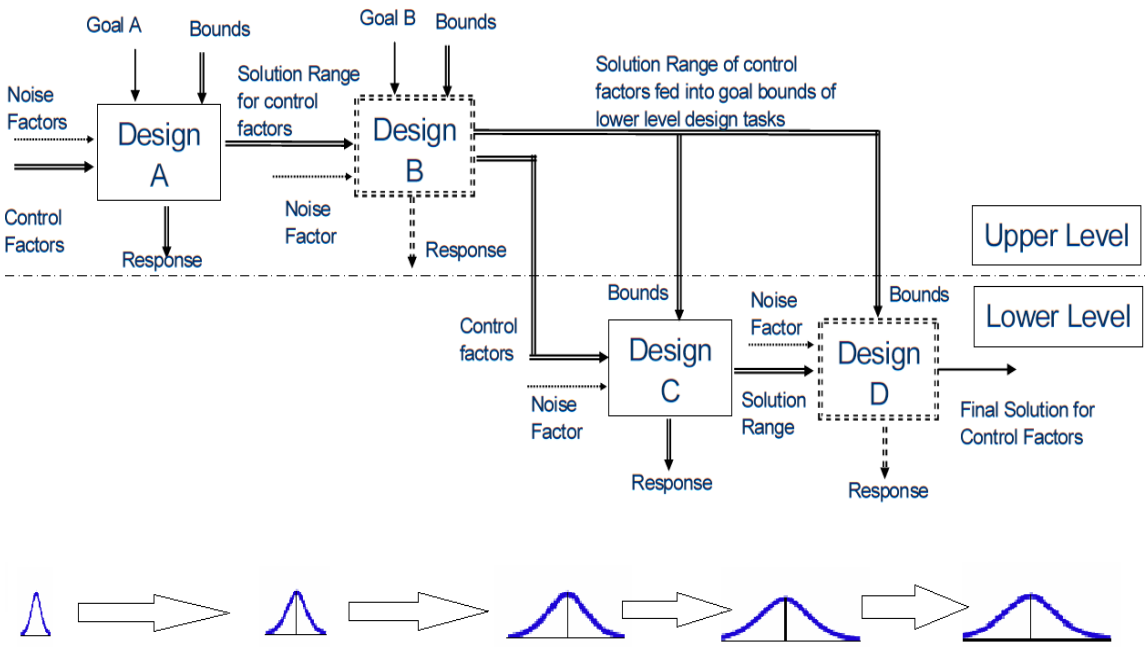

Figure 1.11: Robust design for amplification or reduction of system response along a design process chain[1]

Design process uncertainty emanates from: (a) changes in design specifications as a result downstream or concurrent decisions and design activities or (b) the propagation or potential amplification of uncertainty due to the combined effect of analysis tasks performed in series or in parallel, Figure 1.11. Due to the sequential nature of the design chain mapping, the uncertainty in the noise and control paramaters is amplified by the uncertainty in the model as it propagates through the models in the design chain. Both sources of design process uncertainty are common and important for multidisciplinary design and analysis, including multiscale, multi-physics materials design, with a plethora of shared or coupled variables and analyses performed on multiple length and time levels. The information dependency in multiscale models engenders complex design process chains – hierarchical, parallel, and serial design processes.

Inductive Design Exploration Method: Identify adjustable ranges of control factor (design variable) values under potential uncertainty and uncertainty propagation in a design and analysis process chain in multiscale systems.

For an accurate understanding of the Inductive Design Exploration Method (IDEM)[19] it is important to classify the sources of uncertainty relevant to multiscale systems. We take this up in the next sub-section.

1.2.2. Uncertainty in Multiscale Systems

IDEM is going to be the central framework we build upon in the subsequent chapters. Before we proceed to understanding IDEM, it is necessary to categorize the types of uncertainty in a multiscale system, since quantification of the uncertainty in the model depends on these uncertainty types. Uncertainty can be classified as either *Aleatory* (irreducible) or *Epistemic* (reducible) based on the causes of the uncertainty. *Epistemic* uncertainty can be diminished by improvements in measurements and/or model formulation and/or by increasing the accuracy or sample size of data[13]. *Aleatory* uncertainty, on the other hand, is inherent in the physical system and can only be quantified in a statistical sense[13]. Extending the classification of uncertainty types by Isukapalli and coauthors [20], the types of uncertainty are categorized by Choi et al. [13] is as follows.

a. **Variability (natural uncertainty):** Uncertainty due to the inherent randomness or unpredictability of a physical system; this is irreducible and can only be quantified in a statistical sense. The variability can be further classified as parameterizable and unparameterizable. Parameterizable variability can be configured as variance in numeric form, but unparameterizable variability cannot.
b. **Model parameter uncertainty (data uncertainty):** This is incomplete knowledge of model parameters/inputs due to insufficient or inaccurate data; it is reducible by sufficient data or accurate measurements.
c. **Propagated uncertainty (PU):** this is uncertainty expanded by a combination of the above two types of uncertainty in a chain of models.

d. **Model structure uncertainty (model uncertainty):** This is uncertain model formulation due to approximations and simplifications in a model; it is reducible by improving model formulation.

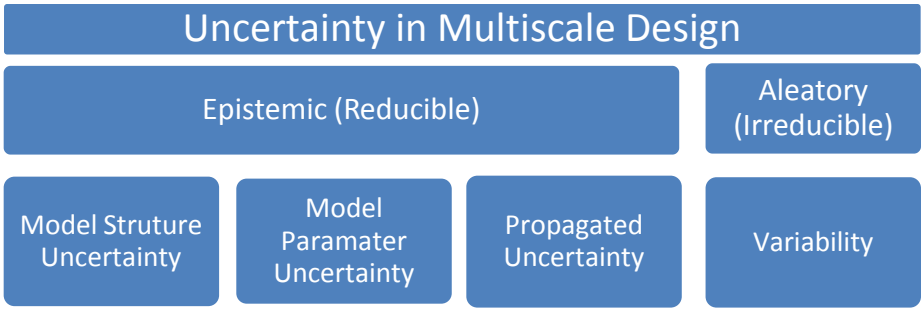

Figure 1.12: Classification of types of uncertainty

These uncertainty types coexist within any system. While one type of uncertainty may dominate, the other type of uncertainty may be negligible. It is an important step of the multiscale design process to identify the key sources of uncertainty and make efforts to mitigate them. In this thesis, we are concerned with all four types of uncertainty and the interrelation with each type of uncertainty is as follows:

a. ***Variability (Natural Uncertainty)***

Variability can be quantified only in the statistical sense. Variability in inherent in any physical phenomena and cannot be mitigated *i.e.* irreducible in nature. Hence, efforts are focused in accurately modelling variability while managing uncertainty. The modelling efforts can in the form of distribution functions (most commonly Gaussian distributions) or intervals. The approach in this thesis to model natural uncertainty as an interval estimate which is formulated as a Taylor series expansion and incorporated in the confidence bound determination. We note that since this uncertainty cannot be reduced, efforts are put only in accounting for variability in robust design of multiscale systems and not reducing it.

b. ***Model Parameter Uncertainty (Data Uncertainty)***

In multiscale systems, there may be several simulation models at different length and time scales. Since it would be computationally very expensive to evaluate feasible spaces for the multiscale system by running simulation models over the entire design

space, we run the simulation models only at a limited number of discrete points in the design space for the design variables with the objective of gaining maximum amount of information about the simulation model reproducing the physical phenomena. To gain the maximum amount of information, we use a design of experiments technique and proceed to evaluate metamodels based on the output from the simulation runs. A metamodel is a 'model of a model' *i.e.* a model that represents the functional relationship between the input and output variables for the simulation model. A linear model for a simulation model with only one design variable (x) will be of the form:

$$Y = b_0 + b_1 x \qquad (1.1)$$

Where, Y is the output of the simulation model, b_0 and b_1 are model parameters and x is the design variable. Such an approximate function can replace the actual simulation model in our analysis of the multiscale system. As the metamodel is an approximation based on the limited data from the actual simulation model, there will an uncertainty component associated with b_0 , $b_1$and x. Ideally, the uncertainty associated with x is only the natural uncertainty or variability. To mitigate model parameter uncertainty associated with b_0 and b_1, we have to acquire additional information about the simulation model over the design space so that we can get better estimates for b_0 and b_1. This translates to running the simulation model over sufficient data points in the entire design space. However, there is no metric to quantify the number of additional runs required to converge to a robust solution or the associated benefit associated in the re-runs. In this Chapter 6, the focus is on reducing the model parameter uncertainty associated with the only the model parameters (b_0 and b_1 in the Equation 1.1) and not with x which comes from two components:

(i) Variability which is irreducible in nature

(ii) Discretization error which can be reduced by making intervals smaller while evaluating robust feasible spaces in IDEM.

However managing discretization error will involve a rigorous study of the computational effort and the benefit associated with reducing the discrete interval approach in IDEM. Hence we are limit our focus to understanding the computational effort and the effort-benefit trade-off associated with modeling parameters for the

metamodel. My approach is to first quantify the model parameter uncertainty and the benefit associated with the refinement of the individual subsystem level simulations. This is taken up in Chapter 6. The idea to first get an initial estimate of the benefit of simulation model refinement on the final design performance and then proceed to proposing the set of data points for re-runs for each simulation model at the subsystem level. This is achieved by reaching a trade-off between the computational cost models for the simulations associated with the anticipated gain on the overall performance requirements of the multiscale system for the system design.

c. Propagated Uncertainty (PU)

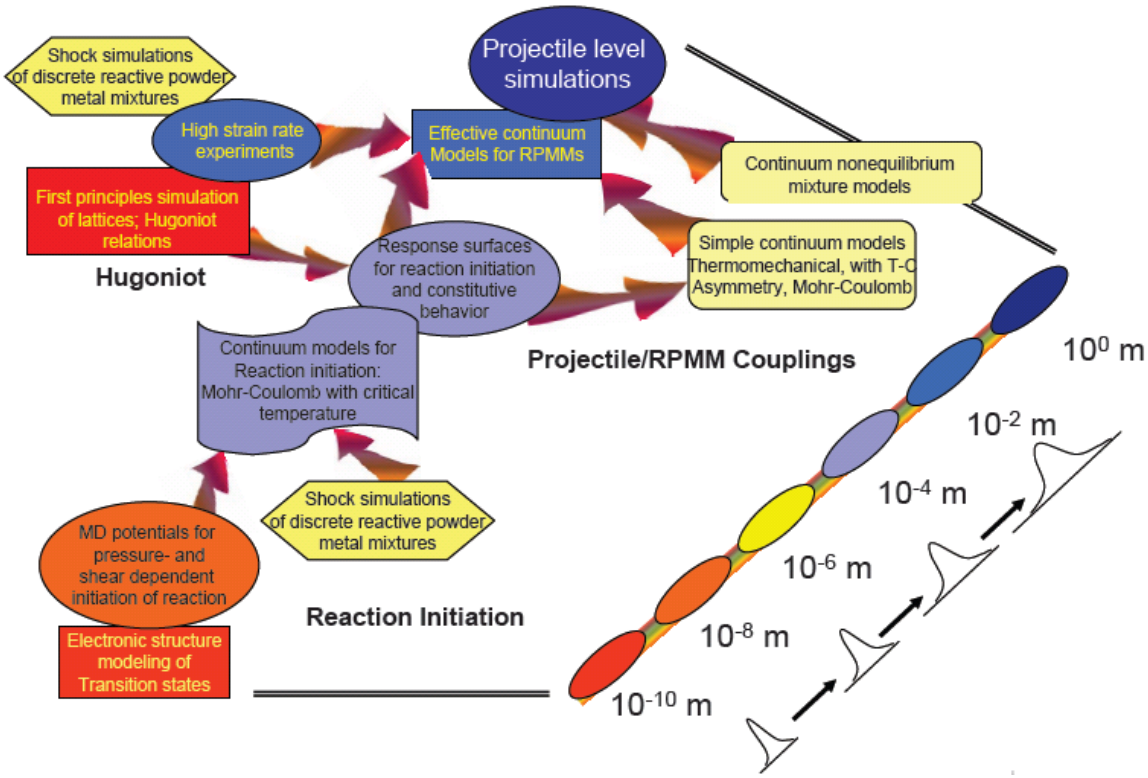

Figure 1.13: Propagation of uncertainty through design chain [1]

Not all subsystems will have the same effect on the final design performance. The uncertainty associated with the simulation models at the micro or nano-scale in the spatial domain will have a greater effect on the performance of the system or product as compared to the models at the macro domain. This is because of the hierarchical nature of multiscale systems and the lower level subsystems will propagate to a greater

extent through the design chain. This propagated uncertainty is managed by our technique of robust design, i.e., IDEM. In order to account for propagated uncertainty while achieving trade-off for further simulation refinement, we account for the propagation by assigning greater weights to simulation models at the smaller scale in the spatial or temporal domain. Figure 1.13 illustrates the propagation of uncertainty through the design model chain along the length scale for the microscale discrete particle shock simulation-based robust design of multifunctional energetic structural materials used by Choi for validating IDEM [1]. The uncertainty is amplified along the design chain. Based on the connectivity between the interlinked models, uncertainty may be reduced too along a design chain.

To further understand the nature of propagated uncertainty which will be crucial for developing weights for the simulation models we look at Figure 1.14. Parameter, x1, is an input to the subsystem model, f1; x1 has a variance associated with it. The y1 is the response from the model in which the input uncertainty is increased because of the combination of variance of x1 and errors in f1 model itself. A Similar thing happens in y2, which is the response of f2 with x2 as the input. The same effect may be applied to model, f3. Variables, y1 and y2, are inputs with variances to f3. The response, z, includes increased uncertainty due to the combination of variances in y1 and y2 and the uncertainty in the model, f3. Therefore, uncertainty accumulates through multiple steps of a model chain and making the variance of the final response unexpectedly large. In order to deal with this kind of uncertainty, the robust design approach for complex systems is necessary and accounted for in IDEM. Also, we see that the uncertainty associated with x1 propagates through two levels in the design chain (f1 and f3) and x2 propagates through two levels in the design chain (f2 and f3) while uncertainty associated with y1 propagated through only one level (f3). Thus we realize that there is a greater benefit in reducing uncertainty in x1 and x2 as compared to variables higher in the design chain. A similar argument can be placed for the models f1, f2 and f3. The uncertainty in f1 and f2 propagate through f3 while f3 has no propagation effect. Thus while developing weights for the simulation models; we should assign greater weights to models lower in the design chain.

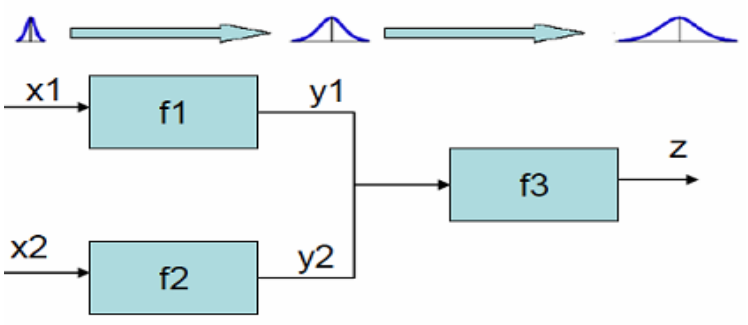

Figure 1.14: Uncertainty propagation through design chain [1]

d. Model Structure Uncertainty (model uncertainty)

Among the types of uncertainty, model structure uncertainty (MSU) is the most difficult type to manage since it is hard to quantify[13]. Choi et al [13] developed IDEM to find robust solution against MSU. Their strategy to deal with MSU is to first find the feasible solution space for given final performance requirements and process constraints considering variability, propagated and model parameter uncertainty. Then proceed to find the best robust solution amongst the identified feasible space against MSU. To reach this trade-off they contend that feasible robust points further away from constraint boundaries considering all interdependent variable spaces are more reliable against unquantifiable model structure uncertainty. For example, in Figure 1.15, even though Design 1 and 2 achieve the same final performance (z space), Design 2 is better than Design 1 because the projected region of Design 2 in the interdependent variable space (y space) is farther from the constraint boundary of the feasible region than Design 1 [13]. In this thesis, we only focus on managing MSU and not reducing it. In order to reduce MSU, value of information needs to be understood holistically. MSU arises from modelling assumptions and hence the computational costs will be more difficult to quantify. One approach is to prepare a comprehensive list of computational programs used in simulations and understanding the impact of refining the model. For example, in structural modelling, the validity of the results is dependent on the mesh size. The computational effort in reducing mesh sizes in FEM softwares like ABAQUS or ANSYS need to be quantified. Also, in numerical simulation in MATLAB we often use approximations which can be tailored. For example a material simulation model may use the Simpsons rule for numerical integration. This can be refined by using Simpsons $3/8^{th}$ rule at an increased computational cost. All these scenarios need to be tabulated

and corresponding computational costs need to be quantified. This is proposed as future work. It is noted that this kind of uncertainty cannot be reduced through additional data acquisition but only through improving the model formulation. For example, if higher order coefficients are ignored in model formulation,additional data will give a set of solution based on the reduced order of the model and will ignore the uncertainty component due to the ignorance of higher order coefficients. Hence the model will need to reformulated accounting for the higher order coefficients to reduce model structure uncertainty.

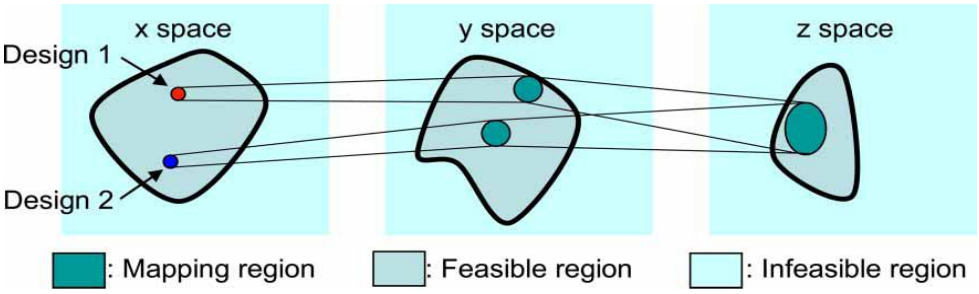

Figure 1.15: Robust design against model structure uncertainty (MSU) [13]

Sources of Uncertainty	Classification of Uncertainty
■ Non-deterministic simulations and analyses ■ Limited data due to intensive computation and expensive experiments ■ Simplifying assumptions and idealization in simulation and analysis models ■ Propagated uncertainty in a simulation and analysis process chain	■ Natural Uncertainty (system variability) □ Parameterizable Variability □ Unparameterizable Variability ■ Model Parameter Uncertainty (parameter uncertainty) ■ Model Structure Uncertainty (model uncertainty) ■ Propagated Uncertainty in a Process Chain (process uncertainty)

Table 1.2: Classification and sources of uncertainty in multiscale systems [1]

In summary, a multiscale design has four sources of uncertainty and the system level designer has to expend resources to quantify and mitigate these sources of uncertainty. In my algorithm robust design is achieved by the Inductive Design Exploration Method (IDEM) which accounts for all the four sources of uncertainty in a multiscale environment. Aleatory uncertainty can be quantified in the statistical sense but epistemic uncertainty can only by mitigated by increasing

the knowledge about the multiscale system. In IDEM, aleatory uncertainty is incorporated in the error bounds for response surface models as a Taylor series expansion at the subsystem level for each of the simulation based subsystems in the multiscale system. Epistemic uncertainty is accounted for by understanding the sources and the quantifying the degree of model parameter uncertainty, model structure uncertainty and propagated uncertainty for the multiscale design. The sources and classification of uncertainty is illustrated in Table 1.2. In the algorithm in Chapter 6, we specifically look at reducing model parameter uncertainty (MPU) while accounting for the other three sources of uncertainty. This is represented in Figure 1.16 and we look at reducing the red error bounds. MSU can reduced by refining the modeling assumptions and would mean a new response surface altogether. NU cannot be reduced while MPU associated with the design variables can be reduced by taking smaller intervals in IDEM.

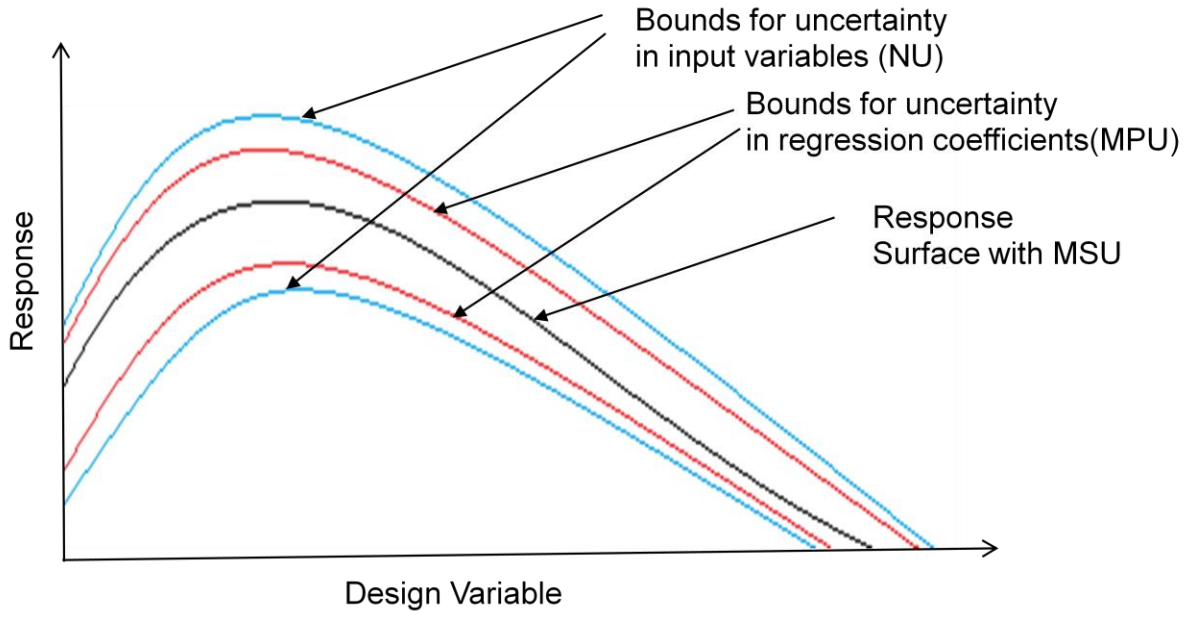

Figure 1.16: Uncertainty management for simulation models

Having understood the sources and classification of uncertainty associated with multiscale design, we proceed to understanding the management of aleatory and epistemic uncertainty in IDEM in the next section.

1.2.3. Inductive Design Exploration Method

The robust design approach for multiscale systems developed by Choi [21] is to identify adjustable ranges of control factor (design variable) values under variability, model uncertainty and uncertainty propagation in a design and analysis process chain. The Inductive Design Exploration Method (IDEM) [21] is proposed as a robust design approach for multiscale systems.

The assumption of IDEM is that the uncertainty which comes from the error of models and then is propagated during the design process can be reduced by keeping the design freedom as large as possible in each design stage. Therefore, IDEM does not provide any specific solutions, but a feasible design space. The specific solution is achieved by the compromise decision support problem (cDSP) approach. In the IDEM approach, the basic idea for finding ranged sets of robust solutions against the propagated uncertainty in a complex model chain is to pass down the feasible solution range in an inductive manner, from desired given final performance ranges to the design space, while the design freedom at each step is kept as large as possible. The design freedom in IDEM is defined as the ratio of the feasible ranges versus entire design space. For identifying feasible solution range, designers use only mathematical surrogate models i.e. the response surface models or theoretical mathematical functions for bottom-up calculation, not the simulation models for the inverse calculation. Designers chose the solutions from this space according to their preferences or experience. The discrete exploration process is implemented in IDEM to explore the whole design space and check whether all individual design variables are able to create feasible performance. Since the discrete exploration process is computationally expensive, the computational time for design problems with a large number of design variables may become exponentially large in IDEM. Therefore, an additional assumption of IDEM is that the design space is small enough to allow for an exhaustive search of all possible design combination. Moreover, due to the discretization of a design space, discretization errors are not avoidable when the algorithm is checking the feasibility of a mean performance based on discretized feasible and infeasible points.

IDEM is a three step algorithm. The steps are as follows[13]:

(i) Rough design space discretization

(ii) Parallel discrete function evaluation

(iii) Inductive discrete constraints evaluation (IDCE)

The overall procedure for IDEM is illustrated in the Figure 1.17.

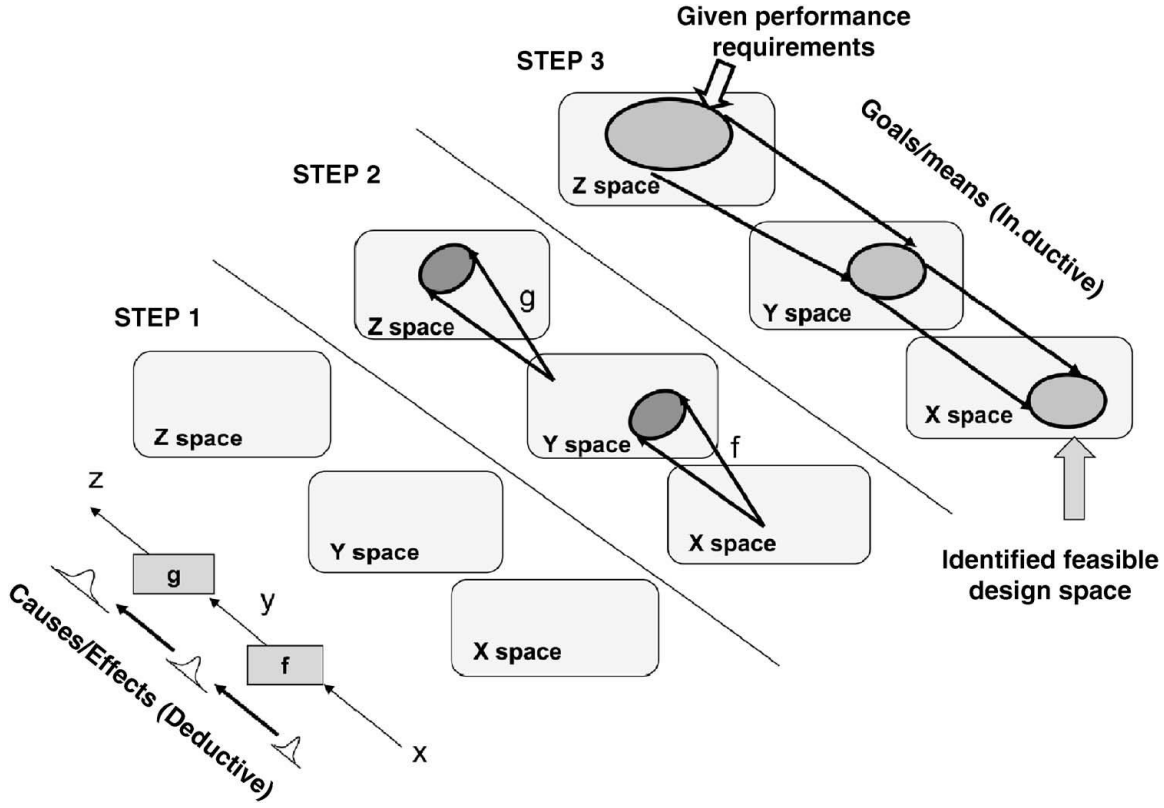

Figure 1.17: Solution search procedure for IDEM [21]

In Step 1 we discretize the design space into intervals as design space exploration is computationally expensive. After Step 1 we generate discrete mapping models between the design variables and the output parameters in the multiscale system. We get ranged sets of feasible design space after Step 2. In step 3 we get the best robust solution by compromising the model structure uncertainty (MSU) with the different models in the multiscale system. We now proceed to look at each of the three steps in greater detail:

Step 1: Discretize Design Space.

IDEM employs search techniques between the mapping models to explore the design spaces at each scale of the multiscale system. The mapping models have to be evaluated for each set of discrete input points and if a model has multiple inputs, a combinatorial set of discrete input sets have to be defined and these sets may become very large for small discretization resolution or large number of inputs. The IDEM performs exhaustive search among these mapping models to find ranged sets of feasible spaces in the lowest level of the material design hierarchy. As a result, the computational time may increase exponentially for small discretization resolutions or choice of large number of response variables. To avoid computational complexity, the design space is discretized and the resolution space is decided so as to have sufficient accuracy while performing the design space search. To this end, the choice of the discrete intervals is decided by the variability or natural uncertainty modeled in the response surface and it is chosen to be equal to twice the variability to cover the entire design space without loss of crucial information, i.e., within limits of error due to natural uncertainty. Also response variables are screened to maintain only the crucial coefficient terms from the mapping models to further decrease computational expense. The parallel discrete function evaluation and inductive constraint design exploration steps are performed on the discretized design space.

Step 2: Parallel Discrete Function Evaluation

After having defined the rough design space (x space in Figure 1.16), the interdependent space (y space in Figure 3.16), and the performance space (z spaces in 1.16), discrete input sets are generated in each of these spaces. The discrete points which are generated are evaluated based on the mapping models (model f and model g in Figure 1.18) and the evaluated data sets which are composed of discrete input points and associated output ranges are stored in a database. These two steps combined are combined in Step 2 and are called parallel discrete function evaluation in IDEM.

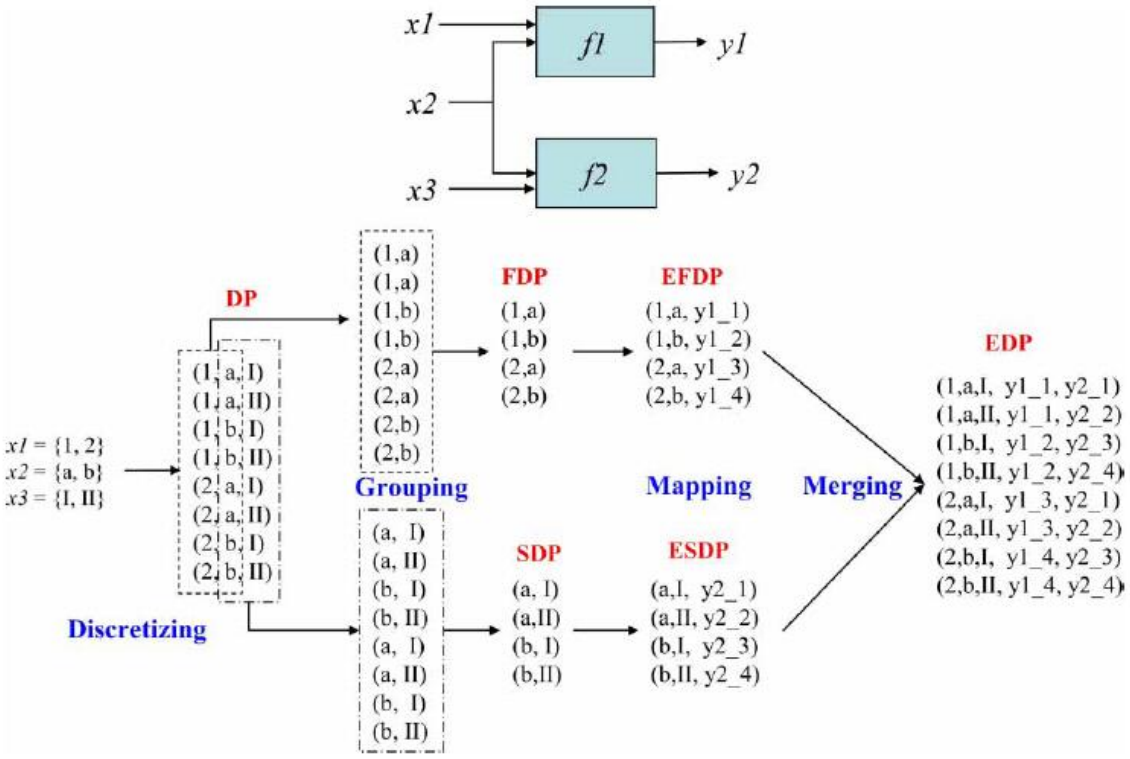

Figure 1.18: Parallel discrete function evaluation in IDEM [13]

Since it is common that an analysis chain includes shared variables with several models, the process for projecting shared input and output space is defined as the following:

- ***Discretization**:* Obtain all combinations of discrete input points of associated input design variables.

- ***Grouping**:* Group the combinations created in the 'discretization' process according the input variables for the mapping models.

- ***Mapping**:* Evaluate the groups created in parallel by the associated mapping model or function. We get the corresponding output as well as the ranges for each input point.

- ***Merging**:* Combine the multiple response ranges obtained from 'Mapping' process in order to formulate response ranges for each point in the original discretization.

For further details of the implementation of the parallel discrete evaluation step, refer Choi's dissertation.

Step 3: Inductive Discrete Constraints Evaluation

Feasible regions in y and x spaces are sequentially identified by a metric for determining whether a discrete point from an input space maps to a feasible design solution in the output space. This metric is called Hyper-Dimensional Error Margin Index (HD-EMI). A visual and mathematical representation of HD-EMI is shown in Figure 1.19.

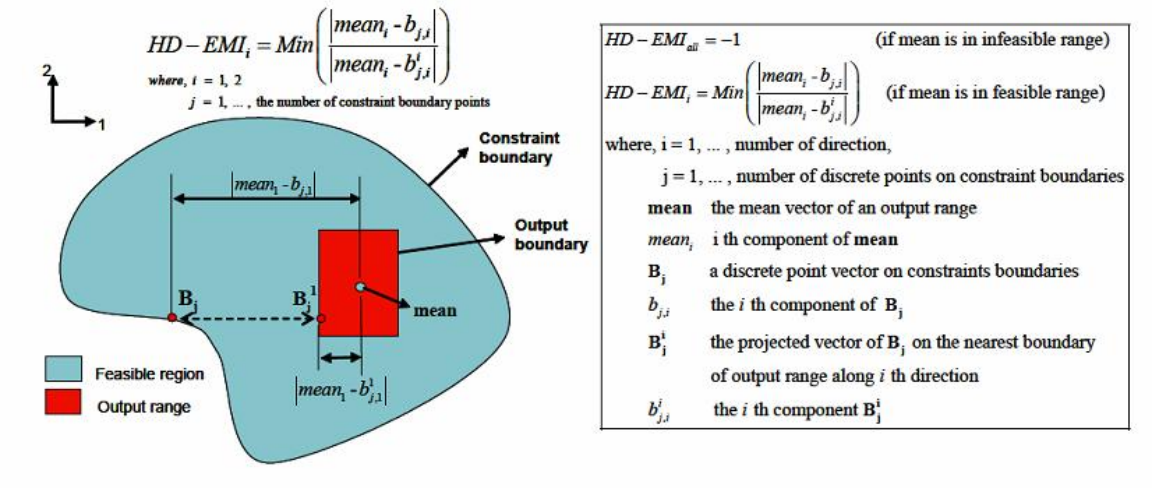

Figure 1.19: Calculation of HD-EMI [1]

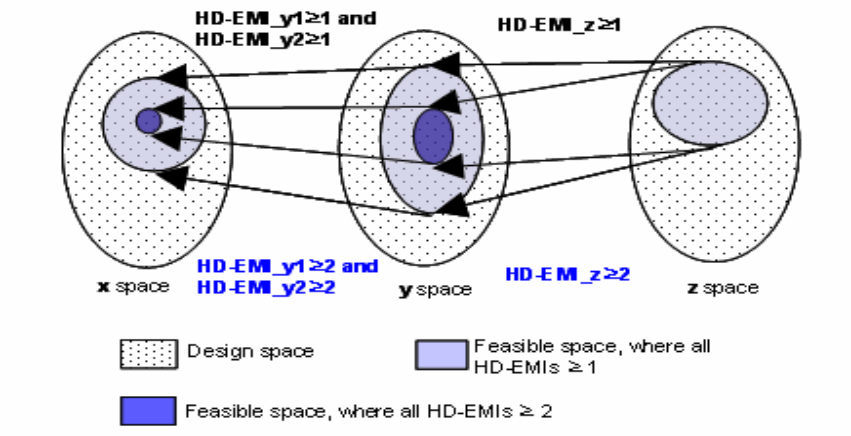

Figure 1.20: An example of the IDCE controlling HD-EMIs [1]

HD-EMI is an extension of the EMI metric [1] developed by Choi from one dimension for a single output model to hyper-dimensional space relevant to multiscale systems with multiple outputs. HD-EMI is a measure of the distance of a design point from the design space boundary divided by variation in system performance. As shown in Figure 1.17, a higher HD-EMI value indicates that the output is further away from the constraint boundaries in the hyper dimensional space and has greater tolerance for model structure uncertainty (MSU). The assumption is that a solution that is far from the constraint boundaries of the feasible design space will remain within the feasible design space in the presence of slight variations. Hence the system level designer can be confident while making design decisions though shifts in the output range are possible due to model uncertainty. Therefore, in IDEM, designers are interested in selecting design points with high values of HD-EMI. Mathematically, a HD-EMI value of 0 indicates that the output is on the constraint boundary along one output direction, i.e., the numerator is 0 and hence indicating the mean output coincides with the nearest constraint boundary point. A HD-EMI value of 1 indicates that either the maximum or minimum output coincides with the constraint boundary range, i.e. , the numerator is equal to the denominator indicating that the distance between the mean output and nearest constraint boundary point is the same as the distance between the mean output and one of either the maximum or minimum output. Hence the nearest boundary point and the output range are coincident along an output direction. These concepts will be used in Chapters 5 and 6 to evaluate robust and feasible discrete points in the design space.

The Inductive Discrete Constraints Evaluation (IDCE) technique is implemented to sequentially find feasible ranges in all intermediate as well as final design spaces based on the HD-EMIs. It is an inverse method in the analysis process chain show in Figure 1.20.

The evaluation procedure starts with an assumption that the required range of the final performance, z, is given as shown in the gray area in z-space in Figure 1.18. From the z-space, a feasible range in y-space is obtained. To achieve this, feasible discrete points in y-space are

found out by evaluating whether the HD-EMI in z-space for the discrete points in y-space are greater than or equal to one. Constraint contours are calculated between the feasible and infeasible discrete points in y-space, by identifying the discrete points in y-space for which the HD-EMIs in z-space are less than or equal to one. Then, the next step is to find feasible regions in x-space based on the identified feasible region in y-space in the same way. The process to find the interpolating point between the feasible and infeasible points is achieved by a numerical root finding method. The method used in this algorithm is the bisection method.[22]

Thus we note that as HD-EMI increases for a particular model, the output range moves farther from the constraint boundary. This means the decision becomes more reliable under potential shift of the output range due to MSU. In the IDCE process, the given specifications are required final performance range and required HD-EMI for the discrete constraints evaluation. These specifications are to be decided by the designer for the product at hand. Therefore, the required HD-EMIs in each space should be selected statistically in order to find the best solution among feasible sets of solutions. Values of HD-EMIs are important in determining the most desirable robust solution against MSU, because HD-EMIs represent the amount of margin for potential errors in the mapping models for estimating output range. A designer may leave wider margins between an output range and constraint boundaries by increasing the HD-EMI for the mapping model whose MSU is larger than others. An additional constraint is that all HD-EMIs should be greater than or equal to one so that entire output range can satisfy the constraints Depending on the value of required HD-EMI, the identified feasible range may be large, small, or unattainable

If there are multiple feasible discrete points in a design space, a designer has more room for tailoring design variables. In this case, the required HD-EMIs in the spaces of y and z can be increased which reduce the feasible ranges in x- and y-spaces, respectively. In order to make product level decisions for the design variables, designers need to compromise the achieved HD-EMI values in the different models so as to get high HD-EMI values for model with high MSU while ensuring product level specifications are met. The IDEM is applied to a multiscale system

in Chapter 2. The limitation of this using IDEM is that if the design process is not sufficiently constrained, it may give large sets of feasible processing spaces in the material design hierarchy and it becomes difficult to choose a single solution from these sets of solution. One approach to overcome this problem is a trial and error approach of increasing the HD-EMI values so that a sufficiently small feasible processing space is obtained and a single solution can be chosen from this small ranged set. However, this may be a painstakingly cumbersome process and the multiscale system is governed by a complex interlinking of dependent and independent variables. The compromise Decision Support Problem (cDSP) can effectively overcome this obstacle and the selection procedure for HD-EMI values is automated using the cDSP approach. This is discussed in the next section.

1.2.4. The compromise Decision Support Problem (cDSP)

The following information on the compromise Decision Support Problem (cDSP) is leveraged with only minor modifications from the Master's Thesis of Markus Rippel[23]. The cDSP is the backbone construct that facilitates the Type I, II and III frameworks presented in the previous sections. The purpose of this section is to review the literature regarding the use of compromise Decision Support Problems in solving engineering design problems in order for it to be applied to multiscale systems. This is undertaken in Chapter 3 using game theoretic protocols. It is further extended by coupling it with IDEM in Chapter 5. Compromise and selection Decision Support Problems are two flavors of DSP. Selection DSPs serve as decision models for selecting between design alternatives. The cDSP provides a mean for solving multi-objective and non-linear design problems [24]. Mathematically, the cDSP is a domain-independent, multi-objective decision model which is a hybrid formulation based on Mathematical Programming and Goal Programming [25]. It is used to determine the values of the design variables, which satisfy a set of constraints and bounds while achieving as closely as possible a set of conflicting goals. Since an important aspect of design is to model and handle multiple trade-offs simultaneously; the compromise DSP is used to model such decisions [26]. The mathematical formulation of the cDSP is shown in Figure 1.21. The word formulation of the cDSP is as follows [27]:

Given: A feasible alternative, assumptions, parameter values and goals

Find: Values of independent system variables (they describe the physical attributes of an artifact) and deviation variables (they indicate the extent to which the goals are achieved.)

Satisfy System constraints, system goals, and bounds on variables

Minimize: Deviation function that measures the deviation of the system performance from that implied by the set of goals and their associated priority levels or relative weights.

GIVEN

An alternative to be improved through modification
Assumptions used to model the domain of interest
Tbe system parameters:

n	number of system variables
p+q	number of system constraints
p	equality constraints
q	inequality constraints
m	number of system goals

$C_l(\mathbf{X})$ Capability of the system
$D_l(\mathbf{X})$ Demand to the system
$g_l(\mathbf{X})$ System constraint function

$$g_l(\mathbf{X}) = C_l(\mathbf{X}) - D_l(\mathbf{X})$$

$f_k(d_l^+, d_l^-)$ Function of deviation variables to be minimized at priority level k the preemptive case

FIND

X_i	System Variables	i = 1,..., n
d_l^+, d_l^-	Deviation Variables	i = 1,..., m

SATISFY

System Constraints (linear, nonlinear)

$g_l(\mathbf{X}) = 0$	i = 1,..., p
$g_l(\mathbf{X}) \geq 0$	i = p+1,..., p+q

System Goals (linear, nonlinear)

$A_i(X) + d_i^- - d_i^+ = G_i$	i = 1,..., m

Bounds

$X_{i,\min} \leq X_i \leq X_{i,\max}$	i = 1,..., n
$d_i^+, d_i^- \geq 0$	i = 1,..., m
$d_i^+ \cdot d_i^- = 0$	i = 1,..., m

MINIMIZE

Deviation function: Archimedean formulation

$$Z = \sum_i W_i (d_i^+, d_i^-) \qquad i = 1,..., m$$

Figure 1.21: Mathematical formulation of cDSP[25]

The system descriptors (system and deviation variables, system constraints, system goals, bounds, and the deviation function) are described in detail by Mistree, Hughes and Bras [25] and are not repeated here. In the compromise DSP, each goal has two associated deviation variables d_i^- and d_i^+ that indicate the extent of the deviation from the target. The deviation variables represent the levels of overachievement and underachievement, respectively, of a goal. The product constraint $d_i^- \cdot d_i^+ = 0$ ensures that at least one of the deviation variables for a particular goal is always zero. The goals may not be equally important. In order to affect a solution on the basis of preference, the goals may be rank-ordered into priority levels. The designers rate certain product qualities higher or lower than other qualities. There are two types of deviation function that can be used in formulating a compromise DSP: the Archimedean solution scheme and the Preemptive approach. In this thesis, the Archimedean approach is used. In the Archimedean approach, the deviation function, Z, is simply a weighted sum of the deviation variables of each of the objectives. In a compromise DSP, the bounds and constraints form the feasible design space. The solution of the compromise DSP is a point selected within the feasible design space based on its degree of satisfaction to a set of conflicting design goals. Satisfaction is evaluated using the value of the deviation function in the compromise DSP. The above two sections lay the groundwork to what follows in the remaining chapters. The organization of work and its validation is described in the next section.

1.3. Validation and Organization of Work

In this section, an overview of the thesis is presented. The reader is also made aware of the running icon that is presented at the end of each chapter. A roadmap is presented and related to the running icon. The reader is presented with another tool to help with his/her navigation through my work. This section is tied to the entire work because it provides the reader with the overall picture of what will be discussed and how it will be presented. Section 1.3.1 has been leveraged from Rippel's thesis[23]

1.3.1. Validation and Verification

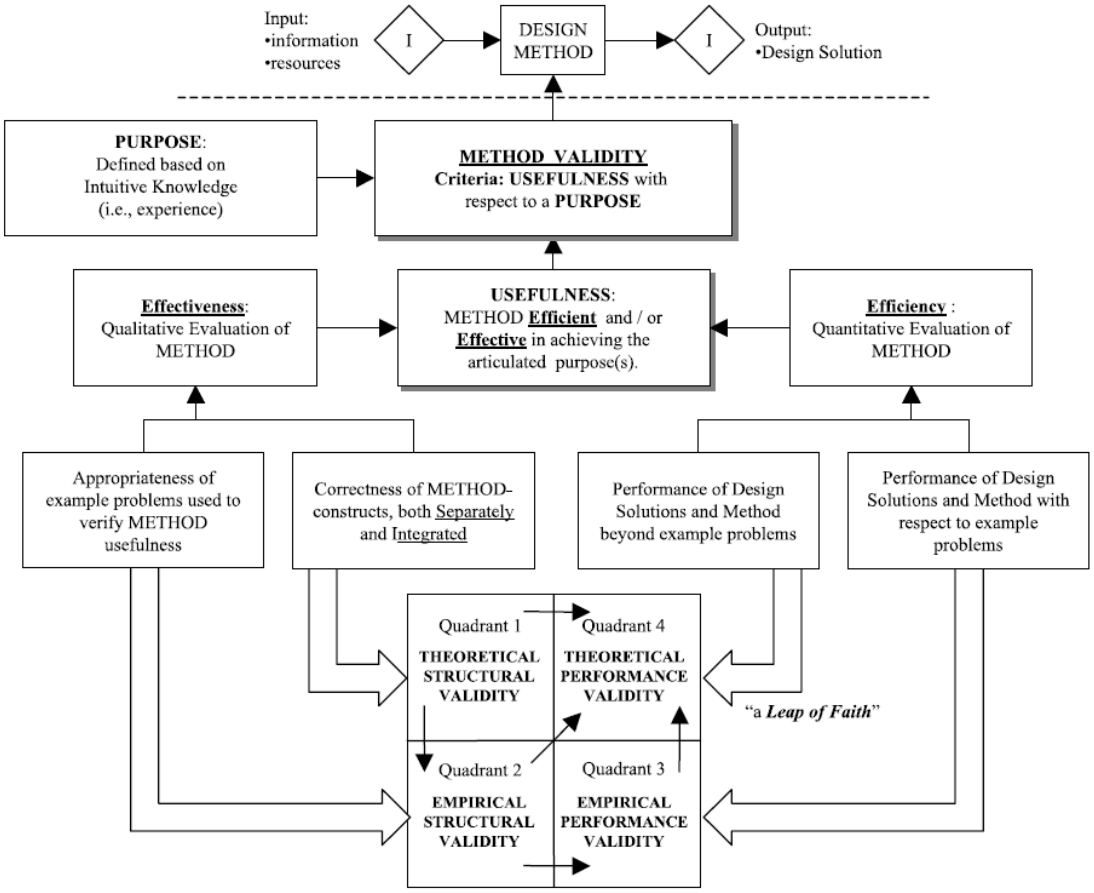

Figure 1.22: The validation square approach [23]

The validation and verification strategy for this thesis is based on the validation square, which was introduced for the validation of design methods[28]. Typically, engineering research is based on formal, quantitative validation through logical induction and/or deduction. However, this approach is problematic for the validation of engineering design methods. As soon as a method is not solely based on mathematical modeling but also on subjective statements, an alternative to logical induction and/or deduction is needed. With the validation square, an approach to the validation of engineering design methods is proposed, which is based on a relativistic notion of epistemology in which "knowledge validation becomes a process of building confidence in its

usefulness with respect to a purpose." The validation square is a framework for validating design methods in which the 'usefulness' of a design method is associated with whether the method provides design solutions correctly (structural validity) and whether it provides correct design solutions (performance validity). This process is illustrated in Figure 1.22. Structural and performance validities are further divided into theoretical and empirical validity which lead to the four quadrants:

Quadrant 1: Theoretical Structural Validity

Theoretical structural validity involves showing the internal consistency of the individual constructs constituting the method as well as showing the overall internal consistency of their assembly. This can be achieved by searching and referencing to literature related to the single constructs, which are already validated elsewhere. Furthermore, the correctness of the information flow throughout the entire design method has to be demonstrated. For this step a flow chart may be useful.

Quadrant 2: Empirical Structural Validity

Empirical structural validity involves building confidence in the appropriateness of the chosen example problems for illustrating and verifying the performance of the developed design method. This means, it has to be shown that the examples are good representations of design problems, for which the method is designed and that the associated data can be used to support a conclusion.

Quadrant 3: Empirical Performance Validity

Empirical performance validity includes showing the usefulness of the method for solving the example problems. The results achieved using the design method have to be analyzed and assessed. Measurements of the usefulness should be related to the desired specifications, which are formulated in the requirements list. Furthermore it has to be shown that the achieved usefulness is, in fact, a result of applying the developed method, for example by comparing the generated outcomes to solutions acquired without the method. The analysis should also include assessment of data with regard to internal consistency, for example multiple starting points and convergence in optimization exercises.

Quadrant 4: Theoretical Performance Validity

Theoretical performance validity involves a "leap of faith" from the usefulness of the design method for the chosen example problems to the general validity of the method, which means building confidence in the generality of the method and accepting that the method is useful beyond the example problems. This can be supported by showing that the example problems are representative for a general class of engineering design problems as well as a final critical analysis of the entire validation process.

Implementation of the Validation Framework in this Thesis

The validation square is a framework that suggests a logical step by step approach for the validation of a design method. Successfully building confidence for the validities in quadrants one, two, and three followed by a critical analysis allows for the "leap of faith" in quadrant four. This "leap of faith" to the general validity of the developed method is characteristic for the validation of design methods that include subjective assumptions. Since this is the case for the methods presented in this thesis, the validation square is an appropriate framework for the validation and verification of the presented work. In Table 1.3, the outline of the validation strategy is presented with regard to the four quadrants of the validation square. The tasks for each step are given with reference to the chapter in which they are addressed. Figure 1.23 captures the flow of information. The quadrants and the chapters for the validation square do not follow a sequential numbering, i.e., Quadrant 1 is addressed in Chapter 1 and we revisit Quadrant 1 after clarifying Quadrant 2. This is done because the work in this thesis followed a sequential approach and the initial work led to further research questions and hypothesis. Hence the study of robust design of multiscale systems taken up in Chapters 2 and 3 led to further refinement of the initial questions and were restated. The work in Chapters 2 and 3 can be associated with Quadrant 3 as it achieves a set of results with an independent set of conclusions, however has been put in Quadrant 2 as it essentially clarifies the foundational constructs on which the subsequent Chapters 5 and 6 are built. Chapter 7 is the Closure and ties to Quadrant 4 in helping up take the leap of faith and apply it to any generic multiscale system. The elements of the validation square will become clearer as we move through the chapters of

my thesis. Figure 1.23 will be used for describing the validation approach at the end of each chapter of this thesis. As seen in Figure 1.23, Chapter 1 ties with motivation for this thesis and introduction of key constructs used in the remainder of the thesis and falls in Quadrant I, i.e., theoretical structural validity. Figure 1.24, shows the organization of work in this thesis.

Table 1.3: The validation approach

Quadrant 1: Theoretical Structural Validation	
• Critical review of literature relating to the components that are foundational for the methods proposed in this thesis. • What are the characteristics, limitations and domains of application of the building blocks? Are the underlying assumptions compatible? How do the individual components relate to the research questions and hypotheses?	Chapters 1 and 4
Quadrant 2: Empirical Structural Validation	
• Presentation and discussion of the current methods and relating it to the research questions and hypotheses. • Discussion of the appropriateness of the example problem • Argue that the example is representative for engineering design problems in the domain the methods are designed for. • Document that the method theoretically is applicable to the example. • Show that the expected data and results can support a conclusion whether the hypotheses are valid or not.	Chapters 2 and 3
Quadrant 3: Empirical Performance Validation	
• Building confidence in the utility of the proposed methods using the example • Demonstrate that the method is working as designed (converges, makes compromises, results in robust points)	Chapters 5 and 6
Quadrant 4: Theoretical Performance Validation	
• Building confidence in the general applicability of the methods beyond the example used in this thesis.	Chapter 7

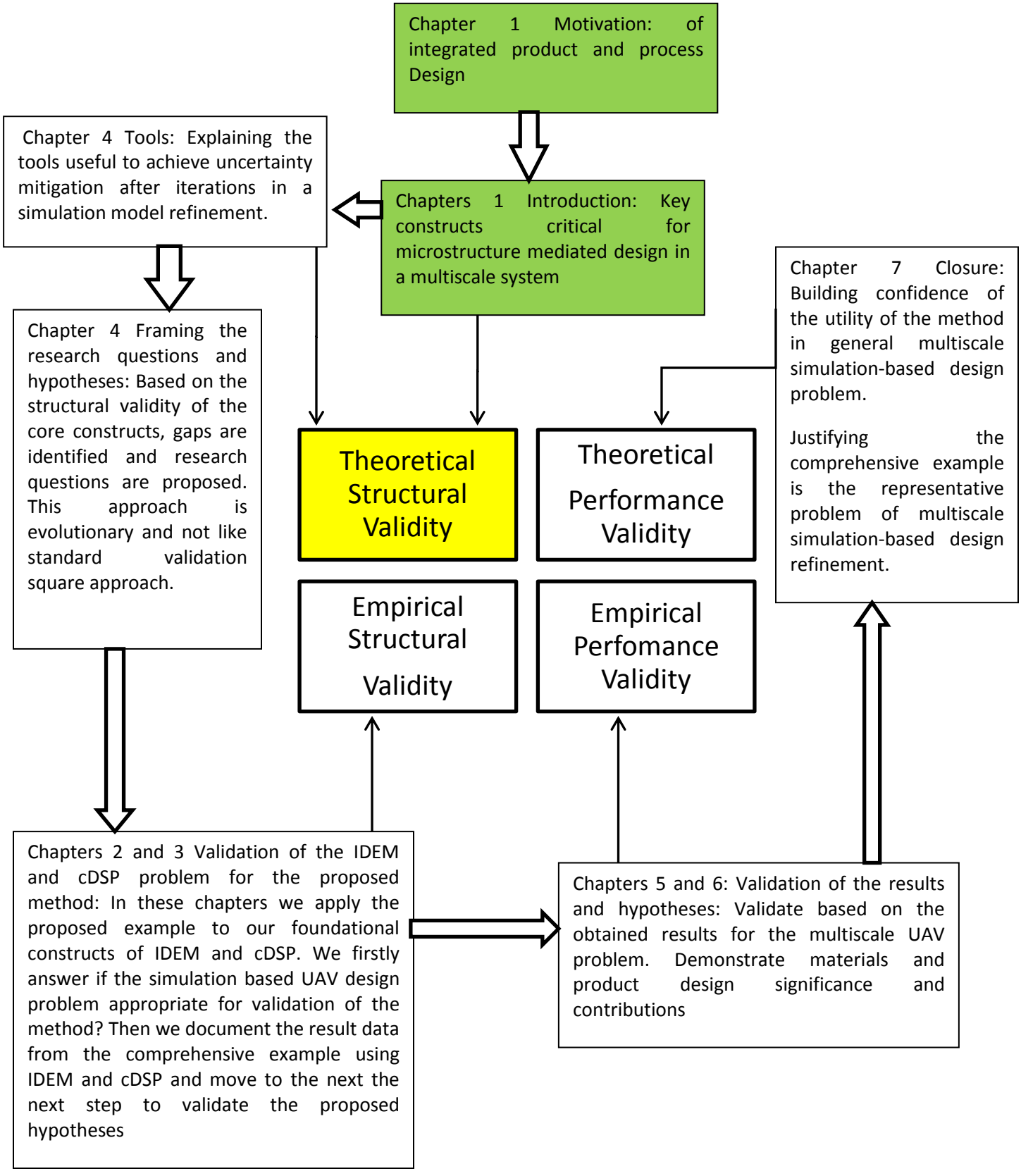

Figure 1.23: The validation square and flow of information

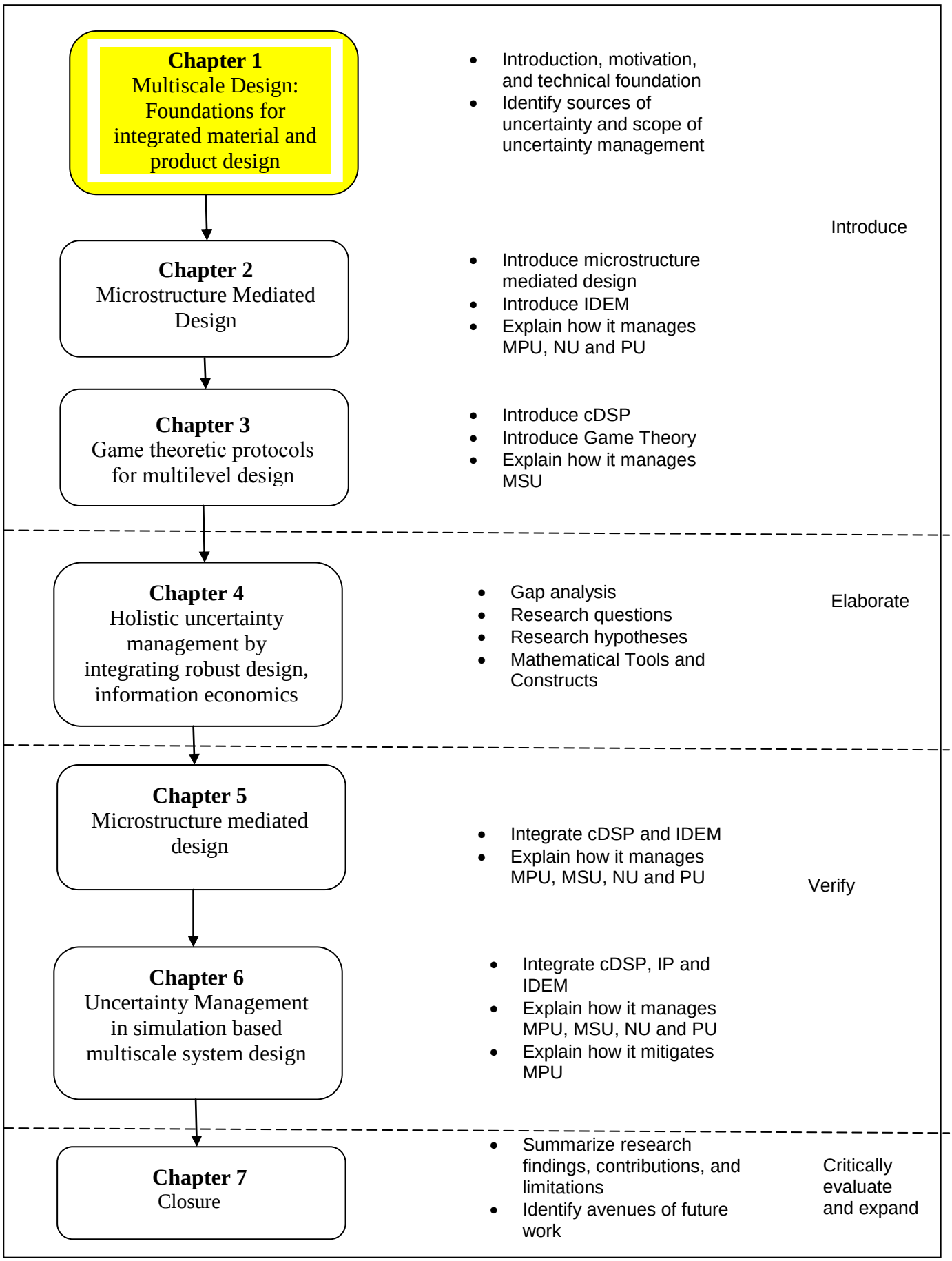

Figure 1.24: Organization of Work

1.3.2. Organization of Work

As explained in the introduction of this chapter, this research work stems from four research article developed during the course of my MS study. Hence the chapters are organized chronologically in the sequence of their development. The organization of work is represented in Figure 1.24.

In **Chapter 1**, the foundation for the thesis is laid with a clear description of multiscale systems, the challenges associated with design of multiscale systems and the notion of multilevel design. Uncertainty is classified and two approaches for managing uncertainty are identified, i.e., robust design and uncertainty mitigation. The core constructs of inductive design exploration method (IDEM) and cDSP are also described in detail which lay the groundwork for the study in Chapters 2 and 3. The validation square approach is discussed to validate and verify the work presented in the thesis.

In **Chapter 2**, the construct of microstructure mediated design is introduced and a sample example of autonomous underwater vehicle (AUV) is modeled for the process-structure-property-performance relationships. The IDEM introduced in Chapter 1 is validated by applying it to AUV and benefits of IDEM for design of multiscale systems are instantiated. This article was presented in the proceedings of ASME, IDETC 2009 conference at San Diego, USA [29]

In **Chapter 3**, game theoretic constructs are used for reaching singular solution or multilevel design. This chapter establishes the groundwork for using cDSP in conjunction with IDEM which identifies ranged sets of solution to identify a single solution from these ranged sets of solution. It also illustrates the efficacy of using cDSP template to reach solution in a collaborative design environment. This study was presented in the proceedings of ASME, IDETC conference ASME, IDETC 2010 conference at Montreal, Canada[28]

In **Chapter 4,** the limitations of the current IDEM are identified and research questions are proposed along with hypotheses to answer them. The crucial limitation of existing multilevel

design methods to reduce uncertainty is identified and tools to overcome this barrier are reviewed which include response surface modeling, design of experiments and value of information.

In **Chapter 5,** the advantages of IDEM and cDSP are unified to get an integrated approach to identify ranged as well as a single solution for multilevel design. We use the microstructure mediated design approach to identify the sources of uncertainty in multiscale modeling and investigate how the cDSP assists IDEM to manage uncertainty by reaching a trade-off amongst the HD-EMI metrics which act as decision nodes for uncertainty management. The results from this chapter are under review to be published in the Journal of Computer Aided Design- Special issue on Multiscale Systems

In **Chapter 6,** an algorithm is developed to assist uncertainty mitigation in multiscale systems and is applied to the MMD construct. Robust design and concepts from information economics are combined to adaptively reach better solutions based on available computational resources. The benefits of using this approach are summarized. . The results from this chapter are under review to be published in the Journal of Mechanical Design- Special issue on Design of Complex Systems

In **Chapter 7**, the thesis is summarized and the research questions are answered by discussing the validity of the hypotheses introduced in Chapter 4. Furthermore, the work is critically reviewed and the contributions are identified. Hereby, emphasis is placed on the underlying assumptions and conditions under which the proposed methods work. For the theoretical performance validation, it is argued that the methods presented in this thesis as well as the conclusions are relevant and valid beyond the AUV problems. Finally, potential future research topics are identified that could enhance the proposed methods and make them more efficient and ideas for holistic uncertainty management are proposed

CHAPTER 2

MICROSTRUCTURE MEDIATED DESIGN

In this chapter, the construct of microstructure-mediated design of material and product is introduced. The microstructure of the material is controlled within feasible bounds to achieve the performance targets of the product. The efficacy of this construct is illustrated via the integrated robust design of submersible and Al-based matrix composites. The integrated design is carried out using an Inductive Design Exploration Method (IDEM) that facilitates robust design in the presence of model structure uncertainty (MSU). Model structural uncertainty (MSU) as described in Chapter 1, originating from assumptions and idealizations in modeling processes, is a form of uncertainty that is often virtually impossible to quantify. In this chapter the Inductive Design Exploration Method (IDEM) introduced in Chapter 1 is demonstrated that facilitates robust design in the presence of model structural uncertainty. Robustness is achieved by trading off the degree of system performance and the degree of reliability based on structural uncertainty associated with system models (i.e., models for performances and constraints). IDEM is demonstrated in the design of a shell of a robotic submersible. The material considered is *in-situ* Al metal matrix composites (MMCs) due to the advantages that the *in-situ* MMCs have over the conventional MMCs. This design task is a representative example of integrated materials and product design problems. The study in this chapter was presented at the proceedings of IDETC 2009, San Diego[30]. The microstructure mediated design approach lays the foundation for a refined algorithm in Chapter 5.

2.1. Framing the Problem

Traditionally materials are selected from databases of experimentally determined materials properties. However, the paradigm is shifting towards the concurrent design of materials and products. This entails tailoring materials for specific performance required in specific products or processes. In order to tailor materials, the approach taken by materials scientists is sequential deductive analysis, with a bottom-up mapping from processing path to nano- and micro-structure, material properties and performance. This corresponds to Olson's materials design hierarchy [4] shown in Figure 2.1 and described in Section 1.1.

The microstructure of a material strongly influences physical, mechanical and chemical properties such as strength, toughness, ductility, corrosion resistance, high/low temperature behavior, etc., which in turn govern the application of these materials. The microstructure represents the interface between structure-property-performance relations including systems design and process-structure relations. A microstructure-mediated design-centered approach has been adopted for concurrent design of materials and product.

A systems-based approach has been adopted. This combines inductive (top-down) engineering with deductive (bottom-up) science; see Figure 2.1. Fundamental to this design approach is an interconnected system of modules (a design process chain) expressed in terms of variables, constraints, and models that embed relevant aspects of the material microstructures through overall system configuration. In this chapter, the method is illustrated through the design of the shell and design of the material from which the shell of a submersible is made. The shell is characterized by both geometrical and material features; see Figure 2.2 [31]. The objective is to design the shell of a robotic submersible for deep sea exploration with the multifunctional requirements of minimizing the mass in walls (wall thickness) for given support superstructure for given maximum depth and associated pressure differential. Other design requirements include a) suitable factor of safety with respect to collapse at target maximum operating depth, b) a large endurance time satisfying the time of operation constraints under water without

resurfacing/refueling/battery changes, c) satisfying geometric and weight constraints. The preferred design must have a) high strength to weight ratio and b) resistance against environmental factors such as corrosion. Recent advances in material processing allow designing the material to attain specific desired properties.

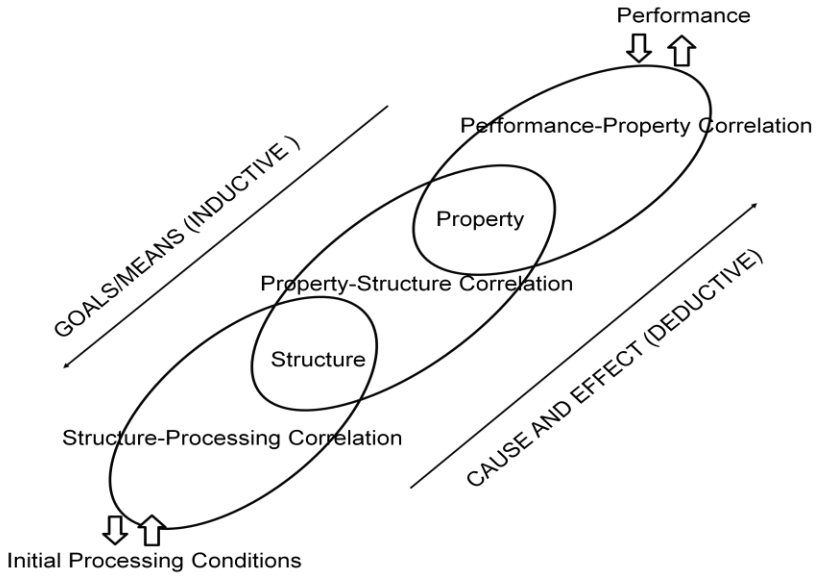

Figure 2.1: Hierarchical materials design [4]

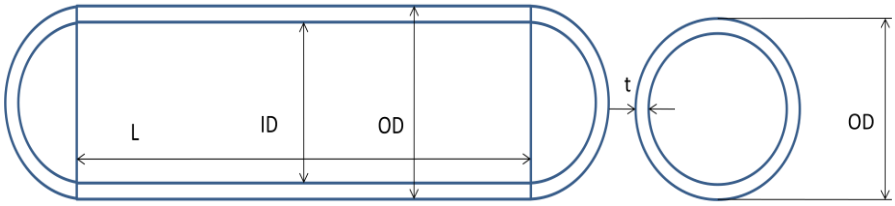

Figure 2.2: Pressure shell of a submersible robot

Al-based metal matrix composite is used to illustrate the proposed method. Metal matrix composites (MMCs), in general, and Al-based MMCs in particular, have been the subject of intense research for the past two to three decades and are being exploited for a range of commercial applications related to aerospace and automotive industries. Al-based metal matrix composites can be divided into two classes, namely, ex-situ and in-situ. In ex-situ composites the reinforcements are added externally [32] whereas in in-situ composites the reinforcing particulates are formed by chemical reaction within the liquid melt. One of the important drawbacks during the processing of ex-situ MMCs is the presence of interfacial impurities and

oxides between reinforcement and matrix resulting in poor wettability and bonding. This has led to the development of in-situ composites, wherein the reinforcements are generated in a metallic matrix via chemical reactions between elements and/or compounds with Al alloy melt during the composite fabrication. The advantages that in-situ MMCs have over conventional MMCs include thermodynamically stable reinforcements in the matrix, clean reinforcement-matrix interfaces resulting in a strong interfacial bonding, finer particle size yielding better mechanical properties and potential for lower cost of production. These advantages make them a strong candidate for the design task at hand. On the other hand, the reinforcement particles in in-situ composites are subject to strong segregation effects and therefore post solidification process strategies are necessary to more uniformly mix the particles.

2.2. Microstructure-Mediated Design

The design approach is based on systems-based integrated top-down (inductive) and bottom-up (deductive) multilevel design as illustrated in Figure 2.3. Multilevel design for the shell design problem involves two activities, namely, process path - structure relationships and structure-property-performance relationships. These two design objectives interact via the microstructure. While on one hand the processing conditions influence the obtained microstructure, the performance of the product depends on the mechanical properties which in-turn are mapped from the microstructure.

In the present study, two major aspects of the design problem, namely, the materials design (rather than just materials selection) and structural design, are combined. The materials design aspect has been divided into three parts based on the different processing steps of the material. The interface between materials design and structural design is the mapping of the processed microstructure to the required mechanical properties.

The Inductive Design Exploration Method (IDEM) is used to effect solution. The design process chain for this application constitutes of six interconnected modules, Figure 2.4. Five modules

account for the modeling of the behavior of the material and the structure. The sixth is used to address uncertainty embodied in the simulation models, the management of uncertainty propagation and tools for design exploration in the presence of propagated uncertainty in the design process chain.

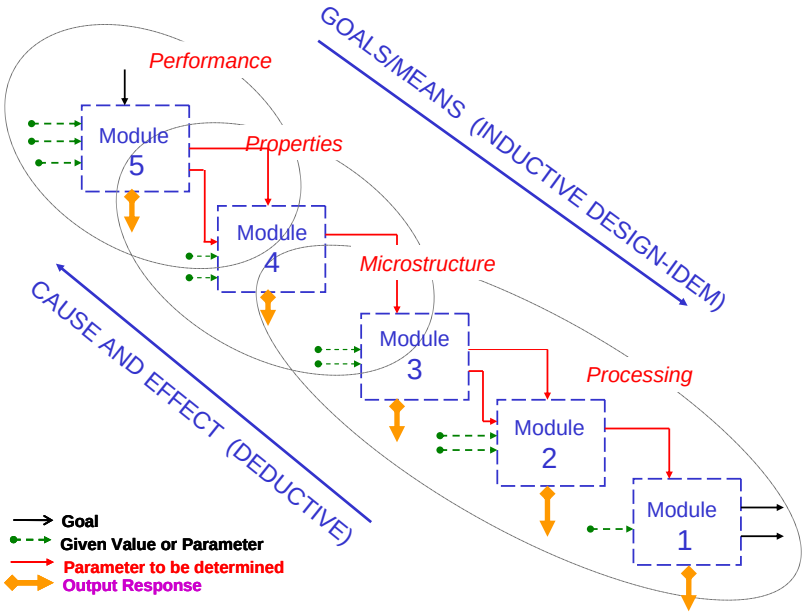

Figure 2.3: Microstructure mediated design of material and structure

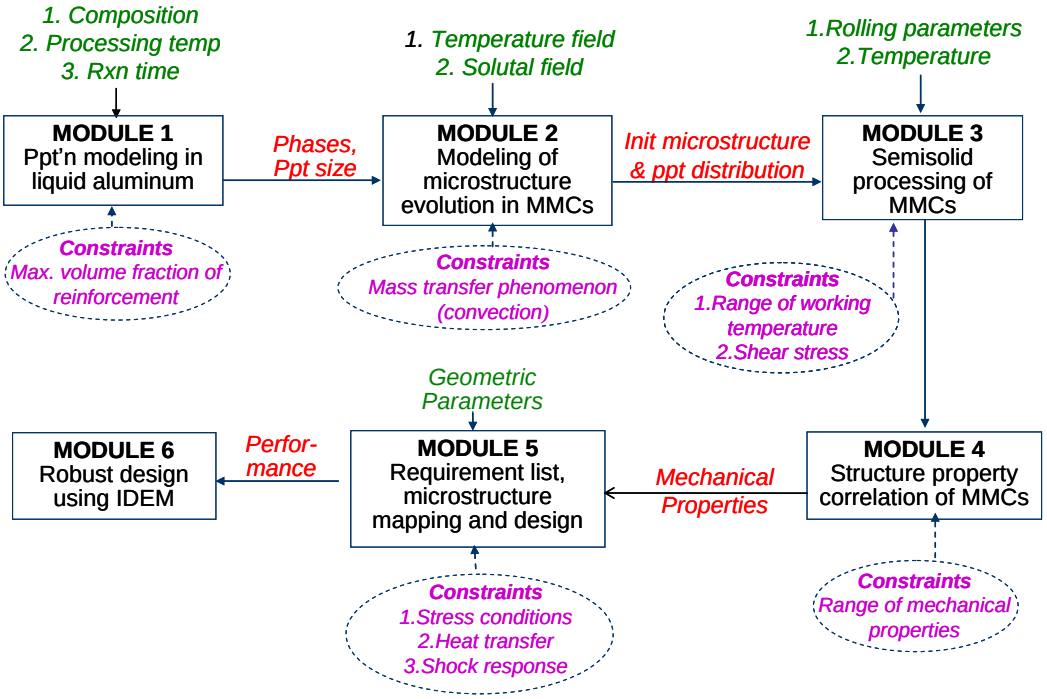

Figure 2.4: Analysis diagram

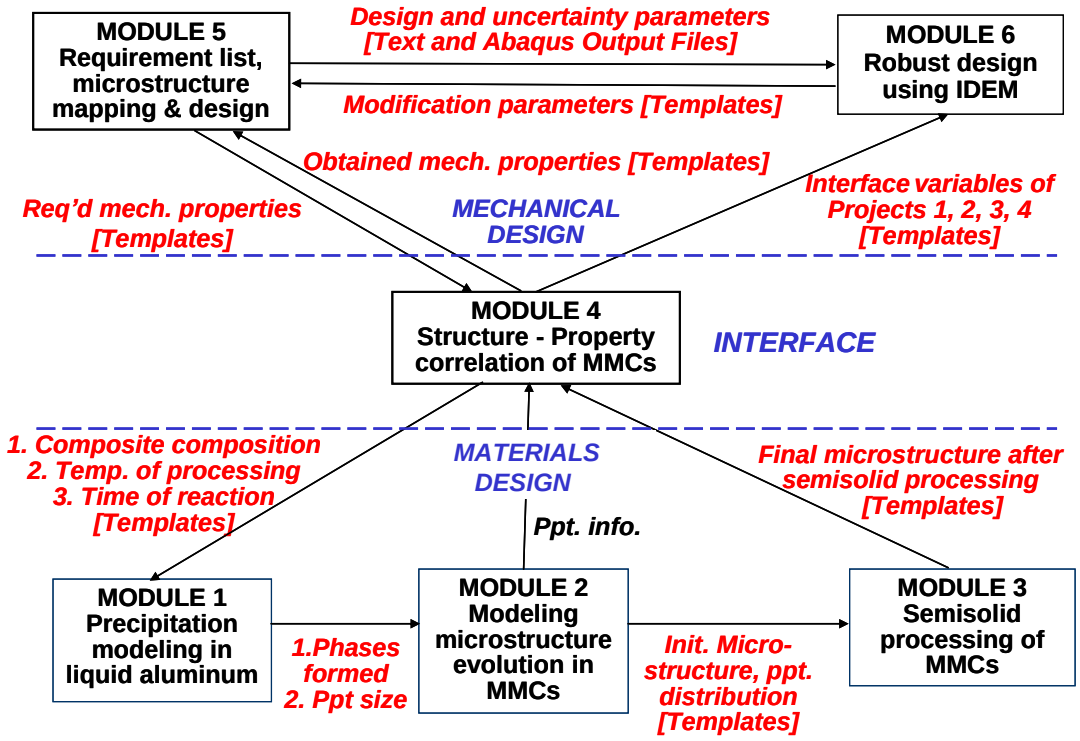

Figure 2.5: Interface diagram

Based on the materials processing steps involved and mechanical design requirements, the interconnected modules that constitute the design process chain for this application are (see Figure 2.3):

MODULE 1: Precipitation modeling in liquid Al.

MODULE 2: Modeling of microstructure evolution in MMCs.

MODULE 3: Evolution of microstructure during semisolid processing of MMCs.

MODULE 4: Structure - property correlations of MMCs.

MODULE 5: Requirement list, microstructure mapping and system-level design.

MODULE 6: Robust design strategy using IDEM to address model structure uncertainty and propagated uncertainty among levels of models.

MODULEs 1, 2 and 3 provide the simulated microstructure after processing. The resulting mechanical properties are estimated in MODULE 4, whereas MODULE 5 maps the required mechanical properties based on the system design considerations.

Given the complexity inherent in the design process chain, it is important to define the variables, the interface and the design constraints between the different modules. In Figures 4, 5 and 6 the analysis is shown, interface and the respective integrated flow diagrams for this design process chain. In the analysis diagram [Figure 2.4] the various independent and dependent variables in the six modules of the design process chain are shown along with the representative modeling constraints. In the interface diagram [Figure 2.5] the connectivity and flow of information between the modules is mapped in the form of design template.

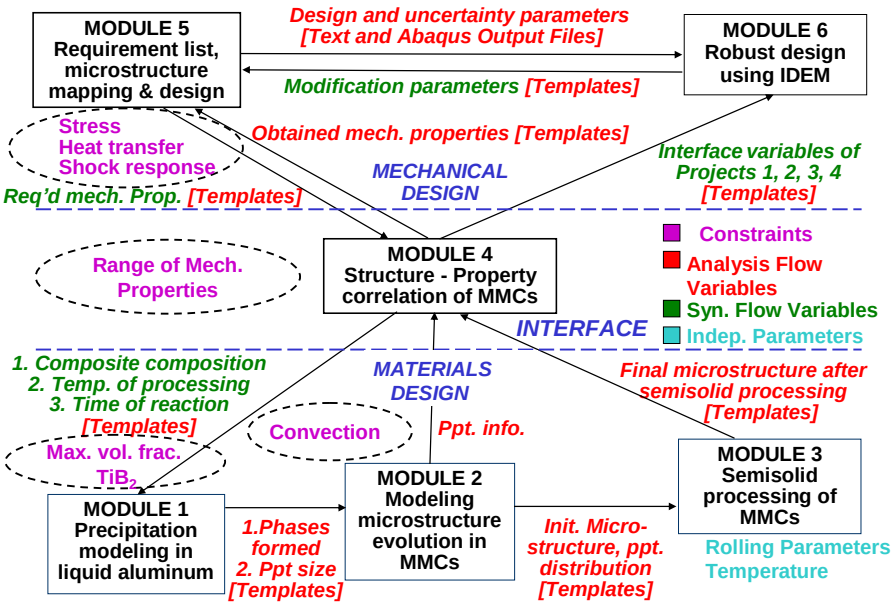

Figure 2.6 Integrated Flow Diagram

MODULE 1 involves the prediction of the precipitation of liquid aluminum based on the composition and processing temperature. The output of MODULE 1 is the information about different phases formed, the size of precipitates and the time required to complete the reaction. This information is used in MODULE 2, which embodies the process of microstructure evolution

and the effect of temperature and solutal fields on the resulting microstructure. The next step is the semi-solid processing of the Al-MMCs through a rolling operation which modifies the material's microstructure. In MODULE 3 the effect of the rolling parameters on the resulting microstructure is predicted. In MODULE 4, this microstructure is used to predict the mechanical properties inherent in the material. These mechanical properties are used in the system-level MODULE 5 to predict the effects of different AUV geometries on overall system performance. As can be seen from the integrated flow diagram [Figure 2.6], the microstructure is the essential link between the design of the material and the design of the undersea submersible appearing the process-structure and structure-property mappings.

In this application, the strength is principally determined by the sizes, shapes and distribution of TiB2 precipitates – in other words the microstructure of the material. The microstructure is determined by processing methods – in this case, it is initially created by precipitation and followed by the evolution of the precipitate size and distribution during semi-solid rolling. The structural design can be modified in two ways, namely, 1) by changing the processing conditions to modify the microstructure, which has an effect on the overall system performance and 2) by changing the geometry of the shell, which in turn not only affects structural performance, but also puts constraints on required mechanical properties of the material. Hence, the material microstructure needs to be designed in such a way that the constraints on the material properties, imposed by the structure, are satisfied. Since the material microstructure acts as the interface between the material and structure, the phrase *microstructure mediated design* has been adopted. Having defined the design variables and the connectivity within the design process chain, the modules described in the sections that follow.

2.2.1 MODULE 1 (Precipitate Modelling in Liquid Aluminium)

A suitable route (Mixed-Salt route) for the in situ Al / TiB_2 composite manufacturing process utilizes the reduction of K_2TiF_6 and KBF_4 with aluminum, generally known as the "halide salt"

process. Yang and coauthors [33] proposed a diffusion mechanism wherein Al_3Ti is formed in the melt initially by a very fast reaction. Boron then diffuses into Al_3Ti particles in the melt, thus forming TiB_2 particles according to the reaction, $Al_3Ti + 2B = 3Al + TiB_2$.

The liquid-state processing techniques to produce in-situ composites include self propagating high temperature synthesis (SHS), exothermic dispersion (XD), reactive hot pressing (RHP), flux assisted synthesis (FAS) and rapid solidification processing (RSP). Any of these processes could be used. K_2TiF_6 and KBF_4 are other precursors that dissolve in the aluminum melt to form intermediate phases Al_3Ti and AlB_2. The reaction between these intermediate phases has been studied to predict the particle size distribution of TiB_2 phase thus formed in the matrix.

A model proposed by Anestiev and coauthors [34] has been used to investigate the diffusion reactions taking place between the intermediate phases. In this model, Al_3Ti and AlB_2 are allowed to react in liquid Al to form TiB_2 particulates. A coordinate system dividing a 2-dimensional space into strips of equal length has been used, half of which contains Al_3Ti and the other half AlB_2 dissolved in the Al melt, shown in Figure 2.7. When these intermediate phases react, random nucleation of TiB_2 particulates is assumed. The kinetics of the formation of TiB_2 particles is governed by unsteady state diffusion equations (solute redistribution theory), which in turn depends on the concentration profile of the intermediate solute phases in the region. The solute consumption rate due to TiB_2 formation is described by volume fraction of the region transformed per unit time. Johnson-Mehl-Avrami analysis[35,36] is used to find the transformed volume fraction from the nucleation and growth rates of the particles as: $\psi = 1 - \exp(-ktn)$ where ψ is is the volume fraction transformed, $k = N G^3/3$ and $n = 4$, N and G are Nucleation and Growth Rate respectively.

The Nucleation rate is primarily a function of the Gibbs energy change associated with the formation of the particle, while the growth rate also depends on its surface energy. The thermodynamic models predicting the Gibbs free energies of the involved phases in the current system are described in Mirkovic et al.[37], Witusiewicz and colleagues[38,39]. The kinetics of

reinforcement particles can be mathematically described by the following set of partial differential equations:

$$\partial X_1/\partial t = D\,(\partial^2 X_1/\partial x^2) - X^1_S\,(\partial \psi/\partial t) \quad (2.1)$$

$$\partial X_2/\partial t = D\,(\partial^2 X_2/\partial x^2) - X^2_S\,(\partial \psi/\partial t) \quad (2.2)$$

where, X_1 and X_2 are the mol fractions of the dissolved Ti and B in the Al matrix respectively, t is the time, D is the diffusion coefficient, X^1_S and X^2_S are the mole fractions of Ti and B in the solid phase (TiB_2). The complex diffusion equations are solved numerically to compute the TiB_2 particle size distribution across the matrix.

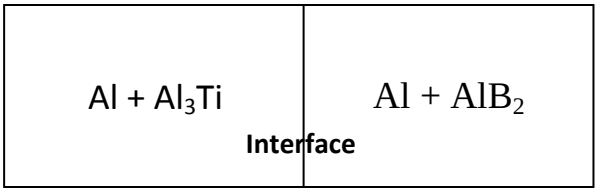

Figure 2.7 Schematic of coordinate system used in MODULE 1

2.2.2 MODULE 2 (Modelling Microstructure Evolution)

Microstructural evolution of materials during various material processes relates key properties such as mechanical strength and electrical properties to the average grain size and the grain size distribution, which are direct consequences of the microstructure evolution. In MODULE 2, microstructure evolution during solidification depends on the thermal and the solutal fields.

The S/L interface evolves in time and has to be found as part of solution. The solidification of a three component alloy is governed by the evolution of temperature T(t, x, y) and concentration field C^{α} (t, x, y) ,where α= 1,2 which satisfies several boundary conditions at the moving S/L interface as well as the initial and the boundary conditions. The equations that describe the physics of solidification process follow. Temperature T in Ω (heat transfer equation):

$$\rho C_p (\partial T/\partial t) = K\Delta T + \rho L(\partial f_s/\partial t) \quad (2.3)$$

Where t is time, (x, y) is the domain co-ordinates, ρ is the density, C_p is the specific heat, *K* is the thermal conductivity, *L* is the latent heat of solidification and f_s is solid fraction. For simplicity the notation $f_L = 1 - f_s$, denotes the liquid fraction. The concentration (C) for the solute (solute diffusion equation)

$$\partial C_L^{\alpha}/\partial t = D_L^{\alpha} \Delta C_L^{\alpha} \quad \text{……For liquid phase} \quad (2.4)$$

$$\partial C_S^{\alpha}/\partial t = D_S^{\alpha} \Delta C_S^{\alpha} \quad \text{…….For solid phase} \quad (2.5)$$

where α = 1,2, D_L^{α} and D_S^{α} are liquid and solid diffusion coefficients of solute α, respectively. The cross diffusion is neglected and zero flux boundary conditions are applied to the four walls of simulation domain Ω.

Fluid flow due to forced or natural convection also influences the microstructure evolution. The present module involves the numerical solution of continuum equations for thermal fields and coupling it with a cellular automata model that computes the evolution of grain structure with solidification time. The measured flux values are used to derive the evolution of the thermal fields with solidification time. Using measured temperature values at the specific points along the metal-mold interface, realistic flux values at the metal-mold interface can be derived which can be fed into a Computation Fluid Dynamics (CFD) modeling tool to obtain accurate thermal fields across the casting domain. These fields are used in the cellular automata model to predict the microstructure evolution as the solidification proceeds.

2.2.3 MODULE 3 (Semi-solid Processing in MMCs)

The present module deals with the simulation of the semi-solid processing of metal matrix composites. The actual process[40,41] consists of passing slabs of as-cast composite material through rollers [Figure 2.8] at such a temperature that part of it is in semi-solid or “mushy” state. Two-high mill rollers of diameter 120 mm and 125 mm barrel width are used in this

process. The sample is heated to temperatures between 610 to 633° C to obtain 10 to 30% liquid in the material. When the slab is passed through the rollers, the grains deform and rearrange and a nearly homogeneous distribution of TiB_2 particles is obtained. Multiple passes are performed to refine the grain size. Such a process enhances the properties of the MMC and homogenizes its composition.

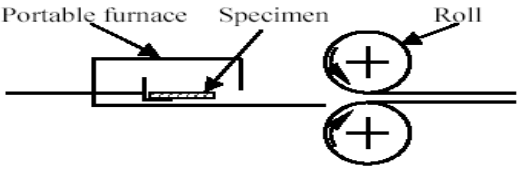

Figure 2.8: Schematic of semi-solid processing

Since this is a novel process and its physics are not yet fully understood, an empirical model is used, based on data taken from a large number of experiments. The model takes as input the processing conditions of semi-solid processing, including ratio, and then predicts the final average grain size and also gives an approximate microstructure. To predict the final grain size it takes in the experimental details and interpolates the grain size. After processing, the TiB_2 particulates rearrange themselves to achieve a more uniform spatial distribution, which is also reflected in the model. Using a genetic algorithm based Voronoi and Monte Carlo code [42], equiaxed globular grains are created. It forms in 100 x 100 matrix grains differentiated by different color codes which can be then be interpreted to render the final microstructure after semi-solid processing.

2.2.4 Module 4 (Structure-Property Correlation of MMCs)

Yield Stress: The matrix yield stress is assumed to obey the Hall-Petch relation, i.e.,

$$\sigma_y = \sigma_0 + k_y (d)^{-0.5} \quad (2.6)$$

where k_y is the strengthening coefficient (a constant unique to each material; for pure Al, k_y = 3.4 MPa-mm), σ_o is a material constant related to lattice resistance (for pure Al, σ_o= 2.95 MPa), d

is the grain diameter, and σ_y is the yield stress. The constants corresponding to matrix properties are assumed to be that of pure Al. The calculation of overall yield stress (σ) also incorporates Orowan particle bypass via dislocation looping [43], i.e.,

$$\sigma = \sigma_y (1 + f_1)(1 + f_2)(1 + f_{orowan}) \qquad (2.7)$$

where f_1 takes the effect of volume fraction of particles, f_2 takes into account the thermal expansion coefficient mismatch between matrix and reinforcement, and f_{orowan} takes into account the effect of particle size (d) and spacing. It receives input from outputs of MODULEs 1 and 3, specifically reinforcement size (d_p, grain size (d), semisolid processing temperature (T) and volume fraction of TiB_2 particles.

Density: The determination of density is based on the average property of each of the constituent phases, i.e.,

$$\rho = \rho_{TiB2} x_{TiB2} + \rho_{Cu} x_{Cu} + \rho_{Al} (1 - x_{TiB2} - x_{Cu}) \qquad (2.8)$$

where ρ, ρ_{TiB2}, ρ_{Cu}, ρ_{Al} are the densities of the composite, TiB_2, copper and aluminum respectively. Also, x_{TiB2} is the volume fraction of TiB_2 and x_{Cu} is the volume fraction of copper (typically 6%).

2.2.5 Module 5 (Property-Performance Correlation of MMCs)

MODULE 5 acts as an interface between the materials design aspect and the design of the structure of the submersible. The performance parameters considered are depth, time of operation and weight of the outer shell of submersible. The objective is to maximize the depth and time of operation while minimizing the weight of the outer shell of the submersible. The formulas used for the calculation of these performance parameters are stated in what follows

Model for Depth (h): Roark's formula [30] for thickness (t) to outer diameter (OD) ratio is used.

$$\frac{t}{OD} = \frac{1}{2}\left(1 - \sqrt{1 - \frac{2P}{\sigma}}\right) \qquad (2.9)$$

where t is the thickness of the shell, OD is the outer diameter of the shell; P is the external pressure and σ is the yield stress of the metal matrix composite. Substituting for P as $\rho_w gh$ where ρ_w is the density of water (1025 kg/m^3), g is the gravitational attraction (9.81 m/sec^2) and h is the depth of submersible below water. Solving for h we get [30]:

$$h = \left(\frac{\sigma}{2\rho_w g}\right)\left[1 - \left(1 - \frac{2t}{OD}\right)^2\right] \qquad (2.10)$$

Model for Weight (*W*): The weight of a cylindrical shell with spherical end caps is calculated.

$$W = \pi \rho L (OD^2 - ID^2) + (4/3) \pi \rho (OD^3 - ID^3) \qquad (2.11)$$

where ρ in eq. (2.11) is the density of the composite, L is the length of the submersible, OD is the outer diameter and ID is the inner diameter of the cylindrical shell with spherical end-caps [Figure 2.2]. The outer diameter (OD) is fixed at 260 mm and the length (L) at 1.6 meter. Thickness (t) can vary from 5 mm to 15 mm as representative parameters of a typical Autonomous Underwater Vehicle as described Kumar et al[44].

Model for Endurance Time (T_{opr})

$$T_{opr} = \frac{0.8(B - W) * eff * Energy\ Density}{FixedLoad + propulsion\ Load} \qquad (2.12)$$

where B is the buoyant weight of the submersible, W (eq.6) is the weight of the cylindrical shell, eff is the efficiency of the battery. The efficiency of a Lithium-Ion battery is typically 60% and its energy density is 128 Watt-Hour/Kg. For the initial design, assuming a slow moving submersible and submergence/surfacing rates, propulsion load is ignored in our calculations and assume a fixed electrical load of 400 Watt-Hour which is typical of the control computers and electronics payloads in a small underwater robotic submersible [31].

2.2.6 MODULE 6 (Robust Design using IDEM)

IDEM is employed to achieve a robust multi-level design that traverses process-structure, structure-property and property-performance relationships; see Figure 2.1. IDEM includes parallel discrete function evaluation and Inductive Discrete Constraints Evaluation (IDCE) based on Error Margin Indices (EMIs) for finding the best solution under MSU [1,45,46,13]. The overall procedure for the IDEM is schematically illustrated in Figure 2.9.

IDEM is exercised to identify adjustable ranges of control factor (design variable) values in a system with uncertainty propagation in a design/analyses process chain and to account for uncertainty in downstream activities and uncertainty propagation. With IDEM, a designer can maximize or maintain ranges of values for design variables or performance parameters that are shared or linked with another designer's robust design process. Thereby, design freedom is preserved for another collaborating designer who can make changes to the design—within specified ranges—without compromising design requirements.

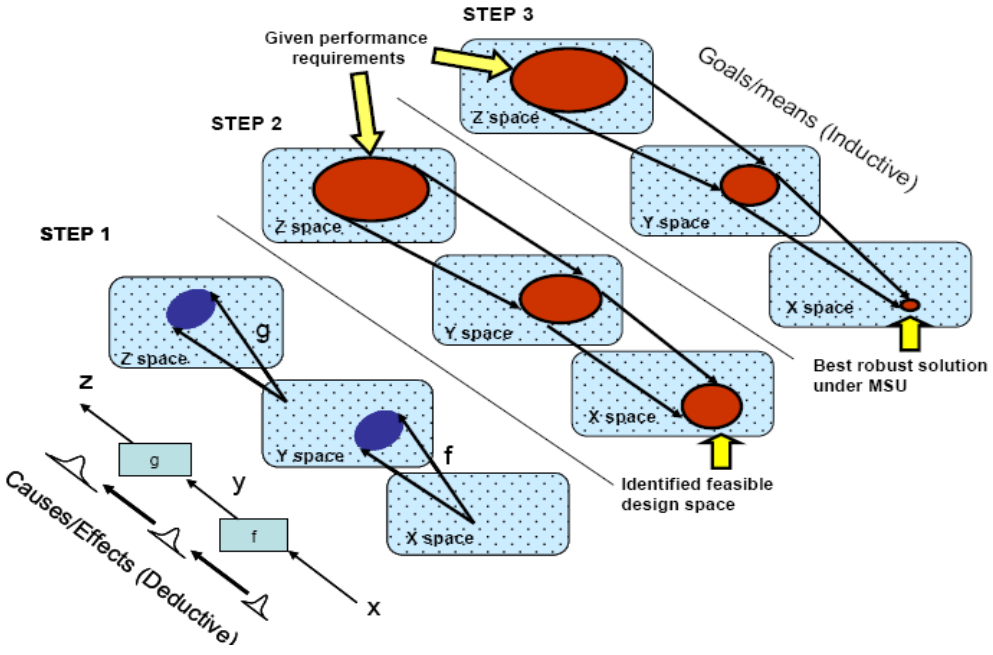

Figure 2.9 Schematic of IDEM [1]

IDEM facilitates multi-level design, the management of uncertainty inherent in the models and the propagation of uncertainty through the design process chain shown in Figure 2.4. In IDEM, we deal with the propagation of uncertainty in design and analysis modules that constitute the design process chain for a particular application. We start with performance and traverse sequentially to process; see Figure 2.1. At each level ranged set of feasible specifications are identified.

IDEM, embodies the concept of Hyper-Dimension Error Margin Indices (HD-EMIs). In this chapter however we employ the Error Margin Indices (EMIs) developed for Type III robust design. The focus of this chapter is to demonstrate the efficacy of IDEM to reach feasible sets of solution for MMD design in a multiscale environment and hence EMIs which are a simplified version of the HD-EMIs are used to affect the solution. However we use the HD-EMI metric in Chapter 5 to illustrate the full potential of IDEM and its ability to manage of all four kinds of uncertainty. EMIs are indicators of the degree of reliability of a decision that it will satisfy the prescribed system constraints or bounds. The procedure for obtaining the EMI is as follows: (a) obtain the upper and/or lower deviation of a response (URL and LRL) and (b) calculate the EMI from this deviation. The EMI is calculated by including the response mean (μ_y) and upper/lower deviations (ΔY_{upper} and ΔY_{lower}) from a combined distribution of a system model and error bounds. The EMI includes the response deviations of a system model due to variations in design variables and the response deviations of error bounds as well as the system model. The mathematical formulations of EMI corresponding to a goal *i* are:

$$EMI_i = (URL_i - f_i(x)) / \Delta Y_{upper} \quad \text{for minimization problems;} \quad (2.13a)$$

$$EMI_i = (f_i(x) - LRL_i) / \Delta Y_{lower} \quad \text{for maximization problems;} \quad (2.13b)$$

$$EMI_i = Min\{\frac{|f_i - URL_i|}{\Delta Y_i}, \frac{|f_i - LRL_i|}{\Delta Y_i}\} \quad (i = 1,2,...,Number\ of\ the\ goals) \quad (2.14)$$

$$\Delta Y_{upper} = Y_{upper} - \mu_y; \quad \Delta Y_{lower} = \mu_y - Y_{lower} \quad (2.15)$$

As shown in Figure 2.9, the objective is to find the best ranged set of design specifications in the space **x** considering uncertainty in mapping functions (*f*) and propagated uncertainty through a design process. IDEM involves finding ranged sets of design specifications by passing feasible solution spaces from performance requirements by way of an interdependent response space to the design space while preserving the feasible solution space as much as possible. The procedure includes the following steps as described in Section 1.2 [13].

- *Step 1:* Define rough design and performance spaces (hyper-dimensional **x**, **y**, and **z** spaces) and generate discrete points in each of these spaces.
- *Step 2:* Conduct parallel discrete function evaluation
  - Evaluate the generated discrete points using the *mapping models* (**f** and **g** in Figure 2.9) that include all quantified amount of uncertainty.
  - Store the evaluated data sets, including discrete input points and output ranges, in a database.
- *Step 3:* Inductive Discrete Constraints Evaluation (IDCE) process: Using information from Step 1, sequentially identify feasible regions in **y** and **x** spaces with a given initial requirement range in **z** space

As EMI increases for a particular model, the output range moves farther from the constraint boundary. This means the decision becomes more reliable under potential shift of the output range due to MSU. In the IDCE process, the specifications, the performance ranges and the initial EMI values for the discrete constraint evaluation are specified by the designer. To determine the best solution among feasible sets of solutions the required EMIs for each space should be anchored in statistics. Values of EMIs are important in determining the most desirable robust solution against model structural uncertainty, because EMIs represent the amount of margin for potential errors in the mapping models for estimating output range. A designer may leave wider margins between an output range and constraint boundaries by increasing the EMI for the mapping model whose MSU is larger than others. An additional constraint is that all EMIs should be greater than or equal to one so that the entire output range can satisfy the

constraints Depending on the value of required EMI, the identified feasible range may be large, small, or unattainable. The solution strategy for this application is outlined in the next section.

2.3. Solution Strategy using IDEM

The solution strategy for this application is illustrated in Figure 2.9. The modeling in MODULE 2 has presented many challenges and these have yet to be resolved. Hence, it is bypassed in illustrating IDEM this application.

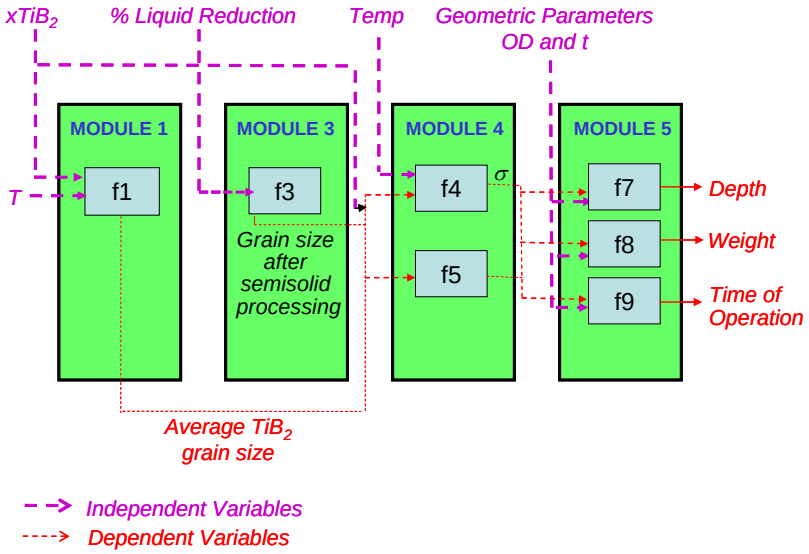

Figure 2.10: Modules used in this application

In Figure 2.10, *f1, f3, f4, f5, f7, f8 and f9* represent the theoretical or empirical models considered at the different levels of design. The inputs to MODULE 1 are the volume fraction of TiB_2 (x_{TiB2}) and temperature of processing in degree K (T).The output of MODULE 1 (*f1)* is the average TiB_2 particle size (d_p) which is one of the inputs to MODULE 4. The independent inputs to MODULE 3 are volume fraction of TiB_2 (x_{TiB2}) and percentage of liquid in processing (%L) and the output of MODULE 3 (*f3)* is the average grain size (d) of microstructure. MODULE 4 receives inputs from the outputs of MODULE 1 and 3 along with the independent inputs of volume fraction of TiB_2 (x_{TiB2}) and temperature of semi-solid processing (temp). MODULE 4 deals with

the structure-property relationships and *f4* gives the density (ρ) and *f5* gives yield stress (σ) as outputs. Finally, MODULE 5 deals with the property-performance relationship of the developed microstructure and *f7* evaluates the performance variable of depth of operation (*h*), *f8* evaluates the weight of the outer shell (*W*) and *f9* evaluates the time of operation (T_{opr}) of the submersible. The independent parameter in this level of design is the thickness of the shell (*t*) and the dependent parameters are density (ρ) and yield stress (σ).The solution scheme for this application is illustrated in Figure 2.11. It is observed that the that the feasible design spaces are inductively passed from MODULE 5 to MODULE 4 and subsequently to MODULES 3 and 1 of design.

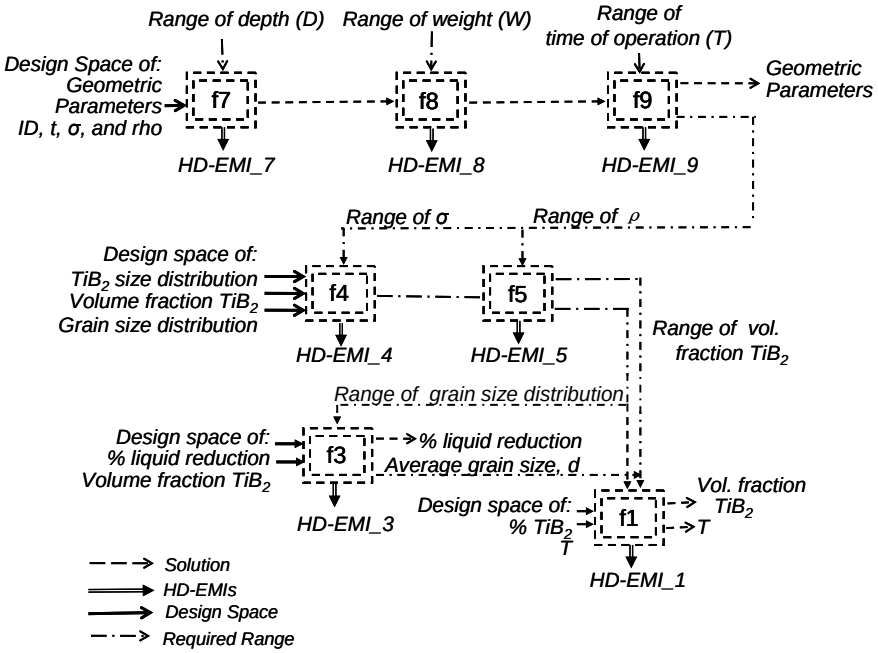

Figure 2.11: Solution strategy using IDEM

It is noted that the volume fraction of TiB_2 is an input to MODULE 1, MODULE 3 and MODULE 4 of design. The responses of MODULE 1 and MODULE 3 are influenced by multiple variables and hence response surface methodology is used for modeling and analysis of the design task at these levels. The Response Surface Methodology employed embodies second order models[47]:

$$Y = \beta_0 + \sum_{i=1}^{k} \beta_i x_i + \sum_{i=1}^{k} \beta_{ii} x_i^2 + \sum \sum_{i<k} \beta_{ij} x_i x_j + \varepsilon \qquad (2.16)$$

where, $\beta_{ij}, i = 1,2,...,k; j = 0,1,2,...,k$ are the regression coefficients and x_j are the regression variables, Y is the response. The Response Surfaces for MODULE 1 and MODULE 3 are generated using MINITAB®. Table 2.1 gives the data set of the variables used to generate the response surface for Module 1.

Table 2.1: Data set for MODULE 1

Volume fraction (xTiB_2, %)	Temperature (*T*, K)	Average particle radius (r, µm)
2.5	1073	0.96
5.0	1073	1.25
7.5	1073	1.22
10.0	1073	1.11
10.0	1173	1.57
10.0	1273	1.74
10.0	1373	1.80

The response surface generated for MODULE 1 is represented by the equation:

$$Y = -17.3246 + 0.2290 x_{TiB2} + 27.7783 T' - 0.0167 x_{tiB2}{}^{2} - 10.4230 T'^{2} \quad (2.17)$$

where *Y* is the response i.e. the average TiB_2 particle grain radius ($d_{p/2)}$, x_{TiB2} is the volume fraction of TiB_2 and *T'* is *T*/1000 where *T* is the temperature in Kelvin.

The data set of the variables used to generate the response surface of MODULE 3 is shown in Table 2.2. The response surface generated for MODULE 3 is represented by the equation:

$$Y = 80.67 - 0.167 x_{TiB2} - 2.25L - 0.3067 x_{ToB2}{}^{2} + 0.01375 L^{2} + 0.202 x_{TiB2} L \quad (2.18)$$

where *Y* is the response i.e., the average grain size(d), x_{TiB2} is the volume fraction of TiB_2 and *L* is the % liquid.

Table 2.2: Data set for MODULE 3

% Volume fraction TiB_2	% Liquid	Grain Size (μm)
2.5	10	62
2.5	20	58
2.5	30	30
5.0	10	54
5.0	20	51
5.0	30	55
7.5	10	62
7.5	20	48
7.5	30	53
10.0	10	49
10.0	20	47
10.0	30	54

2.4. Discussion of Results

The primary design variables in the present case for the submersible's shell [Figure 2.2] are thickness of the shell (t) and volume fraction of TiB_2 ($xTiB_2$). Target requirements include:

- The safe depth of operation of the submersible with a small shell thickness should be as large as possible preferably exceeding 2500 meters and greater depth is better.
- The submersible must have a good endurance with a large time of operation of at least 12 hours without resurfacing or recharging and greater duration of submersion is better.

- Given a weight of the vessel of 76 Kgs and allowing as large a payload as feasible, a representative limit on the weight of the outer shell of the submersible may not exceed 18 kgf, and a lighter shell is preferred.

IDEM has been implemented in MATLAB® for this application. The resolutions for discrete points are fixed as 1(mm), 30 (kg/m^3), 10 (MPa), and 0.5(%) for thickness (*t),* density of composite (*ρ*), yield stress (σ_y), and volume fraction of TiB_2 (x_{TiB2}) respectively. The range for discrete variables are fixed as 5-15(mm), 2700-3300 (kg/m^3), 300-500 (MPa), and 2-10(%) for thickness (*t), density of composite (ρ), yield stress (σ), and volume fraction of* TiB_2 (x_{TiB2}), respectively. These resolutions are reasonably small in order to be able to ignore discretization errors. A 5% performance variability is assumed for each of the mapping models (*f1, f3, f4, f5, f7, f8 and f9).* This is the sum of all quantifiable uncertainty, including natural uncertainty and model parameter uncertainty, of each mapping model. First, the entire feasible ranges are searched in property space (the spaces of *t, ρ* and *σ)* with given performance requirements. The required EMIs (*EMI7, EMI8,* and *EMI9*) for mapping models (*f7,f8, and f9*) are set as greater than or equal to unity, which means all quantified uncertainty is accounted for and the performance output range satisfies the boundary constraints. Among the obtained feasible spaces of *t, ρ,* and *σ,* the value of *t* (thickness of shell) is selected that has the largest feasible space for the rest of the properties (*ρ* and *σ*) because the feasible design domain is to be maintained as large as possible until the end of the design process to achieve robustness under model structure uncertainty.

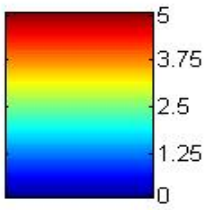

Figure 2.12: Color graph for EMI values

Different colors are used to indicate the variation in the EMI values for different values of variables [Figure 2.12]. Red indicates a EMI value of 5 and the progressively lighter shades denote lower EMI values. The blue diamond points in the figures are the boundary points.

When EMI_7, EMI_8, and EMI_9, are assumed as unity, the largest feasible range in *y* space is achieved at t = 10 (mm). Satisfactory discrete points (circular points) and boundary points (diamond points) between the feasible and infeasible spaces are shown in Figures 2.13, 2.14. With the feasible range achieved in property space, the feasible space of the volume fraction of TiB_2 is identified by setting EMI_4 *and* EMI_5 for mapping models (f_4 *and* f_5) as unity. Then, the entire feasible ranges in the structure space are searched (the feasible spaces of grain size (*d),* TiB_2 particle size (d_p) and volume fraction of TiB_2 ($xTiB_2$)) with given property requirements. The required EMIs (EMI_4 *and* EMI_5) for mapping models (*f4 and f5*) are set as greater than or equal to unity, which ensures satisfaction of the requirement that all quantified uncertainty is within a target level. Among the obtained feasible space of *d,* d_p and $xTiB_2$ the value of temperature of processing (temp) is selected that has the largest feasible space for the rest of the properties (*d,* d_p, and $xTiB_2$) because, as explained previously, it is desired to maintain the feasible region as large as possible until the end of the design process to achieve robustness under MSU.

The achieved feasible space of the volume fraction of TiB2 is within the ranges [0.0322, 0.450] and [0.0656, 0.0995] [Figure 2.15]. This indicates that the achieved space of the volume fraction of TiB_2, [0.0322, 0.450]; [0.0656, 0.0995] and thickness of shell, 10 (mm), with processing temperature of 634 deg C guarantee that the submersible performance satisfies the given requirements while maintaining all quantifiable uncertainty within bounds (5% performance variability), both for each of the mapping models (*f1, f3, f4, f5, f7, f8 and f9)* and for its propagation through the model chain into the final performance space.

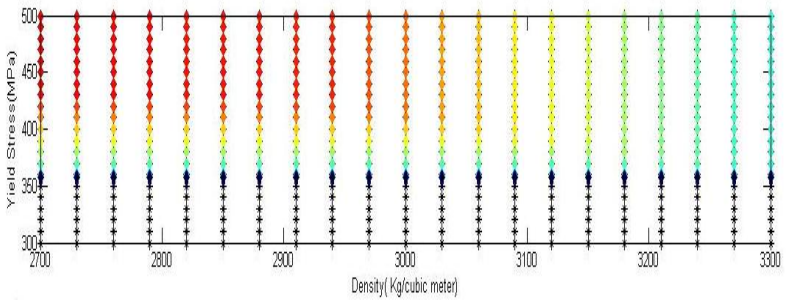

Figure 2.13: Feasible design space for MODULE 5

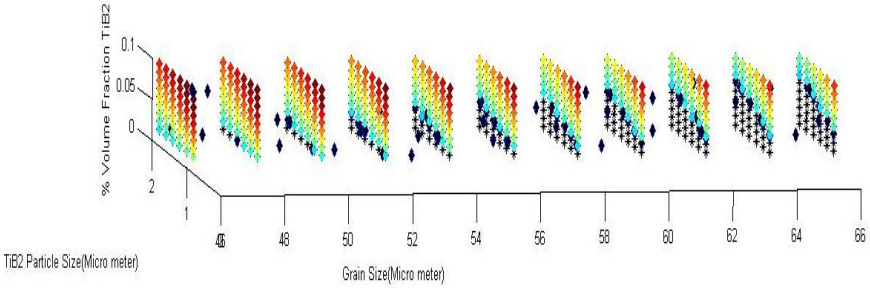

Figure 2.14: Feasible design space for MODULE 4

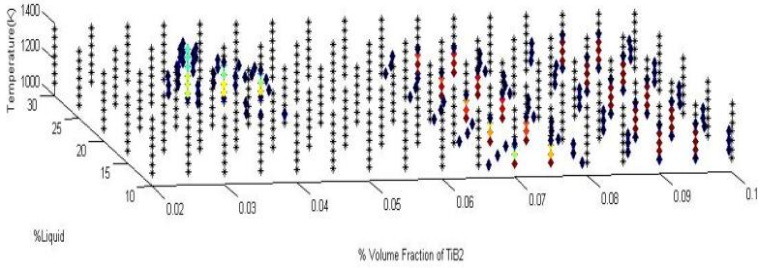

Figure 2.15: Feasible design space for MODULEs 1 and 3

It is seen from Figure 2.13 that higher yield stress σ_y values and lower density ρ values are favorable for the design and are associated with higher EMI values. It can also be concluded from Figure 2.14 that lower grain size (d) and lower TiB2 particle size (d_p) yield higher EMI values and hence are favorable for the design. From Figure 2.17 it can also be concluded that higher volume fraction of TiB_2 yields more feasible design structures of the composite. On increasing the EMI values to [1.4, 1.8, 1.8] for (*f7, f8, f9*) and [1.4, 1.2] for (*f4, f5*) and [1.8, 1.8] for (*f1, f2);* we see in Figures 2.16 and 2.17 that the feasible spaces at each level of design reduces and

feasible space of volume fraction of TiB2 falls to within the range [8.84, 9.75]. As illustrated, considering MSU in the mapping models, a designer may then select the “best” or preferred solution(s) for materials and product using IDEM. Ranged sets of design specifications are identified with given product/system performance requirements considering quantifiable uncertainty. Based on obtained feasible solution sets, designers may have more freedom for choosing their decisions, emphasizing product performance, achieving robustness against MSU, or compromising between them.

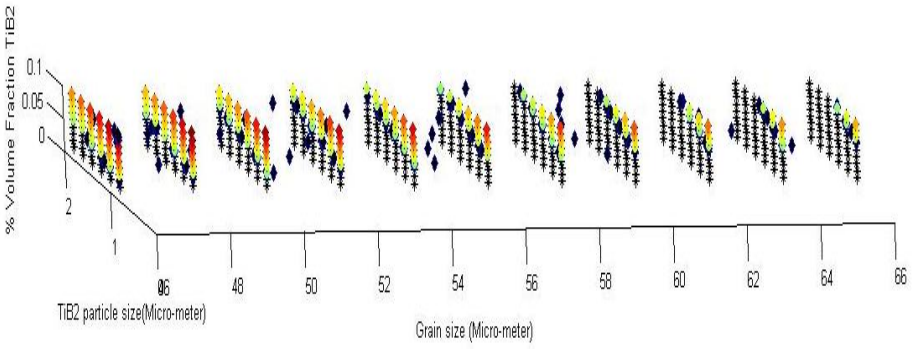

Figure 2.16: Feasible design space for MODULE 4

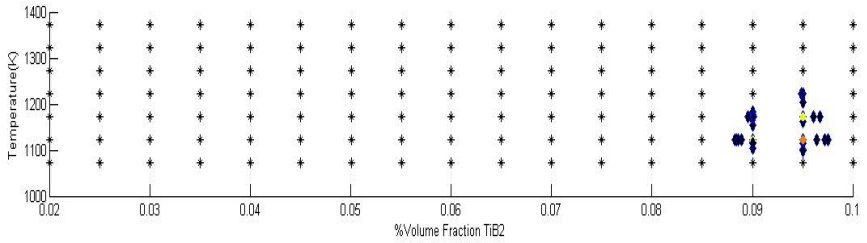

Figure 2.17: Feasible design space for MODULEs 1 and 3

At this point, the reader may wonder what additional information is afforded by this approach in designing or selecting a material beyond the rather obvious effects of reducing particle size and spacing through increase of particle volume fraction. It might seem obvious that these steps would be necessary to develop a high specific strength in situ Al MMC in such an application. However, there are several important points to make. First, the specific ranges of microstructure attributes are directly coupled in the present methodology with the overall systems design

(material plus submersible). Hence, changes in performance requirements are directly reflected in the ranges of microstructure attributes that emerge from application of IDEM. Second, this approach can be readily extended to include performance requirements that impose multifunctional, multiphysics requirements on the material design aspect. For example, if high thermal conductivity is also required as part of the present design (as might be the case for heat transfer from the submersible interior), it may very well drive a decrease in volume fraction of non-metallic particles, which conflicts with strength requirements. Such competing modes of requirements in materials design are common and serve as a compelling basis for the present systems-based robust design approach. Moreover, if one is interested in selecting different process routes (e.g., in-situ versus ex-situ Al MMCs or other matrix materials), the assessment of feasibility is quite difficult without considering the full contributions of the process-structure-property-performance relations. In other words, it is not just a classical materials selection problem [48].

2.5. Thoughts on What has been Presented and What is Next

In this chapter the microstructure-mediated design construct has been introduced. A methodology is presented to pursue concurrent robust design of a robotic submersible and Al-based metal matrix composite that embodies the microstructure-mediated robust design construct. Recently developed tools have been used such as the Inductive Design Exploration Method, which facilitates top-down searching for design solutions including process path and microstructure based on bottom-up simulations.

The work presented in this chapter constitutes one of the most complete applications of IDEM. The primary challenge involves managing uncertainty in over seven empirical and theoretical models over four levels of design. Starting from a hull thickness parameter in MODULE 5, the feasible design spaces for various mechanical properties along with higher yield stress and lower density are identified using IDEM. Similarly, the feasible space of material properties and various material and processing parameters are identified using IDEM, leading to preference for lower

grain size and higher volume fraction of TiB_2 in the MMC; this is based on use of MODULEs 4, 3 and 1. Upon analyzing the results it is concluded that the microstructure mediated design (MMD) construct holds promise in designing both the product and the material from which the product is made. The MMD construct is further refined in Chapter 5 by inclusion of HD-EMI metric instead of EMIs and coupling with cDSP. Having established the functionality of IDEM to reach ranged sets of robust solutions against modeled and propagated uncertainty in multiscale systems, we investigate the applicability of cDSP using game theoretic protocols for managing uncertainty in multilevel design.

In this chapter, one of the founding constructs, i.e., IDEM for the algorithms developed in Chapters 4 and 5 is introduced and hence contributes to the Empirical Structural Validity, i.e., Quadrant II and establishes the internal consistency of algorithm to be developed, Figure 2.18. Detailed description with respect to the validation square is taken up in Chapter 7. Also Figure 2.19 shows where we are in terms of the thesis.

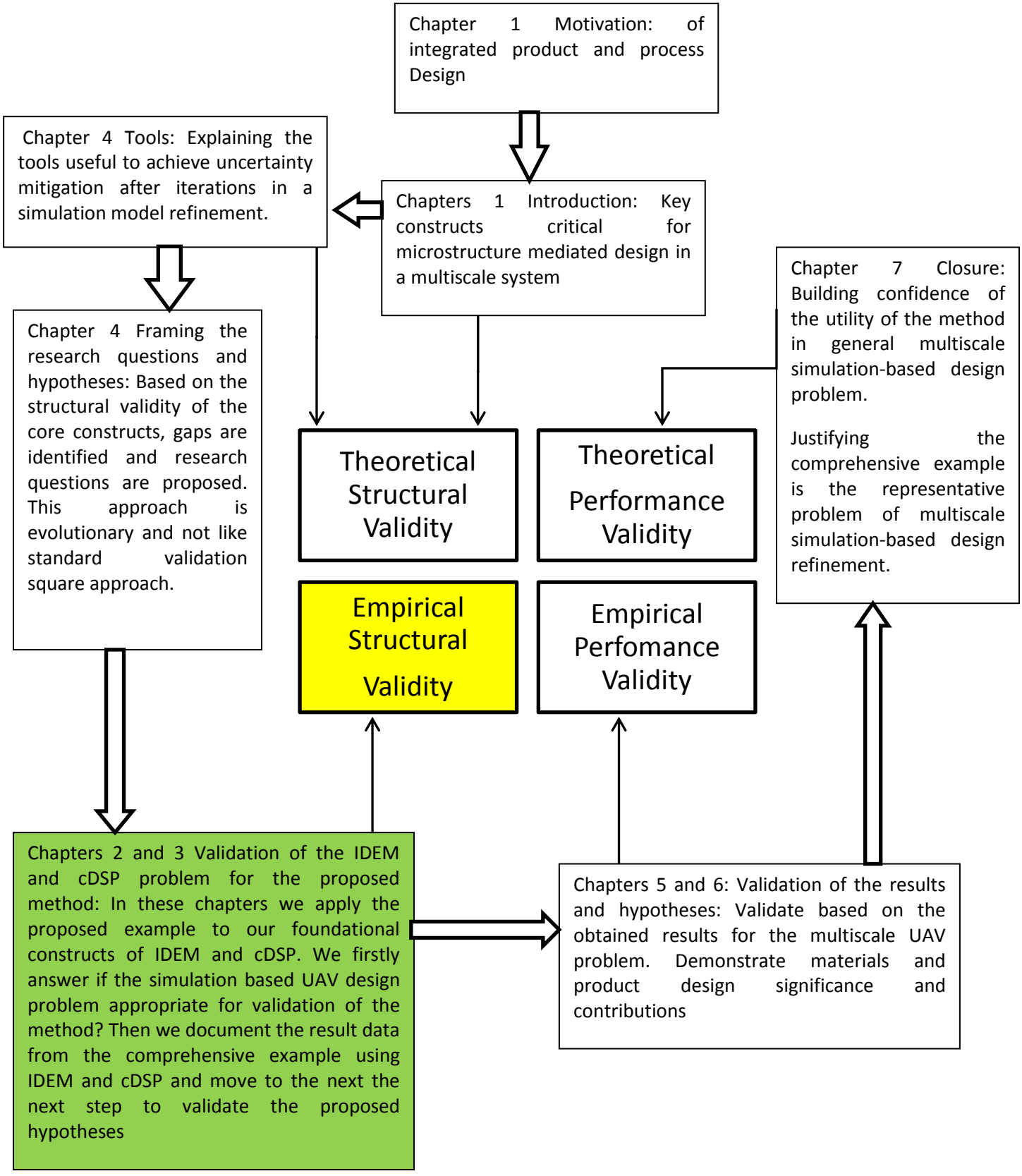

Figure 2.18: The validation square

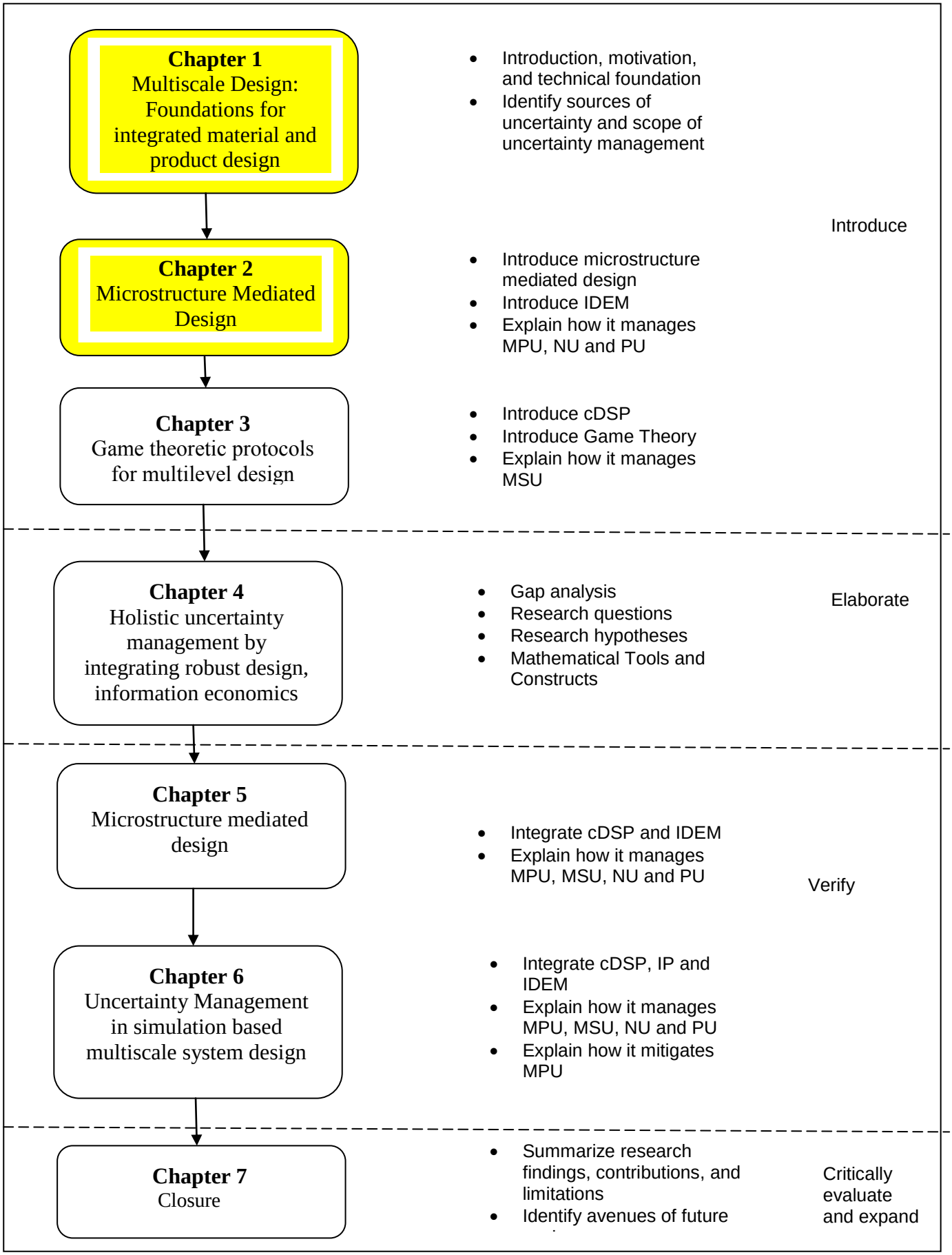

Figure 2.19: Organization of work

CHAPTER 3

DEVELOPMENT OF GAME THEORETIC PROTOCOLS FOR MULTILEVEL DESIGN

The effectiveness of the use of game theory in addressing multi-objective design problems in multiscale systems has been illustrated in this Chapter. For the most part, researchers have focused on design problems at single level. In this chapter, the efficacy of using game theoretic protocols is illustrated to model the relationship between multidisciplinary engineering teams and facilitate decision making at multiple levels. The protocols are illustrated in the context of an underwater vehicle with three levels that span material and geometric modeling associated with microstructure mediated design of the material and vehicle developed in Chapter 2. The solution is reached using the cDSP approach described in Section 1.2. This study was presented at the proceedings of IDETC 2010, Montreal [28].

3.1. Frame of Reference

In the context of engineering design, a game is a decision-making process between multiple teams each of which controls a subset of design variables and seeks to maximize target achievement of system goals subject to individual constraints [49]. In this chapter, game theoretic protocols are applied to model the relationship between multidisciplinary engineering teams and facilitate decision making for a multilevel designing task. The game theoretic construct for multilevel design will be demonstrated through the design of an underwater vehicle as a representative example. This design task is an example of a multilevel design problem with modelling over three levels, i.e., property-performance relationship modelling at the top level, the structure-property relationship modelling in the central level and finally material processing-structure relationship modelling at the lowest level associated with the microstructure mediated

design [29]. The primary objective of the theoretical and empirical modelling considered at the various levels of design is to satisfy the performance constraints in the system.

The efficacy of the game construct is illustrated through the design of the shell and design of the material from which the shell of a submersible vehicle is made. The objective is to design the shell of an underwater submersible for deep sea exploration with the multifunctional requirements of minimizing the mass in walls (wall thickness) for given support superstructure for given maximum depth and associated pressure differential [31]. Other design requirements include a) suitable factor of safety with respect to collapse at target maximum operating depth, b) a large endurance time satisfying the time of operation constraints under water without resurfacing to/refuel the/battery and, c) satisfying geometric and weight constraints.

The advantage of modelling this multilevel multidisciplinary design problem as a game is that each team controls an individual payoff function and facilitates modular decision making, hence removing the burden of disciplinary analysis and decision making at the system level[50]. It also helps reduce iterations among engineering teams for the individual modules. Individual modules are modelled using compromise Decision Support Problems (cDSP) solved by using the JAVA DSIDES software which uses an Adaptive Linear Programming algorithm [51]. Fundamental to this design approach is a system considering variables, constraints, and models that embed relevant aspects of the material microstructures through overall system configuration. This system has been established and details in this chapter will focus on mathematical modelling of the design scheme. For detailed discussion on the design task at hand see Sinha et al [29]

3.2. The Method

In this section material that is needed to understand the foundational elements of the method is presented. This approach is useful for design problem has multiple levels (sometimes called multiple scales). Each level also may have interacting contributions from various groups – or

players. As design requires the successful satisfaction of top-level requirements, we proceed from the highest – or top – level to the lowest level.

(STEP 1) Represent the theoretical or empirical models in multilevel design task as compromise DSPs and instantiate these compromises DSPs into decision templates,

(STEP 2) Use game theoretic protocols to represent interactions and formulate coupled compromise DSP's for cooperating multidisciplinary teams with aid of developed decision templates [52].

(STEP 3) Solve the optimization problem for the deviation function in the coupled cDSP at the top level in my multilevel design task using JAVA DSIDES®.

(STEP 4) Use the solutions in an inductive top-down manner to determine feasible range space and target values for functional models at lower hierarchical levels in the multilevel design. Continue process till you converge to a solution for the lowest level of design.

(STEP 5) Exercise design freedom for individual models by reformulating compromising DSPs using design capability indices (DCI's) [53].

3.2.1 Microstructure Mediated Design

The relevant aspects of MMD are described from Chapter 2. Multilevel design for the shell design problem involves two activities, namely, process path - structure relationships and structure-property-performance relationships. These two design objectives interact via the microstructure. The processing conditions influence the obtained microstructure, and the performance of the product depends on the mechanical properties which in-turn are mapped from the microstructure.

In the present study, the materials design and structural design are combined. The materials design aspect has been divided into three parts based on the different processing steps of the

material. The interface between materials design and structural design is the mapping of the processed microstructure to the required mechanical properties.

In this application, the strength is principally determined by the sizes, shapes and distribution of TiB2 precipitates – in other words the microstructure of the material. The microstructure is determined by processing methods – in this case, it is initially created by precipitation and followed by the evolution of the precipitate size and distribution during the semi-solid rolling. Based on the Olson's Diagram [Refer Figure 2.1]; the design of the underwater vehicle has been divided into design over three levels; processing-structure relationship modeling associated with the microstructure mediated design at the bottom level at level 3; the structure-property relationship modeling in the level 2 and finally property-performance relationship modeling at level 1or the top level. Based on the materials processing steps involved and mechanical design requirements, the interconnected modules that constitute the design process chain for this application are [See Figure 2.3]. For detailed analysis of the modules refer Section 2.2.

MODULE 1: Precipitation modeling in liquid Al.

MODULE 2: Modeling of microstructure evolution in MMCs.

MODULE 3: Evolution of microstructure during semisolid processing of MMCs.

MODULE 4: Structure - property correlations of MMCs.

MODULE 5: Requirement list, microstructure mapping and system-level design.

MODULEs 1, 2 and 3 provide the simulated microstructure after processing. The resulting mechanical properties are estimated in MODULE 4, whereas MODULE 5 maps the required mechanical properties with the performance based on the system design considerations. The modeling in MODULE 2 has presented many challenges and these have yet to be resolved. Hence, it is bypassed in illustrating my method via this application. The problem investigated is shown in the Figure 3.1.

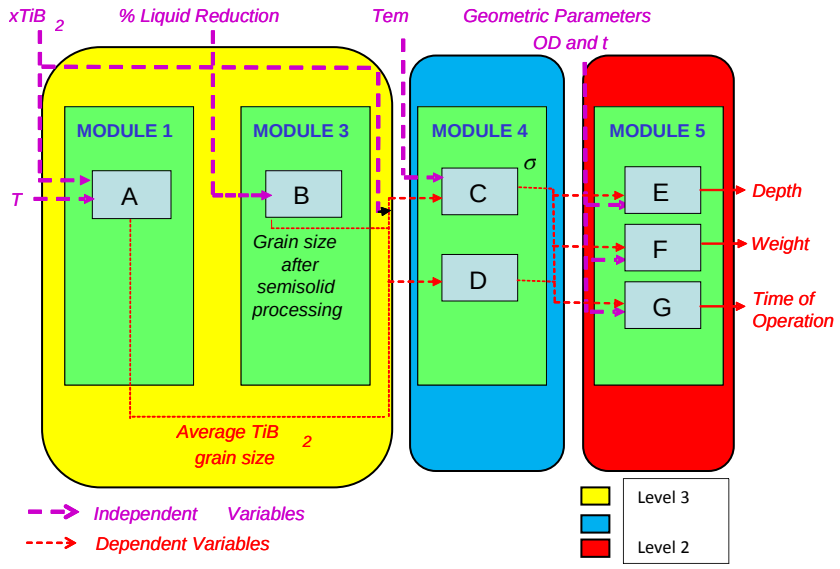

Figure 3.1: Problem analysis diagram

In Figure 3.1; A*, B, C, D, E, F and G* represent the theoretical or empirical models considered over four modules and over three levels of design. As we are evaluating strategic interactions in design teams, the individual modules in Figure 2.10 are represented as players. These levels of design are associated with characteristic relationship modeling between processing-structure; structure-properties or properties-performance. Effectively, these seven models can be viewed as players with their respective outputs as pay-offs. The inputs to MODULE 1 are the volume fraction of TiB_2 (x_{TiB2}) and temperature of processing in degree K (T).The output of MODULE 1 (A*)* is the average TiB_2 particle size (r) which is one of the inputs to MODULE 4. The independent inputs to MODULE 3 are volume fraction of TiB_2 (x_{TiB2}) and percentage of liquid in processing (%L) and the output of MODULE 3 (*B)* is the average grain size (d) of microstructure. MODULE 4 receives inputs from the outputs of MODULE 1 and 3 along with the independent inputs of volume fraction of TiB_2 (x_{TiB2}) and temperature of semi-solid processing (T_1). MODULE 4 deals with the structure-property relationships and *D gives* the density (ρ) and *C gives* yield stress (σ) as outputs. Finally, MODULE 5 deals with the property-performance relationship of the developed microstructure and *E* evaluates the performance variable of depth of operation (h), *F* evaluates the weight of the outer shell (W) and *G* evaluates the time of operation (T_{opr}) of the

submersible. The convention of calling the models in the Modules as Players is followed from here on. The independent parameter in this level of design is the thickness of the shell (t) and the dependent parameters are density (ρ) and yield stress (σ).Thus by Figure 3 we realize that Players A and B belong to Level 3 game while Players C and D fit in to the Level 2 game and finally E, F and G go to Level 1 game design.

3.2.2 Decision Template and Compromise DSP

A compromise DSP is a multi-objective decision model which is a hybrid formulation based on mathematical programming and goal programming in which the objective is to satisfy a set of constraints while achieving a set of conflicting goals as well as possible [54]. The mathematical formulation of the compromise DSP is given in Fig 3.2 and described in detail in Section 1.2. Because of its standardized format, a compromise DSP can be used to model the decision making activities of all of the engineering teams. The compromise DSP formulated in the most elementary entities, *e.g.*, mathematical formulations or computer codes, which are easy to understand by engineering teams and implementable on computer, is called a decision template. In my multilevel design problem, decision templates that represent the player's or engineering team's activities are coupled by shared design variables and state variables that represent interdisciplinary interaction relationships. Game theoretic principles are used to model this interaction and coupled compromise DSP's are developed. Finally a solution is reached using JAVA DSIDES®. The JAVA version of DSIDES (Decision Support in the Design of Engineering Systems) solves the Decision Support Problem (DSP) using an adaptive linear programming (ALP) multi-objective optimization algorithm[55]. It is noted additionally, the ALP algorithm successfully navigates around geometric constraints, although care must be taken when linearizing highly non-linear design spaces.

Given
An alternative to be improved
Target values for goals, G_i, $i = 1,\ldots,n$
Relative importances of goals, w_i
Find
System Variables: $x_j \in X$, $j = 1,\ldots,m$
Deviation Variables: d_i^-, d_i^+
Satisfy
Goals: $A_i(X) + d_i^- - d_i^+ = G_i$,
Constraints: $C_k(X) \le 0$, $k = 1,\ldots,p$
$d_i^- \cdot d_i^+ = 0,\ d_i^-, d_i^+ \ge 0$
Bounds: $lb_j \le X_j \le ub_j$
Minimize
Deviation Function:
$Z = \Sigma w_i \cdot d_i^+ + \Sigma w_i \cdot d_i^-$,

Figure 3.2: Generic form of the compromise DSP[54]

3.2.3 Game Constructs: Pareto or Cooperative Solution

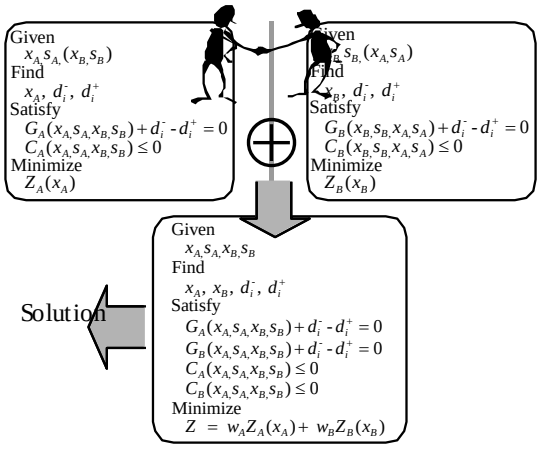

Figure 3.3: Solution of cooperative game [50]

To distinguish a game based approach from other decision making approaches, when solving problems using the principles of game theory, the term "player" is used to represent a disciplinary engineering team with its associated computer-based analysis and synthesis tools (decision templates).The ideal scenario for collaboration is full cooperation between two players in which both players have full access to information about each other's decision making process, including their decision templates and associated engineering tools[56]. Assuming coupled compromise DSPs, A and B respectively represent the decision making activities of player A and B, a full cooperation scenario is solved by combining all players DSPs, hence all

goals, constraints, etc. in DSPs A and B are satisfied in one DSP, as shown in Fig.3.3. Mathematically this is:

$$Z = w_A Z_A(x_A) + w_B Z_B(x_B) \qquad (3.1)$$

3.2.4 Design Capability Indices

In Chapter 2 we used the error margin index metric (EMI) to affect the IDEM solution. In this chapter we employ the design capability index (DCI) which is an alternative to EMI and does not account for model variability. The focus of this chapter is to illustrate the successful compilation of cDSP templates in a multiscale design problem to reach a solution and hence model variability is ignored for illustrative purposes. Chen and co-authors present design capability indices to evaluate performance variations caused by a range of design solutions, and determine whether the design solutions are capable of satisfying a ranged set of design requirements[53].Say, a design variable is represented using x and Δx. f(x) is the formulation of performance measure. The response is measured using y and Δy. Design Capability Indices (DCI's) are represented using:

$$y = f(x) \qquad (3.2)$$

$$\Delta y^2 = \sum_{i=1}^{k} \left(\frac{\partial f}{\partial x_i}\right)^2 \Delta x_i^2 \qquad (3.3)$$

$$C_{dl} = \frac{y - LRL}{\Delta y};\ C_{du} = \frac{URL - y}{\Delta y} \qquad (3.4)$$

$$C_{dk} = \min\{C_{dl}, C_{du}\} \qquad (3.5)$$

LRL and URL represent the lower requirement limit and upper requirement limit for the model, i.e., the range of operation of performance desired. C_{dk}≤1 means that a portion of design solutions falls outside of the requirement limits. Design solutions with C_{dk}≥1 are capable of satisfying design requirements Design capability indices are controlled in the compromise DSP by changing the target values for individual C_{dk}'s. Since constraints C_{dk} ≥1 are added, the deviation function is also changed to maximizing the overachievements of the C_{dk} values.

Compromise DSP for ranged set of decisions is formulated in this manner to ensure that the range of each performance measure not only falls into the corresponding target range, but also achieves the specific target as well as possible [52]. Thus, DCI's operate as a metric for design freedom where higher values of C_{dk} correspond to greater design freedom. However, we shall not solve for the ranged feasible values for the design variables as it has already been illustrated using collaborative optimization [57] and IDEM [29]. The DCI and EMI constructs are extended to the EMI metric in Chapter 5 in order to successfully account for all four types of uncertainty in a multiscale system.

3.3. Mathematical Formulation

Having defined the elements, the modules are described mathematically in the section that follows. For detailed description of the modules, please refer the previous chapter or Sinha et al., 2009 [29].

3.3.1. Level 1

Level 1 is the top level in my design task and consists of property performance modeling or Module 5 in the underwater submersible design The performance parameters are depth of safe operation (Depth or h); minimizing the mass (Weight or W) in walls (wall thickness) for given support superstructure and Time of Operation (Time or T_{opr}) under water without resurfacing. [29]

MODULE 5 (Property-Performance Correlation of MMCs)

MODULE 5 acts as an interface between the materials design aspect and the design of the structure of the submersible. The performance parameters considered are depth, time of operation and weight of the outer shell of submersible. The objective is to maximize the depth and time of operation while minimizing the weight of the outer shell of the submersible. The formulas used for the calculation of these performance parameters are stated in what follows. It comprises of entire Level 1 design task.

PLAYER E: Model for Depth (*h*): Roark's formula[29] is used for thickness (*t*) to outer diameter (*OD*) ratio.

$$\frac{t}{OD} = \frac{1}{2}\left(1 - \sqrt{1 - \frac{2P}{\sigma}}\right) \qquad (3.6)$$

where *t* is the thickness of the shell, *OD* is the outer diameter of the shell; *P* is the external pressure and σ is the yield stress of the metal matrix composite. Solving for *h* we get:

$$h = \left(\frac{\sigma}{2\rho_w g}\right)\left[1 - \left(1 - \frac{2t}{OD}\right)^2\right] \qquad (3.7)$$

Decision Template for PLAYER E (h)

Given:

Target Value for Depth = 3500 m

Range of Depth (2000- 5000m)

Δt = 1(mm), Δσ = 20 (MPa)

$$Depth(h) = \sigma * 10^{-4}(7.779t - 29.921t^2)$$

$$\Delta h = \sqrt{(\frac{\partial h}{\partial \sigma}\Delta\sigma)^2 + (\frac{\partial h}{\partial t}\Delta t)^2}$$

$$\frac{\partial h}{\partial \sigma} = (7.779t - 29.921t^2) * 10^{-4}$$

$$\frac{\partial h}{\partial t} = \sigma * 10^{-4}(7.779 - 2 * 29.921t)$$

Find:

Location of system variable: t, σ

Deviation variables: $d_E^-; d_E^+; d_5^-; d_5^+$

Satisfy:

System Goals

$$C_{dk}^E / C_{dk}^{target} + d_E^- - d_E^+ = 1$$

$$\frac{h}{h_{target}} + d_5^- - d_5^+ = 1$$

System Constraints

Depth ≥ 2000 m

$$C_{dk}^E \geq 1$$

$$d_E^- * d_E^+ = 0; d_5^- * d_5^+ = 0;$$

$$d_E^-, d_E^+ \geq 0; \;\; d_5^-, d_5^+ \geq 0$$

System Bounds

5 ≤ t ≤15 (mm)

300 ≤ σ ≤ 500 (MPa)

Minimize

Deviation Function:

Z= $w_E(-d_E^+) + w_5(-d_5^+)$

PLAYER F: Model for Weight (*W*): The weight of a cylindrical shell with spherical end caps is calculated.

$$W = \pi \rho L (OR^2 - IR^2) + (4/3) \pi \rho (OR^3 - IR^3) \qquad (3.8)$$

where ρ is the density of the composite, *L* is the length of the submersible, *OR* is the outer radius and *IR* is the inner radius of the cylindrical shell with spherical end-caps.

Decision Template for PLAYER F (W)

Given:

Target Value for Weight = 16 kgf

Range of Weight (7- 25 kgf)

Δt = 1(mm), Δρ = 60 (kg/m^3)

$$Weight(W) = \rho * (1.519t - 6.660t^2 + 4.189t^3)$$

$$\Delta W = \sqrt{(\frac{\partial W}{\partial \rho}\Delta\rho)^2 + (\frac{\partial W}{\partial t}\Delta t)^2}$$

$$\frac{\partial W}{\partial \rho} = (1.519t - 6.660t^2 + 4.189t^3)$$

$$\frac{\partial W}{\partial t} = \rho * (1.519 - 2 * 6.660t + 3 * 4.189t^2)$$

Find:

Location of system variable: t, ρ

Deviation variables: $d_F^-; d_F^+; d_6^-; d_6^+$

Satisfy:

System Goals

$$C_{dk}^F / C_{dk}^{target} + d_F^- - d_F^+ = 1$$

$$\frac{W}{W_{target}} + d_6^- - d_6^+ = 1$$

System Constraints

Weight ≤ 25kgf

$$C_{dk}^F \geq 1$$

$$d_F^-, d_F^+ \geq 0;\ d_6^-, d_6^+ \geq 0$$

$$d_F^- * d_F^+ = 0; d_6^- * d_6^+ = 0;$$

System Bounds

5 ≤ t ≤15 (mm)

2936.2 ≤ ρ ≤ 3096 (kg/m^3)

Minimize

Deviation Function:

Z= $w_F(-d_F^+) + w_6(-d_6^+)$

PLAYER G: Model for Endurance Time (T_{opr})

$$T_{opr} = \frac{0.8(B - W) * eff * Energy\ Density}{Fixed\ Load + Propulsion\ Load} (3.9)$$

where *B* is the buoyant weight of the submersible, *W* is the weight of the cylindrical shell, *eff* is the efficiency of the battery.

Decision Template for PLAYER G (T_{opr})

Given:

Target Value for Time = 12 hours

Range of Time = (10- 15 hours)

Δt = 1(mm); Δρ = 60 (kg/m^3)

$$Time(T_{opr}) = 14.823 - 0.1536\rho * (1.519t - 6.660t^2 + 4.189t^3)$$

$$\Delta T_{opr} = \sqrt{(\frac{\partial T_{opr}}{\partial \rho}\Delta\rho)^2 + (\frac{\partial T_{opr}}{\partial t}\Delta t)^2}$$

$$\frac{\partial T_{opr}}{\partial \rho} = -0.1536 * (1.519t - 6.660t^2 + 4.189t^3)$$

$$\frac{\partial T_{opr}}{\partial t} = -0.1536\rho * (1.519 - 2 * 6.660t + 3 * 4.189t^2)$$

Find:

Location of system variable: t, ρ

Deviation variables: $d_G^-; d_G^+; d_7^-; d_7^+$

Satisfy:

System Goals

$$C_{dk}^G / C_{dk}^{target} + + d_G^- - d_G^+ = 1$$

$$\frac{T_{opr}}{T_{target}} + d_7^- - d_7^+ = 1$$

System Constraints

Time ≥ 10 hours

$$C_{dk}^G \geq 1$$

$$d_G^- * d_G^+ = 0; d_7^- * d_7^+ = 0;$$

$$d_G^-, d_G^+ \geq 0; d_7^-, d_7^+ \geq 0$$

System Bounds

5 ≤ t ≤15 (mm)
2936 ≤ ρ ≤ 3096 (kg/m^3)
Minimize
Deviation Function:
Z= w_G $(-d_G^+)$ +$w_7(-d_7^+)$

Coupled Decision Template (PLAYERS E, F and G)

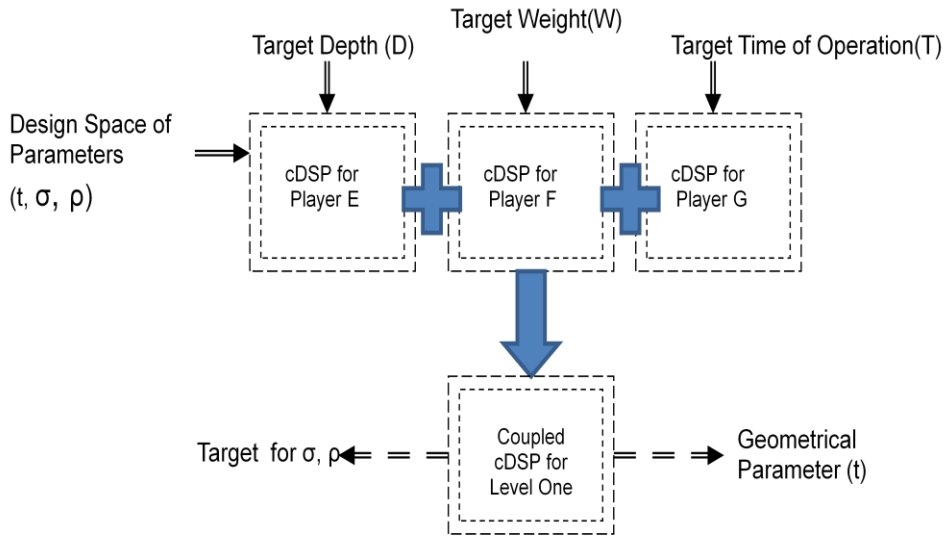

FIGURE 3.4 Coupled decision template (Players E, F and G)

Combining the DSP's for the individual performance parameters, a coupled cDSP is obtained as show in Figure 3.4. The Decision Templates for Weight, Time and Depth are combined and the deviation function is function of the weights of the individual deviation functions. Assigning different weights to the three negative deviation variable (Sum of weights equal to 1), different designing scenarios are calculated. In addition there are three deviation variables to calculate the deviation in objective function for each of the three performance parameters. The output of the coupled cDSP is the target values for elastic modulus (*σ)*, density of composite (ρ) and the thickness of the submersible (t).

Coupled Decision Template (Level 1)

Given:

Target Value for Depth = 4000 m

Target Value for Time = 12 hours

Target Value for Weight = 16 kgf

Weight of Time, Depth, Weight= (w_7, w_6, w_5)

Δt = 1(mm); Δσ = 20 (MPa) ;Δρ = 60 (kg/m^3)

$$Depth(h) = \sigma * 10^{-4}(7.779t - 29.921t^2)$$

$$\Delta D = \sqrt{(\frac{\partial D}{\partial \sigma}\Delta\sigma)^2 + (\frac{\partial D}{\partial t}\Delta t)^2}$$

$$Weight(W) = \rho * (1.519t - 6.660t^2 + 4.189t^3)$$

$$\Delta W = \sqrt{(\frac{\partial W}{\partial \rho}\Delta\rho)^2 + (\frac{\partial W}{\partial t}\Delta t)^2}$$

$$Time(T) = 14.823 - 0.1536\rho * (1.519t - 6.660t^2 + 4.189t^3)$$

$$\Delta T = \sqrt{(\frac{\partial T}{\partial \rho}\Delta\rho)^2 + (\frac{\partial T}{\partial t}\Delta t)^2}$$

Find:

Location of system variable: t, σ, ρ

Deviation variables: $d_E^-; d_E^+; d_F^-; d_F^+; d_G^-; d_G^+;$

$d_5^-; d_5^+; d_6^-; d_6^+; d_7^-; d_7^+$

Satisfy:

System Goals

$$\frac{C_{dk}^i}{C_{dk}^{target}} + d_i^- - d_i^+ = 1 \quad for\ i = E, F, G.$$

$$\frac{X_i}{X_{target}} + d_i^- - d_i^+ = 1 \ \ for\ i = 5,6,7$$

System Constraints

Depth ≥ 2000 m; Weight ≤ 25kgf; Time ≥ 10 hours

$C_{dk}^{i} \geq 1$ For i=E, F, G, 5, 6, 7.

$d_i^- * d_i^+ = 0; \quad d_i^-, d_i^+ \geq 0$

System Bounds

5 ≤ t ≤15 (mm);

300 ≤ σ ≤ 500 (MPa)

2936.2 ≤ ρ ≤ 3096.2 (kg/m^3)

Minimize

Deviation Function: Z= $\sum w_i$*($-d_i^+$) for i=E, F, G, 5, 6, 7

3.3.2. Level 2

Level two is the structure- property relationship modeling level in the design task. The structure parameters are particulate radius(r); grain diameter (d); volume fraction of TiB_2 (x_{TiB_2}) and temperature of processing T_1. The property parameters are elastic modulus (σ) and density (ρ). The target values for the property parameters are solved for the cDSP at Level 1 using JAVA DSIDES.

MODULE 4 (Structure-property correlation of MMCs)

PLAYER C: Yield Stress: The matrix yield stress is assumed to obey the Hall-Petch relation [58], i.e.,

$$\sigma_y = \sigma_0 + k_y (d)^{-0.5} \qquad (3.10)$$

where k_y is the strengthening coefficient (a constant unique to each material; for pure Al, k_y = 3.4 MPa-mm), σ_o is a material constant, d is the grain diameter, and σ_y is the yield stress. The calculation of overall yield stress

$$\sigma = \sigma_y (1 + f_1) (1 + f_2) (1 + f_{orowan}) \qquad (3.11)$$

where f_1 takes the effect of volume fraction of particles, f_2 takes into account the thermal expansion coefficient mismatch between matrix and reinforcement, and f_{orowan} takes into

account the effect of particle size (*d*) and spacing[43]. It receives input from outputs of MODULEs 1 and 3 (Players A and B), specifically reinforcement size(r), grain size (*d*), semisolid processing temperature (T_1) and volume fraction of TiB_2 particles. Because of the complexity in mathematical modeling for Elastic Modulus, the partial derivatives for $\Delta\sigma$ calculation are not presented in closed form and MATLAB has been used to calculate $\Delta\sigma$ using equation 3.2.

Decision Template for PLAYER C (σ)

Given:

Target Value for Elastic Modulus = From Level 1 (σ_{L1})

Range of feasible space for σ= 300-500 MPa

Δx_{TiB_2} = (0.1-0)* 0.1 = 0.01(vol. fraction)

Δd = (65-45)* 0.1 = 2 (μm)

Δr = (2- 0.5)* 0.1 = 0.15(μm)

ΔT_1 = (640- 610)* 0.1 = 3(C)

$\sigma = \sigma_y*(1+f\_1)*(1+f\_d)*(1+f\_orowan)$

$$\Delta\sigma = \sqrt{(\frac{\partial\sigma}{\partial d}\Delta d)^2 + (\frac{\partial\sigma}{\partial r}\Delta r)^2 + (\frac{\partial\sigma}{\partial x_{TiB_2}}\Delta x_{TiB_2})^2 + (\frac{\partial\sigma}{\partial T_1}\Delta T_1)^2}$$

Find:

Location of system variable: x_{TiB_2}, d, r, T_1

Deviation variables: $d_C^-; d_C^+; d_3^-; d_3^+$

Satisfy:

System Goals

$$C_{dk}^C / C_{dk}^{target} + d_C^- - d_C^+ = 1$$

$$\frac{\sigma}{\sigma_{target}} + d_3^- - d_3^+ = 1$$

System Constraints

300 ≤ σ ≤ 500 (MPa)

$$C_{dk}^C \geq 1$$

$$d_C^- * d_C^+ = 0; d_3^- * d_3^+ = 0;$$

$$d_C^-, d_C^+ \geq 0;\ d_3^-, d_3^+ \geq 0$$

System Bounds

$0 \leq x_{TiB_2} \leq 0.1$ (volume fraction)

32 µm ≤ Grain Size (d) ≤ 62 µm
0.8 µm ≤ Particulate Reinforcement size (r) ≤ 1.8 µm
610 ≤ Temperature (T_1) ≤ 640 (Degree Celsius)

Minimize

Deviation Function: Z=$w_C\ (-d_C^+) + w_3(-d_3^+)$

PLAYER D: Density: The determination of density is based on the average property of each of the constituent phases, i.e.,

$$\rho = \rho_{TiB2} x_{TiB2} + \rho_{Cu} x_{Cu} + \rho_{Al} (1 - x_{TiB2} - x_{Cu}) \qquad (3.12)$$

where ρ, ρ_{TiB2}, ρ_{Cu}, ρ_{Al} are the densities of the composite, TiB_2, copper and aluminum respectively.

Decision Template for PLAYER D (ρ)

Given:

Target Value for Density = From Level 1 (ρ_{L1})

Range of feasible space for ρ= (2936.2 -3096) kg/m^3

Δx_{TiB_2} = (0.1-0)* 0.1 = 0.01(vol. fraction)

$$Density(\rho) = 3097.6 - 1{,}620 x_{TiB_2}$$

$$\Delta\rho = \sqrt{\left(\frac{\partial\rho}{\partial x_{TiB_2}} \Delta x_{TiB_2}\right)^2}$$

$$\frac{\partial\rho}{\partial x_{TiB_2}} = -1{,}620$$

Find:

Location of system variable: x_{TiB_2}

Deviation variables: $d_D^-; d_D^+; d_4^-; d_4^+$

Satisfy:

System Goals

$$C_{dk}^D / C_{dk}^{target} + d_D^- - d_D^+ = 1$$

$$\frac{\rho}{\rho_{target}} + d_4^- - d_4^+ = 1$$

System Constraints

$2936 \leq \rho \leq 3096$ (kg/m^3)

$$C_{dk}^D \geq 1$$

$$d_D^- * d_D^- = 0; d_4^- * d_4^+ = 0$$

$$d_D^-, d_D^+ \geq 0; d_4^-; d_4^+ \geq 0$$

System Bounds

$0 \leq x_{TiB_2} \leq 0.1$ (volume fraction)

Minimize

Deviation Function Z= $w_D\ (-d_D^+) + w_4(-d_4^+)$

Coupled Decision Template (PLAYERS C and D)

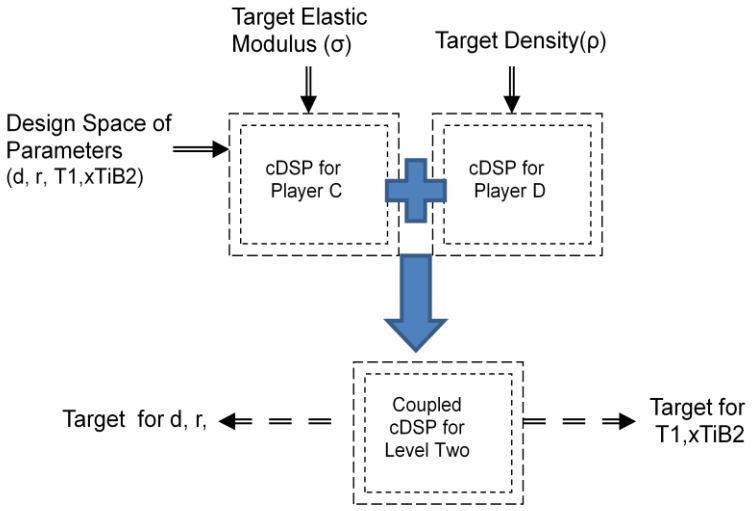

Figure 3.5 Coupled decision template (Players C and D)

Combining the DSP's for Player C and D's parameters, coupled cDSP is obtained as show in Figure 3.5. The Decision Templates for Elastic Modulus (Player C) and Density (Player D) are combined and the objective function for minimization is a function of the weights and values of the individual deviation functions. Assigning different weights to the two deviation variables (Sum of weights equal to 1), we can calculate for different designing scenarios. The output of the coupled cDSP is the target values for grain size (d), particulate size(r), temperature of semisolid processing (T_1) and volume fraction of composite (x_{TiB_2}).

Coupled Decision Template (Level 2)

Given:

Target Value for Density = From Level 1 (ρ_{L1})

Target Value for Elastic Modulus =Level 1 (σ_{L1})

Range of feasible space for σ= 300-500 Mpa

Range of feasible space for ρ = 2936-3096 (kg/m^3)

Weight of Density and Elastic Modulus= (w_3, w_4)

Δx_{TiB_2} = (0.1-0)* 0.1 = 0.01(vol. fraction)

Δd = (65-45)* 0.1 = 2 (μm)

Δr = (2- 0.5)* 0.1 = 0.15(μm)

ΔT_1 = (640- 610)* 0.1 = 3(C)

$$Density(\rho) = 3097.6 - 1{,}620x_{TiB_2}$$

$$\Delta\rho = \sqrt{\left(\frac{\partial\rho}{\partial x_{TiB_2}}\Delta x_{TiB_2}\right)^2}$$

$\sigma = \sigma_y$*(1+f_1)*(1+f_d)*(1+f_orowan)

$$\Delta\sigma = \sqrt{(\frac{\partial\sigma}{\partial d}\Delta d)^2 + (\frac{\partial\sigma}{\partial r}\Delta r)^2 + (\frac{\partial\sigma}{\partial x_{TiB_2}}\Delta x_{TiB_2})^2 + (\frac{\partial\sigma}{\partial T_1}\Delta T_1)^2}$$

Find:

Location of system variable: x_{TiB_2}, d, r, T_1

Deviation variables: $d_D^-; d_D^+; d_C^-; d_C^+; d_3^-; d_3^+; d_4^-; d_4^+$

Satisfy:

System Goals

$$\frac{C_{dk}^i}{C_{dk}^{target}} + d_i^- - d_i^+ = 1 \quad for\ i = C, D.$$

$$\frac{X_i}{X_{target}} + d_i^- - d_i^+ = 1 \ for\ i = 3,4$$

System Constraints

$300 \le \sigma \le 500$ (MPa)

$2936 \le \rho \le 3096$ (kg/m^3)

$C_{dk}^i \ge 1$ For i=C,D,3,4

$$d_i^- * d_i^+ = 0;$$

$$d_i^-, d_i^+ \ge 0$$

System Bounds

$0 \le x_{TiB_2} \le 0.1$ (volume fraction)

32 µm ≤ Grain Size (d) ≤ 62 µm
0.8 µm ≤ Particulate Reinforcement size (r) ≤ 1.8 µm
610 ≤ Temperature (T_1) ≤ 634 (Degree Celsius)

Minimize

Deviation Function:

Z= $\sum w_i * (-d_i^+)$ for i=C, D, 3, 4.

3.3.3. Level 3

There are two modules in the process-structure relationship modeling level. Modules 1 and 2 are considered as Players A and B respectively. The responses of MODULE 1(A) and MODULE 3(B) are influenced by multiple variables and hence we use response surface methodology for modeling and analysis of the design task at these levels. The Response Surface Methodology employed embodies second order models:

$$Y = \beta_0 + \sum_{i=1}^{k} \beta_i x_i + \sum_{i=1}^{k} \beta_{ii} x_i^2 + \sum\sum_{i<k} \beta_{ij} x_i x_j + \varepsilon \qquad (3.13)$$

where, $\beta_{ij}, i = 1,2,...,k; j = 0,1,2,...,k$ are the regression coefficients and x_j are the regression variables, Y is the response. The Response Surfaces for MODULE 1 and MODULE 3 are generated using MINITAB®. TABLE 3.1 gives the data set of the variables used to generate the response surface of MODULE 1 i.e. response surface for Player A.

PLAYER A: MODULE 1 (Precipitation Modeling in Liquid Aluminum)

Table 3.1 Data set for MODULE 1

Volume fraction (xTiB_2, %)	Temperature (*T*, K)	Average particle radius (r, µm)
2.5	1073	0.96
5.0	1073	1.25
7.5	1073	1.22
10.0	1073	1.11
10.0	1173	1.57
10.0	1273	1.74
10.0	1373	1.80

The response surface generated for MODULE 1 is represented by the equation:

$$Y = -17.3246 + 0.2290 x_{TiB2} + 27.7783 T' - 0.0167 x_{tiB2}{}^2 - 10.4230 T'^2 \quad (3.14)$$

where *Y* is the response i.e. the average TiB_2 particle grain radius (R), x_{TiB2} is the volume fraction of TiB_2 and *T'* is T_2/1000 where T_2 is the temperature of precipitate modelling in Kelvin.

Decision Template for PLAYER A (r)

Given:

Target Value f for particulate size (r) = From Level 2 (r_{L2})

Range of feasible space for r= 0.8-1.8 μm

Δx_{TiB_2} = (0.1-0)* 0.1 = 0.01(vol. fraction)

ΔT_2 = (1373- 1073)* 0.1 = 30 (K)

$$r = -17.3246 + 0.2990 * \mathrm{x}_{\mathrm{TiB}_2} + 0.0277783 * T_2 - 0.0167 \mathrm{x}_{\mathrm{TiB}_2}{}^2 - 1.04230 * {T_2}^2 * 10^{-5}$$

$$\Delta r = \sqrt{(\frac{\partial r}{\partial x_{TiB_2}} \Delta x_{TiB_2})^2 + (\frac{\partial r}{\partial T_2} \Delta T_2)^2} \Delta r$$

$$\frac{\partial r}{\partial x_{TiB_2}} = 0.2990 - 2 * 0.0167 * \mathrm{x}_{\mathrm{TiB}_2}$$

$$\frac{\partial r}{\partial T_2} = 0.0277783 - 2 * 1.04230 * T_2$$

Find:

Location of system variable: x_{TiB_2}, T_2

Deviation variables: $d_A^-; d_A^+; d_1^-; d_1^+$

Satisfy:

System Goals

$$C_{dk}^A / C_{dk}^{target} + d_A^- - d_A^+ = 1$$

$$\frac{r}{r_{target}} + d_1^- - d_1^+ = 1$$

System Constraints

0.8 μm ≤ Particulate Reinforcement size (r) ≤ 1.8 μm

$$C_{dk}^A \geq 1$$

$$d_A^- * d_A^+ = 0; d_1^- * d_1^+ = 0;$$

$$d_A^-, d_A^+ \geq 0; d_1^-; d_1^+ \geq 0$$

System Bounds

0 ≤ x_{TiB_2} ≤ 0.1 (volume fraction)

1073 ≤ Temperature (T_2) ≤ 1373 (Kelvin)

Minimize

Deviation Function:

Z= $w_A\ (-d_A^+)+ w_1(-d_1^+)$

MODULE 3 (Semi-Solid Processing in MMCs)

Table 3.2 Data set for MODULE 3

% Volume fraction TiB_2	% Liquid	Grain Size (μm)
2.5	10	62
2.5	20	58
2.5	30	30
5.0	10	54
5.0	20	51
5.0	30	55
7.5	10	62
7.5	20	48
7.5	30	53
10.0	10	49
10.0	20	47
10.0	30	54

The response surface generated for MODULE 3 is represented by the equation:

$$Y = 80.67 - 0.167x_{TiB2} - 2.25L - 0.3067x_{ToB2}{}^2 + 0.01375L^2 + 0.202x_{TiB2}L \quad (3.15)$$

where *Y* is the response i.e., the average grain size(d), x_{TiB2} is the volume fraction of TiB_2 and *L* is the % liquid.

Decision Template for PLAYER B (d)

Given:

Target Value for grain size=Level 2 (d_{L2})

Range of feasible space for d= (32 to 62 µm)

Δx_{TiB_2} = (0.1-0)* 0.1 = 0.01(vol. fraction)

ΔL = (30- 10)* 0.1 = 2(%)

$$d = 80.67 - 0.167 * x_{TiB_2} + \quad - 2.25 * L - 0.3067\, x_{TiB_2}{}^2 + 0.01375 * L^2 + 0.202 * x_{TiB_2} * L$$

$$\Delta d = \sqrt{(\frac{\partial d}{\partial x_{TiB_2}} \Delta x_{TiB_2})^2 + (\frac{\partial d}{\partial L} \Delta L)^2}$$

$$\frac{\partial d}{\partial x_{TiB_2}} = - 0.167 - 2 * 0.3067\, x_{TiB_2} + 0.202 * L$$

$$\frac{\partial d}{\partial L} = \quad - 2.25 + 2 * 0.01375 * L + 0.202 * x_{TiB_2}$$

Find:

Location of system variable: x_{TiB_2}, L

Deviation variables: $d_B^-; d_B^+; d_2^-; d_2^+$

Satisfy:

System Goals

$$C_{dk}^B / C_{dk}^{target} + d_B^- - d_B^+ = 1$$

$$\frac{d}{d_{target}} + d_2^- - d_2^+ = 1$$

System Constraints

45 µm ≤ Grain Size (d) ≤ 65 µm

$$C_{dk}^B \geq 1$$

$$d_B^- * d_B^+ = 0; d_2^- * d_2^+ = 0$$

$$d_B^-, d_B^+ \geq 0;\ d_2^-, d_2^+ \geq 0$$

System Bounds

$0 \leq x_{TiB_2} \leq 0.1$ (volume fraction)

10 ≤ % Liquid ≤ 30 % (%)

Minimize

Deviation Function:

$Z = w_B(-d_B^+) + w_2(-d_2^+)$

Coupled Decision Template (PLAYERS A and B)

Combining the DSP's for the players A and B, a coupled cDSP is obtained as show in the Figure 3.6. The output of the coupled cDSP is the target values for volume fraction of particulate (x_{TiB_2}), temperature for precipitate modeling (T_2) and percentage of liquid (%L) in semisolid modeling. Hence a solution for the processing conditions for the microstructure is reached.

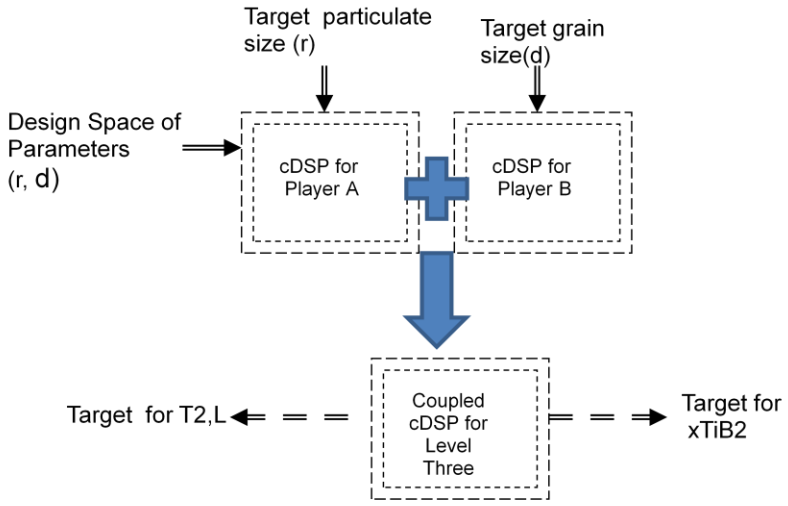

FIGURE 3.6 Coupled decision template (Players A and B)

Coupled Decision Template (Level 3)

Given:

Target Value f for particulate size (r) =Level 2 (r_{L2})

Target Value for grain size=Level 2 (d_{L2})

Range of feasible space for d= (32-62 μm)

Range of feasible space for r = (0.8 – 1.8μm)

Weight of grain size and particulate size= 0.5= (w_1, w_2)

ΔT_2 = (1373- 1073)* 0.1 = 30 (K)

Δx_{TiB_2} = (0.1-0)* 0.1 = 0.01(vol. fraction)

ΔL = (30- 10)* 0.1 = 2(%)

$$d = 80.67 - 0.167 * \mathrm{x}_{\mathrm{TiB_2}} + -2.25 * \mathrm{L} - 0.3067\, \mathrm{x}_{\mathrm{TiB_2}}{}^2 + 0.01375 * \mathrm{L}^2 + 0.202 * \mathrm{x}_{\mathrm{TiB_2}} * \mathrm{L}$$

$$\Delta d = \sqrt{(\frac{\partial d}{\partial x_{TiB_2}} \Delta x_{TiB_2})^2 + (\frac{\partial d}{\partial L} \Delta L)^2}$$

$$r = -17.3246 + 0.2990 * \mathrm{x}_{\mathrm{TiB_2}} + 0.0277783 * T_2 - 0.0167 * \mathrm{x}_{\mathrm{TiB_2}}{}^2 - 1.04230 * T_2{}^2 * 10^{-5}$$

$$\Delta r = \sqrt{(\frac{\partial r}{\partial x_{TiB_2}} \Delta x_{TiB_2})^2 + (\frac{\partial r}{\partial T_2} \Delta T_2)^2}$$

Find:

Location of system variable: x_{TiB_2}, L, T_2

Deviation variables:$d_A^-; d_A^+; d_B^-; d_B^+; d_1^-; d_1^+; d_2^-; d_2^+;$

Satisfy:

System Goals

$$\frac{C_{dk}^i}{C_{dk}^{target}} + d_i^- - d_i^+ = 1 \quad for\ i = A, B.$$

$$\frac{X_i}{X_{target}} + d_i^- - d_i^+ = 1 \ for\ i = 1,2$$

System Constraints

0.5 μm ≤ Particulate Reinforcement size (r) ≤ 2 μm

45 μm ≤ Grain Size (d) ≤ 65 μm

$C_{dk}^i \geq 1$ For i=A,B,1,2

$$d_i^- * d_i^+ = 0;$$

$$d_i^-, d_i^+ \geq 0$$

System Bounds

0 ≤ x_{TiB_2} ≤ 0.1 (volume fraction)

1073 ≤ Temperature (T_2) ≤ 1373 (Kelvin)

10 ≤ % Liquid ≤ 30 % (%)

Minimize

Deviation Function:

Z= $\sum w_i$*($-d_i^+$) for i=A,B,1,2

3.3.4. Coupling of Level 2 and 3

It is seen that x_{TiB_2} is an input parameter to Players A and B at Level 3 and Players C and D at Level 2. If the top-down approach is followed, iteration becomes necessary to converge to a solution for x_{TiB_2}; i.e. the volume fraction of the composite. Instead the two levels of design are coupled as shown in the figure and formulate a coupled cDSP for Level's 2 & 3. The hierarchical optimization solution strategy in JAVA DSIDES is used with Level 2 as the Top Level and Level 3 as the bottom level. This helps us avoid iterating between Level's 2 and 3 and a solution is reached quickly. This can be abstracted as a Stackelberg Leader-Follower Protocol in game theory. Solving this cDSP one arrives at the processing conditions for the microstructure; i.e. target values for volume fraction of particulate (x_{TiB_2}), temperature for precipitate modeling (T_2)and percentage of liquid in semisolid modeling (%L).

Coupled Decision Template (Level 2 and 3)

Given:

Target Value for Density = From Level 1 (ρ_{L1})

Target Value for Elastic Modulus =Level 1 (σ_{L1})

Range of feasible space for σ= (300 to 500) MPa

Range of feasible space for ρ= From Level 1. (2936.2-3096)

Weight of Density and Elastic Modulus= (w_3, w_4)

ΔT_2 = (1373- 1073)* 0.1 = 30 (K)

Δx_{TiB_2} = (0.1-0)* 0.1 = 0.01(vol. fraction)

ΔL = (30- 10)* 0.1 = 2(%); ΔT_1 = (640- 610)* 0.1 = 3(C)

$$Density(\rho) = 3097.6 - 1{,}620x_{TiB_2}$$

$$\Delta\rho = 16.2$$

σ= σ_y(1+f_1)*(1+f_d)*(1+f_orowan)*

$$\Delta\sigma = \sqrt{(\frac{\partial\sigma}{\partial d}\Delta d)^2 + (\frac{\partial\sigma}{\partial r}\Delta r)^2 + (\frac{\partial\sigma}{\partial x_{TiB_2}}\Delta x_{TiB_2})^2 + (\frac{\partial\sigma}{\partial T_1}\Delta T_1)^2}$$

$$d = 80.67 - 0.167 * \mathrm{x}_{\mathrm{TiB_2}} + -2.25 * \mathrm{L} - 0.3067\,\mathrm{x}_{\mathrm{TiB_2}}{}^2 + 0.01375 * \mathrm{L}^2 + 0.202 * \mathrm{x}_{\mathrm{TiB_2}} * \mathrm{L}$$

$$\Delta d = \sqrt{(\frac{\partial d}{\partial x_{TiB_2}}\Delta x_{TiB_2})^2 + (\frac{\partial d}{\partial L}\Delta L)^2}$$

$$r = -17.3246 + 0.2990 * \mathrm{x}_{\mathrm{TiB_2}} + 0.0277783 * T_2 - 0.0167 * \mathrm{x}_{\mathrm{TiB_2}}{}^2 - 1.04230 * T_2{}^2 * 10^{-5}$$

$$\Delta r = \sqrt{(\frac{\partial r}{\partial x_{TiB_2}}\Delta x_{TiB_2})^2 + (\frac{\partial r}{\partial T_2}\Delta T_2)^2}$$

Find:

Location of system variable: $x_{TiB_2}, T_2, T_1, \%L$

Deviation variables: $d_C^-; d_C^+; d_D^-; d_D^+; d_3^-; d_3^+; d_4^-; d_4^+$

Satisfy:

System Goals

$$\frac{C_{dk}^i}{C_{dk}^{target}} + d_i^- - d_i^+ = 1 \quad for\ i = A, B, C, D.$$

$$\frac{X_i}{X_{target}} + d_i^- - d_i^+ = 1 \ for\ i = 3{,}4$$

System Constraints

300 ≤ σ ≤ 500 (MPa)

2936.2 ≤ ρ ≤ 3096 (kg/m^3)

$C_{dk}^i \geq 1$ For i=A,B,C,D,3,4

$$d_i^- * d_i^+ = 0;$$

$$d_i^-, d_i^+ \geq 0$$

System Bounds

$0 \leq x_{TiB_2} \leq 0.1$ (volume fraction)

32 µm ≤ Grain Size (d) ≤ 62 µm
0.8 µm ≤ Particulate Reinforcement size (r) ≤ 1.8 µm
610 ≤ Temperature (T_1) ≤ 634 (Degree Celsius)

Minimize

Deviation Function:

Z= $\sum w_i*(-d_i^+)$ for i=A,B,C,D,3,4

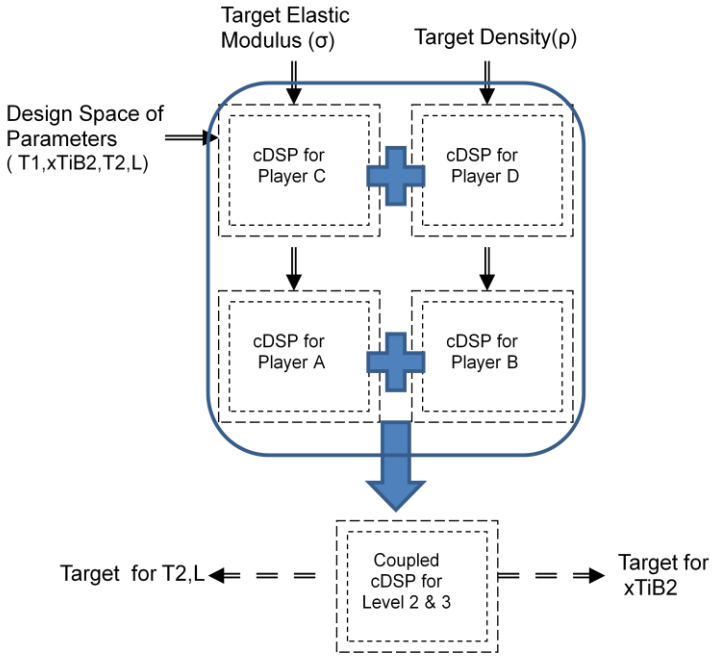

FIGURE 3.7: Coupled decision template (Players A, B, C, D)

Table 3.3 provides a summary of the variables used in the game theoretic formulation. Table 3.4 provides a summary of the Targets and Ranges for each of the Players. NA refers to Not Applicable. Table 3.5 provides a summary of the independent variables, and the modules and corresponding players they are input to.

Table 3.3: List of variables in game formulation

Player	Parameter	Weight Target	Weight DCI	Deviation Targets	Deviation DCI	Level
A	r	w_1	w_A	d_1^-, d_1^+	d_A^-, d_A^+	3
B	d	w_2	w_B	d_2^-, d_2^+	d_B^-, d_B^+	3
C	σ	w_3	w_C	d_3^-, d_3^+	d_C^-, d_C^+	2
D	ρ	w_4	w_D	d_4^-, d_4^+	d_D^-, d_D^+	2
E	h	w_5	w_E	d_5^-, d_5^+	d_E^-, d_E^+	1
F	W	w_6	w_F	d_6^-, d_6^+	d_F^-, d_F^+	1
G	T_{opr}	w_7	w_G	d_7^-, d_7^+	d_G^-, d_G^+	1

Table 3.4: List of targets and ranges

Player	Parameter	Targets	Ranges	Constraint	Level
A	r	r_{L2}	(0.8,1.8)µm	NA	3
B	d	d_{L2}	(32,62) µm	NA	3
C	σ	σ_{L1}	(300,500) MPa	NA	2
D	ρ	ρ_{L1}	(2936,3096)kg/m^3	NA	2
E	h	3500 m	(2000,5000) m	≥2000m	1
F	W	16 kgf	(7,25)kgf	≤25kgf	1
G	T_{opr}	12 hrs.	(0,15)Hrs	≥10 Hrs.	1

Table 3.5 List of independent input variables

Variable	Range	Input Module	Input Player
x_{TiB_2}	(0.02,0.1)%	1,3,4	A,B,C,D
T_2	(1073,1373) K	1	A
T_1	(610,634) C	4	C
%L	(10,30) %	3	B
t	(5,15)mm	5	E,F,G

3.4. Discussion of Results

Performance target requirements at Level 1 for the underwater submersible include:

- The safe depth of operation of the submersible with a small shell thickness should be as large as possible preferably exceeding 2000 meters and the desired target depth is 3500 meters.
- The submersible must have a good endurance with a large time of operation of at least 10 hours without resurfacing or recharging and greater duration of submersion is better.
- Given a weight of the vessel of 76 Kgs and allowing as large a payload as feasible, a representative limit the weight of the outer shell of the submersible may not exceed 25 Kgs, and a lighter shell is preferred.

The cDSP's has been implemented in JAVA DSIDES® for this application.

3.4.1. Level 1 Result

For the coupled decision template at Level 1 ; the range for input variables are derived as 5-15(mm), 2936.2-3096 (kg/m^3), 300-500 (MPa), *for thickness(t), density of composite (ρ) and yield stress (σ)* respectively [Table 3.4,3.5]. The weights for the deviation variables (Targets and Design Capability Index) and the target values for the parameters at Level 1 are displayed in Table 3.6.

Table 3.6: Weights for coupled cDSP Level 1

Player	Parameter	Weight for Targets	Weight for DCI	Target	DCI Target	Level
E	h	0.1666	0.1666	$3500\ m$	8	1
F	W	0.1666	0.1666	16 kgf	8	1
G	T_{opr}	0.1666	0.1666	12 hrs	8	1

Table 3.7: Hierarchical formulation for coupled cDSP Level 1

Player	Variable	Weight	Target	Level
E	d_5^-	0.5	3500	1
	d_E^-	0.33	8	2
F	d_6^-	0.25	16	1
	d_F^-	0.33	8	2
G	d_7^-	0.25	12	1
	d_G^-	0.33	8	2

Table 3.8: Results for Coupled cDSP Level 1

Input/Output	Variable	Value	
Input	t	7.861mm	
	ρ	2936.2 kg/m^3	
	σ	500 MPa	
Output	Player	Variable	Value
	E	Depth (h)	2915.96 m
		C_{dk}^E	2.38
	F	Weight (W)	19.464 kgf
		C_{dk}^F	8.00
	G	Time(T_{opr})	11.83 hrs
		C_{dk}^G	2.83

These weights and the target values represent one design scenario. The designers (Player E, F and G) at Level 1 have the autonomy to tailor the weights and target values as per the design requirement and investigate other design scenarios. Also, instead of a single deviation function that captures all the deviation variables, two deviation functions can be set up hierarchically, where the first deviation function addresses the maximization of target achievement and the second deviation function tackles with design freedom optimization. This feature of hierarchical deviation functions is embedded in JAVA DSIDES®. An illustrative Table 3.7 is presented. We realize that the game theoretic formulation gives the designers at Level 1, the autonomy to control the design evolution via 12 control variables, (6 target values, i.e., 2 for each player E, F

and G, i.e., the target for design capability indices (DCI's) and target for performance requirement. The solution for the coupled cDSP at Level 1 with weights as per Table 3.6 has been displayed in Table 3.8. The input values to Level 1 set the target values for the coupled cDSP for Levels 2 and 3. Hence the target for Player D (*ρ)* is 2936.2 kg/m^3 and for Player C (*σ*) is 500 MPa. We now proceed to the Level 2 result for the illustrative microstructure mediated design of underwater submersible.

3.4.2. Level 2 and 3 Results

For the coupled decision template for Level 2 and 3; the range for input variables are 2-10(%), 610-634(C), 1073-1373 (K) and 10-30(%) for the volume fraction of TiB_2 ($xTiB_2$), processing temperature for Module 4 (T_1), processing temperature for Module 1 (T_2) and liquid percentage for semisolid processing (%L) respectively. The weights assigned and the target values along with the level for hierarchical optimization for the parameters at Level 2 are displayed in the Table 9. The justification for the levels of hierarchical optimization is that for the coupled cDSP for Level's 2 and 3; the primary objective is the attainment of the target values for *ρ (Player D) and σ (Player C)* derived from the Level 1 cDSP solution. The DCI metric associated with Level 2, i.e. , C_{dk}^{C} and C_{dk}^{D} are maximized before maximization of DCI metrics associated with Level 3, i.e., C_{dk}^{A} and C_{dk}^{B} .This is because Level 2 dominates Level 1 for our top down inductive method. This can also be understood from the interpretation that Level 2 acts as a leader and Level 3 as a follower. Hence the variables ρ *and σ* are at the top level for deviation function minimization; C_{dk}^{C} and C_{dk}^{D} are assigned level 2 and C_{dk}^{A} and C_{dk}^{B} are assigned level 3.Again it is seen that the game theoretic formulation gives the designers at Level 2and 3, the autonomy to control the design solution via 10 control variables, i.e., 6 weights for deviation variables and 4 target values for C_{dk}^{i} ; i=A, B, C, D. The solution for the coupled DSP for Levels 2 & 3 has been displayed in Table 3.10.

Table 3.9 Hierarchical formulation: Coupled cDSP level 2and 3

Player	Variable	Weight	Target Value	Level
C	d_C^-	0.5	500 MPa	1
	d_3^-	0.5	8	2
D	d_D^-	0.5	2936.2 kg/m^3	1
	d_4^-	0.5	8	2
A	d_A^-	0.5	8	3
B	d_B^-	0.5	8	3

Table 3.10 Results for coupled cDSP Level 2 and 3

Input/Output	Variable	Value	
Input	xTiB2	0.0996	
	T_2	1143.18 K	
	$\%L$	15.26 %	
	T_1	634 deg C	
Output	Player	Variable	Value
	C	Elastic (σ)	499.9 MPa
		C_{dk}^C	1
	D	Density (*ρ*)	2936.2 kg/m^3
		C_{dk}^D	1
	A	C_{dk}^A	2.53
	B	C_{dk}^B	5.303

As both the Players D (*ρ) and C (σ) variables c*an independently achieve their respective target values as dictated by the Level 1 solution, the final performance values are the same as in Table [3.8]. Else we would have had to recalculate the final performance values for the achieved *ρ, σ* output values at Level 1. Based on obtained solution sets, designers may have more freedom for

choosing their decisions, emphasizing product performance, achieving robustness against MSU, or compromising between them.

3.5. Thoughts on What has been Presented and What is Next

The complexity of modern product realization processes requires multidisciplinary collaboration. Principles from game theory are used to model the relationships between engineering teams and facilitate collaborative decision making, and use design capability indices to help maintain design freedom. In this chapter the design construct for multi-level design is introduced using game theoretic protocols of cooperation and leader-follower mechanism. A methodology is presented to pursue concurrent decision making under in design for an underwater submersible and Al-based metal matrix composite that embodies the microstructure-mediated robust design construct. The principal challenge involved is the performance target achievement in over seven empirical and theoretical models over three levels of design. Starting from a hull thickness parameter in MODULE 5, the feasible design spaces for the mechanical properties are identified using design capability indices. A cooperative solution is reached using the cDSP's for Level 1 and Level 2and 3. Based on our observations it is summarized that the advantages of the game based approach for the proposed multilevel design for the product realization of underwater submersible:

- Interdisciplinary iterations between uncoupled design levels are eliminated, which can greatly reduce the computing cost in multidisciplinary product realization. There are no iterations between modules or levels. This limits the complexity of the decision making process.
- Each team (player) holds its own cost function and makes decisions in its own discipline. Hence, the game based approach greatly increases the autonomy and independence of the disciplinary teams and enables higher parallelism.

- The game theoretical protocols are appropriate to model the relationships between engineering teams, and enable collaborative decision making based on the cooperation styles between teams. JAVA DSIDES is efficient for solving the derived cDSP's as it offers the provision for hierarchical optimization.
- Most importantly, the construct introduced in this chapter can be applied to any complex product. Upstream teams make decisions that remain superior even though the requirements of the downstream teams are yet unknown. Downstream teams can specify final solutions without jeopardizing the satisfaction of the design requirements in upstream activities. Hence, engineering teams can keep the product realization problem open in the early stages of product realization, and make decisions that are superior from the perspective of all disciplines.

In closing, it is noted that compared to other approaches my method does not necessarily lead to a better design. However, for multilevel design tasks especially in the early stages of product realization, the proposed construct is deemed efficient. It is suggested that my method is more practical in the design of multiscale systems. My method also establishes the soundness of using cDSP for design of multiscale systems. IDEM provides ranged sets of solutions as described in the previous chapter and cDSP has potential to manage uncertainty and identify a single best solution from these ranged sets of solution. In this chapter it identifies the best solution by compromising performance achievement and robustness in terms of the DCI metric. Having established the framework for multilevel design using IDEM in the previous chapter and cDSP in this chapter, we proceed to understanding the research gaps and formulate the research questions. The IDEM and cDSP constructs are coupled in Chapter 5 for improved robustness formulate for microstructure mediated design.

This chapter also ties to Quadrant II of the validation square as it establishes the internal consistency of the cDSP used in developing the methods for multiscale systems in Chapters 5 and 6. Figure 3.9 represents the organization of work up to this point in the thesis.

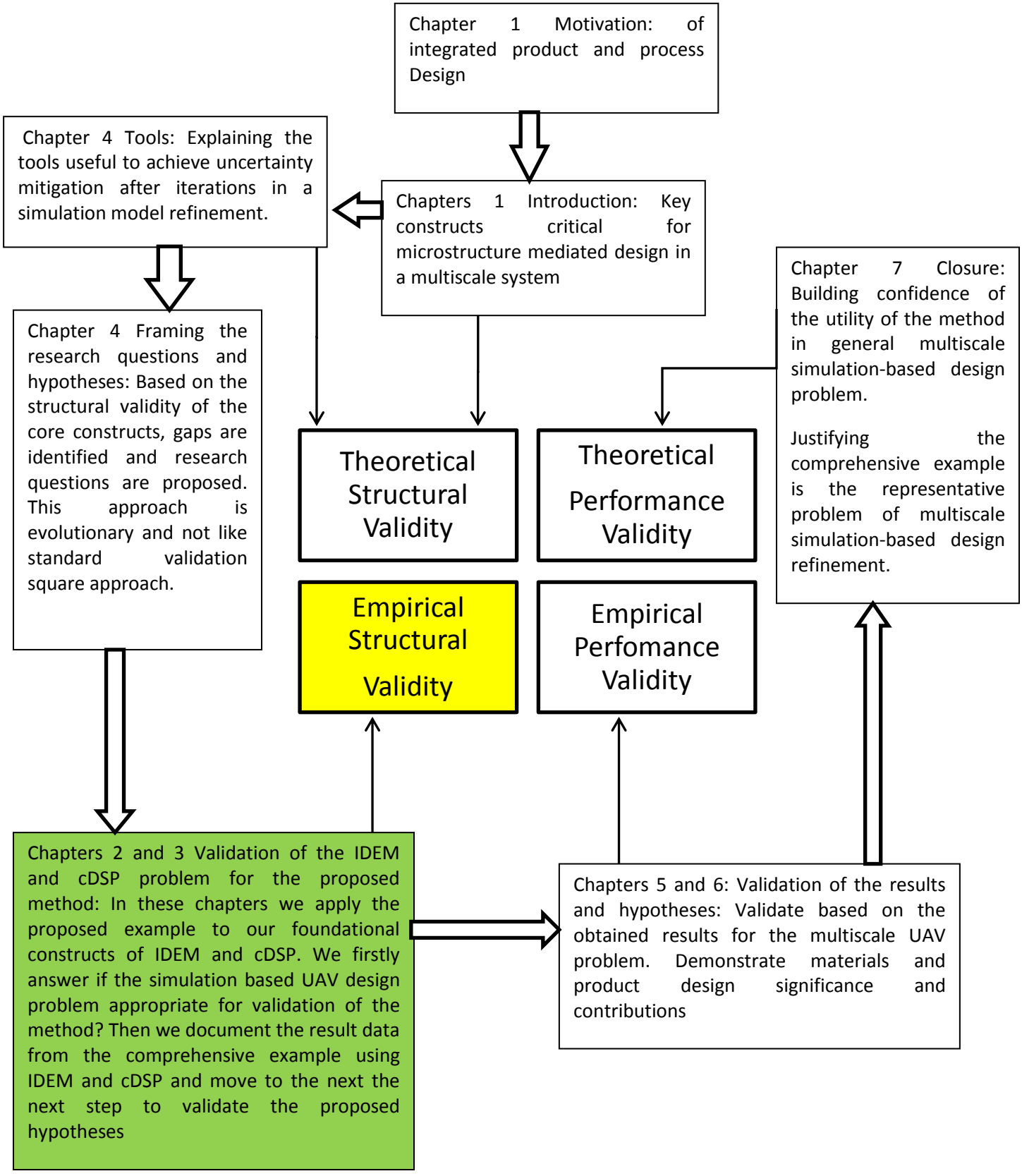

Figure 3.8: The validation square

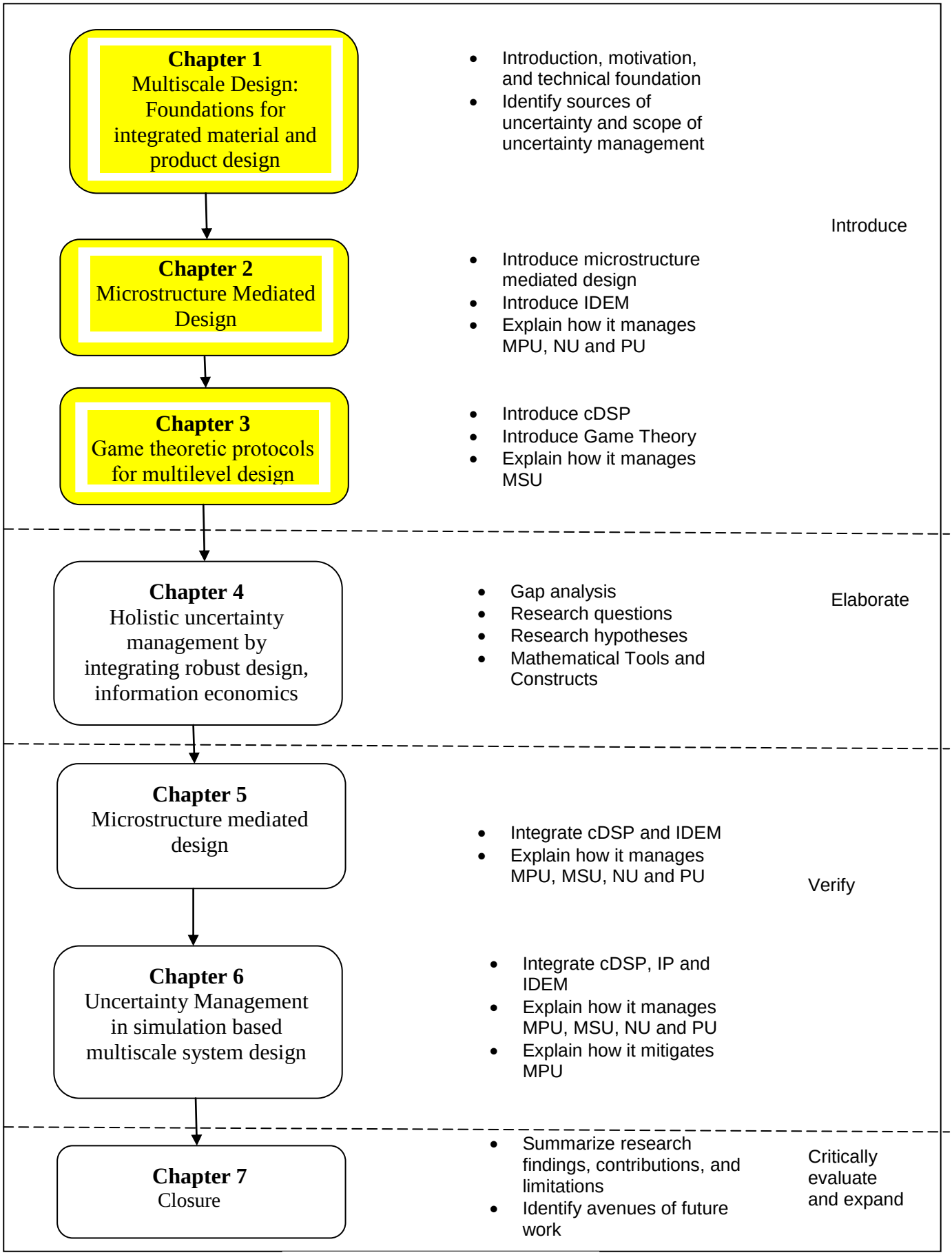

Figure 3.9: Organization of work

CHAPTER 4

HOLISTIC UNCERTAINTY MANAGEMENT BY INTEGRATING ROBUST DESIGN AND INFORMATION ECONOMICS

In this chapter the challenges for design of multiscale systems are reviewed in context of the methods developed in Chapters 2 and 3 and research gaps are identified. The research questions are framed, propose posits to answer them and briefly discuss the overview for the work. The tools used in this work are briefly discussed: the design of experiments, response surface models and value of information.

4.1. Gap Analysis and Research Questions

4.1.1. Gap Analysis

In this section, the gaps in the current research methods for uncertainty management are identified with respect to the challenges identified in Chapter 1. The challenges identified in Section 1.1 with respect to multiscale systems are restated in Table 4.1

Table 4.1: Challenges in design of multiscale systems

a. Balancing the prediction accuracy with computational cost
b. Modeling physical phenomena and interaction between scales
c. Collaborative decision making
d. Collaborative computational infrastructure
e. Managing uncertainty and its propagation
f. The inverse problem

The biggest challenge identified was that of balancing prediction accuracy with computational cost. We saw in Chapter 2 that IDEM facilitates robust decision making in presence of uncertainty and has the capability to tailor prediction accuracy based on the EMI metric. However, it does not account for computational cost for predictions. It also does not provide any means to increase the accuracy. This challenge remains unanswered and is identified as a research gap. The second challenge is alleviated using IDEM as it lays a framework for domain independent modeling of physical phenomena and can account for interdependency amongst linkages in the design chain. Though cDSP allows for collaborative decision making in a multiscale environment as seen in Chapter 3, its integration with IDEM remains to be validated and hence addressing challenge 3, that of collaborative decision making. IDEM diminishes the need for a collaborative computational architecture as its uses mapping models in the form of response surfaces in lieu of simulation models to map between the hierarchical scales. We saw in Chapters 2 and 3, that IDEM was used to successfully manage model parameter uncertainty, propagated uncertainty and natural uncertainty. In addition use of IDEM also establishes the degree of model structure uncertainty which is difficult to quantify unlike the other types of uncertainty. It does so in the form of a HD-EMI metric which defines the reliability of a system model under potential shift of output response due to model structure uncertainty. This metric can be used in cDSP to reach a compromise for its level of attainment and hence manage MSU. However, the integration of IDEM and cDSP relevant to microstructure mediated design (MMD) remains to be validated. Use of IDEM answers the inverse problem by establishing second order mapping models between the input and output response and hence assists in inverse design space exploration. However, it is not explicitly defined in scope of IDEM and this needs to be illustrated with respect to MMD. Based on this discussion, the following gaps are identified for uncertainty management of multiscale systems.

- ***Clarification of multilevel design*****:** Clear definition of the multilevel design and difference from multiscale systems modeling is not clear. Also difference between multiscale modeling and multilevel design for multidisciplinary systems in terms of

hierarchical material design and Olson diagram is not clear from literature and the cDSP and IDEM approaches. Specifically, the inverse problem challenge of multiscale systems needs to be addressed with respect to microstructure mediated design. The presence of decision nodes that arise due to multiscale modeling for multilevel design of systems need to instantiated with respect to material design hierarchy.

- ***Clear definition of the mathematical challenges for uncertainty management and uncertainty mitigation in simulation based multiscale systems***: The discussion of the mathematical challenges for uncertainty management in hierarchical material design using simulation models is scattered throughout literature and not explicit. Chapters 2 and 3 addressed two key components of uncertainty management through robust design. In Chapter 2, the IDEM approach focused on managing modeling uncertainty as it propagates through the design chain. However, explicit modeling of the model parameter uncertainty and natural uncertainty were not discussed and addressed briefly. In Chapter 3, the cDSP approach was tested for collaboratively tailoring the DCI metric to suit management of model structure uncertainty. However, a unified approach which addresses all four types of uncertainty in multiscale systems needs to be established. Also the challenges of methods for mitigating uncertainty in an adaptive way by considering the current prediction accuracy of the multiscale system and scope of further refinement are not found in literature.

- ***Generality of the IDEM*****:** IDEM has not been tested for general design problems that do not necessarily have a one-to-one mapping between variable spaces. IDEM can be used for many-to-one mappings implying multiple solutions in the inverse exploration. Also the question of coming up with a singular solution in presence of multiple solutions arises. MMD is an example to this end. Use of IDEM can find ranged sets of solution; however for general applicability suitable for both initial design space exploration as well as final robust solution, it needs to be extended in order to come up with a singular

solution from the ranged sets of solution. The cDSP approach gives us insight to achieve this.

- ***Establishment of the compatibility between the decision formalisms of value-of-information and robust design*:** In the first chapter it is discussed that multiscale systems are generally a compilation of interlinked simulation models with high computational expense. Hence, acquiring large data sets for uncertainty mitigation is not feasible. Hence current methods like kriging or Monte Carlo simulation are not feasible. It is hypothized that an adaptive formulation for uncertainty mitigation is feasible by acquiring insight into the current multiscale system performance as well as the scope for uncertainty reduction based on value of additional information. Uncertainty mitigation using robust design and information economics raises the question about the compatibility between the decision formulations of robust design and utility theory. Robust design involves finding solutions insensitive to uncertainty while traditional value of information approaches use utility theory to derive an improvement potential metric which focuses on maximization of expected utility. Clearly, optimization and robustness are incompatible and warrants further investigation. Hence, a framework needs to be developed to integrate robust design and information economics in order to achieve uncertainty reduction and move towards holistic uncertainty management, i.e., achieve robustness along with uncertainty reduction.

- ***Formulation of a fundamental, rigorous definition of the tradeoff problem*:** Computational expense or cost will be the common platform for determining the value of information metric for further simulation refinement. A trade-off will need to be achieved between prediction accuracy and computational cost as described in one of the challenges. The proposed method of trading off value versus effort is not found in the literature. It needs to be addressed by establishing a) an approach for quantifying

the effort, and b) a rigorous definition of the tradeoff problem, and c) an approach for making the tradeoff decisions.

- *Justification of the use of information economics over existing techniques*: Information economics uses utility theory to predict the expected value of information. Improvement potential metric was defined for use to engineering systems and applicability to design problem. However, this metric has several shortcomings. The most important one is that it ignores the expected value of information, i.e., it only quantifies the scope of improvement but does not quantify the reduction of the improvement potential metric with additional information. This is identified as a research gap and warrants the improvement potential metric to be extended to suit expected value of information as well as applicability to robust multiscale systems design.

4.1.2. Research Questions and Hypotheses

After having identified the research gaps with respect to multiscale systems the research questions are developed. In Chapters 2 and 3, IDEM and cDSP were structurally validated for application to simulation-based multiscale systems. IDEM successfully provides us ranged sets of solution robust against modeled and propagated uncertainty and also provides a metric for managing model structure uncertainty which is hard to quantify in terms of the developed HD-EMI metric. In Chapter 2, the EMI metric was used instead of HD-EMI metric to simplify the problem at hand though successfully demonstrating its ability to handle model structure uncertainty in terms on constraints placed on the EMI values. In Chapter 3, the cDSP was used in a collaborative game theoretic setting to investigate its applicability to model decisions in a multiscale system. cDSP performed a trade-off between performance achievement and DCI metric which is a alternative formulation to the EMI metric. cDSP arrived at a single solution and hence showed potential to arrive at a single solution from ranged sets of solution if used in

conjunction with the IDEM. However, neither the cDSP not the IDEM provided means for reducing uncertainty in the simulation models. Reducing uncertainty is critical if the initial robust space exploration does not yield sufficiently robust solutions. Hence, the primary research question is formulated as:

Primary Research Question
How does one manage and mitigate uncertainty in simulation-based multiscale systems?

The primary research question has two elements for handling uncertainty- manage and mitigate. The management is achieved through robust design and the mitigation has not been addressed. Hence two research hypotheses for answering the primary research question are formulated as:

1. Integrating constructs from robust design and decision support systems can manage uncertainty

2. Integrating constructs from robust design, information economics and decision support systems can mitigate uncertainty.

IDEM is a robust design method and cDSP falls in the class of decision support systems. Hence it is hypothized that integrating constructs from robust design can help us achieve ranged sets of robust solutions as identified in IDEM and decision support systems can aid in arriving at a single solution from the ranged sets of solution as identified in cDSP. Information economics is the study of value of information. Robust design integrated with decision support systems can identify the best solution for the multiscale system in its current configuration. The system and the associated subsystem simulation models can be viewed as sources of information and a designer can investigate the value additional information from the simulation models has on the overall system performance. To this end, information economics can aid in analyzing the value of additional data from the simulation models in respect to computational time. The objective is to minimize the utilization of computational resources while achieving the maximum benefit from additional data on the system level performance. Hence, for mitigating uncertainty it is

hypothized that integrating constructs from robust design, decision support systems and information economics will aid in systematic reduction of uncertainty.

To manage uncertainty, one of the secondary research questions is formulated as:

Secondary Research Question 1
How can we address model parameter uncertainty, model structure uncertainty, natural uncertainty and propagated uncertainty in multiscale systems?

In Chapter 1, types of uncertainty in multiscale systems were identified as model parameter uncertainty (MPU), model structure uncertainty (MSU), natural uncertainty (NU) and propagated uncertainty (PU). IDEM was verified for managing modeled uncertainty and propagated uncertainty in multiscale systems. However, detailed understanding of modeling uncertainty was not developed. IDEM also provides a metric for managing model structure uncertainty which cannot be modeled in terms of the HD-EMI metric. Arriving at a small set of ranged solution from which the best robust solution can be identified by tailoring the HD-EMI metric was identified as a time-intensive and rigorous task especially as the nature of uncertainty propagation along a complex chain of interlinked models is difficult to comprehend. cDSP was successfully employed to identify single robust solutions by achieving a trade-off between system performance and robustness in terms of the DCI metric. Hence based on this understanding, the following hypotheses are formulated to manage all four kinds of uncertainty in simulation-based multiscale systems for multilevel design:

- IDEM incorporates MPU, NU and PU to give feasible solution sets.
- IDEM develops HD-EMI metric to manage MSU.
- cDSP can used to reach a trade-off amongst HD-EMI values to mange MSU and hence give a single robust solution against MSU, MPU, NU and PU.

Natural uncertainty can be statistically modeled. MPU can be modeled in terms of confidence intervals for the mean metamodel. Thus the mean metamodel along with uncertainty bounds can incorporate the uncertainty due to NU and MPU. This integrated metamodel can serve as the mapping function for multiscale materials design as per Olson's diagram. Propagated uncertainty is minimized by developing exact constraint boundaries in IDEM. The HD-EMI metric is a metric that establishes the reliability of a decision under potential shifts of a model response due to MSU. Hence IDEM can provide robust sets of solution against modeled MPU, NU and PU as well as provides the HD-EMI metric for managing unquantifiable MSU. The cDSP is used to tailor the HD-EMI values from the simulation models in order to reach a single robust solution from the ranged sets of robust solutions identified using IDEM.

For uncertainty mitigation, the second secondary research question is formulated as:

Secondary Research Question 2

How does the system level designer allocate resources for auxiliary simulations based model refinement while ensuring satisfaction of system level design objectives and product requirements in a multiscale integrated product and material design**?**

If the identified robust solution does not meet the standards, auxiliary or additional simulation runs need to be executed to gather additional information about the model and hence contribution to uncertainty mitigation. In order to achieve this, my approach is to integrate the two constructs of robust design and information economics in multiscale simulation based design and reach a trade-off for simulation based model refinement. Ranged sets of robust solution are first identified using concepts from IDEM. At the identified feasible points value of information is defined in terms of the additional information required to reduce the error bounds in the metamodel. To do this, the value of information is defined in terms of improvement potential metric with respect to the model parameter uncertainty in the simulation model. NU is ignored because it cannot be mitigated. Simplistic cost functions are developed which capture the computational effort in reducing the error bounds for the

simulation models. Optimization techniques are then used to reach a trade-off between the cost functions and model refinement to allocate the limited resources to the individual simulation models in the multilevel design. The hypotheses for uncertainty mitigation through resource allocation are:

- Integrating IDEM and cDSP facilitates obtaining a single robust solution against all forms of uncertainty.
- Response surface modelling facilitates defining the improvement potential metric in terms of confidence intervals for mitigating MPU.
- Concepts from value of information and response surface modelling can be integrated to develop predicted improvement potential and corresponding cost functions
- Optimization techniques can be used to reach a trade-off among cost functions.

Based on the hypotheses for the secondary research question 1, it is hypothized that integrating IDEM and cDSP will identify a single robust solution against MPU, NU, MSU and PU as well identify ranged sets of solution robust against MPU, NU and PU. NU is irreducible and PU is in effect a compounded effect of the other three kinds of uncertainty. Individual mitigation of the other 3 kinds will translate into mitigation of PU. Though an element of PU appears at constraints boundaries due to discretization resolution in the IDEM, understanding the value of information for mitigating PU due to discrete resolution is not taken up. Instead it is proposed in future work. MSU and MPU are the two kinds of uncertainty that arise due to incomplete knowledge of the simulation model. MSU arises due to simplifications or assumptions in simulation modeling and mitigating MSU would mean a rigorous understanding of underlying assumptions and its effect of simulation model response. This is a challenging task and is not the focus of this thesis. In this study, the focus is on mitigating MPU which arises due to insufficient information from the simulation models. This insufficient information correlates to larger statistical error bounds or confidence intervals. Hence, the improvement potential metric is

defined so as to capture the degree of MPU in terms of the statistical confidence intervals. Value of information constructs are used to understand the behavior of the confidence intervals with additional data and a correlation is developed between additional data points and improvement potential for the simulation model. Optimization techniques are used to derive maximum benefit in terms of improvement potential metric while minimizing the computational resource. Hence it is hypothized that successful integration of response surface modeling with improvement potential metric can aid in developing accurate cost functions for efficient resource allocation. This will ensure benefit of system level performance while ensuring reduction in MPU. The primary and secondary research questions along with their associated hypotheses are illustrated in Table 4.2. Table 4.3 represents the connectivity between the research questions and the sections they are answered. In this table observed refers to the establishing the theoretical understanding, reflected refers to establishing the connectivity between the established construct and the proposed method. Articulated refers to arriving at results using the proposed hypotheses in context of out example problem of design of AUV using metal matrix composites. This is a representative example for multiscale systems with microstructure mediated design approach.

Table 4.2: Research questions and hypotheses

Research Questions		**Research Question:** How does one manage and mitigate uncertainty in simulation-based multiscale systems?
		Hypothesis: 1. Integrating constructs from robust design and decision support systems can manage uncertainty 2. Integrating constructs from robust design, information economics and decision support systems can mitigate uncertainty.
		Research Question 1: How can we address model parameter uncertainty, model structure uncertainty, natural uncertainty and propagated uncertainty in multiscale systems?
		Hypothesis: 1.1 IDEM incorporates MPU, NU and PU to give feasible solution sets. 1.2 IDEM develops HD-EMI metric to manage MSU 1.3 cDSP can used to reach a trade-off amongst HD-EMI values to mange MSU and hence give a single robust solution against MSU, MPU, NU and PU.
		Research Question 2: How does the system level designer allocate resources for auxiliary simulation based model refinement while ensuring satisfaction of system level design objectives and product requirements in a multiscale integrated product and material design**?**

Table 4.2 continued

		Hypothesis: 2.1 Integrating IDEM and cDSP facilitates obtaining single robust solution against all forms of uncertainty. 2.2 Response surface modeling facilitates defining the improvement potential metric in terms of confidence intervals for mitigating MPU. 2.3 Concepts from value of information and response surface modeling can be integrated to develop predicted improvement potential and corresponding cost functions 2.4 Optimization techniques can be used to reach a trade-off among cost functions.

Table 4.3: Connectivity of research questions and chapters

	Hypothesis	**Chapters Observed**	**Chapters Reflected**	**Chapters Articulated**
RQ: How does one manage and mitigate uncertainty in simulation-based multiscale systems?				
H 1	Uncertainty management	4.1, 5.1	5.2, 5.3	5.3, 5.4
H 2	Uncertainty mitigation	4.1, 6.1	6.2, 6.3	6.3, 6.4
RQ1: How can we address model parameter uncertainty, model structure uncertainty, natural uncertainty and propagated uncertainty in multiscale systems?				
H 1.1	IDEM	5.2	5.3	5.3,5.4
H 1.2	HD-EMI	5.2	5.3	5.3,5.4
H 1.3	cDSP	5.2	5.3	5.3,5.4

Table 4.3 continued

RQ2: How does the system level designer allocate resources for auxiliary simulation based model refinement while ensuring satisfaction of system level design objectives and product requirements in a multiscale integrated product and material design**?**				
H 2.1	IDEM and cDSP	6.2	6.3	6.3, 6.4
H 2.2	Improvement Potential	6.2	6.3	6.3, 6.4
H 2.3	Cost functions	6.2	6.3	6.3, 6.4
H 2.4	Constraint Optimization	6.2	6.3	6.3, 6.4

4.2. LITERATURE REVIEW

The tools to answer the research gaps are the research questions are briefly presented in this section. The constructs and tools used in robust design and information economics are discussed, i.e., design of experiments, response surface modeling and value of information metric referred to as the improvement potential metric. The tools and constructs developed in this section will be used in the remainder of my thesis in Chapters 5 and 6.

4.2.1 Design of Experiments

There are several strategies for the design of experiments like Latin hypercube design, full factorial design, Box-Behnken design, central composite designs etc [59]. Of these, Central composite designs (CCDs) are most popular for building second order response surface models. Central composite designs (CCDs) are used, for calibrating the full quadratic response surface models (RSM) from the simulation models at the subsystem level. A CCD design with axial, center and cube points for a simulation experiment with three parameters in shown in Figure

4.1. A brief description of the procedure for evaluating the design points in CCDs follows. For details of CCD's refer [60,61]. The design matrix for a CCD experiment involving *k* factors is derived from a matrix, **d**, containing three parts. These three parts may vary depending on the type of simulation runs [62]:

1. The matrix **F** obtained from the factorial experiment of the design variables. The factor levels are scaled so that its entries are coded as +1 and −1.
2. The matrix of the center points is represented as **C**. The factor levels will all be coded as 0, i.e., (0, 0, 0... 0), where there are *k* zeros.
3. The third matrix **E** comes from the axial points, with 2*k* rows. For every factor there is a ±α point while assigning 0 to all the other factors. The **E** matrix for the central composite design is represented in Figure 4.2. The flexibility of choosing the α value lies with the designer. A CCD design (d matrix) with three variables is shown in Figure 4.2 However, to make the CCD design rotatable we have to choose specific values of value α given by the formula $\alpha = F^{1/4}$, where F is the number of design variables. These values are represented in Table 4.4. Finally I vertically concatenate these three matrices into the **d** matrix i.e.

d = [F C E]' (4.1)

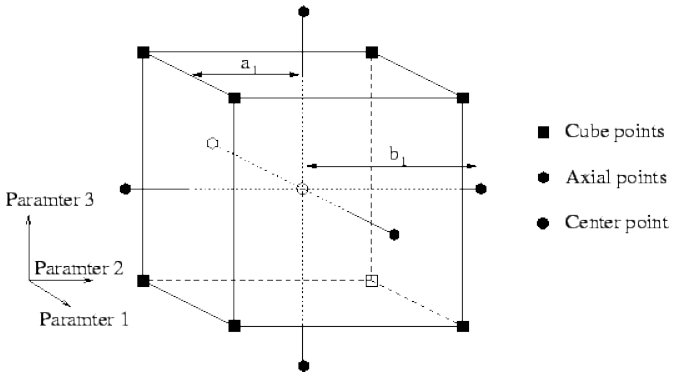

Figure 4.1: CCD for an experiment with three factors[61]

$$\mathbf{E} = \begin{bmatrix} \alpha & 0 & 0 & \cdots & \cdots & \cdots & 0 \\ -\alpha & 0 & 0 & \cdots & \cdots & \cdots & 0 \\ 0 & \alpha & 0 & \cdots & \cdots & \cdots & 0 \\ 0 & -\alpha & 0 & \cdots & \cdots & \cdots & 0 \\ \vdots & & & & & & \vdots \\ 0 & 0 & 0 & 0 & \cdots & \cdots & \alpha \\ 0 & 0 & 0 & 0 & \cdots & \cdots & -\alpha \end{bmatrix}.$$

Figure 4.2: The E matrix for CCD [60]

		A	B	C
Factorial Points (F matrix)	1	-1	-1	-1
	2	-1	-1	+1
	3	-1	+1	-1
	4	-1	+1	+1
	5	+1	-1	-1
	6	+1	-1	+1
	7	+1	+1	-1
	8	+1	+1	+1
Axial Points (E matrix)	9	$-\alpha$	0	0
	10	$+\alpha$	0	0
	11	0	$-\alpha$	0
	12	0	$+\alpha$	0
	13	0	0	$-\alpha$
	14	0	0	$+\alpha$
Center Points (C matrix)	15	0	0	0

Figure 4.3: The d matrix for CCD with 3 variable[60]

The advantages of using CCD's for RSM designs are as follows [63] :

e. A CCD can be run sequentially. It can be naturally partitioned into two subsets of points; the first subset estimates linear and two-factor interaction effects while the second subset estimates curvature effects. If analysis of the data from the first subset points indicates the absence of significant curvature effects we may not run the second set of points. Although in this algorithm existence of interaction effects are assumed and

hence evaluate all the sets of point, this characteristic is useful for reducing the computational effort by sequentially increasing the number of runs to include the second set only if curvature effects exist.

f. CCDs are very efficient, providing information about variable effects over the entire design space and overall simulation error in a small number of required runs. For example a full factorial design with 3 design variables will require 27 runs while a CCD requires only 15 runs. This difference becomes more significant as the number of design variables increase. This is shown in Table 4.4

Table 4.4: Comparison of full factorial 3^n and CCD[61]

Factors	Full Factorial 3^n	CCD	α
3	27	15	1.682
4	81	25	2.000
5	243	27	2.000
6	729	45	2.378
7	2,187	79	2.828

g. CCDs are very flexible. The flexibility in CCD resides in choosing the number of centre runs in the C matrix and the choice of the α value. For computer simulation experiments which are deterministic in nature only one centre run suffices. Based on the α value, there are three varieties of CCD's and hence enables the appropriate use over conditions of the operability in the simulation models and the regions of interest. The three different kinds of CCDs are:

- Face centred CCD
- Circumscribed CCD
- Inscribed CCD

Table 4.5: Classification of central composite design [64]

Central Composite Design Type	Terminology	Comments
Circumscribed	CCC	CCC designs are the original form of the central composite design. The star points are at some distance α from the center based on the properties desired for the design and the number of factors in the design. The star points establish new extremes for the low and high settings for all factors. These designs have circular, spherical, or hyperspherical symmetry and require 5 levels for each factor. Augmenting an existing factorial or resolution V fractional factorial design with star points can produce this design.
Inscribed	CCI	For those situations in which the limits specified for factor settings are truly limits, the CCI design uses the factor settings as the star points and creates a factorial or fractional factorial design within those limits (in other words, a CCI design is a scaled down CCC design with each factor level of the CCC design divided by α to generate the CCI design). This design also requires 5 levels of each factor.
Face Centered	CCF	In this design the star points are at the center of each face of the factorial space, so α = ± 1. This variety requires 3 levels of each factor. Augmenting an existing factorial or resolution V design with appropriate star points can also produce this design.

A comparison of the three types of CCD's is provided in Table 4.5 Based on the conditions of operability, the subsystem level modeler chooses the appropriate CCD for his/her analysis.

After the design of experiments, the subsystem level designer will run the simulation model at the chosen design points. The next objective would be to develop a metamodel with the results from these simulation runs which can replace the simulation model for system analysis. We now look at the metamodel developing, specifically response surface modeling.

4.2.2 Metamodeling Techniques

In the approach in Chapter 5 and 6, the response surface modeling technique is used for developing full quadratic second order models. The general form of response surface (RS) models is a polynomial function of degree d. It is assumed that the pre-selected polynomial model although rigid in nature, is flexible enough to represent the true response surface.

The general RS model can be expressed as the following.

$$y' = b_0 + \sum_j b_j x_j + \sum_j \sum_{k>j} b_{jk} x_j x_k + \sum_j b_{jj} x_j^2 + \sum_j \sum_{k>j} \sum_{l>k} b_{jkl} x_j x_k x_l + \ldots + \sum_j b_{j,j,\ldots,j} x_j^d \qquad (4.2)$$

Although second-order RS models have a limited capability to model accurately non-linear functions of arbitrary shape, they have several advantages. Although higher-order response surfaces can be used to model non-linear design spaces, instabilities arise and it is computationally very expensive to take a sufficient number of sample points in order to estimate all of the coefficients in the polynomial equation, particularly in high dimensions.

The advantage of choosing response surface modeling over other methods is that statistical uncertainty due to estimating system behavior in a continuous space by discrete sampling points may be captured using confidence and prediction interval [65]. These techniques quantify statistical uncertainty due to inadequate sampling data and are intended for quantifying statistical uncertainty due to lack of sampling data. As the focus is on reducing the model parameter uncertainty, these statistical techniques can be extended to understand how additional information from the simulation models can assist in reducing the confidence and prediction intervals. I shall be extending the interval techniques to capture computational effort information look in section 3.3. We now take a deeper look into response surface models and calculating confidence intervals to capture the uncertainty associated in simulation modeling.Second order response surface models can be represented by [65]:

$$Y = \beta_0 + \sum_{i=1}^{k} \beta_i x_i + \sum_{i=1}^{k} \beta_{ii} x_i^2 + \sum\sum_{i<k} \beta_{ij} x_i x_j + \varepsilon \quad (4.3)$$

Where, $\beta_{ij,}$ *i=1, 2… k; j=1, 2… k* are the regression coefficients and x_i, x_j are the regression variables, Y is the response, ε are random errors and k the number of design variables. It is explained how the parameters $\beta_{ij,}$ are estimated for a simple linear regression model. This can be extended in order to determine the regression coefficients for the full quadratic model. Suppose the linear model is:

$$Y' = \beta_0 + \beta_1 x \quad (4.4)$$

The residual, $e_i = y_i - y'_i$ is defined as the difference between the predicted value of the dependent variable as per the model and the true value of the dependent variable. In order to estimate the coefficients β_0, β_1, the method of ordinary least squares is followed which minimizes the sum of the squared residuals (SSE) for each observation i.

$$SSE = \sum_{i=1}^{n} e_i^2 \quad (4.5)$$

Where n is the number of data points. The minimization of this function yields a set of equations in β_0, β_1 , which are solved simultaneously. For the above model the least square estimates are:

$$\beta_1 = \frac{\sum(x_i - x_{av})(y_i - y_{av})}{\sum(x_i - x_{av})^2} \quad (4.6)$$

$$\beta_o = y_{av} - \beta_1 x_{av} \quad (4.7)$$

Where, x_{av} is the average of the *x* values and y_{av} is the average of the *y* values. The estimate of that variance is given by:

$$\sigma^2 = \frac{SSE}{n-2} \quad (4.8)$$

$$\sigma^2 = \frac{SSE}{n-p} \quad (4.9)$$

This is called the mean square error (MSE) of the regression. For a multiple linear regression, the coefficients can be determined in a similar fashion. The estimate of MSE will be given by where p is the number of model parameters. We now proceed to determining confidence intervals.

Confidence Intervals

We realized that the metamodel is an approximation based on the limited data from the actual simulation model and there will an uncertainty component associated with:

(i) Regression coefficients due to limited data and

(ii) Input variables which comes due to the variability

The confidence intervals associated with both these kinds of uncertainty is shown in Figure 4.4.

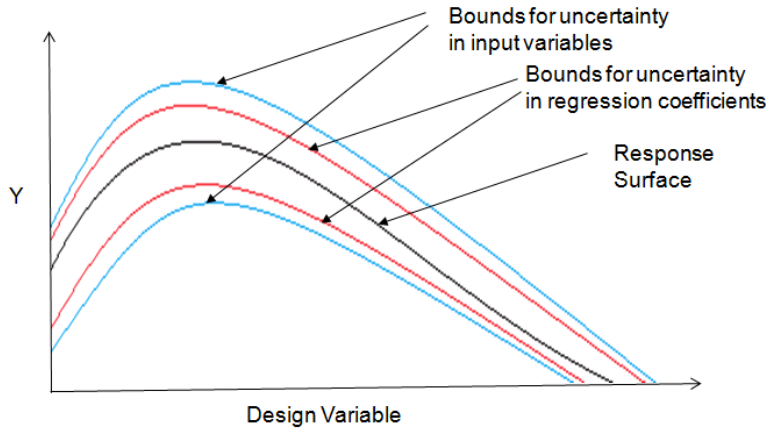

Figure 4.4: Confidence Intervals

(i) The statistical bounds introduced in the metamodel due to uncertainty in regression coefficients can be represented mathematically as:

$$\Delta(\ Regression\ coefficients) = t_{n-p,\alpha/2}\sqrt{MSE}\sqrt{x'_0(X'X)^{-1}x_o} \quad (4.10)$$

Where MSE is the mean square error, X is a (n x p) matrix of the levels of regression variables and x_o is a (n x 1) matrix of the particular point. We note that we are calculating the confidence interval, and $t_{n-p,\alpha/2}$ is the t statistic associated with n data points, p regression coefficients and for 100(1-α) % confidence interval

(ii) The bounds introduced in the metamodel due to uncertain input design parameters can be represented mathematically as:

$$\Delta(\ Input\ Variables) = \sum_{i=1}^{k} \left|\frac{\partial Y}{\partial x_i}\right| \Delta x_i \quad (4.11)$$

Where there are k input variables and Δx_i captures the error in the input variables due to the variability in the input variables. Equation 4.12 is the response variance in the output derived due to variation in the input design variables assuming a first order Taylor series expansion. There are certain underlying assumptions in using this bound. Firstly, there are no noise parameters. In the presence of noise parameters Equation 3.14 would modified as:

$$\Delta(\ Input\ Variables) = \sum_{i=1}^{k} \left|\frac{\partial Y}{\partial x_i}\right| \Delta x_i \ + \sum_{i=1}^{m} |\frac{\partial Y}{\partial z_i}| \Delta z_i \quad (4.12)$$

Where Δz_i is the variation associated with m noise parameters. In my deterministic simulation experiments Δz_i=0. Also the variations are small. If these variations are large, the equation is modified as:

$$\Delta(\ Input\ Variables) = \sqrt{\sum_{i=1}^{k} \left(\frac{\partial Y}{\partial x_i}\right)^2 \sigma_{x_i}^2} \quad (4.13)$$

Where $\sigma_{x_i}^2$ is the variance associated with design variable x_i. In Equation 4.13, the worst case scenario is assumed where all fluctuations occur simultaneously in the worst possible combination. [53] Also in my representation it is assumed the variation

of x_i as an interval estimate $\Delta x_i$and not as variance, primarily because we am not aware of the distribution function of x_i. It is noteworthy to note that in the first order Taylor series representation, the steeper the function is at the point of interest, the higher is the expected variance. This approach works as long as the function is near linear. When dealing with nonlinear functions, this approach can be erroneous and lead to solution converging to a local optimum instead of a robust solution [23]. Rippel suggested the use of the Multiple Point Method for getting better variance estimates and avoiding the problem of the solution converging to a local optimum. The use of the multiple point method for getting variance estimates is proposed in future work.

Thus after having understood the mathematical preliminaries in addressing the uncertainty associated with the input variables and model parameters I can now set the upper and lower confidence intervals of the simulation metamodel as:

$$Y_{max} = Y + (\Delta Y_{CI} + \Delta Y_{IP}) \qquad (4.14)$$

$$Y_{min} = Y - (\Delta Y_{CI} + \Delta Y_{IP}) \qquad (4.15)$$

$$\Delta Y_{CI} = t_{n-p,\alpha/2}\sqrt{MSE}\sqrt{x'_0(X'X)^{-1}x_o} \qquad (4.16)$$

$$\Delta Y_{IP} = \sum_{i=1}^{k} |\frac{\partial Y}{\partial x_i}|\Delta x_i \qquad (4.17)$$

ΔY_{CI} denotes the bounds for a 100(1-α) % confidence interval of the metamodel while ΔY_{IP} arises due to variations in input variables assuming first order Taylor series expansions as illustrated in Equations 4.14-4.17. Δx_i is the error in the input variables and is representative of the the variability of the input parameters. p is the total number of regression coefficients, MSE is the mean square error, X is a (n x p) matrix of the levels of regression variables and x_o is a (n x 1) matrix of the particular point we are calculating the confidence interval. We looked at design of experiments, building the response surface models for the simulation models and the

confidence interval estimates for the response surface. We note that this analysis is done at the subsystem level by the individual design modelers or can also be done by the system level designer is the appropriate information is passed. Having done the system level analysis we proceed to evaluating the robust solution for the entire multiscale problem using the Inductive Design Exploration Method (IDEM). IDEM and cDSP has already been explained in Section 1.2. We now look at the other foundational construct for uncertainty mitigation, i.e., value of information.

4.2.3 Value of Information

The basic notion underlying value of information is that at any stage in the decision-making process, designers possess some information that can be used for selecting the best course of action [66-68]. The designer can either make the decision using available information (e.g., using simpler models), or gather more information (i.e., simulation model refinement) and then making a decision using the updated information. In the context of simulation-based design for multiscale systems, a *simulation model is a source of information* [69]. The system level designer can either make the decision using available information (e.g., using simpler models), or gather more information (i.e., simulation model refinement) and then making a decision using the updated information. Simulation model refinement at the subsystem level can be associated with; (i) refining the modeling assumptions (mitigating MSU) and (ii) acquiring additional data (i.e. , more simulation runs) to better represent metamodels used at subsystem level (mitigating MPU). In this context, the value of this added information is referred to as the *improvement in a designer's decision-making ability*. The primary metric used in engineering design is the expected value of information which accounts only for irreducible uncertainty [70,71]. To address both reducible and irreducible uncertainty, Panchal and coauthors [69] extended the expected value of information to a metric called the improvement potential (P_i). The improvement potential quantifies the maximum possible improvement in a designer's decision (in terms of utility) that can be achieved by refining a simulation model. If the improvement potential is high,

the design decision can possibly be improved by refining the simulation model. However, if the improvement potential is low, then the possibility of improving the design solution is low. The advantages of the metric have been shown for uncertainty mitigation in individual models [72,73]. The metric only quantifies the benefit of gaining more information. It does not account for the effort involved in procuring addition information. However, a key step towards further simulation refinement is to predict the change of improvement potential as additional information is gained from simulation runs or refining modeling assumptions. Quantifying the value of information associated with refining the modeling assumptions will be a rigorous task considering the large number of simulations that assist modeling of various physical phenomena. We need to build a comprehensive list of all the simulation software and associated cost-benefit understanding for each of these. An alternative method would be look at different physical phenomena like thermodynamics, structural dynamics, etc. and common assumptions used in modeling these phenomena. However, in multiscale modeling, different physical laws will be used for modeling subsystems at different length and time scales. Considering the length and time scales can range from quantum or molecular domain to the macro domain of physical products or the nano second to entire product lifecycle which may be years, developing cost models will be a difficult task. In Chapter 6, my investigation is focused on quantifying the value of information gained by additional simulation runs and not on the value of information gained by refining modeling assumptions. Concepts from Lawrence's value of information and response surface modeling are used to predict the change of improvement potential with additional simulation runs. Lawrence provides the *ex-ante* value to decide which information source to choose (i.e., how many simulation runs to choose) in order to evaluate the value-of-information before executing the simulation code and the *ex-post* value to evaluate the value of this additional information after making the decision. Mathematically, the *ex-ante* and *ex-post* value-of-information based metrics are represented as:

Ex-ante value: $v(x, y) = E_{x|y}\pi\left(x, a_y\right) - E_x\pi(x, a_o)$ (4.18)

Ex-post value: $v(x, y) = \pi\left(x, a_y\right) - \pi(x, a_o)$ (4.19)

where $E_x f(x)$ is the expected value of *f (x)* and $E_{x|y} f(x)$is the expected value of *f (x)* given *y*. a_o and a_y represent the actions taken by the decision maker in the absence and presence of information *y* and *π(x, a)* represents the payoff achieved by selecting an action *a*, when the state realized by the environment after the decision is *x*. It is important to realize that the key difference between *ex-ante* and *ex-post* value is that in *ex-post* value, the realization of the state *x* is known whereas the realization of the state *x* is not known in the *ex-ante* value and the expected value of payoff is taken over the uncertain range of state *x* [69]. In the study in Chapter 6, the ex-ante improvement potential is first derived using which the behavior of the improvement potential with the number of simulation runs is predicted. Using these values for the improvement potential computational cost models can be developed for the individual simulation models and the system level designer reaches a trade-off between the computational cost and benefit between these simulation models towards the system level design objectives and allocates resources for further simulation refinement. Once these runs have been made, the ex-post value-of-information is checked against the ex-ante value of information to validate the assumptions and predictive capabilities of the ex-ante Improvement Potential for simulation model refinement.

The formulation of the improvement potential metric is discussed suitable for design of multiscale systems. IDEM gives us the set of discrete feasible points in the design space at different scales in the multiscale problem. The improvement potential metric must capture the scope of refinement allied with the entire design space while accounting for uncertainty bounds. To this end improvement potential for the simulation model, IP_i is defined as:

$$IP_i = \sum_m \frac{1 - \frac{Y_{lower}}{Y_{upper}}}{m} \qquad (4.20)$$

$$Y_{upper} = Y + t_{n-p,\alpha/2}\sqrt{MSE}\sqrt{x'_0(X'X)^{-1}x_o} \qquad (4.21)$$

$$Y_{lower} = Y - t_{n-p,\alpha/2}\sqrt{MSE}\sqrt{x'_0(X'X)^{-1}x_o} \qquad (4.22)$$

The subscript i in IP_i denotes the simulation model the improvement potential metric is calculated for. The improvement potential metric decreases as the error bounds are reduced and will hypothetically be 0 when $Y_{upper} = Y_{lower}$ suggesting no further model refinement is possible. However, this cannot be realized statistically. The improvement potential metric is calculated over all set of feasible design variables to get a true reflection of the scope of refinement without bias. We note that Y_{upper} and Y_{lower} are related to statistical error bounds for the response surface and are different from Y_{max}, Y_{min} which also incorporate the variation of the input variables and the discretization error as first order Taylor series expansions. At this point we may also note that there may be greater value associated with redefining the improvement potential metric in terms of Y_{mean} and Y_{upper} when larger values are desired and Y_{mean} and Y_{lower} when smaller values are desired. The insight about which simulation model is associated with larger/smaller values can be acquired through IDEM. However, most modeling efforts in multiscale systems lead to highly non-linear models where there is little benefit associated with characterizing a simulation model as larger/smaller value is better. Hence the improvement potential is defined in terms of Y_{upper} and Y_{lower} without bias. In this thesis the focus is on extending the improvement potential metric to account for mitigating MPU for the individual simulation models at the subsystem level. I proceed to use this metric to make meta-level decisions involving a trade-off between reduced uncertainty and increased effort as a result of the uncertainty mitigation. The use of value of information for uncertainty mitigation is taken up in Chapter 6.

4.3. WHAT HAS BEEN PRESENTED AND WHAT IS NEXT

In this chapter hypotheses were formulated to address the research questions and also identified the key constructs. They were studied in detail and the theoretical structural validity was established, i.e., Quadrant I of the validation square. I revisit the validation square in greater detail in Chapter 7. Figure 4.6 shows the organization of work.

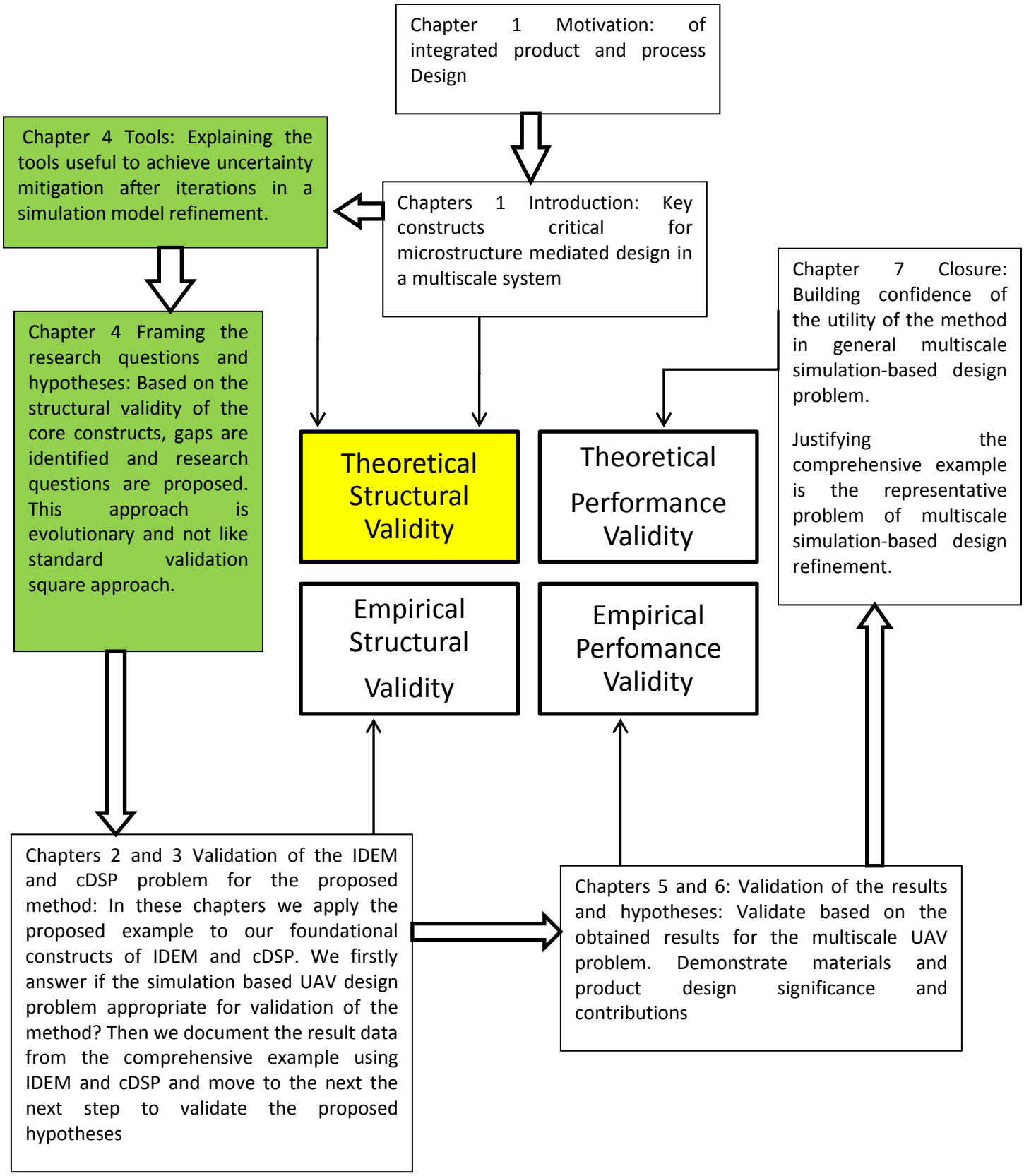

Figure 4.5: The validation square

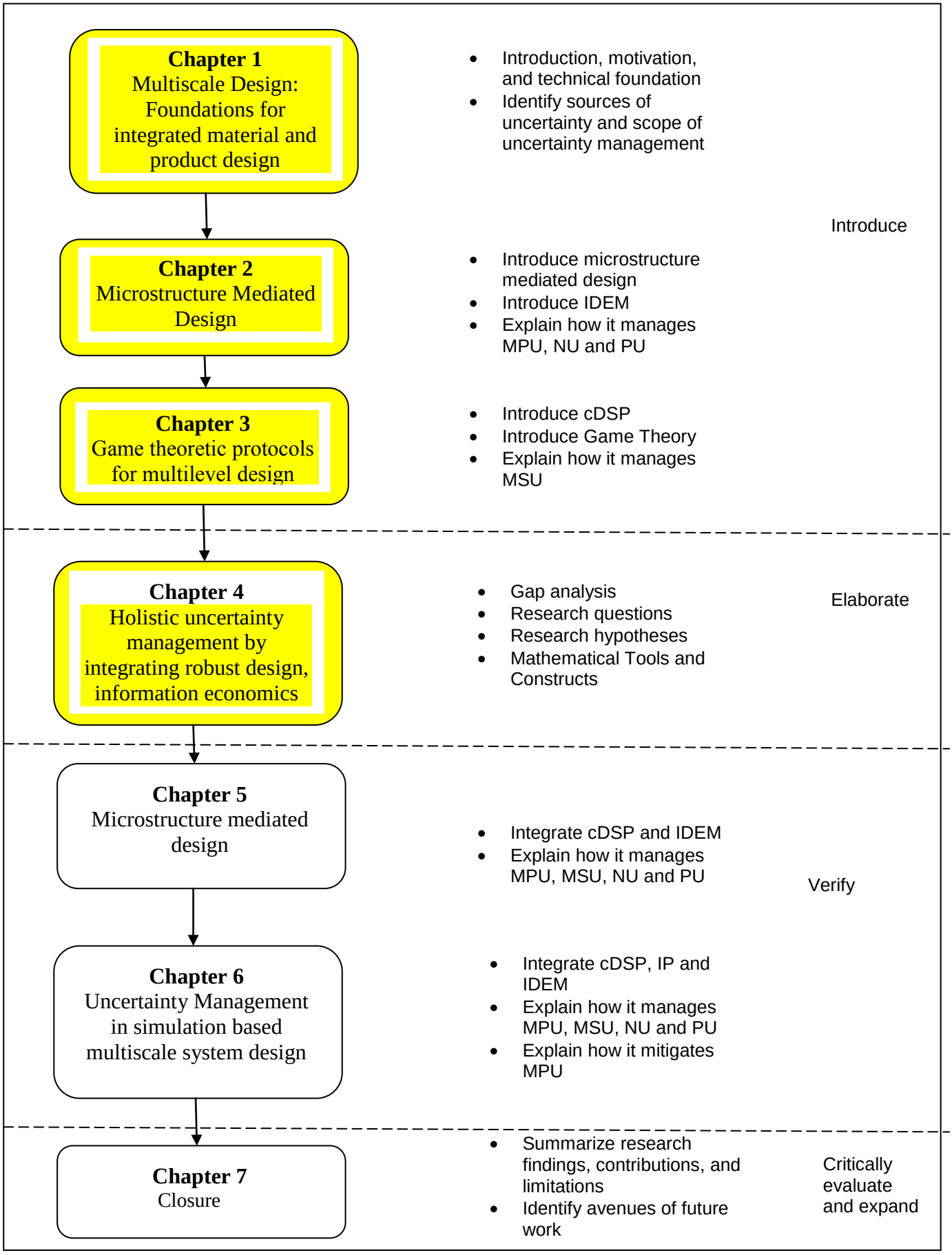

Figure 4.6: Organization of work

CHAPTER 5

MICROSTRUCTURE MEDIATED DESIGN

In this chapter, the construct of microstructure-mediated design of material and product is refined by (i) embedding appropriate aspects of the material microstructure through overall system configuration (i.e., frame multiscale system) (ii) developing hierarchical material models modeling over multiple scales (i.e., multiscale modeling) (iii) controlling the microstructure within feasible bounds subject to uncertainty in design variables, models and its propagation in the multiscale system to achieve the performance targets of the product (i.e., multiscale design) and (iv) Deciding the most suitable processing route among feasible solutions. The efficacy of this construct is illustrated via the integrated design of submersible and Al-based matrix composites as in the previous chapters. The material considered is *in-situ* Al metal matrix composites (MMCs) due to the advantages that the *in-situ* MMCs have over the conventional MMCs. The product considered is a shell of a robotic submersible with performance targets and constraints. The hierarchical system is modeled to identify process-structure, structure-property and property-performance relationships. The integrated design is carried out using an Inductive Design Exploration Method (IDEM) that facilitates robust design in the presence of natural uncertainty (NU), model parameter uncertainty (MPU), model structure uncertainty (MSU) and propagated uncertainty (PU) as explored in Chapter 2. The most suitable processing route is determined using the compromise decision support problem (cDSP) technique coupled with IDEM as established in Chapters 2 and 3. This design task is a representative example of integrated materials and product design problems. The study and results described in this chapter has been submitted for review to the journal of Computer Aided Design[74].

5.1. Frame of Reference- Microstructure Mediated Design

Conventional approaches to product design involve determining the specific material properties for required performance objectives and selecting the appropriate material from databases of experimentally determined material properties, i.e., a top-down approach [75]. Although a lot of modeling literature exists in goal oriented design methods that move from the system level to the component or the part level, designers are restricted to material selection methods due to limited inverse modeling in the material domain. An alternative bottom-up reductionist approach advocating discovery of new materials is simulation-based design of materials using computational material sciences and physics [5]. However this is an idealized process considering the infancy of material design techniques. Using modeling tools at multiple scales (quantum, molecular, micro, continuum), i.e., multiscale modeling; material scientists develop deductive mappings from the processing path to micro-structures, properties and performance, corresponding to Olson's material design hierarchy [4], Figure 5.1. Owing to the cost of modeling and simulation, it becomes critical that top-down (inductive) requirements driven exploration guide the bottom-up (deductive) modeling and simulation techniques. Such a systems-based integrated material and product design approach enables tailoring materials for specific performance requirements in specific products or processes.

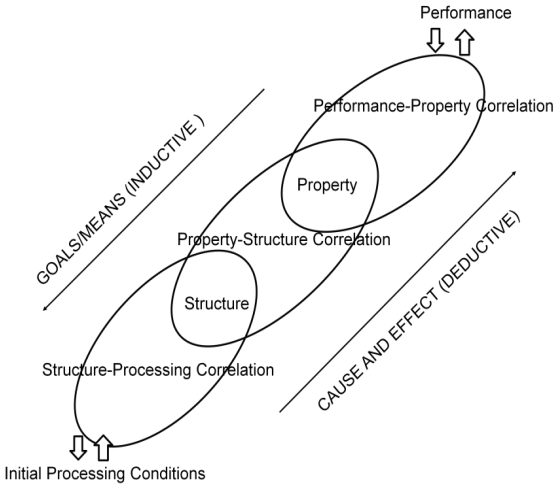

Figure 5.1: Hierarchical materials design[4]

The Olson's diagram was applied to integrated product and material design in Chapter 2. The notions of Olson's material design hierarchy are augmented and the challenges in this system based approach are explained, Figure 5.2. Material design hierarchy is decomposed as a set of mappings, i.e., processing-structure relations; structure-property relations and property-performance relations[5].

a. Process-structure (PS) relations: Establishes feasibility criteria (Thermodynamic, kinetic etc.) and constraints (manufacturing, cost etc.) for the processing conditions.
b. Structure-property (SP) relations: Establishes relations between microstructure features (composition, morphology, phases etc.) and material properties.
c. Property-performance (PP) relations: Establishes relations between desired performance requirements and corresponding material properties required.

The arrows are unidirectional for the PS and SP relations indicating limited inversion, as described in the inverse problem in Section 1.1, due to non-linear, nondeterministic and non-equilibrium characteristic of material behavior with solutions depending on initial conditions. PP relations may be invertible and is the basis for most designers opting for material selection. PS relations constrain the processes of design exploration at higher levels of the hierarchy (due to manufacturing or cost constraints; thermodynamic accessibility; kinetic feasibility etc.) where as SP searches guide exploration of material composition and processing conditions to achieve microstructures satisfying required property sets [5]. The key to material design lies in effectively modeling the microstructure acting as an interface between the PS and SP relations. The microstructure strongly influences physical, mechanical and chemical properties such as strength, toughness, ductility, corrosion resistance, high/low temperature behavior, etc., which in turn govern the application of these materials. In addition, the design of a product can be modified in two ways, namely, i) by changing the material processing conditions to modify the microstructure, which has an effect on the overall system performance and ii) by changing the geometry of the product, which in turn not only affects structural performance, but also puts constraints on required mechanical properties of the material. Hence, the material microstructure needs to be designed in such a way that the constraints on the material

properties, imposed by the structure, are satisfied. Thus, the microstructure acts as a decisive interface in the material design hierarchy including product performance requirements. So a microstructure-mediated design (MMD) centered approach for integrated design of materials and product is adopted. Figure 5.2, can be viewed as reducing the order of modeling resulting in an increased uncertainty component which is discussed next.

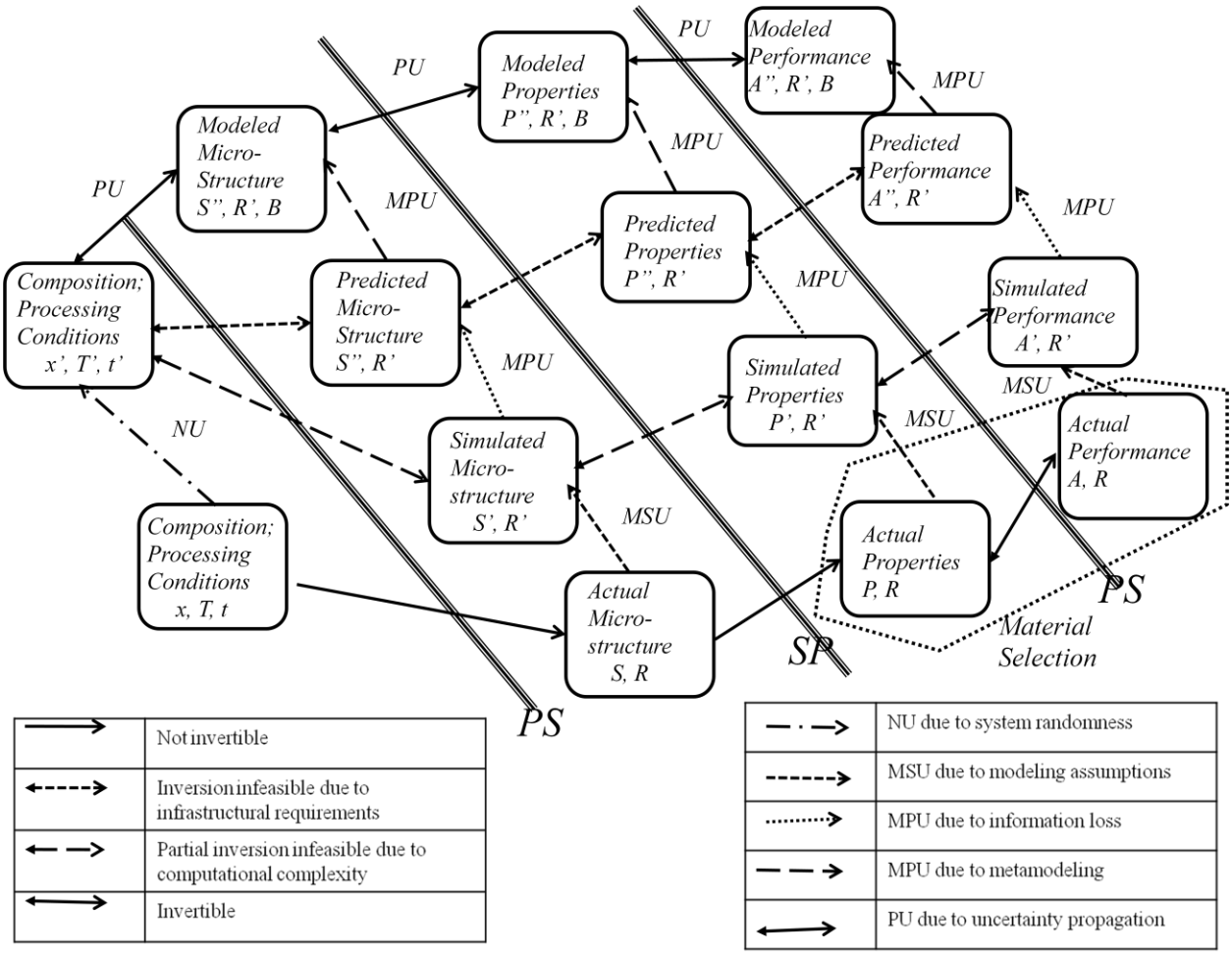

Figure 5.2: Hierarchical mapping in materials design

The second important feature in Figure 5.2 is the lateral transformations at each level of the hierarchy to favor design exploration while introducing different components of uncertainty. The sources of uncertainty are classified as natural uncertainty (NU), model structure uncertainty (MSU), model parameter uncertainty (MPU) and propagated uncertainty (PU) [46]. NU in the processing variables or other independent variables at different levels of the hierarchy is induced

by inherent randomness or variability in composition or operating conditions. For example, the input volume fraction of a material or temperature of processing (control factors) of a material possesses some statistical variance or external processing conditions like humidity (noise factor) vary with time. Serious departures in performance may arise if NU is not considered in modeling. MSU arises due to simplistic assumptions and approximations (e.g., reducing 3D loading to more tractable 2D loading for stress-strain analysis or using a representative volume element for microstructural analysis) while developing simulation models in order to reduce computational complexity. The unquantifiable uncertainty associated with idealizations in multiscale modeling, i.e., quantum, molecular or microscale due to incomplete understanding of physical phenomena at these scales also contributes to MSU. The dotted bidirectional arrows linking the MSU models indicate that though it is technically possible to use the simulation models for design space exploration, the requirement of a complex computational infrastructure linking different simulation and analysis software deems it infeasible. The origination of MPU is categorized as arising due to inaccuracy of inputs and arising due to insufficient information of metamodel parameters. There is loss of information in transforming digital microstructure as normal or log-normal distribution function with reduced degrees of freedom. Although accuracy is conceded for efficiency, it is crucial to consider the inaccuracy in mean and variance of these distributions. Heavy computational costs of non-deterministic simulations costs make it infeasible to mitigate this inaccuracy with large number of replicate runs. Though current advances in microstructure sensitive design (MSD) make it possible to follow the inverse top-down approach in SP relations; infancy of inverse PS relations as new processing techniques emerge constantly and requirement of complex mathematical methods (e.g., n-point correlation functions; spectral methods; discrete Fourier transforms etc.) for optimal microstructure determination among several possibly non-unique SP mappings limit MSD's applicability to integrated material and product design especially in the early stages of design [76]. This drives us towards using metamodeling techniques to permit efficient inversion though with an increased MPU component. The set of possible microstructures or processing conditions is continuous making it imperative to use discrete points to extract relevant information and use response surface modeling to derive

input-output relationships. These metamodel parameters possess MPU due to insufficient information (e.g., 15 discrete CCD points for 3 design variables to represent a continuous physical phenomenon) owing to high cost for large number of runs. The metamodels enable reversibility through the hierarchical material domains but a fourth type of uncertainty, i.e., PU which is a compounded effect of all other three types of uncertainty needs to considered for exploring the hierarchical degrees of freedom associated with material composition and process modifications . Thus for successful integrated design of material and product, we (Figure 5.3) (i) frame a multiscale system, (ii) develop hierarchical models, i.e., multiscale modeling, (iii) use an inductive approach to find feasible processing routes in order to achieve performance targets and, (iv) decide the most suitable processing route among feasible solutions.

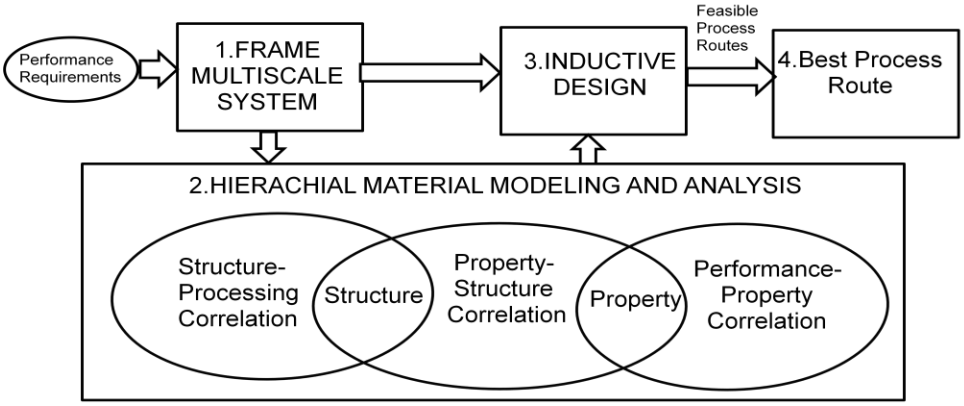

Figure 5.3: Schematic for microstructure mediated design

The integrated design of material and product using the three steps is referred as multiscale design. Design of material refers to controlling the microstructure whereas design of product implies meeting the performance requirements. Often, multiple performance requirements may impose conflicting requirements on the material composition or microstructure (geometry, size, distribution of phases etc.). In order to reach feasible design solutions, a multiscale design approach has been adopted which combines inductive (top-down) engineering with deductive (bottom-up) science for efficient design space exploration. Robust design is employed to minimize effect of uncertainty on process requirements and product performance. Literature

exists for robust design against reducible (MPU, MSU and PU) as well as irreducible uncertainties (NU)[8-13]. For robust design the Inductive Design Exploration Method (IDEM) is employed as it offers the following capabilities with respect to microstructure mediated multiscale design[13]:

(i) Designers can identify multiple feasible solution ranges with IDEM. This advantage is vital owing to non-uniqueness in mapping relations.

(ii) Designers can identify ranged sets of solution for hierarchical systems comprised of models with multiple outputs or shared input variables over different scales using IDEM. This property is useful for multiscale systems with complex interlinking of input and output variables.

(iii) Feasible solution ranges are identified considering all four types of uncertainty. A metric called the Hyper-Dimensional Error Margin Index (HD-EMI) is developed to quantify the degree of MSU. A designer can set constraints for HD-EMI achievement enabling him to tailor the HD-EMI values to make risk-informed decisions against MSU at all hierarchical scales.

(iv) The designer only needs the input and output files for the models being developed. Hence design exploration and simulation analysis can be conducted in parallel reducing computational complexity and saving resources (time, money etc.).

(v) The mapping functions in hierarchical design are modularized implying a change in an analysis model can be incorporated by changing the corresponding mapping function avoiding design iterations.

(vi) The ability to maintain design freedom, i.e., IDEM maintains maximum feasible space in design space while deciding independent design variables. This is useful for early stages in design where the objective is design exploration instead of design optimization and relevant to MMD while we are in the formative years of establishing material design techniques.

The run time for IDEM is large for problems with many design variables. So design variables are screened to eliminate unimportant factors in the design chain. The most robust solution is

calculated by compromising the degree of performance achievement or by reaching a trade-off amongst robust process requirements. For finding the best solution among feasible processing routes the compromise decision support problem (cDSP) is employed [55]. A cDSP is a multi-objective decision model which is a hybrid formulation based on mathematical programming and goal programming and is well suited to satisfy a set of constraints while achieving a set of conflicting targets as well as possible in a multiscale system tasks. For MMD the constraints come from processing conditions, performance achievement and HD-EMI values and targets are set for HD-EMIs and performance. In this approach to the multiscale design, a designer moves from the top-down in Olson's hierarchy using IDEM after completing the bottom-up (deductive) analysis of simulation models. Robustness is achieved by trading off the degree of system performance and the degree of reliability based on MSU associated with system models in the cDSP while quantifying NU and MPU in IDEM. PU is mitigated by developing exact constraint boundaries at the various scales. Current efforts in integrated material and product design focus on employing topological optimization in conjunction with MSD[77]. However, IDEM is employed as it facilitates robustness in integrated hierarchical material and product systems. We note achieving robustness in the presence of uncertainty separates MMD from MSD and other material design techniques employing microstructure information. Considering uncertainty is vital due to the infancy of material design techniques and stress should be on robust design guiding design space exploration instead of performance optimization) [29]. The efficacy of the MMD construct is illustrated via the integrated design of submersible and Al-based matrix composites.

The shell of a typical underwater robotic vessel, namely an autonomous underwater vehicle (AUV)[31], with both geometrical and material features is considered as a test application case for design in this chapter. The objective is to design the shell of the vessel for deep sea exploration with multifunctional requirements of minimizing the mass in walls (wall thickness) for given support superstructure for given maximum depth and associated pressure differential. Other design requirements include a) suitable factor of safety with respect to collapse at target

maximum operating depth, b) a large endurance time satisfying the time of operation constraints under water without resurfacing/refueling/battery changes, c) satisfying geometric and weight constraints d) satisfying operating temperature conditions.

Metal matrix composites (MMCs) are strong and stiff light metal-based composites and with a reinforcement which may be a metal, ceramic or an organic compound[78]. The reinforcement in addition to serving a structural task (reinforcing the compound), also changes the physical properties such as wear resistance, friction coefficient or thermal conductivity. Al-based metal matrix composite is used to illustrate the microstructure mediated design method. Metal matrix composites (MMCs), in general, and Al-based MMCs in particular, have been the subject of intense research for the past two to three decades and are being exploited for a range of commercial applications related to aerospace and automotive industries. Al-based metal matrix composites can be divided into two classes, namely, ex-situ and in-situ[79]. In ex-situ composites the reinforcements are added externally whereas in in-situ composites the reinforcements are formed by chemical reactions within the melt. One of the important drawbacks during the processing of ex-situ MMCs is the presence of interfacial impurities and oxides between reinforcement and matrix resulting in poor wettability and bonding. This led to the development of in-situ composites, wherein the reinforcements are generated in a Al alloy matrix via chemical reactions between elements and/or compounds during the composite fabrication[80]. The advantages that in-situ MMCs have over conventional MMCs include thermodynamically stable reinforcements in the matrix, clean reinforcement-matrix interfaces resulting in a strong interfacial bonding, finer particle size yielding better mechanical properties and potential for lower cost of production. These advantages make it a strong candidate for the design task at hand. In this thesis we deal with the Al-4 % Cu metal matrix composites with TiB_2 reinforcement. The four steps associated with multiscale design of AUV using in-situ Al MMCs are investigated in Section 5.2. Section 5.3 discusses the MMD solution and closing thoughts are presented in Section 5.4.

5.2. Multiscale Design

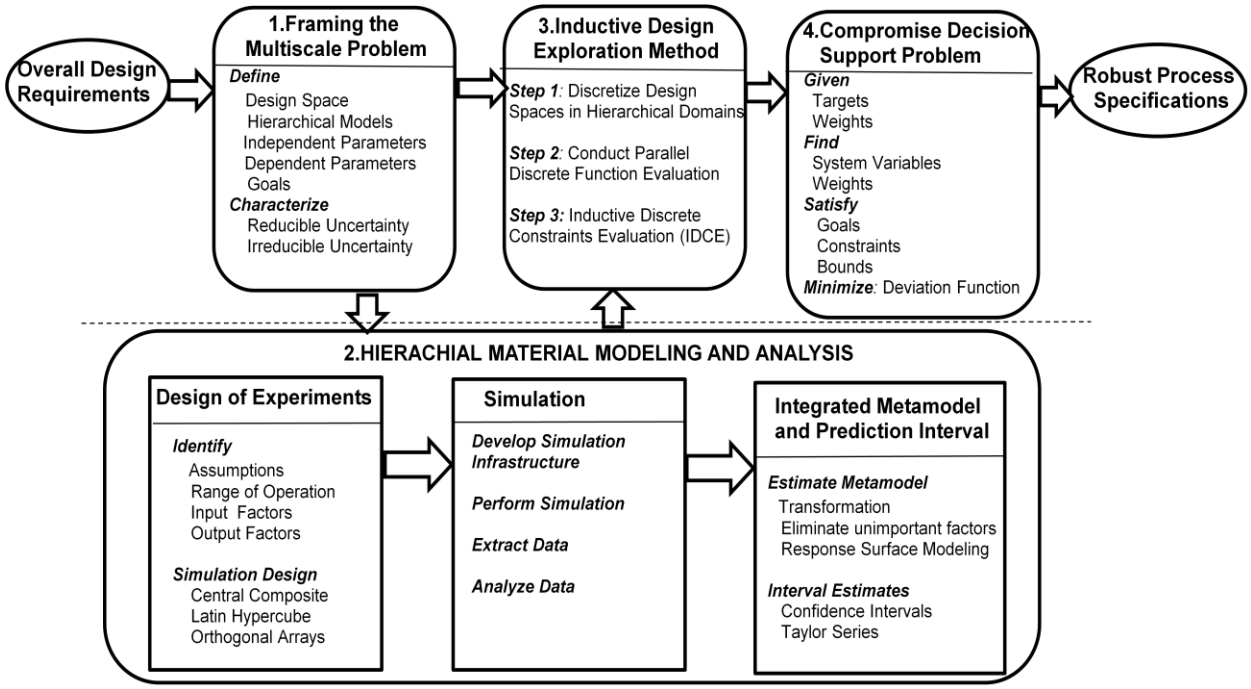

Figure 5.4: Strategy for microstructure mediated design

In Figure 5.4, the 4 steps relevant to MMD of material and product are instantiated. They are:

(i) Step 1: Frame a multiscale system expressed in terms of variables (independent or dependent), targets and models that embed relevant aspects of the material microstructures and define the system goals.

(ii) Step 2: Develop hierarchical material models over multiple length and time scales, i.e., Multiscale modeling. Design of experiments is used to determine the simulation runs and use metamodeling techniques to determine mean response surface model with interval estimates.

(iii) Step 3: Use a top-down (inductive) approach, i.e., IDEM, to control the microstructure within feasible bounds subject to four types of uncertainty and ascertain feasible processing routes in order to achieve performance targets.

(iv) Step 4: Decide the most suitable processing route among feasible solutions using

the cDSP technique.

The multiscale system for AUV design using TiB_2 is framed in Section 5.2.1. In Section 5.2.2 I look at the constitutive models for developing the PS, SP and PP linkages. The steps of IDEM for MMD are explained in Section 5.2.3 and cDSP is explained in Section 5.2.4.

5.2.1. Framing the Multiscale System

The design approach is based on systems-based integrated top-down (inductive) and bottom-up (deductive) multiscale design. Multiscale design for the shell design problem involves two activities, namely, process path-structure relationships and structure-property-performance relationships (Figure 5.1). These two design objectives interact via the microstructure. While on one hand the processing conditions influence the obtained microstructure, the performance of the product depends on the mechanical properties which in-turn are mapped from the microstructure. In this chapter, two major aspects of the design problem, namely, the materials design (rather than just materials selection) and structural design, are combined. The Inductive Design Exploration Method (IDEM) is used to effect solution. The design process chain for this application is constituted of three interconnected modules which account for the modeling of the behavior of the material and the structure. IDEM is used to manage uncertainty embodied in the simulation models, uncertainty arising due to metamodeling and random system variability for design exploration in the presence of propagated uncertainty in the design process chain. Based on the materials processing steps involved and mechanical design requirements, the interconnected modules that constitute the design process chain for this application are:

MODULE 1: Process- Structure Correlation

MODULE 2: Structure-Property Correlation

MODULE 3: Property-Performance Correlation

MODULE 1 provides the simulated microstructure after processing. The resulting mechanical

properties are estimated in MODULE 2, whereas MODULE 3 maps the required mechanical properties based on the system design considerations. MODULE 1 involves the prediction of the precipitation of liquid aluminum based on the composition and microstructure evolution due to the effect of temperature and solutal fields. The output of MODULE 1 is the information about different phases formed, the size of precipitates and the grain size distribution. The microstructure information from MODULE 1 is used in MODULE 2 which predicts the mechanical properties inherent in the material. These mechanical properties are used in the system-level MODULE 3 to predict the effects of different AUV geometries on overall system performance.

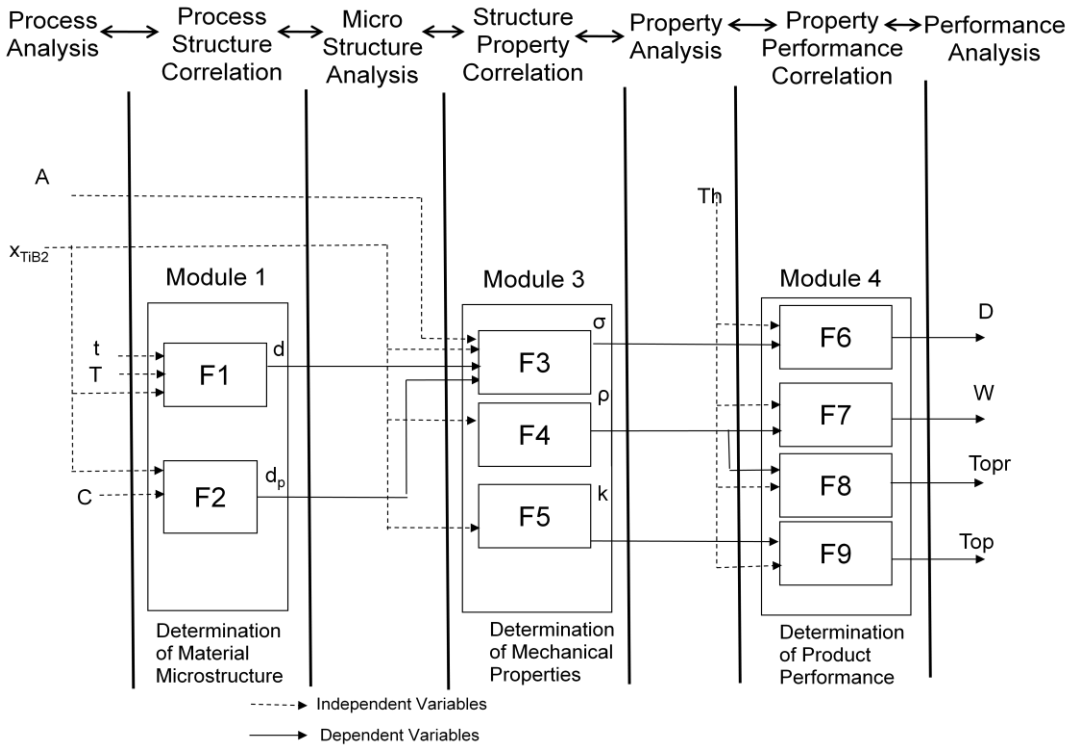

Figure 5.5: The multiscale system for MMD

In this application, the strength is principally determined by the sizes, shapes and distribution of TiB_2 precipitates – in other words the microstructure of the material. The AUV design can be modified in two ways, namely, 1) by changing the processing conditions to modify the MMC microstructure and 2) by changing the geometry of the shell which puts constraints on required mechanical properties of the material while affecting the structural performance. Hence, the

microstructure needs to be designed concurrently with the shell so as to satisfy the imposed constraints on the material properties. Given the complexity inherent in the design process chain, the independent and dependent variables are represented; the models and the information flow between the different modules, Figure 5.5. *F1, F2, F3 and F6* represent simulation models used to design the autonomous underwater vehicle (AUV) while *F4, F5, F7, F8 and F9* represent theoretical or empirical models considered for design. The problem and models have been classified as per the mapping relationships contrary to formulations in previous chapters.

a. MODULE 1: The inputs to *F1* are the volume fraction of TiB_2 (x_{TiB2}), time of reaction (t) and temperature of processing in degree K (T).The output of *F1* is the average TiB_2 particle size (d_p) which is an input to MODULE 2. The independent inputs to *F2* are volume fraction of TiB_2 (x_{TiB2}) and cooling rate (C) and the output of MODULE 2 (*F2)* is the average grain size (d) of microstructure which is another input to MODULE 2. MODULE 1 deals with the process-structure relationships (PS) shown in Figure 6.

b. MODULE 2: This module deals with the structure-property relationships (SP). *F3* gives the yield stress (σ), *F4* gives density (ρ) and *F5* gives the heat transfer coefficient *(k)* as outputs. The model for yield stress (σ) receives inputs from the outputs of MODULE 1 (d_p and d) along with the independent inputs of volume fraction of TiB_2 (x_{TiB2}) and percentage of area fraction (A). The only input to models for density (ρ) and heat transfer coefficient *(k)* is the independent variable of volume fraction of TiB_2 (x_{TiB2}).

c. MODULE 3: This deals with the property-performance (PP) relationship of the developed microstructure. The performance variable of depth of operation (D) is evaluated in *F6*; weight of the outer shell (W) is evaluated in *F7*, time of operation (T_{opr}) for the submersible is evaluated in *F8* and temperature of operation (T_{op}) is evaluated in *F9*. The independent parameter, thickness of the shell (T_h) and is an input to all the models, i.e., *F6, F7, F8 and F9.* The dependent parameters are density (ρ) to weight (*F7)*

and time of operation (*F8)* while yield stress (σ) is an input to depth (*F6)*.

Table 5.1: Dependent parameters

Model	Parameter	Target	Module
F1	d_p (Average particle size)	From Structure-Property mapping	1
F2	*d* (Average grain size)	From Structure-Property mapping	1
F3	σ(Yield stress)	From Property-Performance mapping	2
F4	ρ (Density)	From Property-Performance mapping	2
F5	*k* (Heat transfer coefficient)	From Property-Performance mapping	2
F6	*D* (Safe depth of operation)	Maximize	3
F7	*W* (Weight of outer shell)	Minimize	3
F8	T_{opr} (Time of operation)	Maximize	3
F9	T_{op} (Operating temperature)	Minimize	3

Table 5.2: Independent parameters

Variable	Target	Input Modules	Input Models
x_{TiB_2} Volume fraction of TiB_2	From Property-Structure mapping	1,2	*F1,F2,F3,F4,F5*
T Temperature for precipitate modelling	From Property-Structure mapping	1	*F1*
t Time of reaction	From Property-Structure mapping	1	*F1*
C Cooling rate for microstructure evolution	From Property-Structure mapping	1	*F2*
A Percentage Area Fraction	From Structure-Property mapping	2	*F3*
T_h Shell thickness	From Property-Performance mapping	3	*F6,F7,F8,F9*

Tables 5.1 and 5.2 summarize the models, associates modules and targets for the dependent and independent parameters in the multiscale system. The feasible design spaces are inductively passed (using IDEM) from MODULE 3 to MODULE 2 and subsequently to MODULE 1 of design after completing the deductive analysis. Having defined the design variables and the connectivity within the design process chain, the modules described in the sections that follow.

5.2.2. Hierarchical Material Modelling

MODULE 1: Process-Structure Correlation

Precipitation Modeling in Liquid Aluminum (F1 in Figure 5.5)

A suitable route (Mixed-Salt route) for the in-situ Al / TiB_2 composite manufacturing process utilizes the reduction of K_2TiF_6 and KBF_4 with aluminum, generally known as the "halide salt" process. Yang and colleagues[33] proposed a diffusion mechanism wherein Al_3Ti is formed in the melt initially by a very fast reaction. Boron then diffuses into Al_3Ti particles in the melt, thus forming TiB_2 particles according to the reaction, $Al_3Ti + 2B = 3Al + TiB_2$.

The liquid-state processing techniques to produce in-situ composites include self-propagating high temperature synthesis (SHS), exothermic dispersion (XD), reactive hot pressing (RHP), flux assisted synthesis (FAS) and rapid solidification processing (RSP). Any of these processes could be used. K_2TiF_6 and KBF_4 are other precursors that dissolve in the aluminum melt to form intermediate phases Al_3Ti and AlB_2. The reaction between these intermediate phases has been simulated to predict the particle size distribution of TiB_2 phase thus formed in the matrix.

A model proposed by Anestiev et al.[34] is used to investigate the diffusion reactions taking place between the intermediate phases. This model accounts for the processes taking place at diffusion controlled formation of TiB_2 in liquid Al and is used to predict the mean precipitate size and size distribution of the dispersed TiB_2 particles. The thermodynamics of the phase formation as well as the nucleation and growth kinetics have been taken into account. In this model, Al_3Ti and AlB_2 are allowed to react in liquid Al to form TiB_2 particulates. A coordinate system dividing

a 2-dimensional space into strips of equal length is used, half of which contains Al_3Ti and the other half AlB_2 dissolved in the Al melt (Figure 5.6). When these intermediate phases react, random nucleation of TiB_2 particulates is assumed. The kinetics of the formation of TiB_2 particles is governed by unsteady state diffusion equations (solute redistribution theory), which in turn depends on the concentration profile of the intermediate solute phases in the region. The kinetics of TiB_2 particle formation can be mathematically described by the following set of partial differential equations:

$$\frac{\partial X_1}{\partial t} = D\frac{\partial^2 X_1}{\partial x^2} - X_1^S\frac{\partial \psi}{\partial t} \qquad (5.1)$$

$$\frac{\partial X_2}{\partial t} = D\frac{\partial^2 X_2}{\partial x^2} - X_2^S\frac{\partial \psi}{\partial t} \qquad (5.2)$$

where, X_1 and X_2 are the mole fractions of the dissolved Ti and B in the Al matrix respectively, t is the time, D is the diffusion coefficient, ψ is the volume fraction of the solute reacted per unit time, X^1_S and X^2_S are the mol fractions of Ti and B in the solid phase (TiB_2). The solute consumption rate due to TiB_2 formation is described by the volume fraction of the region transformed per unit time. Johnson-Mehl-Avrami analysis[36] is used to determine the rate of solute consumption due to chemical reaction, described by the increment of the volume fraction reacted (ψ) per unit time. Assuming random dispersion of transformed regions, the volume fraction reacted is given by:

$$\psi = 1 - e^{-V_{ext}} \qquad (5.3)$$

Where, V_{ext} is the extended volume fraction reacted, i.e., the fraction that would be transformed if there was no impingement between the growing particles. Assuming homogenous nucleation and isotropic growth of the particles of the new phase,

$$V_{ext} = \frac{4\pi}{3}\int_0^t I[X_1(x,t'), X_2(x,t')] \times \left(\int_{t'}^t v[X_1(x,t''), X_2(x,t'')]dt''\right)^3 dt' \qquad (5.4)$$

Where, $I[X_1(x,t), X_2(x,t)]$ is the nucleation rate, $v[X_1(x,t), X_2(x,t)]$ is the growth rate of the new

phase, t', t'' are variables for integration from time 0 to t. According to the theory of solute redistribution[81] the growth velocity of the new phase depends on the chemical compositions of the phases as:

$$v[X_1(x,t), X_2(x,t)] = v_0\left(1-\exp(\frac{z-\Delta G}{RT})\right) \qquad (5.5)$$

$$z = \frac{2\sigma_s V_m}{r} \text{ and } \Delta G = \Delta G^L - \Delta G^S + \frac{\partial \Delta G^L}{\partial X_1}(X_1^S - X_1) + \frac{\partial \Delta G^L}{\partial X_2}(X_2^S - X_2) \qquad (5.6)$$

Where, σ_s is the surface tension of the matrix melt, V_m is the molar volume of the precipitate phase, r is the radius of the individual particle, ΔG_L and ΔG_S are the Gibbs free energies of the liquid and the solid phase respectively. As it is difficult to determine the radii of each individual particle, the average radius of the particles formed is used:

$$r_{av} = \left(\frac{3\psi(x)}{\frac{4\pi}{\delta x}\int_{\delta x}[\int_0^t I(X_1, X_2)dt']d(\delta x')}\right)^{1/3} \qquad (5.7)$$

The nucleation rate can be derived from the classical nucleation theory [82] as:

$$I = I_0 \exp\left(\frac{-E}{kT}\right)\exp\left(\frac{-\Delta G^*}{kT}\right) \qquad (5.8)$$

Where, E is the activation energy accounting for the ionic mobility, ΔG* is the Gibbs free energy for the formation of critical nuclei. For the solution of the above system of equations, numerical methods are implemented in MATLAB™, as their analytical solution is not possible. The partial differential equations are solved using the finite difference scheme while Simpson's 3/8th rule are used to solve the integrals. The values of constants or parameters used in the above equations are: D = 5x10^{-9} m^2/s, V_m = 1.55x10^{-5} m^3/mol, σ = 1 N/m [34], Q = 326.3 kJ/mol. The particle size d_p is twice the particle radius r_{av}. The TiB_2 particle size distribution is determined across the matrix over a reaction time of one hour after which the reaction is complete. The mole fractions of Ti and B (X_1 and X_2) are correlated to volume fraction of TiB_2, x_{TiB_2}. For additional details of modeling refer thesis by Patra, 2009 [82].

Figure 5.6: A schematic of the coordinate system used for precipitate modeling [82]

Modeling Microstructure Evolution (F2 in Figure 5.5)

Microstructure evolution of materials during various material processes relates key properties such as mechanical strength and electrical properties to the average grain size and the grain size distribution, which are direct consequences of the microstructure evolution. The microstructure evolution during solidification depends on the thermal and the solutal fields. Fluid flow due to forced or natural convection also influences the microstructure evolution. The final grain structure of the composite is determined by three main phenomena: the heterogeneous nucleation of grains, the preferential growth orientations and the growth kinetics of a dendrite tip[83]. They are used in conjunction with the thermal-solutal fields in the cellular automata model to predict the microstructure evolution as the solidification proceeds. The mathematical description of the dendritic solidification process of a three component alloy (Al, Cu and TiB_2) in two dimensional square solidification domain (Ω) follows. For details refer to thesis by Lenka, 2009 [84].

The solid/liquid (S/L) interface evolves over time and is found as part of solution. The solidification of a three component alloy is governed by the evolution of temperature T(t,x,y) and concentration field $C^{\alpha}(t,x,y)$,where α= 1,2 which satisfy the initial conditions as well as boundary conditions at the moving S/L interface. The equations that describe the physics of solidification process are:

$$\rho C_p \frac{\delta T}{\delta t} = k\Delta T + \rho L \frac{\delta f_s}{\delta t} \qquad (5.9)$$

Where T is temperature, t is time, (x,y) is the domain co-ordinates, ρ is the density, C_p is the specific heat, k is the thermal conductivity, L is the latent heat of solidification and f_s is solid fraction. $\delta f_L = 1 - \delta f_s$, denotes the liquid fraction. The boundary condition at the walls of the domain is:

$$-k\nabla T \bullet n = h\left(T - T_\infty\right) \qquad (5.10)$$

Where n is normal to the wall, h is the convective heat transfer coefficient and T_∞ is the environmental temperature. The concentration (C) for the solute (solute diffusion equation) are given by the following two equations:

$$\frac{\delta C_L^\alpha}{\delta t} = D_L^\alpha \Delta C_L^\alpha \quad \text{for liquid phase} \quad (5.11)$$

$$\frac{\delta C_S^\alpha}{\delta t} = D_S^\alpha \Delta C_S^\alpha \quad \text{for solid phase} \quad (5.12)$$

Where α = 1,2, D_L^α and D_S^α are liquid and solid diffusion coefficients of solute α, respectively. The cross diffusion is neglected and zero flux boundary conditions are applied to the four walls of simulation domain. The solute conservation equation at S/L interface is:

$$\left(C_L^{\alpha,*} - C_S^{\alpha,*}\right) V_n = (D_S^\alpha \nabla C_S^\alpha - D_L^\alpha \nabla C_S^\alpha).n \qquad (5.13)$$

V_n , n are the normal velocity and the normal vector of the interface pointing into the liquid respectively. The notation '*' indicates evaluation of interface. The local equilibrium equation at the S/L surface is given by:

$$C_S^{\alpha,*} = K^\alpha C_L^{\alpha,*} \qquad (5.14)$$

Where K^α is the equilibrium partition coefficient for solute α. The interface temperature , T^* is defined as:

$$T^{*} = T_{L}^{EQ} + \sum_{\alpha=1}^{2}(C_{L}^{\alpha,*} - C_{o}^{\alpha})m_{L}^{\alpha} - \tau k f(\varphi,\theta) \qquad (5.15)$$

Where C_{o}^{α} is the initial concentration for solute α, T_{L}^{EQ} is the equilibrium temperature of the liquid phase, i.e., the liquidus temperature at the initial composition, m_{L}^{α} is the slope of liquidus for solute α, τ is the Gibbs Thompson coefficient, is the curvature of S/L interface, θ is the angle of preferential growth direction (generally <100> crystallographic orientations for cubic metals), and φ is the angle of the normal to the interface with respect to same axis. For heterogeneous nucleation modeling, the work done by Rappaz et al. [85] has been adopted. The total density of nucleated grains, n(ΔT) accounting for extinction of nucleation sites by growing grains is given by:

$$n(\Delta T) = \int_{0}^{\Delta T} \frac{dn}{d(\Delta T')}[1 - f_{s}(x_{TiB_2}, T')]d\Delta T \qquad (5.16)$$

Where ΔT is the given undercooling and f_s is the volume fraction of solid already formed which is a function of volume fraction of TiB_2, x_{TiB_2}. Gaussian distributions are used to describe heterogeneous nucleation both at the mould surface and in the bulk of the melt. After having described the heterogonous nucleation, I describe the growth orientation of a nucleated grain. The probability of a newly nucleated grain to have a dendritic growth direction in the range [θ, θ + dθ] is given by [84]:

$$dp(\theta) = \frac{2}{\pi}d\theta \qquad (5.17)$$

The relationship between the growth rate of the dendrite tip, v, and its undercooling, ΔT, is calculated with the aid of the Kurz-Giovanola-Trivedi model[86] and given by the solution of following equations:

$$\Omega = \frac{c' - c_0}{c'(1-k)} = Iv(P_e) \qquad (5.18)$$

$$R = 2\pi\sqrt{\frac{\tau}{mG_c - G}} \qquad (5.19)$$

$$Pe = \frac{Rv}{2D} \qquad (5.20)$$

$$\Delta T = mc_0[1-\frac{1}{1-\Omega(1-\chi)}] \qquad (5.21)$$

Ω is the supersaturation, c_0 is the initial concentration of the alloy, c' is the concentration in the liquid at the tip, χ is the partition coefficient, m is the slope of the liquidus, D is the diffusion coefficient in the liquid, G is the Gibbs-Thomson coefficient, G_c is the solute gradient in the liquid at the tip and P_e is the solutal Peclet number. Iv (P_e) is the Ivantsov function of the Peclet number. The present model determines the numerical solution of continuum equations for thermal-solutal fields. The computed flux values at the specific points along the metal-mold interface are fed into FLUENT™ to obtain accurate thermal fields over time across the casting domain. These fields are used in a state transition matrix generated in the cellular automata code to predict the microstructure evolution as the solidification proceeds. When the temperature becomes lower than the liquidus point, the cells in the matrix become solid as governed by mechanisms of heterogeneous nucleation, growth orientations and growth kinetics of a dendrite. The cellular automata code is implemented in FORTRAN™ [84].

MODULE 2: Structure-Property Correlation

Yield Stress (F3 in Figure 5.5)

The variation of the periodic hexagonal array (PHA) is used to predict the local stress and strain fields and stiffness properties based on the stress field, the volume fraction of the phases and the constituent mechanical properties[87,88]. The composite structure region is assumed to be a two dimensional hexagonal model with uniform grain size and split into a hard phase comprised of uniformly distributed TiB_2 particles in the Al-Cu alloy and a soft phase consisting of the pure

Al-Cu alloy. The hard phase takes into account the segregation of particulate reinforcements along the grain boundary region in the composite. It is assumed that the soft phase has no particulate reinforcements. The model is constrained to maintain contact between the hard phase and soft phase. The interfacial tying between the matrix region and the boundary region is done by creating contact surfaces on both phases. A representative volume element (RVE) is selected to cover the entire macroscopic volume of the composite with identical local stress and strain within each RVE (Figure 5.7). The elasto-plastic analysis of the mechanical behavior for the composite is reduced to the analysis of the RVE subject to periodic boundary conditions. A fixed percentage of the area along the boundaries of the RVE constitutes the hard phase. This area fraction correlates to the volume fraction of TiB_2, x_{TiB_2}. The periodic boundary conditions for the nodes are set so as to have equal displacement along a direction. Mathematically, the equations are:

$$u_{12} - u_{v4} = u_{11} - u_{v1} \qquad (5.22)$$

$$u_{22} - u_{v1} = u_{21} - u_{v2} \qquad (5.23)$$

$$u_{v3} - u_{v2} = u_{v4} - u_{v1} \qquad (5.24)$$

Where u_{ij} is the displacement vector for any boundary point joining vertices v_i and v_j of the RVE and u_{vi} the displacement vector for the vertex v_i of the RVE. For the hard phase (Al-4Cu-xTiB2), Young's modulus was calculated using Voigt upper bound (traditional rule of mixtures approach). The value of yield stress is determined using:

$$\sigma_c = \sigma_m(1+f_1)(1+f_d)(1+f_{orowan}) \qquad (5.25)$$

σ_c is the yield strength of the MMC, σ_m is the yield strength of the monolithic matrix, f_1 is the improvement factor associated with the load-bearing effect of the reinforcement, f_d is the improvement factor related to the dislocation density in the matrix, caused by the thermal mismatch between the matrix and the reinforcement particles f_{orowan} is the improvement factor associated with Orowan strengthening of the particles[43]. The expression for f_1 is:

$$f_1 = 0.5x_{TiB_2} \qquad (5.26)$$

The expression for f_d is:

$$f_d = 1.25 G_m b \sqrt{\omega} / \sigma_{ym} \qquad (5.27)$$

Where G_m is the shear modulus of the matrix, b is the Burgers vector, ω is the enhanced dislocation density given by [43]:

$$\omega = 12 \frac{\Delta\alpha \Delta T x_{TiB_2}}{b d_p (1 - x_{TiB_2})} \qquad (5.28)$$

Where $\Delta\alpha$ is difference in the coefficients of thermal expansion between metal matrix and particulate and ΔT is difference between processing and test temperatures. The σ_m value varies with grain size *d*, given by the modified Hall-Petch equation [89] as:

$$\sigma_y = [(\sigma_o + 22.6\ C_o) + (k_y + 1.04\ C_o) d^{-1/2}] \qquad (5.29)$$

Where C_o is the weight % of Cu (4%), k_y is the strengthening coefficient for pure metal and σ_o is a material constant related to lattice resistance. For the soft phase, yield stress and plastic strain are defined using the plasticity model. The constants used for calculating the elastic and plastic behaviors of the constituent phases are determined from experimental values[43]. A numerical solution for the elastoplastic behavior of the periodic hexagonal array (PHA) RVE (i.e., stress-strain response curve) subject to uniform tensile stresses is calculated at nodes using the finite element software ABAQUS™. Yield strength values are calculated using 0.2% offset from linear part of the stress-stress curve and is averaged over the nodes. For additional details refer to Mishra, 2010 [89].

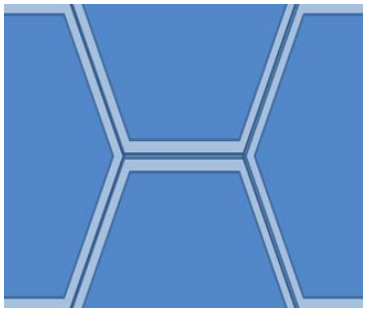

Figure 5.7: Representative volume element (RVE)

Density (F4 in Figure 5.5)

The determination of density is based on the average property of each of the constituent phases, i.e.,

$$\rho = \rho_{TiB_2} x_{TiB_2} + \rho_{Cu} x_{Cu} + \rho_{Al}(1 - x_{TiB_2} - x_{Cu}) \quad (5.30)$$

Where ρ, ρ_{TiB2}, ρ_{Cu}, ρ_{Al} are the densities of the composite, TiB_2, copper and aluminum respectively. Also, x_{TiB2} is the volume fraction of TiB_2 and x_{Cu} is the volume fraction of copper (4%).

Heat Transfer Coefficient (F5 in Figure 5.5)

The Maxwell model is used as representative of all classical models for thermal conductivity. Particle size has not been accounted for in any classical models. Based on Maxwell's work, the effective thermal conductivity (*k*) can be predicted as [90]

$$k = \frac{k_{TiB_2} + 2k_{Al-Cu} + 2(k_{TiB_2} - k_{Al-Cu}) x_{TiB2}}{k_{TiB_2} + 2k_{Al-Cu} - (k_{TiB_2} - k_{Al-Cu}) x_{TiB2}} k_{Al-Cu} \quad (5.31)$$

Where, k_{TiB_2} is the thermal conductivity of TiB_2, k_{Al-Cu} is the thermal conductivity of the Al-Cu matrix, and x_{TiB2} is the particle volume fraction of TiB_2.

MODULE 3 : Property-performance correlation

Depth (F6 in Figure 5.5)

This analysis was carried out by Bera, 2010 [91]. A finite element analysis is performed for the pressure hull to determine the collapse depth of the underwater submersible. A cylindrical shell with hemispherical end caps is considered (Figure 5.8). The outer radius is fixed at 125 mm, inner radius being variable and length fixed at 1650mm. In order to obtain the operating depth of the underwater vehicle a static buckling analysis of the pressure hull was done. The material used for the purpose was isotropic elastic material with variable yield strength and Poisson's ratio assumed constant equal to 0.3. A homogeneous solid section was assigned to the part and

the analysis was completed in three steps. In the first step the static boundary conditions were defined and the two ends of the pressure hull were pinned to the reference frame. In the second step a static pressure of 1MPa was applied on the structure. In the third step a liner buckling analysis of the pressure hull was done and another uniform pressure load of 1 MPa was applied and a minimum of four eigenvalues were requested. The element type used for the analysis was C3D20R which is a 20 node quadratic brick element suitable for linear elastic calculations. All 20 nodes have three translational degrees of freedom in the nodal x, y and z direction. The element has 27 integration points. The location of the integration points in this element enables capturing the stress concentrations at the surface of a structure. The C3D20R element employs a reduced integration scheme to decrease the number of calculations thus simplifying the overall computational complexity of the model without sacrificing accuracy. Seed size used for the problem was 10. The stress distribution and buckling pressure of the pressure hull are predicted using the finite element package ABAQUS™ [91]. A factor of safety of 1.5 is used for deriving the relationship between collapse pressure and safe depth

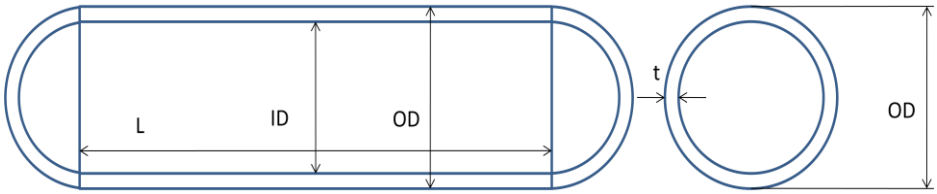

Figure 5.8: Pressure Shell of an Autonomous Underwater Vehicle

Weight (F7 in Figure 5.5)

The weight of a cylindrical shell with spherical end caps is calculated as:

$$W = \frac{\pi\rho L}{4}\left(OD^2 - ID^2\right) + \frac{4\pi\rho}{24}(OD^3 - ID^3) \qquad (5.32)$$

Where ρ the density of the composite, *L* is the length of the submersible, *OD* is the outer diameter and *ID* is the inner diameter of the cylindrical shell. The outer diameter (*OD*) is fixed at 260 mm and the length (*L*) at 1.65 meter. Thickness (T_h) varies from 5 mm to 15 mm as

representative parameters of a typical Autonomous Underwater Vehicle

Time of Operation (F8 in Figure 5.5)

$$T_{opr} = \frac{0.8(B\text{-}W).eff.E_d}{L_f + L_p} \qquad (5.33)$$

Where B is the buoyant weight of the submersible, *W* is the weight of the cylindrical shell and *eff* is the efficiency of the battery, E_d is the energy density of the battery, L_f is the fixed load for the submersible and L_p is the propulsion load for the submersible. The efficiency of a Lithium-Ion battery is typically 65% and its energy density is 128 Watt-Hour/Kg. For the initial design, assuming a slow moving submersible and submergence/surfacing rates, we shall ignore propulsion load in these calculations and assume a fixed electrical load of 400 Watt-Hour which is typical of the control computers and electronics payloads in a small underwater robotic submersible.

Temperature Conditions (F9 in Figure 5.5)

$TS_1 \text{ and } TS_2$ are the temperatures at the outer radius and inner radius of cylinder respectively. The operating temperature inside the cylindrical shess is predicted by solving the following set of equations:

$$T_{op} = TS_2 + \frac{q}{4K} ID^2 \qquad (5.34)$$

$$q = \frac{2\pi kL(TS_2 - TS_{1)}}{\ln(OD/ID)} \qquad (5.35)$$

$$0.5\dot{q}OD = h(TS_1 - T_\infty) \qquad (5.36)$$

Where $\dot{q}$ is the internal heat generated per unit volume, *OD* is the outer diameter of the shell, *ID* is the inner diameter, *K* is the thermal conductivity for the equipment inside (assume it to be

a solid cylinder), k is the thermal conductivity for the composite, h is the convective coefficient for water and T_∞ is the convective temperature of water. Having looked at the hierarchical models and IDEM in detail, IDEM is explained in respect to MMD.

5.2.3. Inductive Design Exploration Method (IDEM)

IDEM was described in detail in Section 1.2. IDEM is employed to achieve a robust multiscale design that traverses property-performance; structure-property and process-structure relationships after the bottom-up mappings are evaluated. IDEM includes parallel discrete function evaluation and Inductive Discrete Constraints Evaluation (IDCE) based on Hyper-Dimensional Error Margin Indices (HD-EMIs)[46]. IDEM is exercised to identify adjustable ranges of control factor (design variable) values in a system with uncertainty in a design/analyses process chain with complex interlinking of design variables and output responses. IDEM facilitates multiscale design, the management of uncertainty inherent in the models and the propagation of uncertainty through the design process chain. We start with performance and traverse inductively to process using IDEM. At each level a ranged set of feasible specifications is identified. The steps of IDEM for MMD are:

- *Step 1:* Rough design spaces (hyper-dimensional performance, property, structure, and process spaces) are defined and discrete points in each of these spaces are generated.
- *Step 2:* Discrete function evaluation (DFE):
  - The generated discrete points are generated using the mapping models in PS, SP and PP domain that include all quantified amount of uncertainty. The number of mapping models is larger than the number of models if a model in the multiscale system produces multiple outputs.
  - The evaluated data sets, including discrete input points and output ranges, are stored in a database.
- *Step 3:* Inductive Discrete Constraints Evaluation (IDCE) process: Using information from

Steps 1 and 2, feasible regions in property, structure and process spaces are sequentially identified with a given initial requirement range in performance space based on the Hyper Dimensional-Error Margin Index (HD-EMI) metric.

HD-EMIs are indicators of the degree of reliability of a decision that it will satisfy design space constraints or performance bounds if it undergoes a shift in the output range due to uncertainty. The HD-EMI values are calculated in each output direction in a hyper-dimensional output space, Figure 5.9. HD-EMI for output direction *i*, is represented as[46]:

$$\mathrm{HD-EMI_i} = \min\left(\frac{|(\mathrm{mean}-\mathrm{B_j})\bullet \mathrm{u_i}|}{|(\mathrm{mean}-\mathrm{B_j^i})\bullet \mathrm{u_i}|}\right) \qquad (5.37)$$

Where *j* is the set of all points on constraint boundaries, mean represents a vector of output responses, B_j is one point on the constraint boundary, B_j^i is a projection vector of B_j onto the output range along the desired output direction and u_i is a unit vector of output responses along the output direction[46]. $\mathrm{HD-EMI_i}$ is the minimum of all values calculated based on all constraint boundary points. HD-EMI metric is reliable even if there are multiple isolated feasible regions (even single points) since every feasible point will have its corresponding ensemble of constraint boundary points.

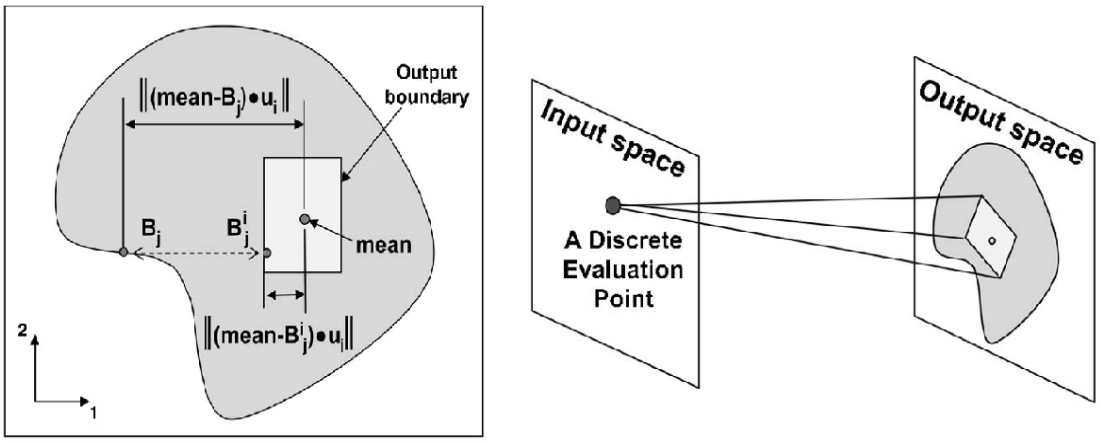

Figure 5.9: HD-EMI calculation in an output direction[46]

As the simulation models used in the multiscale system are computationally expensive, simulation experiments are systematically planned and executed at a small number of discrete points to extract relevant input-output information. The procedure for obtaining the mean and output range used in the HD-EMI calculation for simulation models is as follows:

(i) Second order response surface models are used to determine the mean response Y from the input-output data sets. Second order response surface model is represented as[65]:

$$Y=\beta_0+\sum_{i=1}^{\eta}\beta_i x_i+\sum_{i=1}^{\eta}\beta_{ii}x_i^2+\sum\sum_{i<\eta}\beta_{ij}x_i x_j+\varepsilon \qquad (5.38)$$

Where, $\beta_{ij,}$ i=1, 2… k; j=1, 2… k are the coefficients and x_i, x_j are the input design variables, ε is the random error and η the number of design variables. β_{ij}'s are calculated using least-square fit. As IDEM is computationally expensive, the fitted response surface model is analyzed to eliminate the unimportant linear, quadratic or interaction terms using stepwise regression methods[47]. The backward elimination technique is used starting with the full quadratic response surface model.

(ii) The output range is determined using the maximum ΔY_{max} and minimum ΔY_{min} deviations from the mean response Y. First the upper ΔY_{upper} and lower ΔY_{lower} deviations are calculated using statistical confidence intervals as[65]:

$$Y_{upper}=Y+\Delta Y_{CI} \qquad (5.39)$$

$$Y_{lower}=Y-\Delta Y_{CI} \qquad (5.40)$$

$$\Delta Y_{CI}=t_{n-p,\frac{\alpha}{2}}\sqrt{MSE}\sqrt{x'_0\left(X'X\right)^{-1}x_o} \qquad (5.41)$$

ΔY_{CI} denotes the statistical bounds for a 100(1-α) % confidence interval. n is the number of simulation runs and p is the total number of regression coefficients, MSE is the mean square error, X is a (n x p) matrix of the levels of regression variables

and x_o is a (p x 1) matrix of regression variables for the particular point we are calculating the confidence interval. ΔY_{CI} models the MPU due to insufficient data and not include the variability (NU) in the input variables. Assuming the variations Δx_i in the input variables are small, the maximum Y_{max} and minimum Y_{min} responses estimated using a first-order Taylor series expansion are given by[92]:

$$Y_{max} = Max\left[Y_j(x) + \sum_{i=1}^{\eta} \left| \frac{\partial Y_j}{\partial x_i} \right| \Delta x_i \right] \qquad (5.42)$$

$$Y_{min} = Min\left[Y_j(x) - \sum_{i=1}^{\eta} \left| \frac{\partial Y_j}{\partial x_i} \right| \Delta x_i \right] \qquad (5.43)$$

Where j= mean, upper and lower deviation of responses. Hence the ΔY_{max} and ΔY_{min} are determined as:

$$\Delta Y_{max} = Y_{max} - Y \qquad (5.44)$$

$$\Delta Y_{min} = Y - Y_{min} \qquad (5.45)$$

The ΔY_{max} and ΔY_{min} for theoretical models follow a similar procedure where ΔY_{upper} and ΔY_{lower} are set by the designer depending on the expected degree of deviation from theoretical response Y due to MPU.

Using the above equations, HD-EMIs can be qualitatively explained as:

(a) A HD-EMI value less than zero indicates that the mean output vector is outside the constraint boundaries and is infeasible as the numerator will be negative and denominator positive in the vector calculations,

(b) A value greater than 0 indicates the mean output vector is within the constraint boundaries, i.e. both the numerator and denominator are positive and hence is a feasible input point, further a value of 0 indicates that the length of mean output vector

from the constraint boundary is 0 and hence is coincident on the constraint boundary,

(c) A value of 1 indicates the maximum or minimum output deviation coincides with nearest constraint boundary point and hence is robust against modelled NU and MPU as discussed in description of IDEM in Section 1.2.

(d) A value of HD-EMI greater than 1 indicates the output range is further away from constraint boundaries and has a larger margin for potential error due to MSU for estimating output range.

In the IDCE process, the specifications, the performance ranges and the initial HD-EMI values for the discrete constraint evaluation are specified by the designer. A designer may leave wider margins between an output range and constraint boundaries by increasing the constraint HD-EMI value for the mapping model whose MSU is larger than others. Depending on the value of required HD-EMI, the identified feasible range may be large, small, or unattainable. Exact constraint boundaries are identified in a top-down manner using the bisection method to avoid propagated errors, i.e., combined effect of NU and MPU. The discretization resolution in IDEM is set as twice the variability so as to continuously cover the design space and identify all feasible regions unless the region is smaller than the resolution. Discretization errors due to coarse resolution occur in the vicinity between feasible and infeasible points due to which few infeasible points are deemed feasible. However, it can be reduced by more conservative resolutions at an increased computational time. IDEM is implemented in MATLAB^{TM}. Using the feasible solution spaces from IDEM, the best processing route is determined using the cDSP, described in the next section.

5.2.4. Compromise Decision Support Problem (cDSP)

Compromise decision support problem (cDSP**)** as described previously in Section 1.2, is a multi-objective decision model which is a hybrid formulation based on mathematical programming and goal programming [55]. The cDSP is explained with respect to MMD. The system goals are

normalized and achievement is evaluated using deviation variables. Weights are assigned to goals and the cDSP minimizes the weighted sum of the deviation function (Archimedean formulation). Preemptive (lexicographic) formulations are also possible in cDSP enabling hierarchical minimization of multiple deviation functions. It has the advantage of including equality and inequality constraints over traditional goal programming. For MMD, the selection of deviation variables is formulated using the cDSP. It is achieved by setting targets and constraints for the HD-EMIs and trading off their achievement to identify the design variables which minimize the deviation for the targets. The cDSP is segmented as given, find, satisfy and minimize (Figure 5.10).

Given n, number of decision variables
p, number of equality constraints
q, number of inequality constraints
m, number of system goals
$g_i(x)$, constraint functions

Find x (system variables)
d_i^-, d_i^+ (deviation variables)

Satisfy

System constraints:

$$g(x)=0 \quad i=1,\ldots,p$$
$$g(x)\leq 0 \quad i=p+1,\ldots,p+q$$

System goals:

$$A_i(x)/G_i + d_i^- - d_i^+ = 1$$

Bounds:

$$X_i^{min} \leq X_i \leq X_i^{max}$$
$$d_i^-, d_i^+ \geq 0 \text{ and } d_i^- \cdot d_i^+ = 0$$

Minimize

$$Z = [f_1(d_i^-, d_i^+), \ldots, f_k(d_i^-, d_i^+)] \text{ preemptive}$$
$$Z = \Sigma W_i (d_i^- + d_i^+) \text{ Archimedean}$$

Figure 5.10: The mathematical formulation for cDSP[55]

The given information in the cDSP includes constraints or ranges for the system performance, targets for HD-EMIs and information from the DFE and IDCE process which includes the mapping models, constraint boundaries in the hierarchical space and feasible solution ranges. HD-EMIs are constrained to be greater than one, guaranteeing the final solution is robust against modeled MPU and NU. The overachievement of HD-EMI values indicates robustness against MSU in the corresponding PS, SP or PP mapping models. This aspect is illustrated in Figure 5.11. If x represents the processing space, y represents the intermediate structure/property space

and z represented the final performance space, although both design solutions (Design 1 and 2) have identical final performances, Design 2 is more robust against MSU than Design 1 as its mapped region is further away from the constraint boundaries. Integrating IDEM and cDSP provides the advantage of considering MSU in intermediate models while making design decisions over traditional robust design approaches which focus only on final performance spaces[13]. The cDSP finds the design variables within bounds subject to HD-EMI evaluation using constraint boundaries to minimize target deviation and hence weighted HD-EMI goal achievement. cDSP is implemented in JAVA™ with a MATLAB™ builder. Different scenarios for HD-EMIs will be evaluated in Section 3.4.

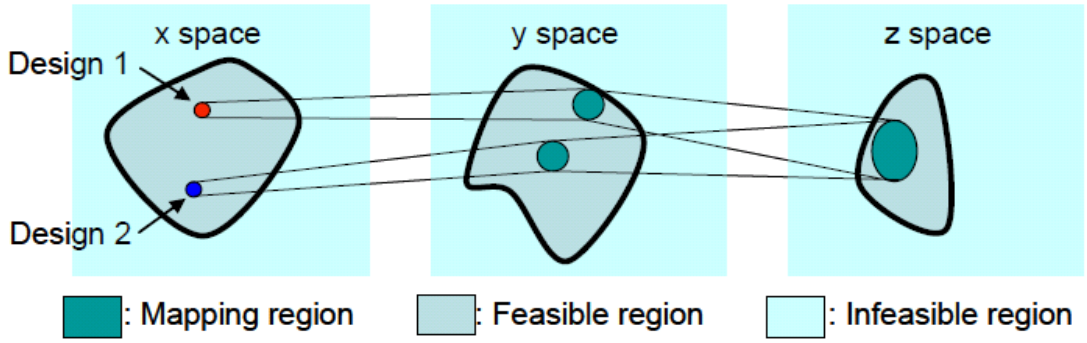

Figure 5.11: Robustness against MSU[13]

5.3. Discussion of Results

In Figure 5.12, the 4 steps are depicted in order to find the best solution for MMD of material and product. In perspective of the discussion in Section 5.2, they are:

(i) The bounds and variability of the processing variables are set for the framed multiscale system. The constraints and targets for the system goals along with ranges and resolution for the process-structure-property-performance spaces are defined. This information is used in the Step 1 of IDEM.

(ii) Using the results from the hierarchical material models, second order response surface models are developed and variables are screened using backward

elimination technique. The mean response surface models along with interval estimates are input to Step 2 of IDEM. We traverse sequentially from process to structure to property to final performance space to complete the deductive analysis.

(iii) Using information from the previous 2 steps, IDEM is employed to control the microstructure within feasible bounds subject to four types of uncertainty. Ranged feasible property, structure and processing spaces are evaluated in an inductive manner in order to achieve performance targets.

(iv) The DFE and IDCE process is input to cDSP along with HD-EMI targets to decide the best processing route among multiple feasible solutions by trading off the HD-EMI achievement.

Each step is described in greater detail in the succeeding sub-sections.

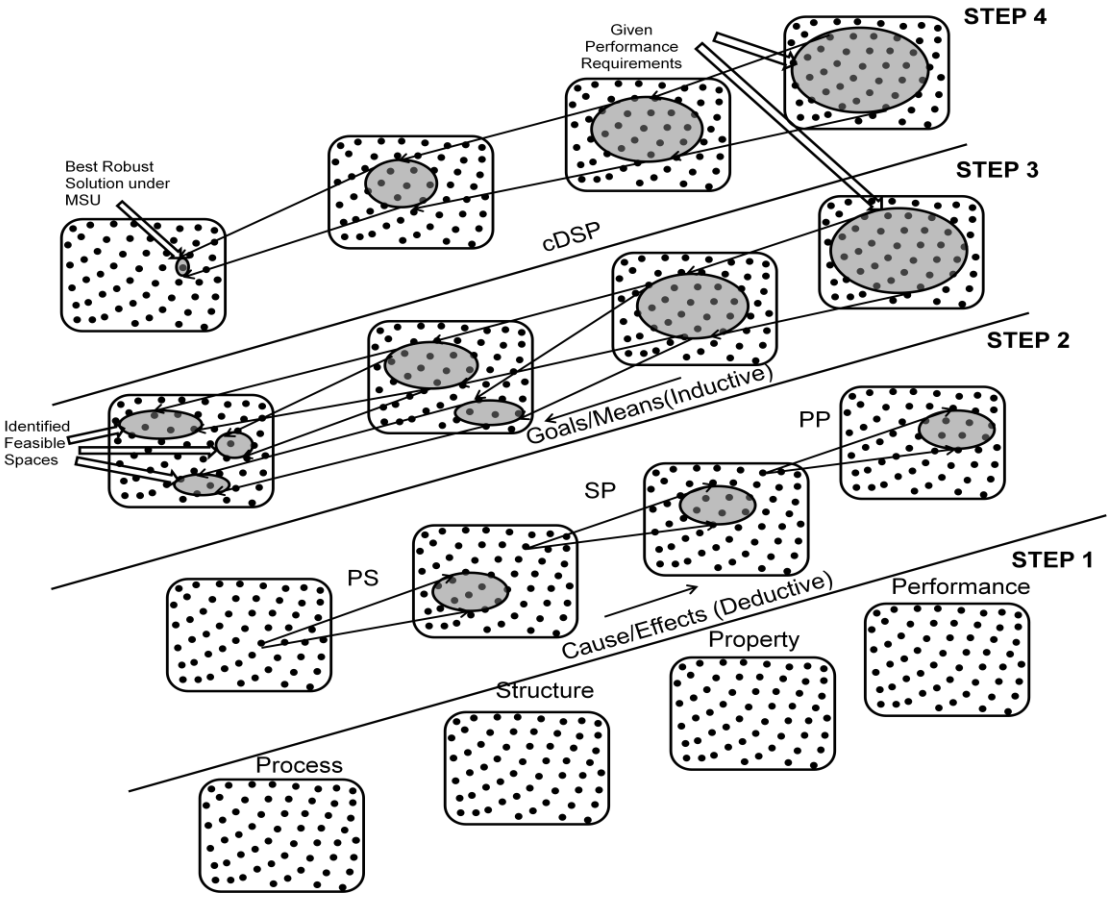

Figure 5.12: Steps for MMD

5.3.1. Quantify the Multiscale System for MMD

The multifunctional performance requirements of AUV are quantified as:

- The safe depth of operation of the submersible with a small shell thickness should be as large as possible exceeding 3000 meters and greater depth is better. The target depth is set at 5000 meters.
- The submersible must have a good endurance with a large time of operation of at least 12 hours without resurfacing or recharging and greater duration of submersion is better. The target time of operation is set at 15 hours.
- Given a weight of the vessel of 80 kilograms and allowing as large a payload as feasible, a representative limit the weight of the outer shell of the submersible may not exceed 18 kilograms and a lighter shell is preferred. The target for weight is 15 kilograms.
- The operating temperature of the submersible should not exceed 20 degree Celsius. We set an operation temperature target of 18 degree Celsius.

Table 5.3: Dependent parameters

Model	Parameter	Ranges	Resolution	Variability Δx	Model Variability	Target	Const-raint
F1	d_p	[0.1,4.2] µm	0.1 µm	0.05 µm	RSM	IDCE	NA
F2	*d*	[10,150] µm	5 µm	2.5 µm	RSM	IDCE	NA
F3	*σ*	[140,300] MPa	5MPa	2.5 Pa	RSM	IDCE	NA
F4	*ρ*	[2600,3200] kg/m^3	10 kg/m^3	5 kg/m^3	±2.5%	IDCE	NA
F5	*k*	[200,260] W/m-K	5 W/m-K	2.5 W/m-K	±2.5%	IDCE	NA
F6	*D*	[500,25000] m	25 m	NA	RSM	5000 m	≥3000m
F7	*W*	[5,30] kgs	0.5 gs	NA	±2.5%	15 kgs	≤18 kgs
F8	T_{opr}	[8,16] hrs	0.25rs	N	±2.5%	14 hrs.	≥12 Hrs.
F9	T_{op}	[16,22] C	0.C	A	±2.5%	18 C	≤20 C

Table 5.4: Independent parameters

Variable	Range	Resolution	Variability Δx	Input Modules	Input Models
x_{TiB_2}	[2,10] %	0.25 %	0.15%	1,2	*F1,F2,F3,F4,F5*
T	[1073,1273] K	10 K	5 K	1	*F1*
t	,60] mins	3 mins	1.5 mins	1	*F1*
C	[0.2,9.0] K/sec	0.4 K/sec	0.2 K/sec	1	*F2*
A	[15,30] %	3 %	1.5%	2	*F3*
T_h	[5,15] mm	0.25 mm	0.125 mm	3	*F6,F7,F8,F9*

We note that the discretization resolution for IDEM is set twice the variability so as to cover the entire design space and reasonably small enough to avoid discretization errors. Model variability due to MPU is determined using response surface confidence intervals for the simulation models and set equal to ±2.5% for the theoretical models. The response surface models along with sources of MSU and modeling of MPU and NU are briefly described in the next section. Tables 5.3 and 5.4 summarize the models, ranges, resolution, targets and constraint values for the dependent and independent parameters in the multiscale system.

5.3.2. Response Surface Modelling

The mean responses of simulation models (*F1, F2, F3* and *F6)* are analyzed using response surface modeling for modeling for the design task. As mentioned previously 0.10 value is used for the F-to-remove statistic in the backward elimination technique from the full quadratic response surface model. All variables are scaled from -1 to 1 corresponding to the ranges in the respective data sets and are denoted using symbols as described in Tables 1 and 2. The mean square error and R^2 statistic values are evaluated.

Response Surface Modeling for TiB_2 precipitate size (*F1 in Figure 5.5)*

The response TiB_2 particle size (d_p) is simulated with change in reaction temperature (T) and different initial concentrations of Ti and B which correlates to the volume fraction (x_{TiB_2}) after the reaction is complete in approximately one hour. The evolution of particle size with time (t) is determined by calculating the $d_{p.}$ in intervals of 10 minutes for a range of one hour. A sample output response is depicted if Figure 13. Thus the response d_p is a function of three variables, i.e., x_{TiB_2} , T and t (Table 5.5).

$$d_p(\mu m) = 1.42 + 0.16x_{TiB_2} + 0.61T + 1.37t - 0.20x_{TiB_2}{}^2 + 0.09x_{TiB_2}T + 0.54Tt + 0.27x_{TiB_2}t \quad (5.46)$$
$$MSE = 2.58\times10^{-2}; R^2 = 0.98$$

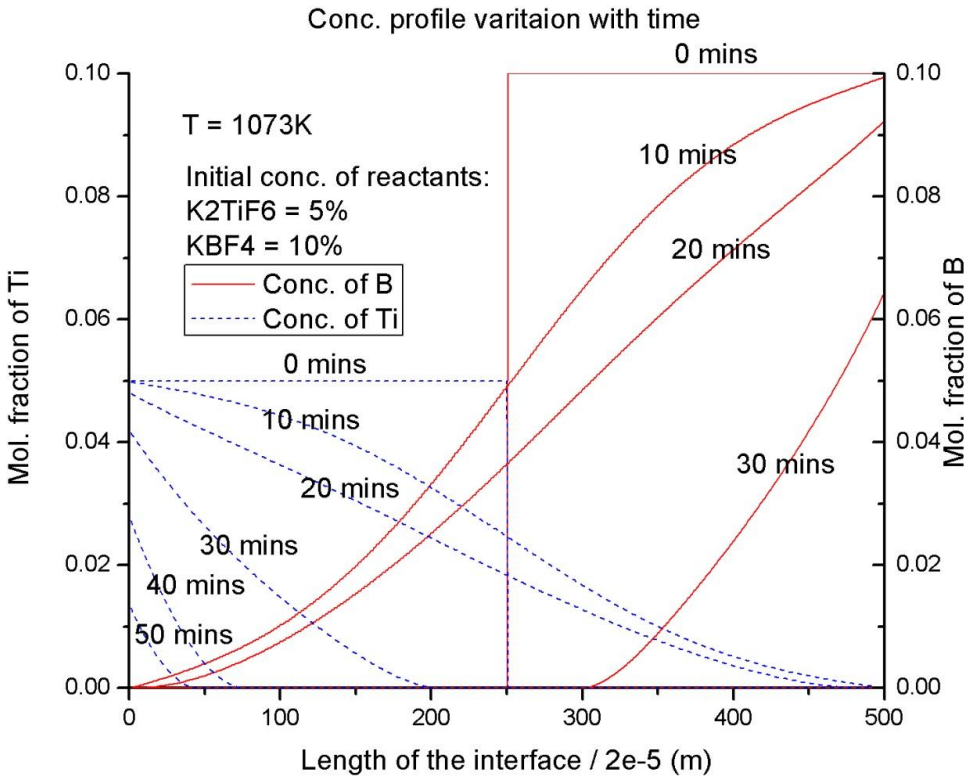

Figure 5.13: Evolution of concentration profile with time, T = 1073K, initial concentration: Ti 0.05, B 0.1 mole fraction [82]

Table 5.5: Partial data set for F1

Temperature (T) (K)	Volume Fraction (x_{TiB_2}) (%)	Time (t) (minutes)	Precipitate Size (d_p) µm
1073	2.5	60	0.885
1073	5	60	1.725
1073	7.5	60	1.683
1173	2.5	60	2.725
1173	5	60	3.1
1173	7.5	60	2.997
1273	2.5	60	3.091
1273	5	60	3.788
1273	7.5	60	4.202

The sources of MSU in *F1* are:

- In the mixed salt route TiB_2 is formed from the reaction of K_2TiF_6 and KBF_4 rather than Ti and B in elemental form as assumed in this model.
- It has been assumed that all of the Ti and B added into the melt convert to TiB_2, which is not the case. Some amount of unreacted Ti and B still remain in the melt.
- The presence of any metastable phases such as Al_3Ti and AlB_2 has been neglected in the final particulates.
- Assuming that the melt is constantly stirred during the process, gravity or viscous drag is ignored.
- The precipitate size is determined by averaging over the strips in 2-dimensional space, i.e., first order statistic.

For a time step size of 0.04 seconds, the MATLAB model has a run time of approximately 72 hours for the simulated time of one hour of the reaction. Due to the heavy computational time, the simulation model is run for a set of 9 combinations of x_{TiB_2} and T. MPU due to insufficient information from the simulation model is modeled using confidence intervals as described in Eq 41. The NU is modeled using first order Taylor series as described in Eqs 42 and 43. The

variability (Δx) values are mentioned in Table 2. The same procedure for modeling MPU and NU is followed for the rest of the simulation models.

Response surface modeling for grain size (*F2 in Figure 5.5*)

The response grain size (*d*) is simulated with change in the volume fraction (x_{TiB_2}) and evolution over decreasing temperature flux values which correlates to the cooling rate (*C*) in the mould. Thus the response *d* is a function of three variables, i.e., x_{TiB_2} and *C* (Table 5.6). The initial fitted response surface model has a low R^2 statistic suggesting poor fit and power-transformation was performed on the output response so as to improve the fit [47]. λ=0 is obtained using Box-Cox transformation suggesting *ln* power-transformation of the response. The final response surface using power transformation is:

$$\begin{aligned} d(\mu m) &= 3.50 - 0.54 x_{TiB_2} - 0.34C \\ MSE &= 0.0134, R^2 = 0.96 \end{aligned} \qquad (5.47)$$

The sources of MSU in *F2* are:

- A two dimensional square solidification domain (Ω) has been assumed for temperature flux determination to decrease the computational complexity of the model.
- <100> crystallographic orientation is assumed, idealizing $\mathrm{TiB_2}$ reinforced bimetallic composite as a cubic metal.
- Grain nucleation and redistribution due to Brownian motion is neglected.
- The average grain size is determined using a normal grain size distribution over the 2D matrix (e.g., 250x500 cells in a 500x 1000 μm matrix in Figure 5.14)

Table 5.6: Data set for F2

Cooling Rate (*C*) (K/sec)	Volume Fraction (x_{TiB_2}) (%)	Grain Size (*d*) µm
0.2	2.5	90.099
0.2	5	70.297
0.2	7.5	45.297
0.8	2.5	60.1485
0.8	5	49.0099
0.8	7.5	32.9208
5.5	2.5	39.8515
5.5	5	30.198
5.5	7.5	20.0495
7.2	2.5	32.1782
7.2	5	24.0099
7.2	7.5	17.0792
9	2.5	29.9505
9	5	20.0495
9	7.5	13.8614

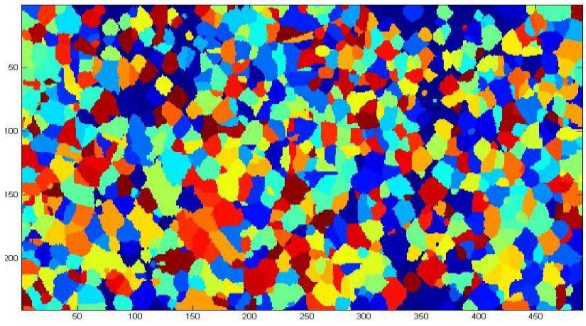

Figure 5.14: Grain distribution in 250x500 cells with a cell size of 2 µm[84]

Response Surface Modeling for Yield Strength (*F3 in Figure 5.5*)

The response yield strength (σ) is simulated with change in the volume fraction (x_{TiB_2}), varying the area fraction (*A*), grain size (*d*) and precipitate size (d_p). Thus the response *d* is a function of three variables, i.e., x_{TiB_2} and *C* (Table 7). The final response surface is:

$$\sigma(MPa) = 243.33 - 16.44x_{TiB_2} - 2.21d_p - 5.88d + 10.30L - 1.12x_{TiB_2}d_p + 4.50d_pL$$
$$MSE = 1.78; R^2 = 0.99 \quad (5.48)$$

Table 5.7: Data set for F3

Volume Fraction (x_{TiB_2}) %	Grain Size (e) µm	Precipitate Size (d_p) µm	Area Fraction *(A)* %	Yield Strength (σ) MPa
2.5	150	0.5	15	216.61
2.5	150		15	15.21
2.5	50	0.5	15	227.1
2.5	50	1	15	225.4
7.5	150	0.5	15	240.66
7.5	150	1	15	237.2
7.5	50	0.5	15	254.33
7.5	50	1	15	247.7
2.5	150	0.5	30	228.55
2.5	150	1	30	225.8
2.5	50	0.5	30	239.67
2.5	50	1	30	23674
7.5	150	0.5	30	271.36
7.5	150	1	30	264.21
7.5	50	0.5	30	286.12
7.5	50	1	30	276.64

The sources of MSU in *F3* are:

- The analysis of the yield strength for the MMC composite has reduced to a more tractable 2D RVE analysis.
- It is assumed that the particulate reinforcements are entirely segregated along the grain boundaries in the hard phase and the soft phase has no particulate reinforcements.
- The stresses in the PHA RVE are idealized to uniform tensile stresses
- The stress-strain response curve analyzed using dummy nodes over the RVE introduces MSU (Figure 5.15)

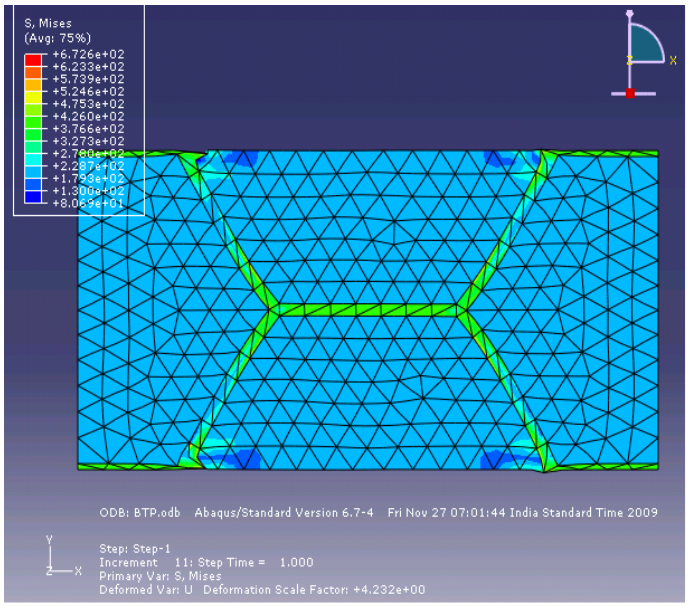

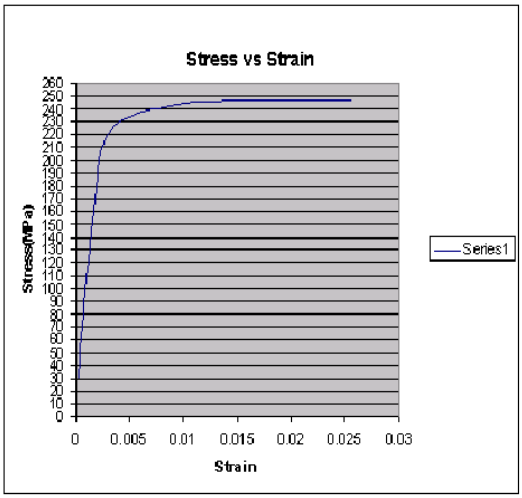

Figure 5.15: Stress distribution for Al-4Cu-2.5TiB$_2$ (Grain size=100 µm, Particle size = 0.5 µm, Area fraction of harder phase = 15%)

Response Surface Modeling for Depth (*F6 in Figure 5.5*)

The response depth (*D*) is simulated with change in thickness (x_{TiB_2}) and yield strength (σ)

$$D(m) = 1000(2.75 + 3.31t - 1.04\sigma - 1.36t^2 + 1.17\sigma^2); MSE = 6534.4; R^2 = 1 \qquad (5.49)$$

Table 5.8: Data set for F6

Thickness (T_h) mm	Yield strength (σ) *MPa*	Depth (*D*) m
6	220	701.93
8	180	1211.55
8	60	1750.05
10	140	1755.48
10	220	2758.61
10	300	3761.73
2	180	3835.7
12	260	5540.19
14	220	7433.23

Data set is given in Table 5.8. MSU in *F6* arises due to idealizing the pressure hull to be a cylinder with hemispherical end caps. The MPU and NU are modeled as described for *F1*.

5.3.3. Robust Design Spaces using IDEM

The solution for IDEM takes the structure as shown in Figure 5.16. Ranged set of performance targets are set in the top level of the MMD problem and based on property-performance (PP) mapping models and constraining the HD-EMI values ($HD\text{-}EMI_6$, $HD\text{-}EMI_7$, $HD\text{-}EMI_8$ and $HD\text{-}EMI_9$) to be greater than 1, ranged sets of discrete property space points are inductively determined along with the constraint boundaries. The HD-EMI values constrained to be greater than 1 ensure that the range of discrete property points are robust against modeled NU and MPU for performance variables.

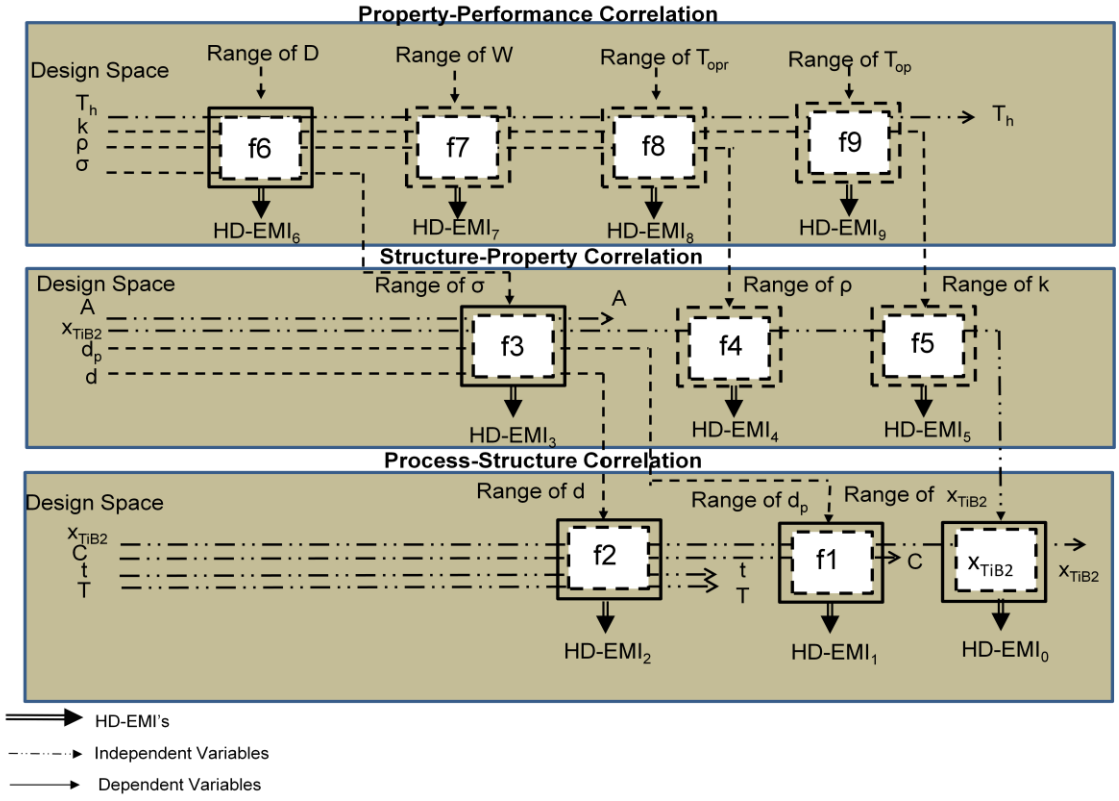

Figure 5.16: Solution strategy for MMD using IDEM

The range of property space determined by bisection method to mitigate PU is passed to the structure-property (SP) domain in the multiscale system. The independent variable, *t,* is selected by maximizing design freedom, i.e., the value which maximizes the number of discrete feasible sets in the property domain range. The same procedure is repeated with the structure-property (SP) mapping models and ranged sets of structure points and constraint boundaries are passed into the process-structure (PS) domain. The independent variable *A,* is selected in a manner similar to *t*, i.e., by maximizing design freedom. IDEM is run in the process-structure domain and finally get ranged sets of robust process variables. A dummy model is introduced for the volume fraction as x_{TiB_2} is an input to both PS and SP domains. The HD-EMI value is constrained to be greater than 1 for the property and structure models (HD-EMI$_1$, HD-EMI$_2$, HD-EMI$_3$, HD-EMI$_4$ and HD-EMI$_5$) indicating the mean output vector is within the constraint boundaries, i.e., is a robust input point. A HD-EMI value of 1 indicates that the maximum or minimum output deviation coincides with nearest constraint boundary point and hence is robust against modeled NU and MPU while a higher value of HD-EMI indicates the output range is further away from constraint boundaries and has a larger margin for potential error in the mapping model due to MSU for estimating output range. Exact constraint boundaries are identified in a top-down manner using the bisection method to avoid propagated errors, i.e., combined effect of NU and MPU. IDEM is executed and feasible and robust design points are identified in the property, Figure 5.17; structure, Figure 5.18; and processing, Figures 5.19 and 5.20, design space based on the interlinked mapping models.

The robust space of the volume fraction of TiB_2 (processing variable) lies within the ranges [0.0225, 0.035]; [0.045, 0.0525]; [0.06, 0.0675] and [0.075, 0.0775] (Figures 5.19 and 5.20). This indicates that the achieved space of the volume fraction of TiB_2, 0.0225, 0.035]; [0.045, 0.0525]; [0.06, 0.0675]; [0.075, 0.0775], thickness of shell, 10.75 mm, and area fraction, 30%, guarantees satisfactory submersible performance while maintaining all quantifiable uncertainty (MPU and NU) and its propagation within bounds. We see from Figure 17 that higher yield strength σ

values and lower density ρ values are favorable for the design and are associated with higher HD-EMI values. It can also be concluded from Figure 18 that lower grain size (d) and lower TiB_2 particle size (d_p) yield higher HD-EMI values and hence are favorable for the design. From Figures 5.18 and 5.19 it can also be concluded that higher volume fraction of TiB_2 yield higher HD-EMI values and hence more favorable design structures of the composite. The color legend for HD-EMI attainment is shown to the right of each figure. The black diamond points indicate the constraint boundary points. The absence of constraint boundary points along an axis (e.g., Thermal conductivity k) indicates that the entire range meets the desired requirements subject to modeled uncertainty. IDEM facilitates the designer to determine ranged sets of processing variables robust against modeled MPU, NU and PU. The most suitable processing route from the ranged sets is determined using the cDSP by compromising the HD-EMI attainment and hence robustness against MSU as illustrated in Section 5.3.4.

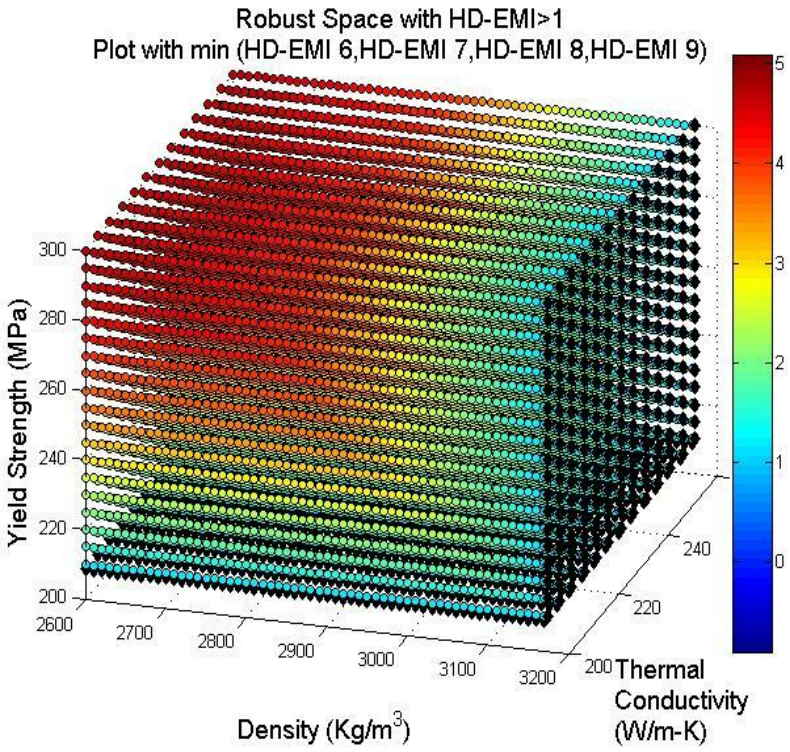

Figure 5.17: Robust design space for MODULE 3

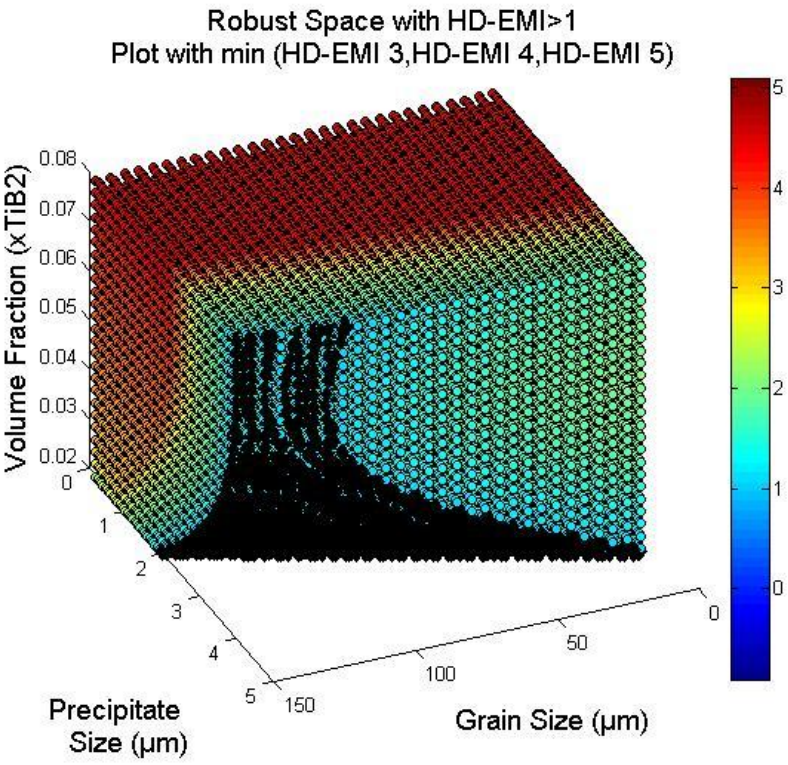

Figure 5.18: Robust design space for MODULE 2

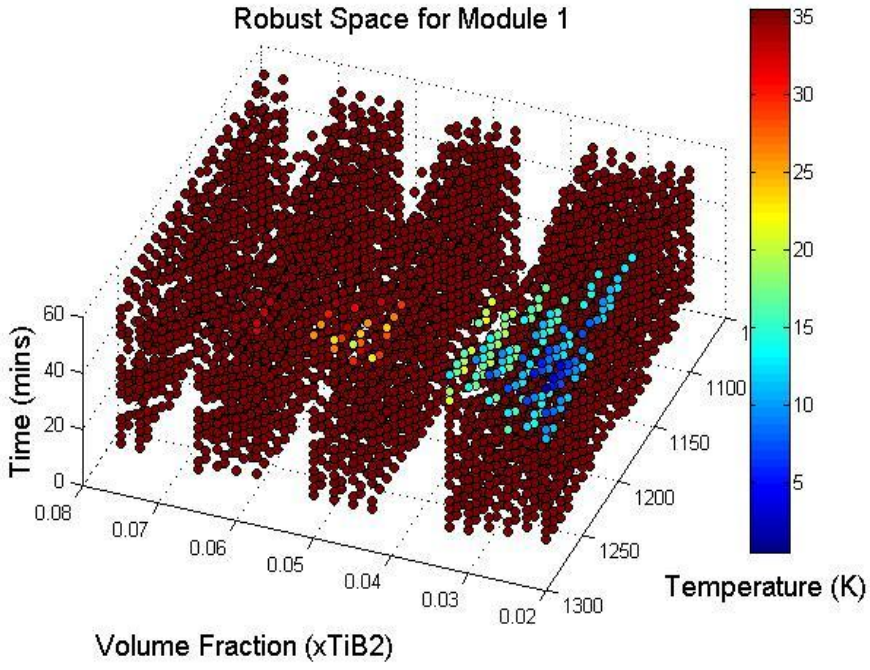

Figure 5.19: Robust design space for MODULE 1 (Precipitate size)

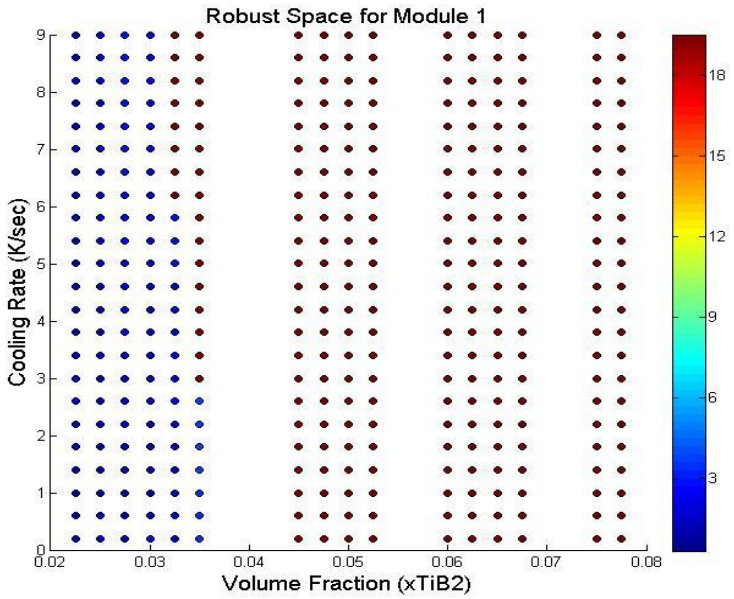

Figure 5.20: Robust design space for MODULE 1 (Grain size)

5.3.4. Compromise Decision Support Problem for HD-EMI's

The cDSP is coupled with the IDEM process in order to reduce the robust design space and find the best set of process variables by minimizing the weighted summation of deviations between the achieved objectives and target objectives. Three scenarios for the objective deviation function is formulated based on either HD-EMI values for MSU management or performance objectives:

• *Scenario 1*: Find the optimal design specifications for the process variables that optimize the performance objectives, i.e., depth, time of operation, weight and operating temperature.

• *Scenario 2*: Find the robust design specifications for process variables that incorporate modeled uncertainty in the mapping models (MPU, NU, PU) in order to optimize the performance objectives.

• *Scenario 3*: Find the robust design specification for process variables considering MSU in the mapping model in addition to modeled uncertainty in order to optimize the HD-EMI attainment.

For Scenarios 1 and 2, the deviation function is formulated using performance objectives with equal weights while in Scenario 3, the deviation function is formulated using HD-EMI value attainment and the robust solution for the multiscale system, i.e., values of the design variables, is calculated by minimizing the deviation of the HD-EMIs from target values (10 for all models and equal weights). While only one scenario for robust design specification is analyzed, the cDSP provides for setting different target values based on provision for potential MSU and hierarchical optimization of deviation functions and other scenarios can be set as deemed appropriate by system level designer. For Scenario 2 and 3, the constraints on all HD-EMIs must be greater than or equal to 1 and the number of solution sets found by the IDCE in IDEM must be at least 1. The results of the design exploration are shown in Table 5.9. The achieved HD-EMI values are infinite when no constraint boundaries exist in the output direction. The HD-EMI value is -1 when the mean output lies outside the ranged specifications. The values of independent variables, T_h and *A*, are 10.75 mm and 30% respectively as found out using IDEM.

Scenario 1 gives us the optimal performance achievement, however, HD-EMI$_1$ is -1 indicating the d_p is outside the prescribed range and hence suggesting uncertainty consideration in the interdependent variables is vital along with final system performance. In Scenario 2 the HD-EMI values are constrained to be greater than 1 and process variables yield robust final performance considering modeled NU, MPU and PU. In Scenario 3, the deviation function formulated using HD-EMI values is minimized yielding most suitable solution under potential MSU. In Scenarios 2 and 3, system performance is compromised to account for uncertainty. The consideration of modeled MSU using the HD-EMI metric in addition to modeled MPU, NU and PU in IDEM provides robustness against incorrect mapping functions due to inappropriate assumptions or limited knowledge. The HD-EMI target values can be altered in the cDSP formulation to consider higher or lower potential MSU by the material modeler or system level designer. Thus, the cDSP identifies the best solution amongst the ranged sets by compromising performance or HD-EMI attainment.

Table 5.9: cDSP solutions

Variables			Scenario 1	Scenario 2	Scenario 3
HD-EMI Variables	*F1 (d_p)*	$HDEMI_1$	-1	∞	∞
	F2 (d)	$HDEMI_2$	∞	∞	∞
	F3 (σ)	$HDEMI_3$	11.77	13.02	12.90
	F4 (ρ)	$HDEMI_4$	4.27	4.21	4.21
	F5 (k)	$HDEMI_5$	∞	∞	∞
	F6(D)	$HDEMI_6$	12.59	12.75	12.79
	F7 (W)	$HDEMI_7$	18.04	18.05	18.05
	F8 (T_{opr})	$HDEMI_8$	4.20	4.21	4.21
	F9 (T_{op})	$HDEMI_9$	5.44	5.45	5.45
Design Variables	x_{TiB_2}		0.080	0.0775	0.0775
	T(K)		1073	1163	1073
	C(K/sec)		9.0	8.6	0.20
	t(mins)		15	12	21
Perfor-mance Variables	*D(m)*		4674.5	4571.4	4551.4
	W(kgs)		15.62	15.65	15.64
	T_{opr}(hrs)		13.45	13.45	13.45
	T_{op}(C)		17.51	17.50	17.50

5.4. Thoughts on What has been Presented and What is Next

A robust design approach for MMD is investigated by coupling IDEM and cDSP by making system level performance insensitive to MPU, MSU, PU and NU without eliminating its sources. Ranged sets of process variables are identified for MMD using IDEM while maximizing design freedom and considering quantifiable uncertainty (MPU, NU and PU). A singular robust solution is identified by compromising product performance for achieving robustness against MSU using

cDSP and HD-EMI metric. The key features using a coupled IDEM and cDSP approach are:

- IDEM facilitates top-down searching for design solutions including process path and microstructure based on bottom-up simulations. The specific ranges of microstructure attributes are directly coupled in the present methodology with the overall systems design (material plus submersible). Hence, changes in performance requirements are directly reflected in the ranges of microstructure attributes that emerge from application of IDEM.
- All sources of uncertainty are accounted in identifying a singular robust solution. NU, MPU and PU are accounted for in IDEM which provides ranged sets of robust solutions. NU or variability is dealt with first order Taylor series expansion.MPU is dealt by defining confidence intervals for response surface models developed. PU is dealt by developing exact constraint boundaries in a top-down manner using bisection technique. MSU is dealt by trading off the HD-EMI attainment from the robust ranged sets of solution.
- Feasibility of process paths is assessed by considering the full contributions of the process-structure-property-performance relations. The approach can be ready extended to include additional competing modes of microstructure requirements or existing mapping models in the design chain can be altered without revaluating the entire design exploration. This is possible due to the modular nature of the mapping models and as the uncertainty modelled in mapping functions is decoupled from design exploration.
- With material modelling techniques at its infancy, consideration of potential MSU serve as a compelling basis for the present systems-based robust design approach. Although the approach does not guarantee robustness against unquantifiable or unrecognizable MSU, it facilitates robust decision making under potential MSU by aiding for the desired level of MSU mitigation in terms of HD-EMI targets or constraints.

The work presented in this chapter constitutes one of the most complete applications of uncertainty management for integrated material and product design. Uncertainty is successfully

managed over three modules and nine analysis models in the PS, SP and PP domains for MMD. The MMD approach determines robust processing routes to pursue concurrent design of a robotic submersible and Al-based metal matrix composite that embodies the microstructure-mediated robust design construct and holds promise for early design space exploration in designing both the product and the material from which the product is made. The advantage of this method is the use of simple input-output mappings in the form of response surface models to calculate the system robust solution. The uncertainty arising due to use of the response surfaces is systematically accounted in the form of statistical confidence intervals. IDEM can be applied without resorting to complex material knowledge and mathematical formulations but only through having access to the input output functions and the range of operation of the simulation model. It is noted that the MMD approach is different from the MSD approach as a designer uses response surface models as input-output relationships instead of direct data from the simulation models. The flexibility of this approach enables a designer to use other mathematical relationships instead of second order response surface models as illustrated in the MMD approach. A material designer, once he/she has access to a better model can use the improved data set to build new response surface models and plug it into the IDEM infrastructure without having to iterate the entire design process. This enables saving time and resources as well as increases the flexibility of the IDEM. The IDEM is also capable of using the data itself in form of sub-routines in the main MATLAB function. A designer has the flexibility to use these sub-routines for direct measurements of the response based on the original simulation model instead of resorting to response surface modeling. Though this will result in increased computational cost, it has the benefit of increased accuracy based on real-time design of experiment setting. This possibility of IDEM greatly increases the flexibility to couple it with MSD exploits while avoiding re-calculation of the entire design process to provide robust feasible sets. It is also useful for maintaining design freedom in initial design exploration while material design modeling techniques are at its infancy. A detailed description is provided in I-Statement in the Section 7.2. Having looked at robust design for a multiscale system, the next frontier of uncertainty management is explored, i.e., uncertainty reduction in the next chapter.

In this chapter the secondary research question 1 (Section 4.1) was answered by integrating the constructs of IDEM and cDSP. Uncertainty modeling was systematically established in multiscale systems for MMD and validated the hypotheses proposed for the secondary research question. Results were achieved and it fits into the Empirical Performance Validity, i.e., Quadrant III of the validation square. The organization of work is depicted in Figure 5.22.

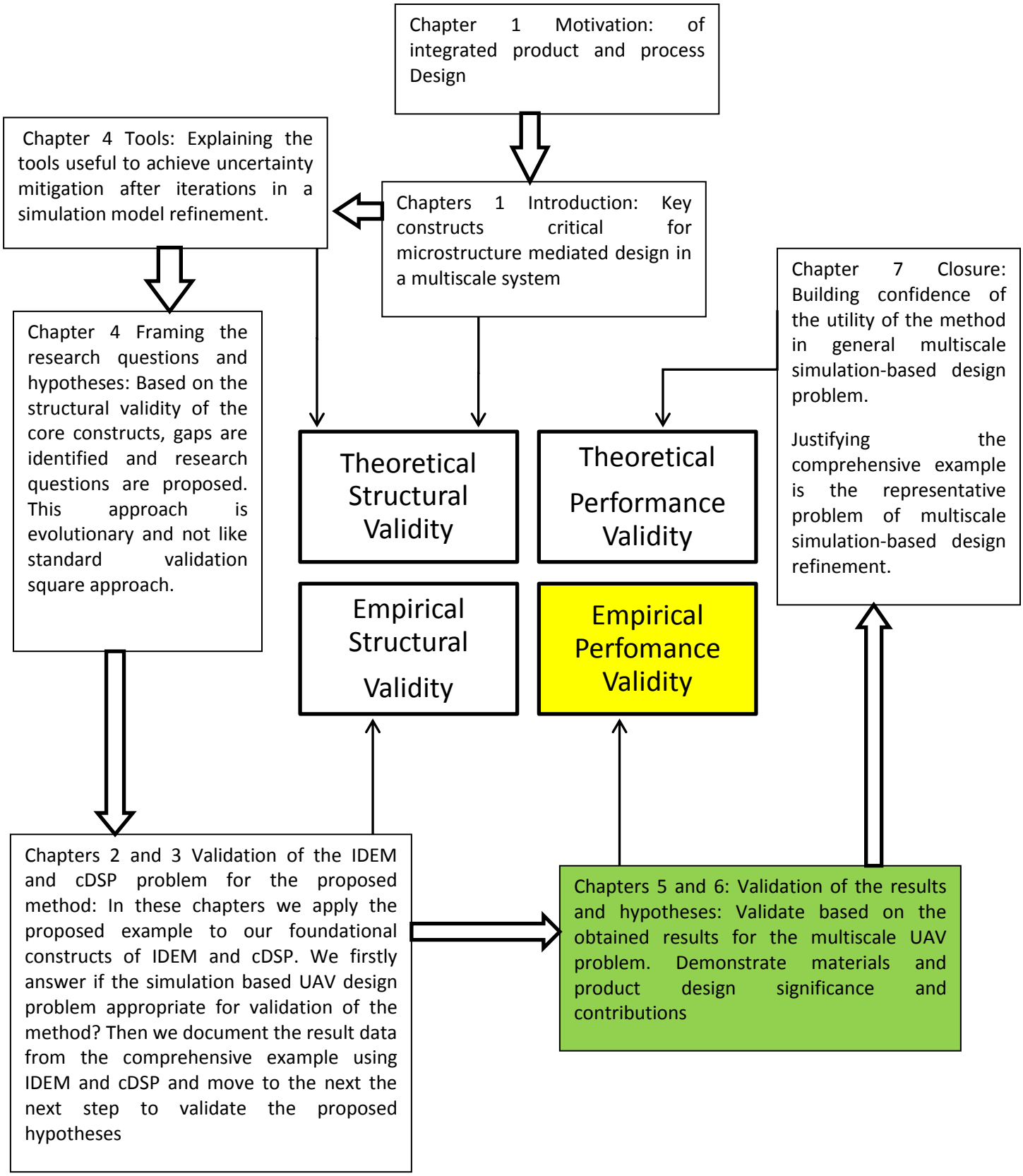

Figure 5.21: The validation square

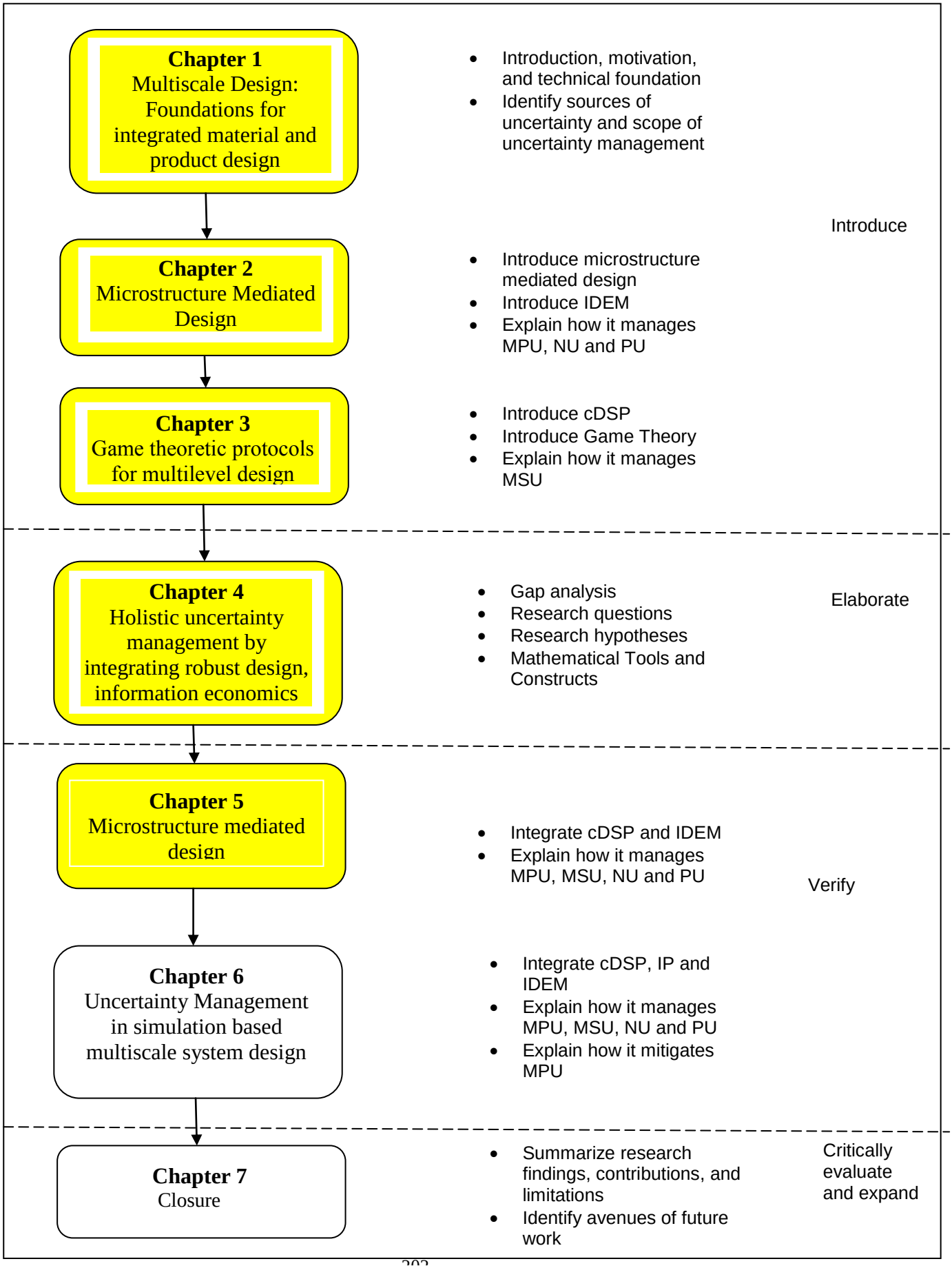

Figure 5.22: Organization of work

CHAPTER 6

UNCERTAINTY MANGEMENT IN SIMULATION BASED MULTISCALE SYSTEMS

Chapter 5 was dedicated to arriving at ranged sets and a single robust solution in multiscale systems. This was achieved for the microstructure mediated design task. In this chapter, the opportunities for managing uncertainty in simulation-based design of multiscale systems are explored using constructs from information management and robust design. A multiscale system is simulated with models at multiple length and time scales. The accuracy of the simulated performance is determined by the trade-off between computational cost for model refinement and the benefits of mitigated uncertainty from the refined models. Hence, the motivating question: 'How should a system level designer allocate resources for auxiliary simulation model refinement while satisfying system level design objectives and ensuring robust process requirements for multiscale systems? My approach consists of integrating: (i) a robust design method for multiscale systems, and (ii) an information economics based approach for quantifying the cost-benefit trade-off for mitigating uncertainty in simulation models. Specifically, this approach focuses on allocating resources for reducing model parameter uncertainty arising due to insufficient data from simulation models. A comprehensive multiscale design problem, the concurrent design of material and product is used to demonstrate my approach. System level designers can efficiently allocate resources for sequential simulation model refinement in multiscale systems using the approach presented in this chapter.

6.1. Frame of Reference: Uncertainty Management in Simulation-Based Multiscale Systems Design

Uncertainty in simulation-based design is particularly important in systems at multiple length and time-scales, referred to as multiscale systems. Multiscale systems design (multiscale design) is characterized by a number of challenges[29] such as: a) the presence of both *reducible* and *irreducible* uncertainties, b) the presence of uncertainties within individual models, which are due to uncertain parameters, approximations, assumptions, etc., c) propagation of uncertainties in networks of interconnected models through multiple scales, d) evolving simulation models, resulting in multiple fidelities of models at different points in a design process, and e) significant model development and execution costs, necessitating judicious use of computational resources.

Robust design alleviates the consequence of uncertainty without removing the underlying sources[12]. Most published approaches for robust design are focused on mitigating reducible uncertainties to the extent possible and developing accurate representations of irreducible uncertainty[8-13]. In the context of simulation based multiscale design, both approaches are associated with an increase in effort. Uncertainty mitigation necessitates additional simulation runs or modeling effort, whereas increasing the information about uncertainty demands increased computational effort. In the multiscale design, this increase in effort is so significant that it can prevent design exploration and has proven an impediment to the development of efficient methods that facilitate robust design. Instead of striving to mitigate reducible uncertainty and getting meta-information about irreducible uncertainty, the paradigm of *managing uncertainty* is proposed by balancing: a) the need to reduce uncertainty (by gathering more information, refining modeling assumptions, accurate representations etc.), and b) making decisions that are robust against various sources of uncertainty in simulation-based multiscale design. The motivating question for this chapter is: *'How does a system level designer allocate*

his/her limited resources for auxiliary simulation model refinement while ensuring a robust design and satisfaction of system level design objectives in multiscale design?' It is postulated this can be addressed by integrating constructs from robust design and information economics.

Information economics guides the best course of action between using available information (e.g., using simpler models) or gathering more information (i.e., simulation model refinement) in the decision-making process[66-68]. The integration of information economics and robust design is challenging because in addition to the design decisions involving the system's performance objectives, there is an additional layer of meta-level decisions involving the tradeoff between uncertainty reduction and effort. These meta-level tradeoff decisions require the knowledge of the effort and costs associated with uncertainty mitigation. My approach to address the motivating question is to separate the multiscale design problem into two sets of decisions: a) robust design constructs are used for the recommendation of product parameters (i.e., design variables) in the presence of uncertainty, and b) information economics constructs to quantify the cost-benefit trade-off. Integration of these twin constructs is achieved via auxiliary simulation model refinement. My belief is that successful integration of information economics and robust design enables efficient allocation of resources (time/money) to improve system level performance while satisfying robust process requirements. This integrated algorithm is developed in Section 6.2 and a comprehensive multiscale example of concurrent product and material development is used to clarify each step and validate my algorithm in Section 6.3. Closing thoughts are presented in Section 6.4.

6.2. Integrating Robust Design and Information Economics

6.2.1. Uncertainty

Simulation models are used to generate information about physical phenomena when it is impractical or expensive to measure the outcomes using experiments or direct measurements. Simulation models are built on underlying assumptions under which the models are valid. They

guide the development of the predictive capabilities between the desired response (output) and the design variables (input). Often, these simulation models are computationally expensive making it infeasible to search the design space for satisfying responses. Instead, simulation experiments are systematically planned and executed to extract relevant information and approximate mathematical surrogates, i.e., metamodels which represent input-output relationships. These relationships are used in multiscale systems to search for desired solutions of design variables. The uncertainty associated with these assumptions or approximations may further be amplified as it propagates through a chain of simulation models at different length and time scales with interlinked parameters as is often the case with multiscale systems.

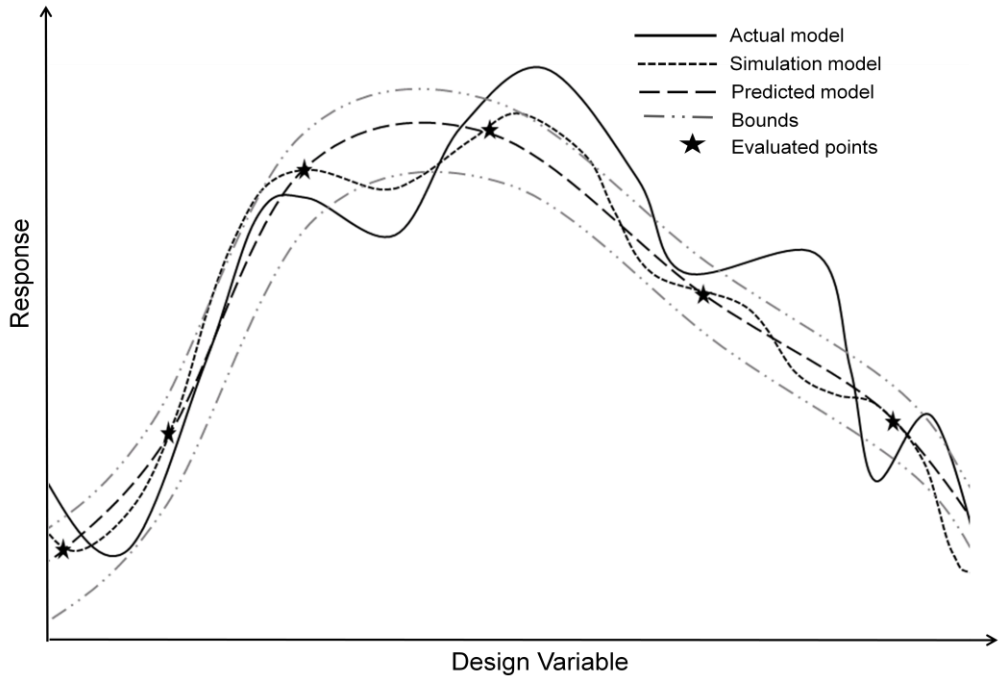

Figure 6.1: Uncertainty in simulation models.

It is critical to understand the sources of uncertainty in multiscale systems in order to manage the uncertainty efficiently and hence it is mentioned again from Section 1.2. In the context of simulation-based design for multiscale systems uncertainty is classified as[13]:

- **Variability (Natural Uncertainty):** Variability is irreducible and can be quantified in a statistical sense. It arises due to inherent randomness of noise and control factors in physical systems.
- **Model Parameter Uncertainty (Data Uncertainty):** It arises due to uncertainty in model parameters of a surrogate model used to represent the simulation model. It can be reduced by additional information.
- **Model Structure Uncertainty (Model Uncertainty):** This uncertainty is introduced due to the assumptions and approximations used while building a simulation model. It can be reduced by model refinement, i.e., better assumptions or approximations, usually at a greater computational cost.

These sources of uncertainty are represented graphically in Figure 6.1. A hypothetical physical phenomenon is represented with a solid curve. A simulation model with simplifications and assumptions predicts this phenomenon under model structure uncertainty (---- curve). Running the simulation model at a small number of inputs (star points) and building a metamodel to represent the input-output relationship introduces model parameter uncertainty (— — — —curve). Further the inputs also possess variability. Upper and lower bounds are built (dotted curves) on this metamodel to capture variability of inputs and statistical confidence intervals for the error in model parameters, i.e., these bounds quantify the model parameter uncertainty (MPU) and natural uncertainty (NU) in a simulation model. However, model structure uncertainty (MSU), i.e., information about the simplifications and assumptions is not captured by these bounds. My hypothesis is that by systematically reducing these error bounds over simulation models at different length and time scales, i.e., at the subsystem scales/levels, I achieve robustness (insensitivity to NU and MPU) in the system process as well reliable performance targets. Variability is aleatory (irreducible) in nature but we can mitigate the other two types of epistemic (reducible) uncertainty with additional effort. There are two ways to refine simulation models at an added cost to achieve better performance: a) refine the model

formulation to reduce model structure uncertainty (mitigate MSU) and b) accumulate more data to reduce model parameter uncertainty (mitigate MPU). In this chapter, the focus is on developing metrics to reduce MPU. Reducing MSU is challenging because there are different physical laws governing different length and time scales and only an accurate understanding of these laws along with comprehensive knowledge about modeling techniques can quantify the relative uncertainty of model structure in order to reduce it.

6.2.2. Method for simulation model refinement in multiscale systems

An eight step method is proposed for a system level design to be able to allocate resources to subsystem level simulation model refinement in multiscale systems by integrating constructs from robust design and information economics, Figure 6.2. This approach relies on the ability to uncouple individual subsystem modules from the overall calculation.

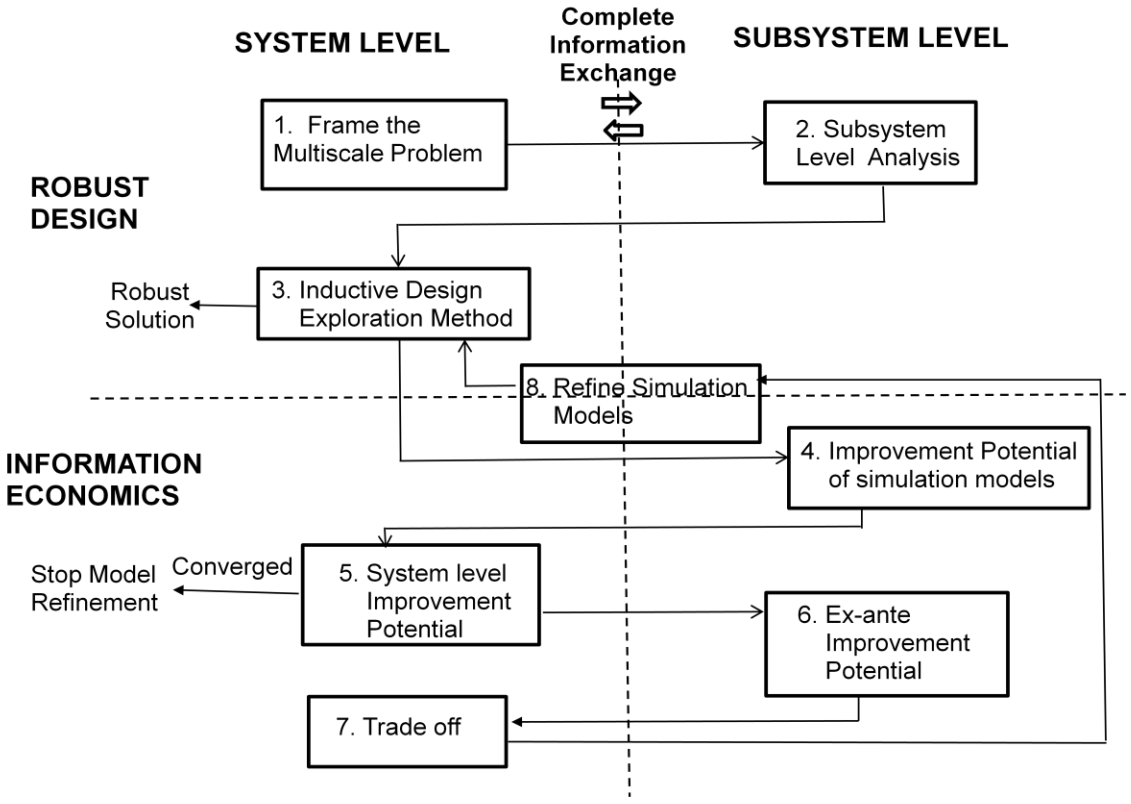

Figure 6.2: Simulation model refinement for uncertainty management in multiscale systems

Step 1. Frame the Multiscale Problem

The system level designer comprehensively represents the design process chain, simulation modeling techniques at subsystem levels and dependent/independent parameter values/ranges interlinked with individual subsystems in a multiscale system. This step ensures system level connectivity with subsystem level models for multiscale design.

Step 2. Subsystem Level Analysis

The subsystem level modelers analyze the simulation models in the multiscale system, i.e.:

(i) Perform design of experiments to plan simulation runs;

(ii) Execute simulation models;

(iii) Develop response surface models or other metamodels and;

(iv) Establish bounds

The response surface models along with bounds are passed to the system level designer.

Step 3. Robust Design Exploration

The system level designer performs robust exploration to determine possible sets of solutions under MPU, MSU, NU and a compounded combination of all three uncertainty types due to propagation in the design chain and determines the best solution amongst the feasible sets. It passes the ranged sets of solution to the subsystem modelers. For robust exploration and to determine a robust solution the use of the Inductive Design Exploration Method (IDEM) is proposed.[13] IDEM facilitates hierarchical design of multiscale systems while accounting for all three kinds of uncertainty in simulation models and its propagation[93]. It identifies ranged sets of discrete design variables in each domain at the subsystem scales in an inductive way and determines a desirable solution against MSU[13].

Step 4. Subsystem Level Value-of-Information

Subsystem level designers quantify the value-of-information associated with: a) refining assumptions/approximations in inputs or modeling techniques for simulation models and b)

gathering additional information from existing simulation models. In this work, the focus is on the latter and, in the context of simulation refinement, this added information correlates to mitigating MPU and hence improving the model's ability to recommend good decisions. Specifically, a metric is developed to quantify insufficiency of data from simulation runs, the improvement potential metric (IP_i)[69]. Each subsystem designer calculates the IP_i metric corresponding to its simulation model.

Step 5. System Level Value-of-Information

Using these improvement potential metrics, the system level designer calculates the improvement potential metric *(IP)* for the multiscale system, i.e., system-level improvement potential *(IP),* to check for convergence and ensure there is added value in further simulation model refinement. A weighted sum approach is used for this calculation where weights are derived as degrees of influence of simulation models on system-level performance objectives.

Step 6.Cost-Benefit Analysis

The subsystem level modelers develop a functional relationship between the computational cost for auxiliary simulation runs and the benefit in terms of improvement potential metric referred to as the *ex-ante* improvement potential (IP'_i). IP'_i is the predicted benefit associated with additional simulation runs without performing the simulation runs.

Step 7. Trade-Off

The system level designer uses the functional relationships between computational costs and IP'_i to make the meta-level decision trade-off. That is, to minimize total computational time versus constraining system level *ex-ante* improvement potential in order to find an *IP'* below convergence criterion) and assigns computational resource for further simulation refinement.

Step 8. Refine Simulation Models

The subsystem level modelers run the next set of simulations based on assigned resources and provide improved metamodels for the robust exploration step (Step 3). The algorithm is iterated until the system level improvement potential (*IP*) is equal to or drops below the desired convergence criterion.

The entire algorithm can be thought of as being divided into four quadrants. Steps 1 to 3 are linked to robust design while steps 4 to 7 deal with information economics. Step 8 integrates robust design and information economic constructs. Steps 1,3,5,7 are performed by the system level designer while Steps 2, 4 and 6 are performed by the subsystem level modelers. An important assumption here is that there is complete information exchange between the system and the subsystem level designers, i.e., total collaboration. I proceed to explain each step in the context of my example multiscale system, i.e., concurrent design of material and product in Section 6.3.

6.3. Concurrent Design of Material and Product

6.3.1. Design of Autonomous Underwater Vehicle (AUV) using In-Situ Al-Based Metal Matrix Composite (MMCs)

The paradigm of concurrent design of materials and product entails tailoring materials to meet specific performance requirements. Design of material refers to controlling the microstructure and design of product implies meeting the performance requirements. Hierarchy exists over multiple length and time scale in the process-structure [PS], structure-property [SP] and property-performance [PP] relationships, Figure 6.3. Hence, concurrent material and product development can be viewed as a multiscale problem. There is significant uncertainty associated with simulation modeling in the material domain scales, i.e., quantum, molecular or microscale as physical phenomena at these scales is not fully understood and modeling assumptions lead to

increased uncertainty. The computational cost of executing simulation runs at these levels is high and efforts to reduce computational cost result in model simplification using metamodeling techniques and hence lead to an increased uncertainty component. Hence, concurrent design of material and product is a representative example for uncertainty management in multiscale systems and is useful for demonstrating the integration of robust design and information economics.

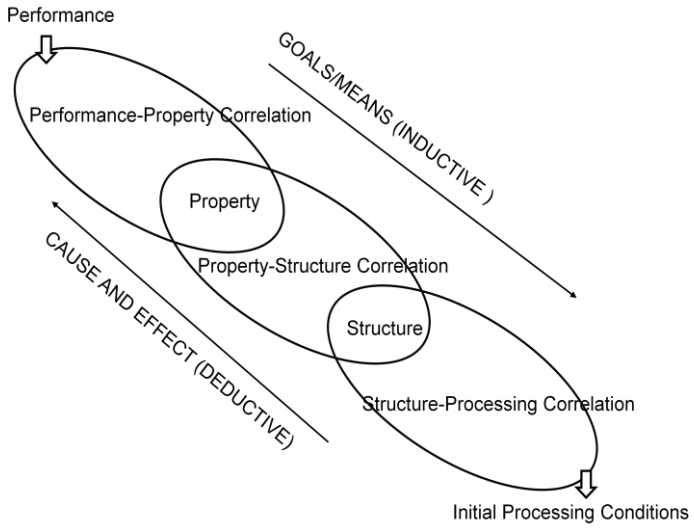

Figure 6.3: Hierarchical materials design[4]

Design of an Autonomous Underwater Vehicle(AUV) is considered with the following multifunctional requirements:[29]

- The safe depth of operation of the submersible with a small shell thickness should exceed 5000 meters and the greater the depth the better.
- The submersible must have a time of operation of at least 12 hours without resurfacing or recharging. Greater duration of submersion is better.
- Given the weight of vessel to be 80 kilograms and allowing as large a payload as is feasible, a representative limit for the weight of the outer shell of the submersible may not exceed 18 kilograms, and a lighter shell is preferred.
- The operating temperature of the submersible may not exceed 20 degree Celsius to

ensure safe operation of the electronic equipment within the submersible.

Metal matrix composites (MMCs) are strong and stiff light metal-based composites and with a reinforcement which may be a metal, ceramic or an organic compound[78]. A new category of materials known as in-situ composites have been developed, wherein the reinforcements are generated in a metallic matrix via chemical reactions between elements and/or compounds during the composite fabrication[80]. This example deals with the processing route of in-situ Al composites. In this chapter we work with an Al-Cu matrix strengthened with TiB_2 reinforcement. The 8 steps for are followed the example (Figure 6.4).The steps associated with robust design are demonstrated in Section 3.2 and those with information economics in Section 6.3.3. In Section 6.3.4 the integration of the two constructs is achieved via sequential simulation refinement.

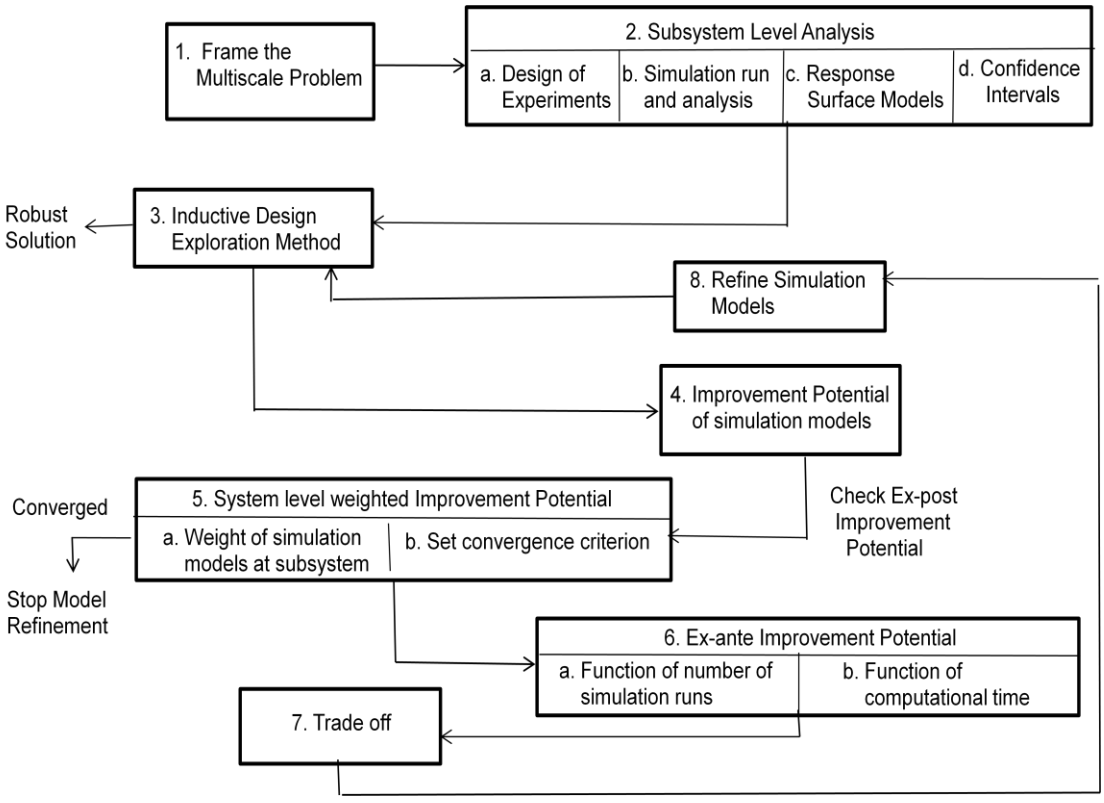

Figure 6.4: Simulation model refinement for multiscale design

6.3.2. Robust Design of the AUV using In-Situ Al-Based MMCs

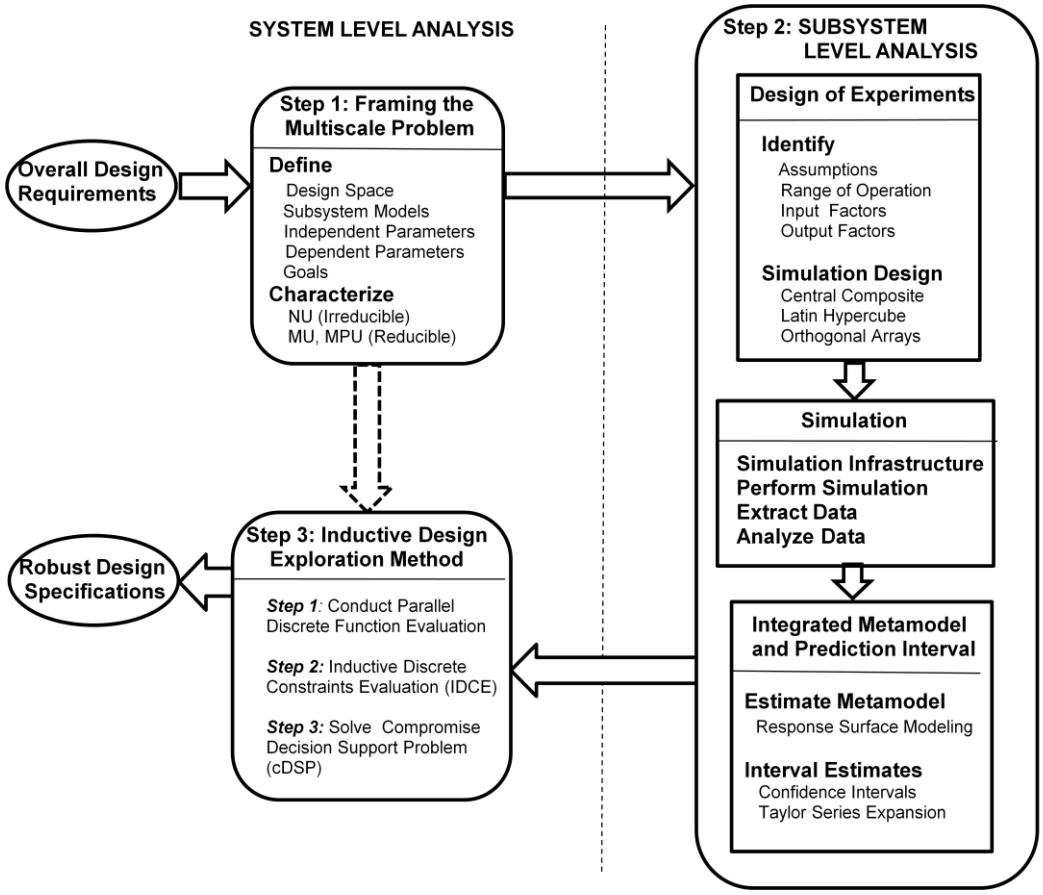

Figure 6.5: Robust design of multiscale systems using IDEM

The Inductive Design Exploration Method[13] is used for robust design of my multiscale system. This corresponds to Steps 1-3 in Figure 6.2. The steps of IDEM are:

- ***IDEM Step 1:*** **Parallel Discrete Function Evaluation for Each Subsystem**

The design space (design variables), interdependent space (dependent variables) and the performance space (performance variables) are defined and discrete points are generated. These generated points are evaluated based on mapping models (i.e., surrogate models) and the evaluated data sets composed of discrete input points and associated output ranges are stored in a database.

- ***IDEM Step 2:*** **Inductive Discrete Constraints Evaluation (IDCE)**

Feasible and robust regions in interdependent and design spaces are sequentially identified with constraints in the performance space based on a metric called the Hyper Dimensional-Error Margin Index (HD-EMI) indicating the degree of reliability of the model if it undergoes a shift in the output range due to uncertainty.

- ***IDEM Step 3:*** **Compromise Decision Support Problem (cDSP) for System Level Design.**

The cDSP[55] is used to calculate the most desirable robust solution from the feasible set of solutions for the design parameters by reaching a trade-off among the HD-EMI values.

With IDEM, ranged sets of feasible specifications (discrete points) are identified and a robust solution is calculated under different kinds of uncertainty. The ranged sets of specifications are used for calculating the improvement potential metric while the robust solution indicates the design variables for robust process requirements once the algorithm has converged. The robust design method for my multiscale example is shown in Figure 6.5. Each step is discussed in detail.

Step1: **Framing the Multiscale Problem**

To frame the multiscale problem, the multiscale design process is represented in Figure 6 which shows the dependent/independent parameter values interlinked with individual subsystems, the models and the modeling techniques, the performance requirements and goals associated with multiscale design task. In Figure 6.6, *f1, f2, f3 and f6* represent simulation models (shaded boxes) used to design the autonomous underwater vehicle (AUV) while *f4, f5, f7, f8 and f9* represent theoretical or empirical models considered for design. The inputs to MODULE 1 are the volume fraction of TiB_2 (x_{TiB2}) and temperature of processing in degree K (T).The output of MODULE 1 (*f1)* is the average TiB_2 particle size (d_p) which is an input to MODULE 3. The independent inputs to MODULE 2 are volume fraction of TiB_2 (x_{TiB2}) and cooling rate (C) and the

output of MODULE 2. (*f2)* is the average grain size (*d*) of the microstructure which is another input to MODULE 3. MODULE 1 and MODULE 2 deal with the process-structure relationships [PS] shown in Figure 3. MODULE 3 deals with the structure-property relationships [SP]: *f3* gives the yield stress (*σ*), *f4* gives density (*ρ*) and *f5* gives the heat transfer coefficient *(k)* as outputs. The model for yield stress (*σ*) receives inputs from the outputs of MODULE 1 and 2 along with the independent inputs of volume fraction of TiB_2 (x_{TiB2}). The only input to models for density (*ρ*) and heat transfer coefficient *(k)* is the independent variable of volume fraction of TiB_2 (x_{TiB2}). Finally, MODULE 4 deals with the property-performance [PP] relationship of the developed microstructure. The performance variable of depth of operation (*D*) is evaluated in *f6*; weight of the outer shell (*W*) is evaluated in *f7*, time of operation (T_{opr}) for the submersible is evaluated in *f8* and temperature of operation (T_{op}) is evaluated in *f9*. The independent parameter, thickness of the shell (*t*) and is an input to all the models, i.e., *f6, f7, f8 and f9.* The dependent parameters are density (*ρ*) to weight (*f7)* and time of operation (*f8)* while yield stress (*σ*) is an input to depth (*f6)*. The feasible design spaces are inductively passed from MODULE 4 to MODULE 3 and subsequently to MODULES 2 and 1 of design.

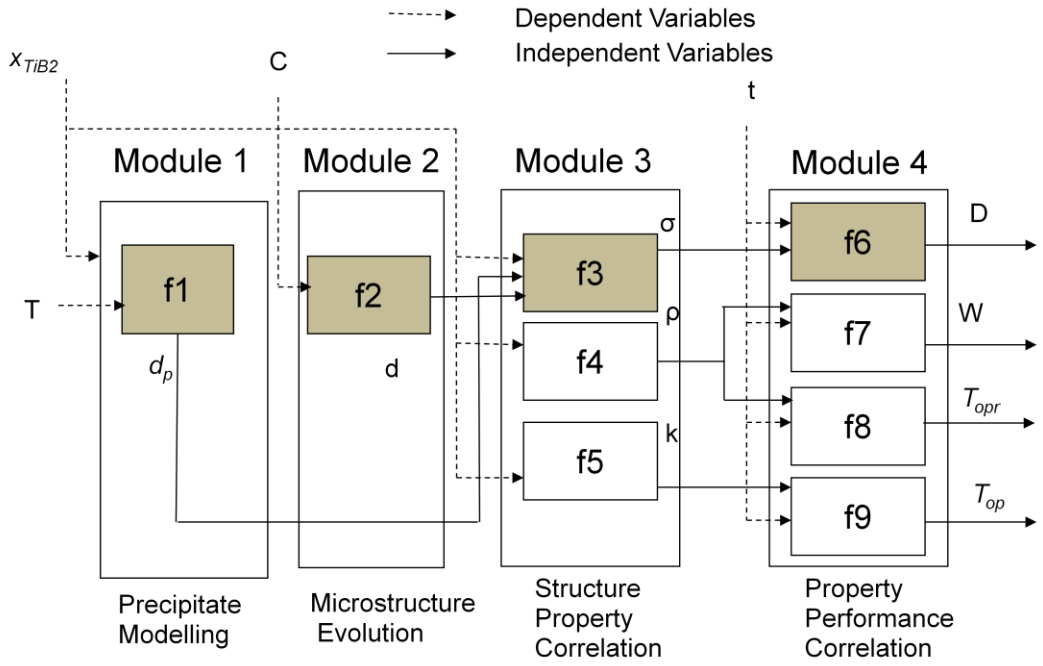

Figure 6.6: Multiscale system for concurrent design of material and product

Table 6.1: Dependent parameters

Model	Parameter	Range	Resolution	Variability	Constraint	Module
f1	d_p Average prep size	[0.1,2.1] µm	0.1 µm	0.05 µm	NA	1
f2	*d* Average grain size	[10,150] µm	5 µm	2.5 µm	NA	2
f3	*σ* Yield stress	[400,500] MPa	5 MPa	2.5 MPa	NA	3
f4	*ρ* Density	[2700,3100] kg/m^3	10 kg/m^3	5 kg/m^3	NA	3
f5	*k* Heat transfer coefficient	[200,260] W/m-K	5 W/m-K	2.5 W/m-K	NA	3
f6	*D* Safe depth of operation	[500,25000] m	25 m	NA	≥5000 m	4
f7	*W* Weight of outer shell	[5,30] kgs	0.5 kgs	NA	≤18 kgs	4
f8	T_{opr} Time of operation	[10,15] hrs	0.25 hrs	NA	≥12 Hrs.	4
f9	T_{op} Operating temperature	[15,22] C	0.1 C	NA	≤20 C	4

Table 6.2: Independent parameters

Variable	Range	Resolution	Variability Δx	Input Module	Input Models
x_{TiB_2} Volume fraction of TiB_2	[2,10] %	0.25 %	0.125%	1,2,3	*f1,f2,f3,f4,f5*
T Temperature for precipitate modelling	[1073,1273] K	10 K	5 K	1	*f1*
C Cooling rate for microstructure	[0.2,9.0] K/sec	0.5 K/sec	0.25 K/sec	2	*f2*
t Shell thickness	[5,15] mm	0.25 mm	0.125 mm	4	*f6,f7,f8,f9*

The performance constraints are:

- The safe depth of operation (*D*) of the submersible must exceed 5000 meters.
- The submersible must have a time of operation (T_{opr}) of at least 12 hours.
- The weight of the outer shell (*W*) of the submersible may not exceed 18 kgs.
- The operating temperature (T_{op}) of the submersible may not exceed 20 degree Celsius.

For the multiscale problem, simulation models are used for precipitate modeling (*f1),* microstructure evolution (*f2),* modeling the yield stress of the composite (*f3)* and for determining the depth of operation (*f6)*. All simulation models carry underlying assumptions (resulting in MSU) and are run for a relatively small number of design variable settings as they are computationally expensive (resulting in MPU). The solution technique IDEM is used to evaluate outputs for discrete input points and the discretization resolution in IDEM is modeled to reflect the variability (NU) in the input variables. However, discretization errors are introduced in calculating feasible and infeasible points. Tables 6.1 and 6.2 summarize the models, associated modules, ranges, discretization resolution and constraints for the dependent and independent parameters in my multiscale system. These ranges, resolution values and constraints are used in IDEM. The modeling techniques and assumptions of the simulation models are briefly discussed and I proceed to determine a robust solution and metrics to mitigate MPU by refining the simulation models. The details of the other models can be found in Chapter 5.

MODULE 1: Precipitation Modeling in Liquid Aluminum (f1 in Figure 6.6)

A suitable route for the in situ Al / TiB_2 composite manufacturing process is the reduction of K_2TiF_6 and KBF_4 with aluminum. A model proposed by Anestiev and co-authors[34] has been used to investigate the diffusion reactions taking place between the intermediate phases of Al_3Ti and AlB_2. A coordinate system dividing a 2-dimensional space into strips of equal length is used, half

of which contains Al_3Ti and the other half AlB_2 dissolved in the Al melt. Random nucleation of TiB_2 particulates is assumed. The kinetics of the formation of TiB_2 particles are governed by unsteady state diffusion equations, which, in turn, depend on the concentration profile of intermediate solute phases in the region. The solute consumption rate due to TiB_2 formation is described by the volume fraction in the region per unit time. Johnson-Mehl-Avrami analysis[35,36] is used to find the volume fraction from the nucleation and growth rates of the particles. The nucleation rate is primarily a function of the Gibbs energy change associated with the formation of the particle, while the growth rate also depends on the particle's surface energy. The thermodynamic models predicting the Gibbs free energies of the phases are described Mirkovic et al.[20], Witusiewicz and colleagues[21-22]. The complex diffusion equations are solved numerically in MATLAB™ to compute the TiB_2 particle size distribution across the matrix for a reaction time of one hour [82]. The mean particle size is determined by calculating the average particle size over the entire matrix.

MODULE 2: Modeling Microstructure Evolution (f2 in Figure 6.6)

The microstructure evolution during solidification depends on the thermal and the solutal fields. Fluid flow due to forced or natural convection also influences microstructure evolution. The model numerically calculates the solution of continuum equations for thermal fields and couples the solution with a cellular automata model that computes the evolution of grain structure with solidification time. Measured flux values are used to derive the evolution of the thermal fields with solidification time. Using measured temperature values at specific points along the metal-mold interface, realistic flux values at the metal-mold interface are derived which are then fed into the Computation Fluid Dynamics (CFD) modeling tool, *FLUENT*™**,** to obtain accurate thermal fields across the casting domain. These fields are used in the cellular automata model developed in FORTRAN™ to predict the microstructure evolution and the grain size distribution as the solidification proceeds [84].

MODULE 3: Structure-Property Correlation of Yield Stress (f3 in Figure 6.6)

The variation of the periodic hexagonal array is used to predict the local stress and strain fields and stiffness properties based on the stress field, the volume fraction of the phases and the constituent mechanical properties[87,88]. The composite structure region is assumed to be a two dimensional hexagonal model with uniform grain size and is split into a hard phase comprised of uniformly distributed TiB_2 particles in the Al-Cu alloy and a soft phase consisting of the pure Al-Cu alloy. A representative volume element is selected to cover the entire macroscopic volume of the composite. The elastic and plastic behaviors of the constituent phases are either described using experimental values or calculated theoretically[43]. Grain size is varied using the Hall-Petch relation and a numerical solution for the elastoplastic behavior of the PHA RVE (i.e., a stress-strain curve) and subject to uniform tensile stresses is calculated using the finite element software ABAQUS™. Yield strength values are calculated using 0.2% offset from the linear part of the stress-stress curve [89].

MODULE 4 : Property-Performance Depth Correlation (f6 in Figure 6.6)

A finite element analysis is performed for the pressure hull to determine the collapse depth of the underwater submersible. A cylindrical shell with hemispherical end caps is considered. The stress distribution and buckling pressure of the pressure hull are predicted using the finite element package ABAQUS™ [91]. A factor of safety of 1.5 is used for deriving the relationship between collapse pressure and safe depth.

Step 2: **Subsystem Level Analysis**

Second order response surface models are used to capture the non-linearity of the input-output relationships. Designers can opt for higher order response surface models or other metamodeling techniques to model highly non-linear phenomena. Central composite designs[94] (CCDs) are used for calibrating the full quadratic response surface models from the simulation models at the subsystem level. CCDs estimate linear, quadratic and interaction effects in a minimum number of simulation runs. The input variables are scaled from -1 to 1 in the CCD to

calibrate second order response surface models represented as[65]:

$$Y = \beta_0 + \sum_{i=1}^{\kappa} \beta_i x_i + \sum_{i=1}^{\kappa} \beta_{ii} x_i^2 + \sum \sum_{i<\kappa} \beta_{ij} x_i x_j + \varepsilon \quad (6.1)$$

Where, $\beta_{ij,}$ *i=1, 2… k; j=1, 2… k* are the coefficients and x_i, x_j are the input design variables, *Y* is the response, ε are the random errors and κ the number of design variables. The upper and lower confidence intervals of the simulation metamodel are calculated as[60,11,46]:

$$Y_{upper} = Y + \Delta Y_{CI} \quad (6.2)$$

$$Y_{lower} = Y - \Delta Y_{CI} \quad (6.3)$$

$$\Delta Y_{CI} = t_{n-p,\alpha/2} \sqrt{MSE} \sqrt{x'_0 \left(X' X \right)^{-1} x_o} \quad (6.4)$$

ΔY_{CI} denotes the statistical bounds for a 100(1-α) % confidence interval. n is the number of simulation runs and p is the total number of regression coefficients, MSE is the mean square error, X is a (n x p) matrix of the levels of regression variables and x_o is a (p x 1) matrix of regression variables for the particular point I am calculating the confidence interval. ΔY_{CI} is the response variation due to insufficient data (MPU) and does not include the variability (NU) in the input variables. Assuming the variations Δx_i in the input variables are small, the maximum and minimum responses are estimated using a first-order Taylor series expansion and are given by:

$$Y_{\max} = Y_{upper} + \Delta Y_{IP} \quad (6.5)$$

$$Y_{\max} = Y_{lower} - \Delta Y_{IP} \quad (6.6)$$

$$\Delta Y_{IP} = \sum_{i=1}^{k} \left| \frac{\partial Y}{\partial x_i} \right| \Delta x_i \quad (6.7)$$

ΔY_{IP} arises due to variability in the input variables. The discretization resolution in IDEM is twice the deviation, Δx_i in the input variables (NU) so as to cover the entire design space. We note that the deviation Δx_i in inputs to models higher in the multiscale hierarchy (x_i is an output response from a model at lower hierarchy) are set independently assuming worst case scenario and are not equal to the variability of the output response. The α value is 0.05, i.e., a 95% two-

sided confidence interval. The response surface models for the simulation models, calculated in MATLAB™ along with their MSE and R^2 statistic are as follows:

$$d_p(\mu m) = 3.12 + 0.36x_{TiB_2} + 1.13T - 0.27{x_{TiB_2}}^2 - 0.37T^2 + 0.07x_{TiB_2}T; MSE = 6.2\times10^{-2}; R^2 = 0.97 \quad (6.8)$$

$$d(\mu m) = 30.25 - 12.67x_{TiB_2} - 22.35C - 0.61{x_{TiB_2}}^2 + 14.47C^2 + 6.84x_{TiB_2}T; MSE = 10.88, R^2 = 0.99 \quad (6.9)$$

$$\begin{aligned}\sigma(MPa) = {} & 444.11 - 0.62x_{TiB_2} - 10.62d_p - 61.62d + 9.94{x_{TiB_2}}^2 + 14.94{d_p}^2 + 48.94d^2 \\ & -5.50x_{TiB_2}d_p - 19.50x_{TiB_2}d + 6.50d_p d; MSE = 561.54; R^2 = 0.87\end{aligned} \quad (6.10)$$

$$D(m) = 1000(5.64 + 6.77t - 0.65\sigma - 2.67t^2 + 0.002\sigma^2 + 0.72t\sigma); MSE = 24543; R^2 = 0.99 \quad (6.11)$$

Step 3: **Inductive Design Exploration Method (IDEM)**

The solution for IDEM takes the structure as shown in Figure 6.7. Ranged sets of performance targets are set in the top level of the multiscale design problem and based on property-performance [PP] mapping models, ranged sets of feasible property space discrete points are inductively passed to the structure-property [SP] domain in the multiscale system. In this chapter, feasible points are defined as a discrete evaluation point whose output response falls within the constraint boundaries. The independent variable, *t,* is selected by maximizing design freedom, i.e., the value which maximizes the number of discrete feasible sets in the property domain range. The same procedure is repeated with the structure-property [SP] mapping models and ranged sets of feasible structure are passed into the process-structure [PS] domain. Finally we get ranged sets of feasible process variables. A dummy model is introduced for the volume fraction as x_{TiB_2} is an input to both PS and SP domains. The best robust solution against MSU, MPU and NU is calculated by adjusting the hyper dimensional-error margin indices (HD-EMIs) obtained from each mapping model. HD-EMIs indicate the degree of reliability of chosen design variables that it will satisfy hierarchical constraints or bounds.

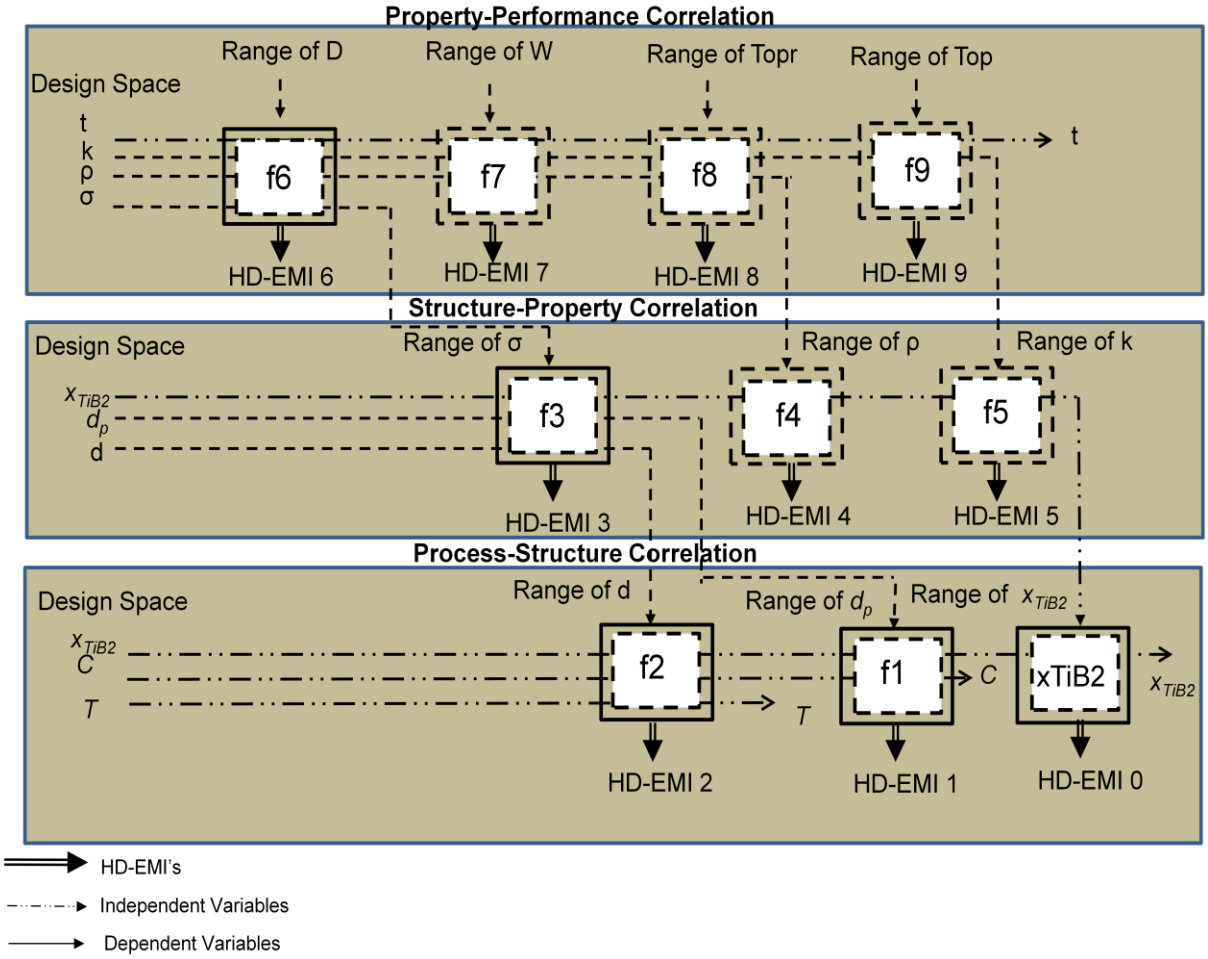

Figure 6.7: IDEM for multiscale design

The HD-EMI values are calculated in each output direction in a hyper-dimensional output space, Figure 6.8. HD-EMI for output direction *i*, is represented as:

$$HD-EMI_i = \min\left(\frac{|(mean - B_j).u_i|}{|(mean - B_j^i).u_i|}\right) \tag{6.12}$$

Where *j* is the set of all points on constraint boundaries, mean represents a vector of output responses, B_j is one point on the constraint boundary, B_j^i is a projection vector of B_j onto the output range along the desired output direction and u_i is a unit vector of output responses along the output direction[46]. $\mathrm{HD-EMI_i}$ is the minimum of all values calculated based on all constraint boundary points. An HD-EMI value greater than 0 indicates the mean output vector is

within the constraint boundaries, i.e., is a feasible input point, while a value of 1 indicates that the maximum or minimum output deviation coincides with nearest constraint boundary point and hence is robust against modeled NU and MPU. The corresponding input point will be referred to as a robust point. A higher value of HD-EMI indicates the output range is further away from constraint boundaries and has a larger margin for potential error in the mapping model due to MSU for estimating output range. Exact constraint boundaries are identified in a top-down manner using the bisection method to avoid propagated errors, i.e., combined effect of NU and MPU. IDEM is executed and feasible design points are identified in the property, Figure 6.9; structure, Figure 6.10; and processing, Figure 6.11, design space based on the interlinked mapping models.

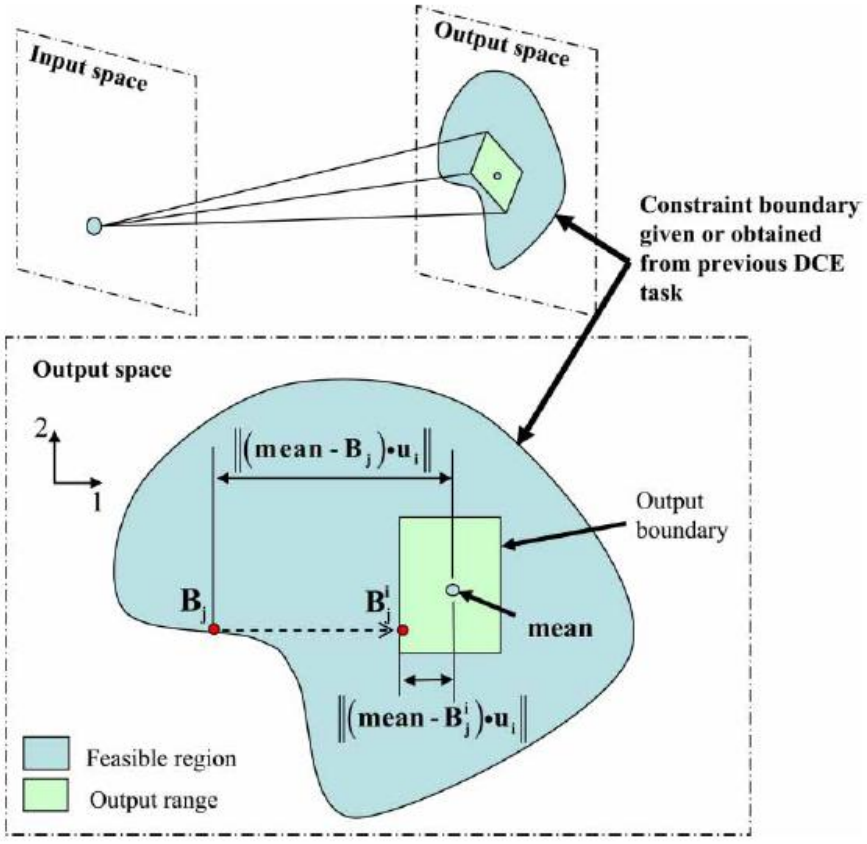

Figure 6.8: HD-EMI calculation in an output direction[46]

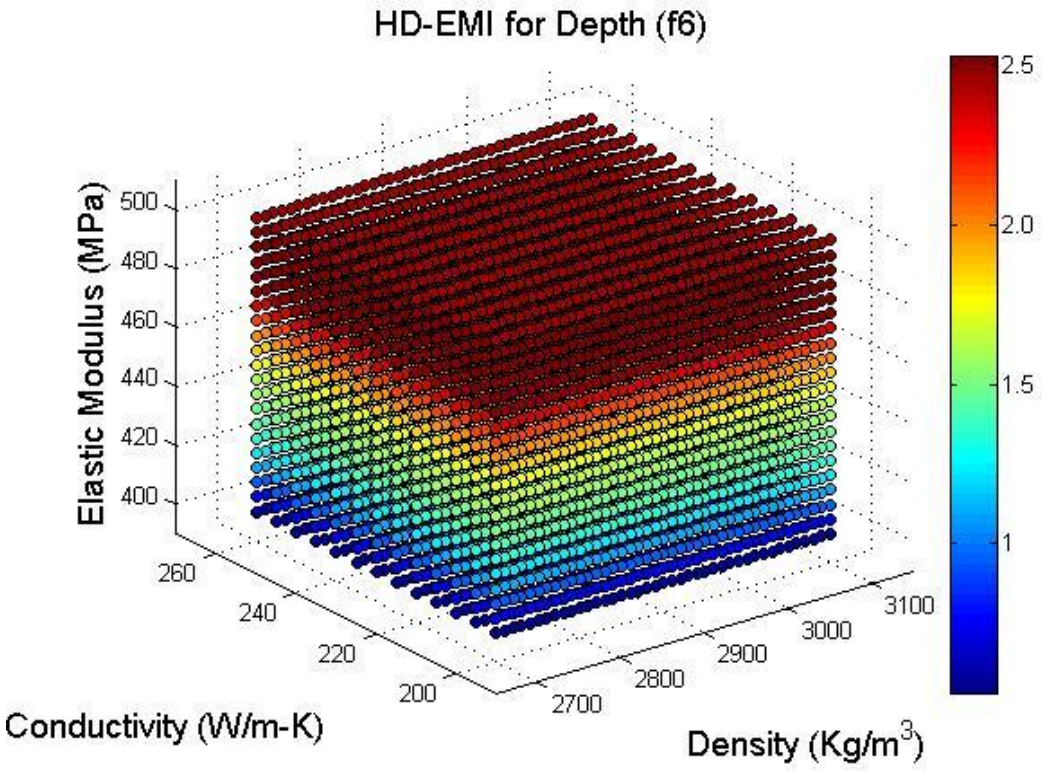

Figure 6.9: Feasible property (MODULE 4) design space

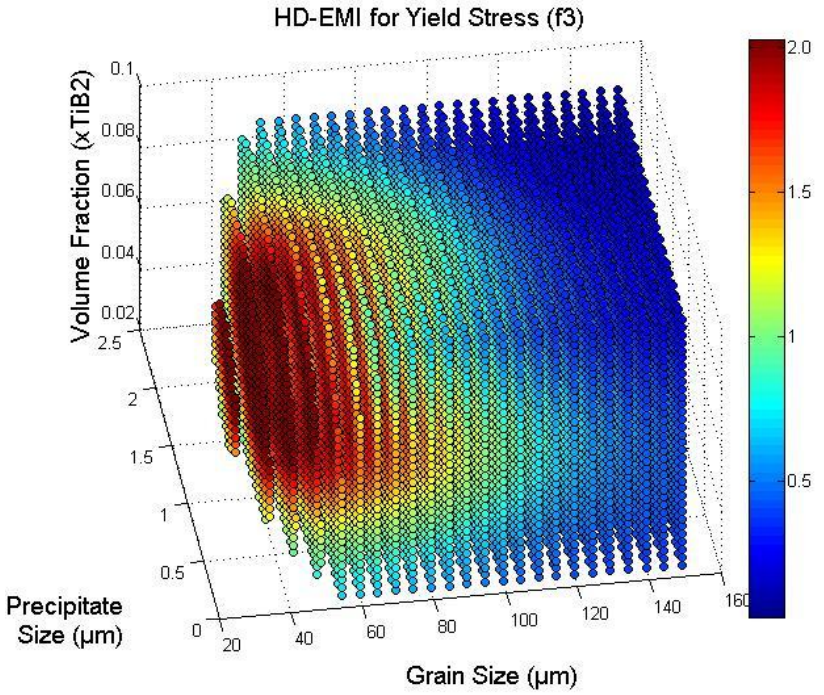

Figure 6.10: Feasible structure (MODULE 3) design space

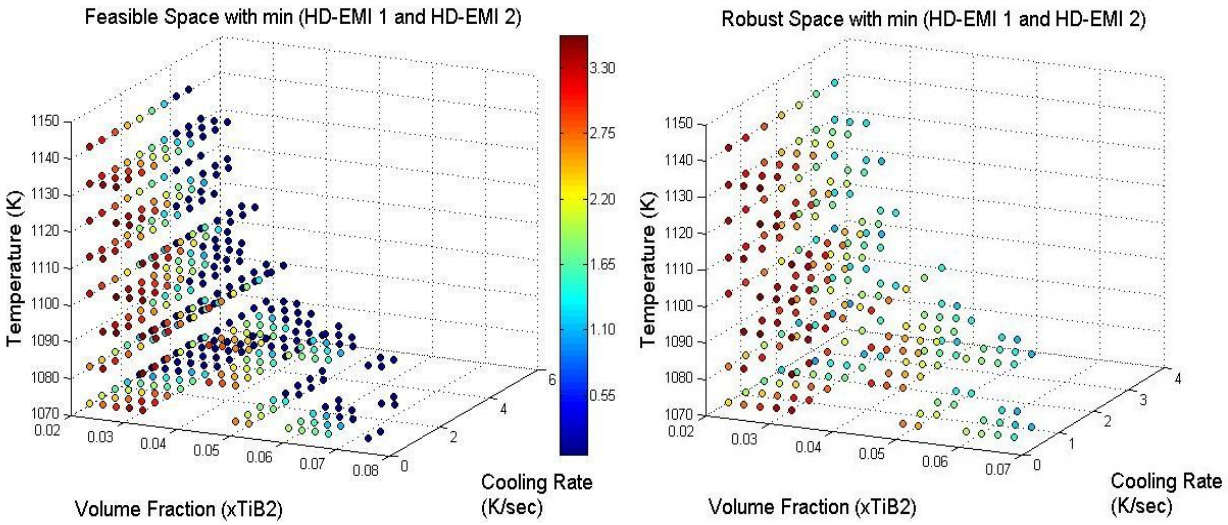

Figure 6.11: Feasible and robust processing design space (MODULES 1 and 2)

The feasible space of the volume fraction of TiB_2 (processing variable) lies within the ranges [0.0225, 0.035]; [0.045, 0.0525]; [0.06, 0.0675] and [0.075, 0.08] (Figure 6.11) while the robust space lies within the ranges [0.0225, 0.035]; [0.045, 0.0525]; [0.06, 0.0675]. This indicates that the achieved space of the volume fraction of TiB_2, [0.02, 0.035]; [0.045, 0.0525]; [0.06, 0.0675] and thickness of shell, 10.25 mm, guarantees satisfactory submersible performance while maintaining all quantifiable uncertainty (MPU and NU) and its propagation within bounds.

The best solution for the multiscale system, i.e., values of the design variables, is calculated by minimizing the deviation of the HD-EMIs from target values (10 for all models and equal weights). This solution along with the achieved HD-EMI values and system level performance is shown in Table 3. The HD-EMI values indicate that *f2* and *f6* are relatively robust against MSU while the low values for *f1* and *f3* indicate the best compromise solution is close to the constraint boundaries. The performance exceeds the requirements for the submersible and the achieved depth (D) from *f6* is 6098 meters. The number of robust points is 237 from a resolution space of 13167 points. I compare the HD-EMI values from the simulation models, depth performance after simulation model refinement and number of robust points in Section 6.3.4.

The feasible design space points are used for improvement potential calculations.

Table 6.3: System level solution

f1 *(d_p)*	***f2*** *(d)*	***f3*** *(σ)*	***f4*** *(ρ)*	***f5*** *(k)*	***f6****(D)*	***f7*** *(W)*	***f8*** *(T_{opr})*	***f9*** *(T_{op})*
HDEMI1	**HDEMI2**	**HDEMI3**	**HDEMI4**	**HDEMI5**	**HDEMI6**	**HDEMI7**	**HDEMI8**	**HDEMI9**
1.06	5.82	116	2.24	3.81	8.92	17.62	4.04	5.53

Design Variables				**Performance**			
x_{TiB_2}	*T(K)*	*C(K/sec)*	*t(mm)*	*D(m)*	*W(kgs)*	*T_{opr}(hrs)*	*T_{op}(C)*
0.035	1073	0.536	10.25	6098.81	15.31	13.50	17.52

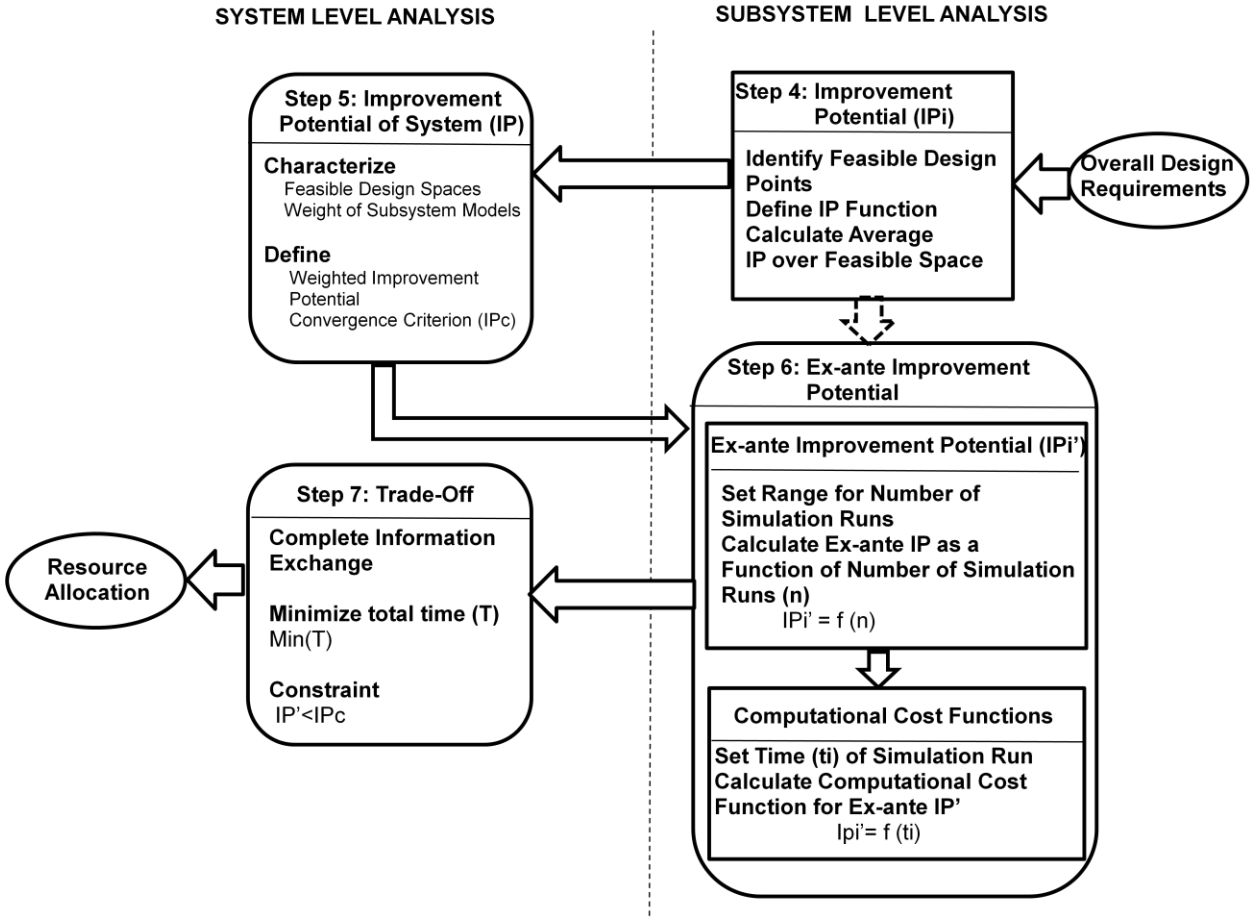

Figure 6.12: Schematic for improvement potential trade-off

6.3.3. Information Economics

In the context of simulation-based design of multiscale systems, a *simulation model is a source of information*[69]. Using information economics, we wish to decide the best course of action for resource allocation to gather additional information based on available information. The additional information should specifically mitigate MPU while meeting performance requirements. To this end, the improvement potential (P_i)[69] metric developed by Panchal and co-authors capture the expected value of information in terms of utility[70,71]. A high improvement potential value indicates a greater value associated with refining the simulation model compared to a low value. The metric only quantifies the benefit of gaining more information. It does not account for the effort involved in procuring additional information. In this section the improvement potential metric is defined in terms of the response surface models to suit robust design of multiscale systems and develop cost-benefit functions for auxiliary runs on mitigating MPU in a simulation model. These functions are used to decide resource allocation by reaching a trade-off between reduced uncertainty and increased effort for additional simulation runs. The first step towards developing the cost-benefit functions is to predict the change in improvement potential with additional simulation runs. Concepts from value of information[66-68] and response surface modeling[60] are used to predict this change. Specifically, the predicted value without executing the simulation model is termed the *ex-ante* improvement potential and the realized value based on the refined metamodels is termed the *ex-post* improvement potential. Comparing the *ex-post* improvement potential against the *ex-ante* improvement potential metric guides the predictive capabilities of the *ex-ante* metric. The steps for information economics relevant to the multiscale problem are shown in Figure 6.12. In Section 6.3.3 the improvement potential metric for the simulation models and system is developed. Also, the cost-benefit models are developed in terms of the *ex-ante* improvement potential.

Step 4: **Improvement Potential**

IDEM gives us the set of discrete feasible points in the design space at different scales in the multiscale problem. The improvement potential metric must capture the scope of model refinement. Using the feasible sets from IDEM, the improvement potential for the simulation model, IP_i is defined as:

$$IP_i = \sum_{m} \frac{1 - \frac{Y_{lower}}{Y_{upper}}}{m} \tag{6.13}$$

$$Y_{upper} = Y + t_{n-p,\alpha/2} \sqrt{MSE} \sqrt{x'_0 \left(X'X \right)^{-1} x_o} \tag{6.14}$$

$$Y_{lower} = Y - t_{n-p,\alpha/2} \sqrt{MSE} \sqrt{x'_0 \left(X'X \right)^{-1} x_o} \tag{6.15}$$

The subscript *i* in IP_i denotes the simulation model for improvement potential metric. The improvement potential metric decreases as the error bounds are reduced and will hypothetically be 0 when $Y_{upper} = Y_{lower}$ suggesting no further model refinement is possible. However, this cannot be realized statistically unless MSE=0, i.e., the model fits the data perfectly. The improvement potential metric is calculated over all set of feasible design points (m) to get a reflection of the scope of refinement without bias. I note, the feasible design points refer to corresponding output responses being inside the constraint boundaries and robust points to the entire range being inside the boundaries. It is expected that few feasible points to get converted to robust points as the associated output range decreases with simulation model refinement. The improvement potential metric is defined to capture the degree of uncertainty in model parameters due to insufficient data, i.e., in terms of Y_{upper} and Y_{lower} related to statistical error bounds for the response surface. Y_{max} *and* Y_{min} additionally incorporate the variability as first order Taylor series expansions. As variability is irreducible, it is not considered. The resolutions of design variables in IDEM are twice the variability so as to continuously cover the design space. However, discretization errors occur in the vicinity between feasible and infeasible points and can be reduced by more conservative resolutions at

an increased computational cost.

The improvement potential values associated with *f1, f2, f3* and *f6,* i.e., the simulation models in the multiscale system are 0.527 (IP_1), 0.242 (IP_2), 0.25 (IP_3) and 0.109 (IP_6) respectively. These values suggest that *f1* has the maximum potential for refinement while that of *f6* is the least.

Step 5: **System Level Improvement Potential**

At the system level, (i) determine the weights for the individual simulation models as a function of the impact on the system level performance; (ii) calculate the overall Improvement Potential of the system. A convergence criterion is set as an indication of when to stop further simulation model refinement. This criterion is based on the current improvement potential, the α value for confidence interval and the computational resources available to a system level designer. A system level designer has freedom to choose this value based on the degree of uncertainty mitigation desired. A higher convergence criterion for the overall system level improvement potential should be set for larger percentage of confidence intervals, i.e., for small α values as convergence may be statistically unattainable if it is set too low.

i. **Weights for Simulation Models:** The relative weight of importance for a simulation model is calculated as a multiplicative factor of the weight of the performance objective and the corresponding degree of influence of its output. It is to be summed over all performance objectives. This is:

$$W_i = \sum_{PO} W_{PO} H_e \tag{6.16}$$

Where, W_i is the weight of the simulation model, W_{PO}, is the weight of the system level performance objective, and H_e is the highest exponent of the simulation output parameter that appears in the performance function. As we consider second

order response models for simulation models or closed form empirical functions for other models in the multiscale system, H_e can be derived explicitly. The product of W_{PO} and H_e is summed over every performance objective it appears in and a cumulative weight for the simulation model is obtained. The designer can also assign weights independently as per his/her discretion.

Weight for *f1*: The output from *f1* (d_p) appears in one performance objective, i.e., depth (*D*). Depth is a function of yield strength with highest order 2, i.e., *D*= $a_0 + a_1 f(\sigma) + a_2\sigma^2$. Also, yield strength (σ) is a second order function of d_p, i.e. $\sigma = a_0 + a_1 f(d_p) + a_2 {d_p}^2$.

Therefore it is derived *D*= $a_0 + a_1 f(d_p, {d_p}^2, {d_p}^3) + a_2 {d_p}^4$ and the highest exponent of d_p in depth *(D)* is 4. If all performance objectives have equal weight of 0.25, the weight of *f1* will be 0.25x4, i.e., 1.

Weight for *f2:* The output from *f2* (d) appears in one performance objective, i.e., depth (*D*). Following a similar calculation, the weight of *f2* is determined to be 1.

Weight for *f3:* The output from f3 (σ) appears only in the performance objective depth (*D*). As depth is a function of yield strength with highest order 2, the weight of *f3* is 0.5.

Weight for *f6:* The weight of the objective *D* will be its performance weight, i.e., 0.25.

Thus, models (*f1* and *f2*) in lower hierarchy of the multiscale system have a higher weight suggesting there is greater value in mitigating the uncertainty in these models. This is justified as the uncertainty is these models will be propagated to a greater extent in the design chain as compared to ones in the top of the hierarchy.

ii. **System Improvement Potential (*IP*):** The system improvement potential is calculated as a weighted average over the weights of the simulation models (W_i) and their corresponding improvement potentials (IP_i). The system level designer sets a convergence criterion IP_c for the system improvement potential and further simulation model is stopped once that threshold value is reached, i.e., $IP \leq IP_c$. The system level improvement potential can be expressed as:

$$IP = \frac{\sum_{i=1}^{s} W_i . IP_i}{\sum_{i=1}^{s} W_i} \tag{6.17}$$

Where *s* is the number of simulation models in the multiscale system. Based on the weights and improvement potential values of the simulation models the system improvement potential is determined to be 0.335. It is checked for three convergence criterion equal to 0.25, 0.20 and 0.15

***Step 6: Ex-ante* Improvement Potential**

Cost-benefit models are developed based on the *ex-ante* improvement potential. It is noted that although this ties to the sample size determination for an experiment, traditional sample size determination techniques are based using the operating characteristic curve for null hypothesis treatment or a trial and error confidence interval estimation[47]. These techniques are only suitable for calibration experiments and not my simulation-based multiscale design task as there are several computational models (experiments) and cost factors which need to be accounted for. Developing cost-benefit models helps scale the benefit of uncertainty mitigation in terms of the common parameter-computational time. Assigning computational resources based on the IP_i metric can lead to inefficiency because a model with a high IP_i value can have significant computational time. Instead, there may be greater value in using this resource to run a model with lesser computational time. The underlying mathematics for deriving the cost-benefit models is presented below. Combining Eqs. 6.13, 6.14 and 6.15, the improvement potential

metric is:

$$IP_{i,n} = \sum_{m} \frac{1 - \frac{Y_{lower}}{Y_{upper}}}{m} = \sum_{m} \frac{1 - \frac{Y - t_{n-p,\alpha/2}\sqrt{MSE}\sqrt{x_0'\left(X'X\right)^{-1}x_o}}{Y + t_{n-p,\alpha/2}\sqrt{MSE}\sqrt{x_0'\left(X'X\right)^{-1}x_o}}}{m} \tag{6.18}$$

Where *n* is the number of simulation runs. The mean square error is calculated as:

$$MSE = \frac{SS_E}{n-p} = \frac{\sum e_i^2}{n-p} \tag{6.19}$$

e_i are the residual errors between the actual values and the fitted values by the regression model. A critical part of evaluating the *ex-ante* improvement potential is to estimate how the mean square error will vary with an increase in the number of data points. It is assumed the residual error per observation, *e* will remain constant. However for small sample sizes as with the CCD, this will underestimate the *MSE*[95]. Hence the predicted *MSE'* is modified using Eqn. 6.20:

$$MSE' = \frac{ne^2}{n-p-1} \tag{6.20}$$

The factor of 1 in the denominator can be interpreted as Bessel's correction for the sample MSE from the population of (unrealized) simulation runs. Therefore for r additional runs or data sets, the *MSE'* will vary as:

$$MSE_r' = \frac{(n+r)e^2}{n+r-p-1} = \frac{(n+r)(n-p-1)}{(n+r-p-1)(n)}MSE' = \frac{(n+r)(n-p-1)}{(n+r-p-1)(n)}MSE \tag{6.21}$$

Where the value for *MSE'* for n runs is known, i.e., *MSE.* Varying r from 1 to larger values, the *ex-ante* improvement potential is determined as a function of additional simulation runs as:

$$IP'_{i,n+r} = \sum_{m} \frac{1 - \frac{Y - t_{n+r-p,\alpha/2}\sqrt{MSE_r'}\sqrt{x_0'\left(X'X\right)^{-1}x_o}}{Y + t_{n+r-p,\alpha/2}\sqrt{MSE_r'}\sqrt{x_0'\left(X'X\right)^{-1}x_o}}}{m} \tag{6.22}$$

The subsystem level designers can approximate the time required for r simulation runs as

$T_i = a + rt_i$ where *a* in the set up time and the constant t_i represents the time per simulation for the i^{th} simulation model with *r* additional runs. Thus the improvement potential can be evaluated as a function of computational time. This function will decrease with increase in computational time and is represented using an exponential function shown in Eqn. 6.23, where the constants a_0, a_1, a_2, a_3 and a_4 are found by a least square fit in MATLAB™. These functions are calculated by subsystem modelers and used by the system level designer for trade-off and assigning computational resources.

$$IP'_i = f\left(T'_i\right) = a_0 + a_1 \exp^{\frac{T'_i}{a_2}} + a_3 \exp^{\frac{T'_i}{a_4}} \tag{6.23}$$

Thus the *ex-ante* improvement potential metric is devised in terms of the number of simulation runs and further correlated with the computational time/cost. These functional relationships are used by the system level designer to achieve trade-off and assign resources for further simulation refinement. For my multiscale system no set-up time is assumed, i.e. a=0; and the functions between improvement potential and computational time are represented as:

$$IP'_1 = 0.20 + 0.22\exp^{\frac{T'_1}{75.53}} + 0.099\exp^{\frac{T'_1}{566.31}}; t_1 = 36hrs \tag{6.24}$$

$$IP'_2 = 0.08 + 0.11\exp^{\frac{T'_2}{9.49}} + 0.047\exp^{\frac{T'_2}{73.73}}; t_2 = 5hrs \tag{6.25}$$

$$IP'_3 = 0.11 + 0.08\exp^{\frac{T'_3}{13.88}} + 0.05\exp^{\frac{T'_3}{87.93}}; t_3 = 4hrs \tag{6.26}$$

$$IP'_6 = 0.03 + 0.05\exp^{\frac{T'_3}{0.90}} + 0.02\exp^{\frac{T'_3}{7.16}}; t_6 = 0.5hrs \tag{6.27}$$

Step 7: **Trade-Off Mechanism**

An ideal scenario is assumed where a system level designer has complete information about the cost functions and *ex-ante* improvement potentials and there is full information exchange between the system level designer and subsystem level modelers. Constraint optimization techniques are used to minimize the total computational time in order to order to reach the

convergence criterion IP_c. $T = \sum_{i=1}^{s} T_i$ is minimized with constraints $IP_c \geq IP'$ where IP' is the weighted system level *ex-ante* improvement potential metric. The solution for the number of runs for each model approximated to the nearest integer value is shown in Table 6.4.

Table 6.4: Trade-off solution

Convergence Criterion	Simulation Model	Time for runs (hours)	Number of runs
0.25	*f1*	34.30	~1
	f2	19.28	~4
	f3	7.19	~2
	f6	2.05	~4
0.20	*f1*	108.78	~3
	f2	31.49	~6
	f3	21.95	~6
	f6	3.30	~7
0.15	*f1*	419.40	~12
	f2	140.33	~28
	f3	100.59	~25
	f6	14.75	~30

6.3.4. *Step 8:* Refine Simulation Models and Iteration

Once the resource allocation has been determined, the simulation models are re-run by the subsystem modelers. IDEM in Step 3 gives us the set of feasible solution sets and the simulation models are re-run for set of input values for which the improvement potential values are maximum. After the re-runs, the modified metamodels and used to re-run IDEM (STEP 3). This procedure is continued until convergence is reached. For my multiscale system, the simulation models are re-run as per the trade-off solution. The refined response surface models are:

Convergence Criterion: 0.25

$$d_p(\mu m) = 3.12 + 0.36x_{TiB_2} + 1.13T - 0.27{x_{TiB_2}}^2 - 0.37T^2 + 0.08x_{TiB_2}T; MSE = 4.7\times10^{-2}, R^2 = 0.98 \quad (6.28)$$

$$d(\mu m) = 30.15 - 12.41x_{TiB_2} - 22.34C - 1.03{x_{TiB_2}}^2 + 14.85C^2 + 6.85x_{TiB_2}T; MSE = 5.26; R^2 = 0.99 \quad (6.29)$$

$$\begin{aligned}\sigma(MPa) &= 455.39 - 0.86x_{TiB_2} - 11.64d_p - 63.11d - 4.65{x_{TiB_2}}^2 + 0.34{d_p}^2 + 34.34d^2 \\ &+2.65x_{TiB_2}d_p - 7.55x_{TiB_2}d - 1.65d_p d; MSE = 455.46; R^2 = 0.87\end{aligned} \quad (6.30)$$

$$D(m) = 1000(5.62 + 6.77t - 0.65\sigma - 2.69t^2 - 0.01\sigma^2 + 0.73t\sigma; MSE = 10609; R^2 = 1.0 \quad (6.31)$$

Convergence Criterion: 0.20

$$d_p(\mu m) = 3.10 + 0.40x_{TiB_2} + 1.18T - 0.31{x_{TiB_2}}^2 - 0.37T^2 + 0.02x_{TiB_2}T; MSE = 6.1\times10^{-2}, R^2 = 0.97 \quad (6.32)$$

$$d(\mu m) = 29.40 - 12.45x_{TiB_2} - 22.23C - 0.48{x_{TiB_2}}^2 + 15.21C^2 + 6.84x_{TiB_2}T; MSE = 4.95; R^2 = 0.99 \quad (6.33)$$

$$\begin{aligned}\sigma(MPa) &= 455.91 - 0.91x_{TiB_2} - 11.59d_p - 63.27d - 5.10{x_{TiB_2}}^2 - 0.45{d_p}^2 + 33.48d^2 \\ &+2.78x_{TiB_2}d_p - 7.05x_{TiB_2}d - 0.88d_p d; MSE = 293.68; R^2 = 0.89\end{aligned} \quad (6.34)$$

$$D(m) = 1000(5.63 + 6.76t - 0.65\sigma - 2.68t^2 - 0.007\sigma^2 + 0.84t\sigma; MSE = 8420; R^2 = 1.0 \quad (6.35)$$

Convergence Criterion: 0.15

$$d_p(\mu m) = 3.04 + 0.44x_{TiB_2} + 1.21T - .30{x_{TiB_2}}^2 - 0.35T^2 + 0.004x_{TiB_2}T; MSE = 3.7\times10^{-2}, R^2 = 0.97 \quad (6.36)$$

$$d(\mu m) = 27.89 - 10.21x_{TiB_2} - 17.97C - 0.04{x_{TiB_2}}^2 + 13.71C^2 + 5.07x_{TiB_2}T; MSE = 14.01; R^2 = 0.95 \quad (6.37)$$

$$\begin{aligned}\sigma(MPa) &= 453.63 + 3.68x_{TiB_2} - 8.23d_p - 61.61d - 3.09{x_{TiB_2}}^2 - 0.32{d_p}^2 + 38.95d^2 \\ &+10.33x_{TiB_2}d_p - 0.99x_{TiB_2}d - 4.44d_p d; MSE = 139.45; R^2 = 0.89\end{aligned} \quad (6.38)$$

$$D(m) = 1000(5.64 + 6.69t + 0.64\sigma + 2.66t^2 - 0.02\sigma^2 + 0.79t\sigma; MSE = 7356; R^2 = 1.0 \quad (6.39)$$

IDEM is re-run and the cDSP solutions for all three cases are shown in Table 6.5. The *ex-post* improvement potential values for the simulation models are shown against the *ex-ante* values in Table 6.6. We see that the *ex-post* values are in close comparison with the *ex-ante* value being overestimated apart from *f2* (convergence criterion 0.15) and *f1* (convergence criterion 0.20 and

0.25). The overestimation of the *ex-ante* value can be elucidated as the simulation models are run at the points of maximum improvement potential thus ensuring an advantageous reduction in improvement potential. The underestimation for *f2* (convergence criterion 0.15) and *f1* (convergence criterion 0.20) can be explained due to the rise in MSE for the refined response surface model suggesting the behavior of microstructure and precipitate evolution is highly non-linear and require higher order response surface models to capture the simulation behavior. The underestimation for *f1* (convergence criterion 0.25) is within tolerance limits for only one additional simulation run. The weighted system level improvement potential is equal to 0.239 (convergence criterion 0.25), 0.196 (convergence criterion 0.20) and 0.127 (convergence criterion 0.15) suggesting the convergence criterion has been reached for all three cases and no further simulation refinement is necessary. Thus for:

- Convergence Criterion 0.25, a total computational time of 499.5 hours (433.5 hours for the initial CCD runs and 66 hours for iterated runs) is required,
- Convergence Criterion 0.20, 599 hours (433.5 hours for the initial CCD runs and 165.5 hours for iterated runs) is required, and
- Convergence Criterion 0.15, 1120.5 hours (433.5 hours for the initial CCD runs and 687 hours for iterated runs) is required

The system level improvement potential has reached the corresponding convergence criterion in a single iteration for all three cases. The robust solution for the design variables and the system performance is the solution shown in Table 5. The HD-EMI values progressively increases with simulation refinement indicating greater robustness against MSU. The weighted average HD-EMI value for the 4 simulation models increases from 4.24 for initial CCD runs to 6.49 for criterion 0.25, 7.52 for criterion 0.20 and 8.39 for criterion 0.15. The HD-EMI metric can be used to gauge qualitatively the relative levels of refinement required to mitigate MSU to achieve greater robustness at the system level. There is a progressive increase in achievement of safe

depth to 6155 meters as compared the 6098 meters from the first cDSP solution suggesting simulation model refinement was beneficial in terms of performance objectives at the system level. The number of robust points increases to 332 points for criterion 0.25, to 380 points for criterion 0.20 and finally 385 points for criterion 0.15, Figure 6.13, indicating an increase in robust space due to simulation model refinement. The range for robust points spans from [0.0225, 0.075] for criterion 0.15 as compared to [0.0225, 0.0675] for initial CCD runs suggesting a few infeasible/feasible points have been converted to robust points by uncertainty mitigation. The solution in Table 6.5 is robust against all forms of uncertainty as determined by IDEM with the achieved degree of refinement determined by the system level improvement potential metric. Contingent on the assumption of MSE variation, the algorithm provides the most effective resource allocation for further simulation refinement to converge below the convergence criterion and reach a robust solution for the multiscale system.

Table 6.5: System level solution

Convergence Criterion:0.25								
f1 *(d_p)*	***f2*** *(d)*	***f3*** *(σ)*	***f4*** *(ρ)*	***f5*** *(k)*	***f6****(D)*	***f7*** *(W)*	***f8*** *(T_{opr})*	***f9*** *(T_{op})*
HDEMI1	**HDEMI2**	**HDEMI3**	**HDEMI4**	**HDEMI5**	**HDEMI6**	**HDEMI7**	**HDEMI8**	**HDEMI9**
1.01	8.47	1.32	2.25	3.7	15.17	17.2	4.03	5.53

Design Variables				**Performance**			
x_{TiB_2}	*T(K)*	*C(K/sec)*	*t(mm)*	*D(m)*	*W(kgs)*	*T_{opr}(hrs)*	*T_{op}(C)*
0.036	1084	0.743	10.25	6135.74	15.31	13.51	17.52

Convergence Criterion:0.20								
f1 *(d_p)*	***f2*** *(d)*	***f3*** *(σ)*	***f4*** *(ρ)*	***f5*** *(k)*	***f6****(D)*	***f7*** *(W)*	***f8*** *(T_{opr})*	***f9*** *(T_{op})*
HDEMI1	**HDEMI2**	**HDEMI3**	**HDEMI4**	**HDEMI5**	**HDEMI6**	**HDEMI7**	**HDEMI8**	**HDEMI9**
1.64	8.86	1.71	2.18	3.57	6.03	7.64	4.05	5.52

Table 6.5 continued							
Design Variables				**Performance**			
x_{TiB_2}	*T(K)*	*C(K/sec)*	*t(mm)*	*D(m)*	*W(kgs)*	T_{opr}*(hrs)*	T_{op}*(C)*
0.033	1087	0.896	10.25	6151.59	15.33	13.50	17.52
Convergence Criterion:0.15							
f1 *(*d_p*)*	***f2*** *(d)*	***f3 (***σ*)*	***f4*** *(*ρ*)*	***f5*** *(k)*	***f6****(D)*	***f7*** *(W)*	***f8*** *(*T_{opr}*)*	***f9*** *(*T_{op}*)*
HDEMI1	**HDEMI2**	**HDEMI3**	**HDEMI4**	**HDEMI5**	**HDEMI6**	**HDEMI7**	**HDEMI8**	**HDEMI9**
3.78	8.73	2.71	2.11	3.25	18.37	17.65	4.06	5.52
Design Variables				**Performance**			
x_{TiB_2}	*T(K)*	*C(K/sec)*	*t(mm)*	*D(m)*	*W(kgs)*	T_{opr}*(hrs)*	T_{op}*(C)*
0.029	1082	0.20	10.25	6155.78	15.36	13.50	17.52

Table 6.6: Ex-ante vs. Ex-post values of improvement potential

Convergence Criterion	*Improvement Potential*	*f1*	*f2*	*f3*	*f6*
0.25	*Ex-ante*	0.425	0.133	0.205	0.058
	Ex-post	0.451	0.106	0.176	0.040
0.20	*Ex-ante*	0.337	0.119	0.168	0.049
	Ex-post	0.366	0.100	0.132	0.032
0.15	*Ex-ante*	0.246	0.887	0.130	0.375
	Ex-post	0.211	0.105	0.056	0.014

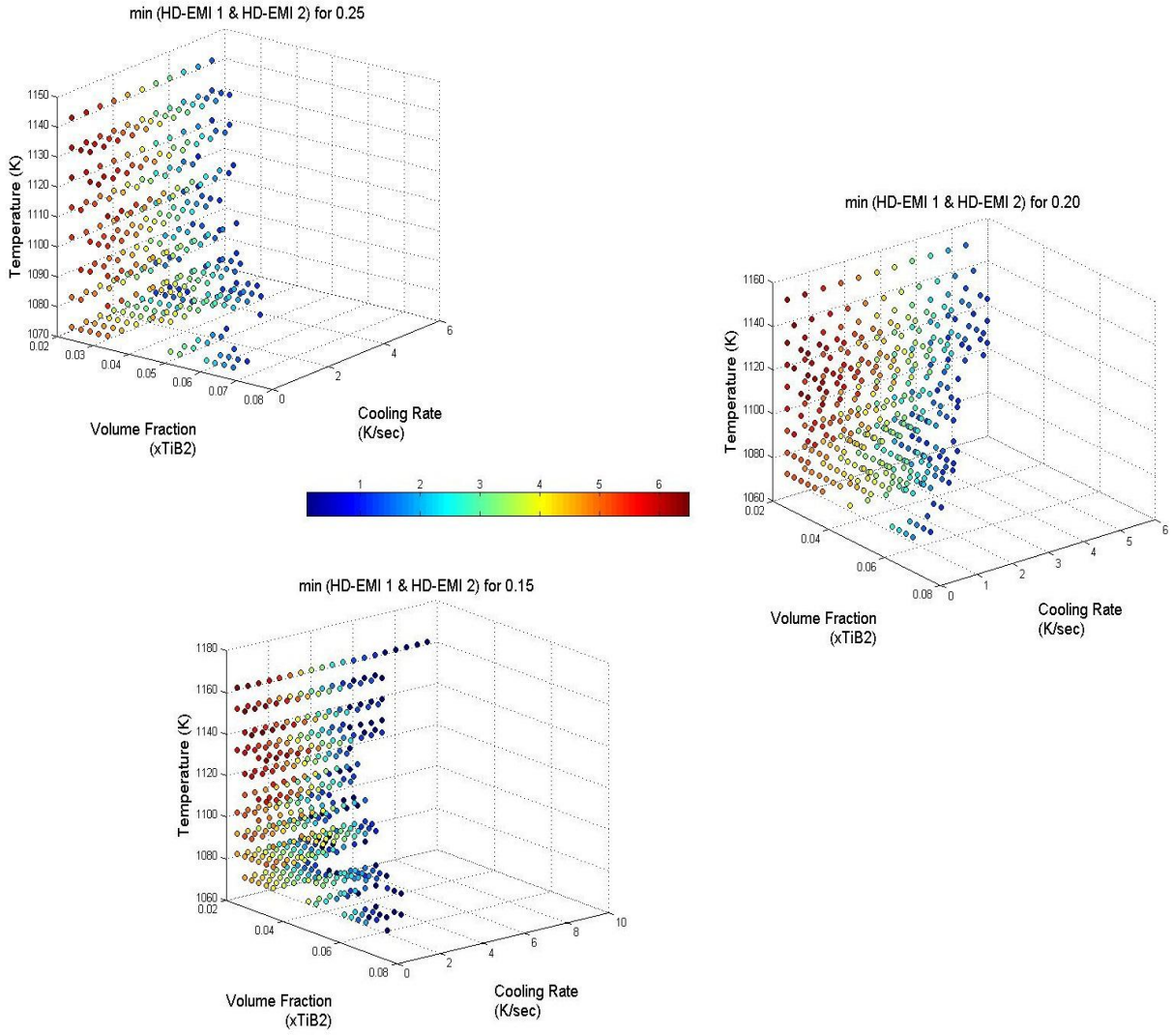

Figure 6.13: Robust processing space for 0.25, 0.20 and 0.15 convergence criterion.

6.4. Thoughts on What has been Presented and What is Next

The question posed in this chapter is 'How should a system level designer allocate resources for auxiliary simulation model refinement while satisfying system level design objectives and ensuring robust process requirements in multiscale systems?' In multiscale systems a qualitative answer is not possible due to the hierarchical nature of subsystem integration and complex coupling of the dependent and independent parameters. To provide a quantitative answer to

the question, sources of uncertainty are differentiated as MSU, MPU and NU. An algorithm to mitigate MPU arising due to insufficient data is developed using constructs from robust design and information economics. Using this algorithm, a system level designer is able to allocate resources as follows:

- Robust design against all three types of uncertainty and its propagation is facilitated using IDEM for multiscale systems. Ranged feasible sets are identified in addition to a single robust solution enabling use of these ranges for improvement potential evaluation until a final solution is reached. It assists in avoiding design iteration due to shifts in model responses.
- MPU due to insufficient data is quantified by the improvement potential metric in terms of statistical confidence intervals of a second order response surface model. The metric can be extended to higher order response surface models or other metamodeling techniques in order to represent non-linear phenomena of various fidelities.
- Correlation between benefit in terms of improvement potential and associated effort is made possible by the *ex-ante* improvement potential metric based on an empirical variation of MSE. It allows designers to account for computational cost in addition to uncertainty quantification and differentiates this metric from existing value-of-information based metrics.
- The computational time for iterations is minimized using constraint optimization techniques, hence allowing intelligent and judicious allocation of resources. Although the algorithm does not guarantee convergence in a single iteration, it assists a system level designer to allocate resources efficiently and enables the advantageous mitigation of MPU to reach the convergence criterion in a small number of iterations.
- Modularizing the algorithm into system and sub-system levels and decoupling robust design and information economics evaluations allows parallel computations in distributed design environments. Parallel computing techniques in combination with efficient resource allocation can cut down convergence time for a final robust solution.

This algorithm lays a general framework applicable to any multiscale system with a complex interlinking of simulation models. The consideration of simulation model weights in developing system level *ex-ante* improvement potential addresses the need for uncertainty mitigation at different levels of hierarchy. Coupled with the power of IDEM in identifying feasible ranged sets of designs, the proposed algorithm effectively allocates resources in simulation-based multiscale systems by integrating constructs from robust design and information economics. The focus in this chapter was on mitigating MPU and the method lays the foundation for holistic uncertainty management in simulation-based multiscale systems. The current algorithm uses second order response surface models to capture the input-output relationships. In the I-Statement in Section 7.2, posits have been laid down to choose the order of response surface based on the computational cost and the physical phenomena governing the simulation model. Also, the algorithm focuses on reducing model parameter uncertainty without consideration of performance objectives. Mixing performance measures with robust design measures is not a suitable approach. However, brief comments have been added to the I-Statement to suit uncertainty mitigation in terms of performance objectives. Also, as the focus was on mitigating MPU, additional insight cannot be obtained about the uncertainty from the value of the improvement potential metric alone. Separate metric needs to be evaluated for mitigation of MSU discussed in the I-Statement in Section 7.2.

In this chapter the secondary research question 2 in Section 4.1 was answered by integrating the constructs of robust design and information economics. Uncertainty modeling was systematically established in multiscale systems and validated the hypotheses proposed for the secondary research question. The eight step algorithm provides a framework for efficient resource allocation to mitigate MPU. Results were achieved and it fits into the Empirical Performance Validity, i.e., Quadrant III of the validation square. The organization of work is shown in Figure 6.15.

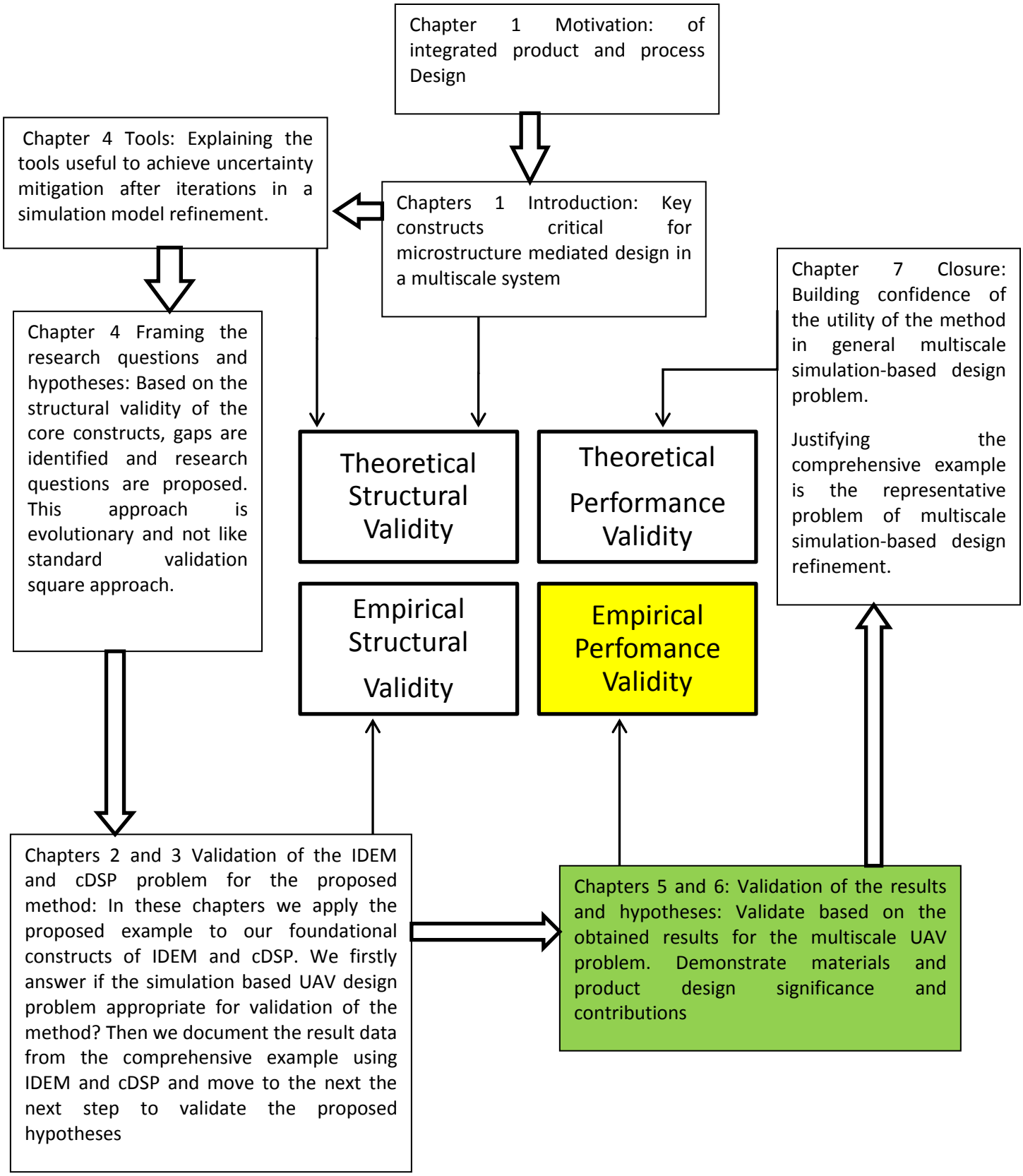

Figure 6.14: The validation square

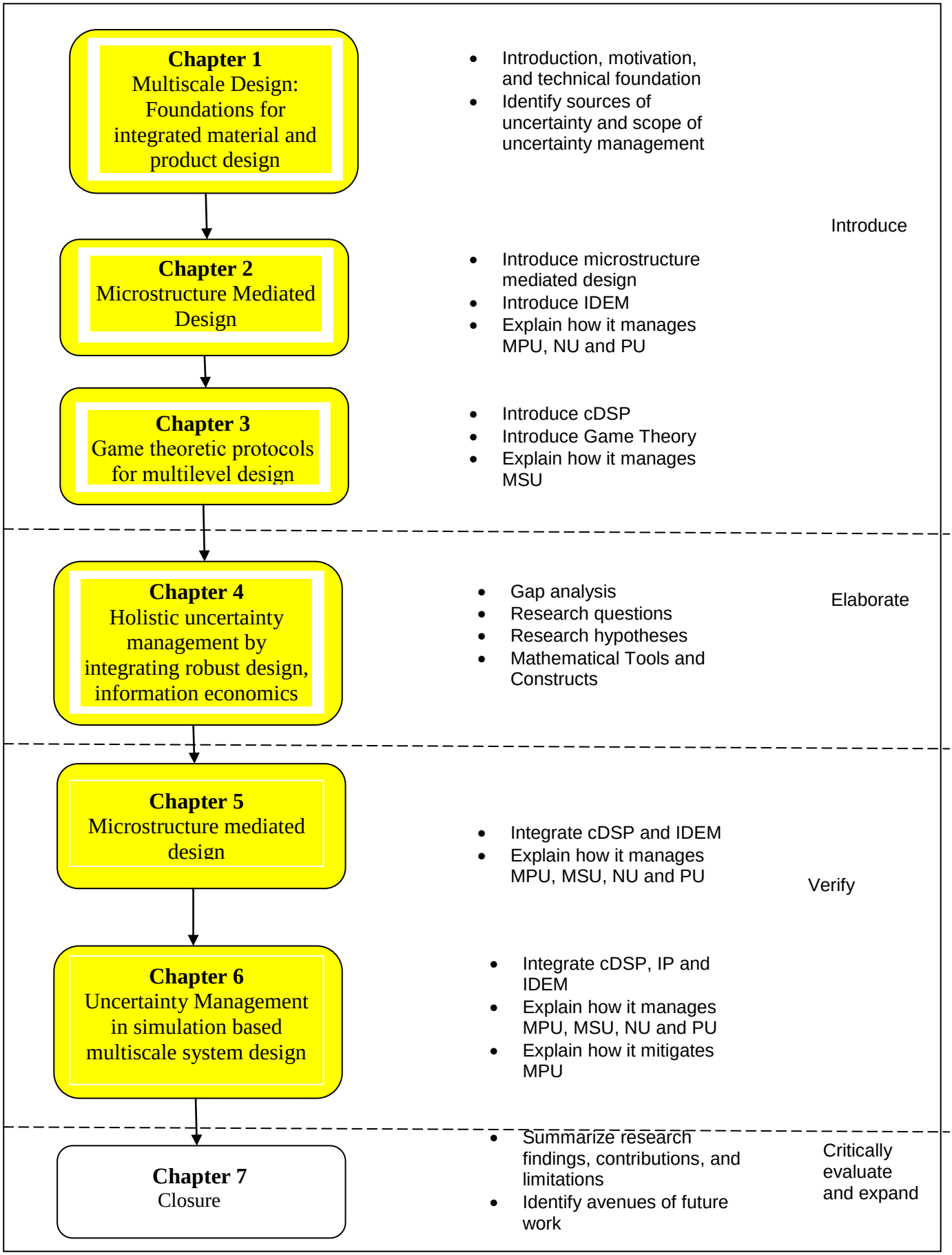

Figure 6.15: Organization of work

CHAPTER 7

CLOSURE

In this chapter, if the objectives for the work have been achieved and if the intellectual questions posed in Chapter 3 have been addressed. Finally, future work is discussed and the relevant contributions of the work are outlined in the I-statement. The relevant section titles and the status of each section are as follows.

7.1. A Look Back: Revisiting Research Questions and Hypotheses

The primary research question is:

'How does one manage and mitigate uncertainty in simulation-based multiscale systems?'

It is postulated that integrating constructs from robust design and decision support systems facilitate uncertainty management while integrating constructs from robust design, information economics and decision support systems aid mitigation of uncertainty.

To address the primary research question two secondary research questions are postulated:

1. How can we address model parameter uncertainty, model structure uncertainty, natural uncertainty and propagated uncertainty in multiscale systems?
2. How does the system level designer allocate resources for auxiliary simulation based model refinement while ensuring satisfaction of system level design objectives and product requirements for multiscale integrated product and material design?

To answer the first secondary research question the following three hypotheses are postulated:

1.1 Inductive Design Exploration Method (IDEM) incorporates model parameter uncertainty, propagated uncertainty, natural uncertainty and model structure uncertainty to give feasible solution sets.

1.2 IDEM uses hyper dimensional error margin index metric (HD-EMI) to manage model structure uncertainty

1.3 Compromise Decision Support Problem (cDSP) can be used to reach a trade-off amongst HD-EMI values to mange model structure uncertainty and hence gives a single robust solution against model structure uncertainty, model parameter uncertainty, propagated uncertainty and natural uncertainty.

To answer the second secondary research question following four hypotheses are postulated:

2.1 Integrating IDEM and cDSP facilitates giving single robust solution against all forms of uncertainty.

2.2 Response Surface Modeling allows us to define the improvement potential metric in terms of confidence intervals for mitigating model parameter uncertainty.

2.3 Concepts from value of information and response surface modeling can be integrated to develop predicted improvement potential and corresponding cost functions

2.4 Optimization techniques can be used to reach a trade-off among cost functions.

The first of the secondary research questions dealt with management of uncertainty in multiscale systems. Specifically management of model parameter uncertainty (MPU), model structure uncertainty (MSU), natural uncertainty (NU) and propagated uncertainty arising in multiscale systems are considered. The sources of these four kinds of uncertainty were described in context of simulation based multiscale systems. A comprehensive multiscale system was developed interlinking simulation as well as theoretical models over multiple length and time scales. The multiscale system comprised of material models in the process-structure (PS) and structure-property (SP) correlation. These material models simulated the microstructure and developed the property space for the material considered, i.e., in-situ aluminum based metal matrix composites. Further, simulation tools and theoretical models were used to map into the performance space for the product using property-performance (PP) relationships. Thus the mapping models moved in a bottom-up manner from the processing space to the structure space to the property space and finally to the performance space. Based on the materials processing steps involved and mechanical design requirements, the analysis of the

material and the structure was carried out using nine models (Section 5.2) : 1) precipitation model of the metal, 2) model of the evolution of microstructure in PS domain, 3) model for yield strength, 4) model for density, 5) model for thermal conductivity in SP domain and 6) model for depth, 7) model for time of operation, 8) model for weight and 9) model for operating temperature in the PP domain. The first three models and model for depth were simulation models and the rest were theoretical or empirical models considered. The sources of uncertainty arising in the simulation models as well as theoretical models were understood and quantified when possible. NU was quantified as a first order Taylor series expansion, MPU was quantified in terms of confidence intervals in response surface models and a metric indicating reliability of model performance against model structure uncertainty was incorporated, i.e., HD-EMI for multiscale system design. The constraints for HD-EMI were set as 1 indicating robustness against MPU and NU. The information from the response surface models and corresponding uncertainty bounds were input to IDEM which is capable of managing uncertainty in hierarchical systems. IDEM was employed to identify robust sets of solution against MPU and NU in the property, structure and processing space given performance requirements in an inductive top down fashion. PU was controlled by developing exact constraint boundaries using the bisection technique while moving top-down from performance space to processing space. Thus bottom-up analysis and top-down exploration were combined in IDEM based on Olson's material design hierarchy over SP, PS and PP domains in Section 5.3. Once robust sets of design variables were identified against MPU, NU and MPU we proceeded to manage model structure uncertainty by setting target goals for HD-EMI metrics in models and the weights for the target achievements. A higher value of achieved HD-EMI indicated greater robustness against model structure uncertainty which is difficult to quantify. The target values, individual models, corresponding uncertainty bounds were input to cDSP to reach a trade-off among possible sets and emerge with a single solution with the highest weighted sum of HD-EMI values. This single solution from the robust solution sets is most reliable against model structure uncertainty. Thus all four kinds of uncertainty MPU, NU, MSU and PU are managed in Section 5.3.

To summarize the conclusions in Section 5.4:

- NU or variability is dealt with using first order Taylor series expansion. The discretization resolution in IDEM is set equal to the variability in order to cover the entire design space.
- MPU is managed by defining confidence intervals for response surface models.
- PU is alleviated by developing exact constraint boundaries in a top-down manner using bisection technique. While passing the information in a top-down manner, the HD-EMI value is constrained to be greater than one which indicates robustness against NU and MPU.
- MSU is managed by trading off the HD-EMI values from the robust sets of solution using cDSP technique with a weighted sum deviation function. The deviation function is minimized for set HD-EMI goals.

The second of the secondary research questions dealt with mitigation of uncertainty in multiscale systems. The types of uncertainty are classified as reducible or irreducible. Natural uncertainty is irreducible in nature. Model parameter uncertainty and model structure uncertainty are reducible in nature. Propagated uncertainty (PU) is a compounded effect of the other three types of uncertainty and hence it can be mitigated by reducing model parameter uncertainty or model structure uncertainty. The IDEM technique employs exact constraint boundary technique and hence minimizes discretization error due to discrete resolution space and aiding mitigation of PU. Specifically mitigation of model parameter uncertainty (MPU) was considered in simulation models. Using the knowledge gained from the first secondary research question, IDEM was employed in conjunction with cDSP to identify a single solution from the feasible solution sets. A single solution once the level of improvement in simulation models has been reached is calculated using the cDSP and setting constraint for HD-EMI values to be greater

than 1. The error bounds developed for response surface model use the Taylor series expansion for NU and confidence intervals for MPU. As the concern is only mitigating MPU, the improvement potential metric is defined in terms of the lower and upper confidence intervals for the response surface models. The initial response surface models were built using central composite design. The improvement potential metric is devised in such a way that a low value of improvement potential indicates a lower value for simulation refinement as compared to a greater value for improvement potential. The improvement potential is averaged over all satisfying points to get a reflection without bias. A weighted sum approach for determining the system level improvement potential was developed in terms of the degree of influence of a simulation model on final performance objectives. This meant that models lower in the design hierarchy had greater weights which is justified as models lower in the hierarchy are propagated to a greater extent in the design chain and hence more value rests in mitigating the MPU in the lower models of the multiscale hierarchy. A convergence criterion was set to stop further simulation model refinement. The predicted or ex-ante improvement potential was then developed in terms of the number of subsequent simulation runs. To develop the ex-ante improvement potential, an empirical relation to capture the deviation of mean square error (MSE) was devised. Though MSE is erratic in nature, this relation guides resource allocation by correctly estimating the variation for models that must be adequately described using second order models. Overestimating or underestimating the MSE will lead to needless loss of resources or design iterations. Then based on the ex-ante improvement potential, computational cost functions are developed. This helps gauge scope of refinement in terms of the common parameter, computational time. The computational time was minimized in order for the system level improvement potential to reach the convergence criterion. The simulation models were re-run at points of maximum improvement potential and hence ensured advantageous reduction of MPU. With simulation model refinement we saw the number of robust feasible sets increased with a decrease in convergence criterion as expected. Also, the average HD-EMI value for the simulation models saw a progressive increase with a corresponding increase in achievement of depth. Thus simulation model refinement was

beneficial in terms of performance achievement and uncertainty mitigation. To summarize the conclusions in Section 6.4:

- Robust design against all three types of uncertainty and its propagation is facilitated using IDEM and cDSP for multiscale systems. Ranged feasible sets are identified in addition to a single robust solution. Ranged sets are used for improvement potential evaluation.
- MPU due to insufficient data is quantified by the improvement potential metric in terms of statistical confidence intervals of a second order response surface model.
- Correlation between benefit in terms of improvement potential and associated effort is made possible by the *ex-ante* improvement potential metric based on an empirical variation of MSE.
- The computational time for iterations is minimized using constraint optimization techniques, hence allowing intelligent and judicious allocation of resources.
- Modularizing the algorithm into system and sub-system levels and decoupling robust design and information economics evaluations allows parallel computations in distributed design environments.

Thus MPU is mitigated while MPU, MSU, NU and PU are managed. It sets the set for holistic uncertainty management and uncertainty mitigation. The algorithm was developed for MMD which is a representative example of a multiscale system. The constructs used to validate the primary research questions were founded on fundamental tools applicable to any generic system. Experiments were planned using a central composite design approach. Data was analyzed using a step-wise regression method to screen out unimportant variables for microstructure mediated design and decrease complexity. Integrated metamodels were developed using a second order response surface modeling. Prediction intervals were determined using statistical confidence intervals. These tools are applicable to any model with input and output. The improved IDEM formulation with coupled cDSP can be applied to any

generic multiscale system with mapping functions. For uncertainty mitigation the improvement potential metric was developed based on response surface and value of information constructs. The algorithm can be applied to any complex system with hierarchical mapping between the models. Weights for the simulation models were calculated using an empirical approach based on degree of influence. Optimization techniques were used to minimize the total computation time based on second order exponential functions for ex-ante improvement potential metric. The illustration of the algorithm was in terms of the MMD. However, MMD is representative of a multiscale design approach with interconnectivity established between the different material design hierarchy in terms of mapping functions. For any generic multiscale system, the mapping functions can be replaced by the representative mapping functions for the particular simulation model. As these methods are applicable to any generic simulation model, we can take a leap of faith and conclude the developed algorithm can manage and mitigate uncertainty in multiscale systems. This will be strengthened in the I-Statement. Thus we reach Quadrant IV of the validation square and establish theoretical performance validity. Figure 7.1 represents the validation square in context of the current chapter.

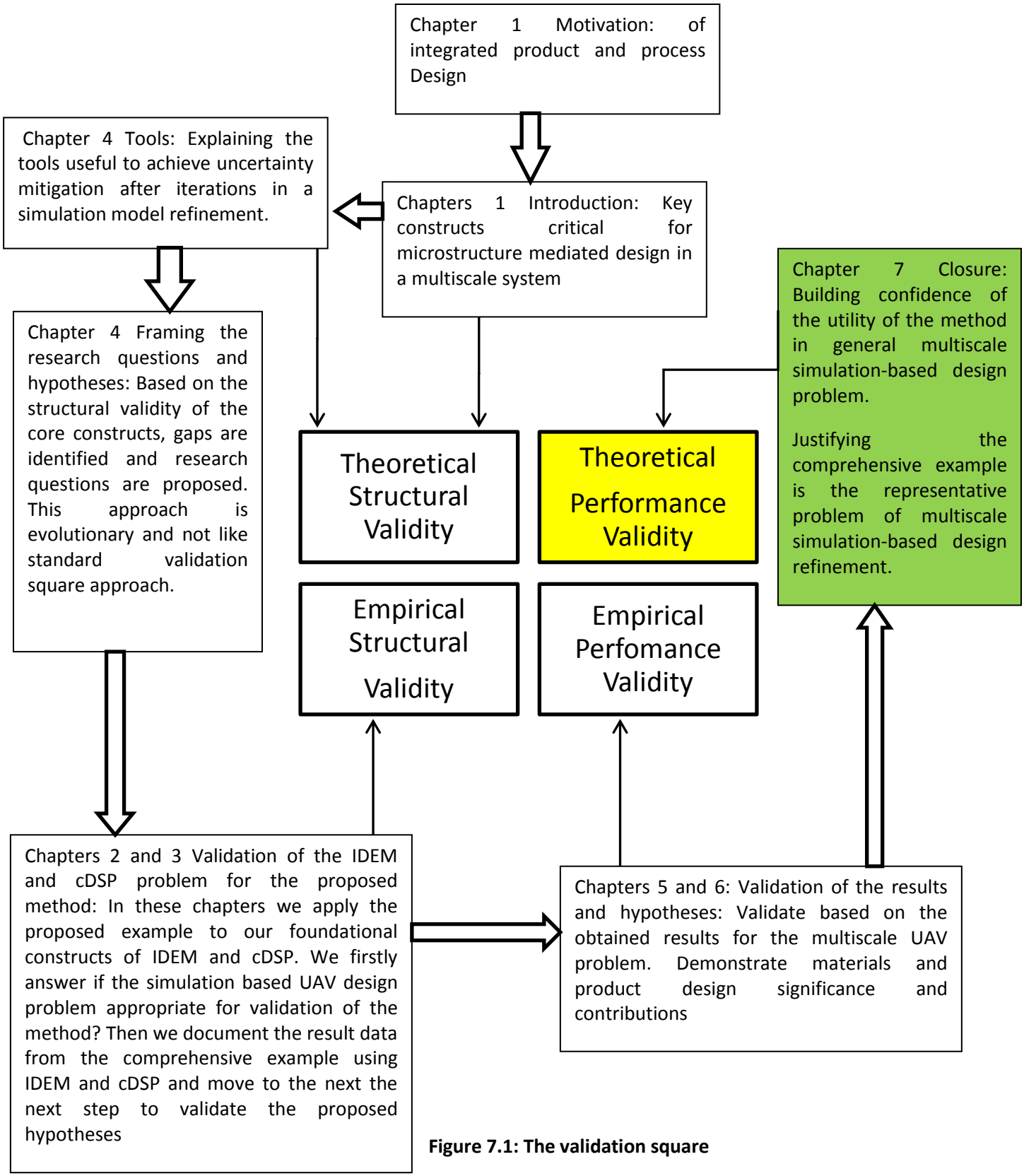

Figure 7.1: The validation square

7.2. I-Statement

In my thesis, I explored the paradigm of uncertainty management using the constructs from information economics, game theory and robust design. I used IDEM for robust design and improvement potential metric for information economics. Game theoretic protocols were used to asses different design environment. To develop a system level understanding of what has been achieved, I looked in greater detail on types of uncertainty as developed by Choi et al.

- Variability (natural uncertainty)
- Model parameter uncertainty (data uncertainty)
- Model structure uncertainty (model uncertainty)
- Propagated uncertainty: It is a combined effect of all three types of uncertainty.

I developed a multiscale problem- integrated material and product design. Microstructure mediated design task was investigated by developing models over the hierarchical material domain, specifically (Section 2.2):

- Process-structure (PS) relations: I established feasibility criteria (Thermodynamic, kinetic etc.) and constraints (manufacturing, cost etc.) for the composition and processing conditions.
- Structure-property (SP) relations: I established relations between microstructure features (composition, morphology, phases etc.) and material properties.
- Property-performance (PP) relations: I established relations between desired performance requirements and corresponding material properties required.

The following are the contributions from the tasks:

Table 7.1: Contributions from Chapters 2 and 3

Chapter	Contributions
Chapter 2 Microstructure mediated design	• The specific ranges of microstructure attributes are directly coupled in the present methodology with the overall systems design (material plus submersible). Hence, changes in performance capability are directly reflected in the ranges of microstructure attributes that emerge from application of IDEM. • The approach can be readily extended to include performance requirements that impose multifunctional, multiphysics requirements on the material design aspect. Competing modes of requirements in materials design are common and serve as a compelling basis for the present systems-based robust design approach. • If one is interested in selecting different process routes (e.g., in-situ versus ex-situ Al metal matrix composites or other matrix materials), the assessment of feasibility is quite difficult without considering the full contributions of the process-structure-property-performance relations. In other words, it is not just a classical materials selection problem. • Inductive Design Exploration Method facilitates top-down searching for design solutions including process path and microstructure based on bottom-up simulations. • The work presented in Chapter 2 constitutes one of the most complete applications of IDEM. The primary challenge involves managing uncertainty in over seven empirical and theoretical models over four levels of design.
	• Interdisciplinary iterations between uncoupled design levels are eliminated, which can greatly reduce the computing cost in multidisciplinary product realization. The complexity of the decision

Table 7.1 continued

Chapter 3 Game Theoretic protocols for multilevel design	making process is limited by eliminating iterations between modules or levels. • Each team (player) holds its own cost function and makes decisions in its own discipline. Hence, the game based approach greatly increases the autonomy and independence of the disciplinary teams and enables higher parallelism. • The game theoretical protocols are appropriate to model the relationships between engineering teams, and enable collaborative decision making based on the cooperation styles between teams. Java DSIDES is efficient for solving the derived cDSP as it offers the provision for hierarchical optimization. • The construct introduced in the corresponding chapter can be applied to any complex product. Upstream teams make decisions that remain superior even though the requirements of the downstream teams may not be known yet. Downstream teams can specify final solutions without jeopardizing the satisfaction of the design requirements in upstream activities. Hence, engineering teams can keep the product realization problem open in the early stages of product realization, and make decisions that are superior from the perspective of all domains. • Compared to other approaches my method does not necessarily lead to a better design. However, for multilevel design tasks especially in the early stages of product realization, the proposed construct is deemed efficient. I do suggest that my method is more practical in the design of complex engineered systems.

Following these two tasks, research gaps were identified and addressed in Chapters 4 and 5.

The gaps identified were as follows in Section 4.1:

1. *Clarification of multilevel design*: Clear definitions of the multilevel design and difference from multiscale system modeling were not clear with respect to

microstructure mediated design. Also the difference between multiscale modeling and multilevel design for multidisciplinary systems in terms of hierarchical materials design was not clear from literature and the IDEM and cDSP approaches.

2. *Clear definition of the mathematical challenges for uncertainty management and uncertainty mitigation in simulation based multiscale systems*: The discussion of the mathematical challenges for uncertainty management in hierarchical material design using simulation models is scattered throughout literature and not explicit. Also the challenges for uncertainty mitigation are not found in literature.

3. *Generality of the IDEM method*: The IDEM method has not been tested for general design problems that do not necessarily have a one-to-one mapping between variable spaces. IDEM can be used for many-to-one mappings implying multiple solutions in the inverse exploration. Also the question of coming up with a singular solution in the presence of multiple solutions arises. MMD is an example to this end.

4. *Establishment of the compatibility between the decision formalisms of value-of-information and robust design*: Uncertainty mitigation using robust design and information economics raises the question about the compatibility between the decision formulations. Robust design involves finding solutions insensitive to uncertainty while value of information uses utility theory to derive improvement potential metric which focuses on maximization of expected utility. Clearly, optimization and robustness are incompatible and this warrants further investigation.

5. *Formulation of a fundamental, rigorous definition of the tradeoff problem*: The proposed method of trading off value versus effort is not found in literature. It needs to be addressed by establishing a) an approach for quantifying the effort, and b) a rigorous definition of the tradeoff problem, and c) an approach for making the tradeoff decisions.

6. *Justification of the use of improvement potential over existing expected value of information*: Improvement potential metric ignores of the expected value of information

in the sense it only quantifies the scope of improvement but does not quantify how much the improvement potential will be reduced with additional information. This is identified as a research gap.

To answer this question, the challenges are split into two chapters:

- Microstructure mediated design: multiscale design of material and product (Chapter 5)
- Uncertainty management in simulation-based multiscale systems (Chapter 6)

Relevant to each chapter, the gaps are classified as follows:

Table 7.2: Classification of Gaps

Microstructure mediated design: Multiscale design of material and product (Chapter 5)	**Uncertainty management in simulation-based multiscale systems (Chapter 6)**
Clarification of multiscale design	Establishment of the compatibility between the decision formalisms of value-of-information and robust design
Clear definition of the mathematical challenges for uncertainty management and uncertainty mitigation in simulation based multiscale systems	Formulation of a fundamental, rigorous definition of the tradeoff problem
Generality of the IDEM method	Justification of the use of improvement potential over existing expected value of information

I discuss how these gaps have been addressed:

1. *Clarification of multiscale design*:

- Multiscale modeling involves coming up with hierarchical simulation models over

multiple length and time scales ensuring system level connectivity of the information flow. Multiscale modeling is discussed in Sections 4.2.1 and 4.2.2 in context of MMD of material and product.

- Multilevel design seeks making risk-informed decisions at the various levels in a hierarchical system. If the hierarchical system is a multiscale system, i.e., with models simulated over different scales, it corresponds to multiscale design. Specifically the risk-informed decisions are made using the HD-EMI metric which establishes the degree of reliability of a model in a multiscale system under potential shifts in the output range.

2. *Clear definition of the mathematical challenges for uncertainty management and uncertainty mitigation in simulation based multiscale systems*.

For both uncertainty management and uncertainty mitigation, the primary challenge is identifying and classifying all sources of uncertainty that may arise in a multiscale system. To identify the challenges, sources of uncertainty were classified as:

- Variability (natural uncertainty)
- Model parameter uncertainty (data uncertainty)
- Model structure uncertainty (model uncertainty)
- Propagated uncertainty

Variability was quantified using Taylor series expansion. MPU was quantified using statistical error bounds. MODEL STRUCTURE UNCERTAINTY was evaluated using the HD-EMI metric. Propagated uncertainty was avoided by exact constraint boundary calculation. For MPU mitigation, improvement potential metric is devised using bounds from response surface models.

3. *Generality of the IDEM method*: The generality of the IDEM method is illustrated using hierarchical material design over PS, SP and PP mappings over process-structure-property-performance domains. These domains may have many-to one mapping in the bottom up approach and the input-output relationship is quantified using response

surface models. The top-down or inductive approach identifies all sets of feasible or robust solutions that may arise from many-to-one mappings in the bottom-up approach. The singular solution is identified by compromising the degree of HD-EMI achievement in the individual simulation or theoretical models using cDSP technique.

4. *Establishment of the compatibility between the decision formalisms of value-of-information and robust design*: To ensure compatibility between optimization and robustness, improvement potential metric is devised in terms of the confidence intervals used for robust design. This ensures the base for making robust design decisions for product parameters or design variables is the same as improvement potential metric used for making simulation refinement decisions for models or process variables.

5. *Formulation of a fundamental, rigorous definition of the tradeoff problem*: The proposed method of trading off value versus effort is addressed by establishing

- An approach for quantifying the effort for reducing MPU in terms of the number of simulation runs,
- MPU is reduced by decreasing the confidence intervals. This is achieved by an empirical relation for MSE variation.
- The simulation runs are correlated to computational time and time is used as a common base trade-off
- Tradeoff decisions to allocate resources for further simulation refinement are achieved optimization techniques in MATLAB so that the system level improvement potential drops or becomes equal to the convergence criterion.

6. *Justification of the use of improvement potential over existing expected value of information*: Improvement potential metric extends the current improvement potential metric and is able to quantify the scope of improvement as well as the reduction of the improvement potential with additional information.

Table 7.3: Contributions from Chapters 5 and 6

Topic	Contributions
Chapter 5 Microstructure mediated design	• NU or variability is dealt with first order Taylor series expansion.MPU is dealt by defining confidence intervals for response surface models developed. PU is dealt by developing exact constraint boundaries in a top-down manner using bisection technique. Model structure uncertainty is dealt by trading off the HD-EMI values from the robust sets of solution using cDSP technique with a weighted sum deviation function. • The specific ranges of microstructure attributes are directly coupled in the present methodology with the overall systems design (material plus submersible). Robust solution ranges are identified using IDEM • IDEM is used in conjunction with design of experiments and response surface modeling to reduce computational cost. • The HD-EMI metric allows us to tailor the final solution based on the desired mitigation of model structure uncertainty. • The assessment of feasibility for different routes considers full contributions of the process-structure- property-performance relations and singular robust solution is identified using cDSP. • Inductive Design Exploration Method facilitates top-down searching for design solutions including process path and microstructure based on bottom-up simulations. • The work presented in this chapter constitutes one of the most complete applications of uncertainty management. The primary challenge involves managing uncertainty in over nine empirical and theoretical models over three levels of design.
	• Ranged feasible sets are identified using IDEM in addition to a single robust solution using cDSP enabling use of these ranges for improvement potential evaluation until a final solution is reached. It assists in avoiding design iteration due to shifts in

Table 7.3 continued

Chapter 6 **Uncertainty management in simulation-based multiscale systems**	model responses. • The improvement potential metric can be extended to higher order response surface models or other metamodeling techniques in order to represent non-linear phenomena of various fidelities. • The *ex-ante* improvement potential metric allows designers to account for computational cost in addition to uncertainty quantification and differentiates this metric from existing value-of-information based metrics. • Although the algorithm does not guarantee convergence in a single iteration, it assists a system level designer to allocate resources efficiently and enables the advantageous mitigation of MPU to reach the convergence criterion in a small number of iterations. • Parallel computing techniques are made possible due to modularization of algorithm and in combination with efficient resource allocation can significantly cut down convergence time for a final robust solution. • This algorithm lays a general framework applicable to any multiscale system with a interlinking of simulation models. • The consideration of simulation model weights in developing system level *ex-ante* improvement potential addresses the need for uncertainty mitigation at different levels of hierarchy. • My focus in this thesis is on mitigating MPU and I believe the method lays the foundation for holistic uncertainty management in simulation-based multiscale systems.

The algorithm for uncertainty mitigation is developed on some core assumptions. The most important one being that the system can be modeled using second order response surfaces. The MSE error variation is also a critical assumption contributing to the solution. In order to improve

the algorithm, I propose the following for future work.

Table 7.4: Scope for future work

WRT	Improvement
Discretization error effort	In my algorithm for uncertainty management, I looked at MPU specifically linked with model parameters and how value of information can be used for simulation model refinement for multiscale systems. This value of information understanding needs to be extended to mitigating uncertainty in design variables i.e. understanding the computational effort in reducing discretization error in IDEM. This can be achieved by understanding simulation run times for different discretization resolutions.
Model structure uncertainty	Model structure uncertainty arises from modeling assumptions and hence is more difficult to quantify. One approach is to prepare a comprehensive list of computational programs used in simulations and understanding the impact of refining the model. For example, in structural modeling, the validity of the results is dependent on the mesh size. The computational effort in reducing mesh sizes in FEM softwares like ABAQUS or ANSYS need to be quantified. Also, in numerical simulation in MATLAB we often use approximations which can be tailored. For example a material simulation model may use the Simpsons rule for numerical integration. This can be refined by using Simpsons $3/8^{th}$ rule at an increased computational cost. All these scenarios need to be tabulated and corresponding computational costs need to be quantified.
Design of experiments	I used central composite design for space filling experiments. Although CCD's have several advantages over other space filling experiments, other possibilities exist Latin hypercube, orthogonal arrays or D-optimal designs which may be more effective for space filling experiments. These need to be evaluated

Table 7.4 continued

Response surface modeling	I used a second order full quadratic model for developing metamodels for simulation outputs. We can start with linear models and based on p-values or F-statistic and determine when it is appropriate to consider second order models which require a larger number of runs to evaluate the regression coefficients correctly. Also, there are other alternatives to response surface models like Kriging, Adaptive Response Surface Modelling (ARSM) or Probabilistic collocation which need to be evaluated in terms of computational efficiency and appropriateness for application to IDEM.
Confidence intervals	I used a t-statistic confidence interval to determine the uncertainty bounds of a response surface model. Literature suggests that this prediction interval estimate is not appropriate for certain simulation based design with large data sets and can lead to incorrect variance estimates. Other confidence interval methods need to be rigorously studied and checked for validity with respect to different kind of simulation models.
IDEM	IDEM has been used for robust design. While evaluating metamodels the design space has been kept constant throughout the algorithm. Design space reduction will lead more quickly to convergence towards a robust solution. However, it would also mean the triviality of initial simulation runs outside the reduced feasible space and corresponding increase in uncertainty of associated metamodels. This needs to be understood in greater detail.
Improvement potential	The improvement potential metric has been evaluated in terms of upper and lower bounds of metamodel. It may make greater sense to redefine the improvement potential metric in terms of mean and upper bound when larger values are desired and mean and lower bound when smaller values are desired.
Trade-off	For trade-off, I assumed a hierarchical leader –follower game theoretical protocol similar to Stackelberg mechanism. In the Stackelberg leader-follower trade-off mechanism with complete information exchange, a very simplistic case has been assumed. We

Table 7.4 continued

	need to test game theoretic protocols for realistic design environments
Algorithm	The algorithm has been developed after the first set of simulation runs has been run and we have a starting point for uncertainty management. It will be interesting to refine the algorithm and understand how the system level designer can mitigate uncertainty from scratch without any prior simulation runs and only computational cost information.

In summary, I have achieved the objective of integrating robust design and information economics in my algorithm which mitigates MPU in Chapter 6. This needs to be extended to the other two kinds of reducible uncertainty, i.e., model structure uncertainty and propagated uncertainty.

For mitigating PU, we need to investigate the increase of computational time with increase in discretization resolution in IDEM. This exercise is fairly straightforward. However, uncertainty propagation in other robust multiscale techniques needs to be tested for efficiency against IDEM. Mitigation of model structure uncertainty is more challenging as it is hard to quantify and it is difficult to interpret how MSU varies with modeling assumptions and incomplete knowledge. To mitigate model structure uncertainty we can take leads from the HD-EMI value and computational resources should be invested in simulation models that yield low HD-EMI values indicating the mean response is close to constraint boundaries and more susceptible to error under potential shift of the output response due to model structure uncertainty. The cost models need to be systematically developed and the following discussion is in respect to cost modeling for mitigating model structure uncertainty. With any cost modeling the end goal is to have a little more insight into the future, before the cost is incurred. This is true whether the cost is time, money or other resources. Cost modeling is extremely important especially in the field of systems engineering, where an engineer, and ultimately a company, will benefit greatly from this estimated cost early on in a products life cycle. With this benefit being so important, many cost models have emerged. In 1981 Boehm produced a model called the constructive cost model (COCOMO) to estimate cost, schedule and effort for software engineering projects. This model was later replaced with COCOMO II in 1997 and later published in 2000, soon after

becoming widely accepted [96]. In 2002, another cost model emerged called the Constructive Systems Engineering Cost Model (COSYSMO) which was developed by Valerdi [97]. This cost model was primarily developed through an analysis of COCOMO II along with Delphi exercises. COSYSMO has also become widely accepted and has been implemented in many aerospace and defense companies [98].

Through the analytical inspection of the relationship between how the COSYSMO model was developed from the COCOMO II model we can formulate an outline of how to create an analogous cost model for the domain of simulation-based design. From Valerdi's dissertation [97], which gives insight to how COSYSMO was developed, I have extracted these analogues steps needed to create a general cost model for model structure uncertainty:

1. *Specify/Identify the Problem*: As stated before the goal of the system level designer is to quantify the cost associated with using existing models or developing new ones for the purpose of information economics. Unlike COSYSMO or COCOMO II, the system level designer is more interested in cost of the model itself rather than the elaborate costs of an overall project.
2. *Model Definition*: The system level designer needs to identify the scope, boundaries and range of this cost model. In other words, the he needs to find the parameters in which my cost model needs to work, and will eventually be calibrated to this spectrum. This will give a clear view of what his end result will look like.
3. *Identify the Significant Factors*: The system level designer needs to determine what variables will be the drivers in his cost model. What factors and components will affect and make up this model? In the example of COSYSMO, three main types of drivers were defined: additive, exponential, and multiplicative. Several questions need to be answered at this stage of a general cost model. Some of these questions include: What factors will be analogous to the COSYSMO drivers? How will they be similar? How will they be different? Will a general model take a similar form?
4. *Determine and Calibrate Design Exploration Costs:* As with any creation of a model one must allocate time, energy and resources to design exploration. The design of experiments and strategies must be considered since both can incur a large cost. The system level designer will need to determine these costs so that the model does not over look significant hidden costs. Leads from HD-EMI values from initial design space

exploration can be used to affect mitigation of MODEL STRUCTURE UNCERTAINTY.

5. *Determine and Calibrate Person-Hour Costs*: Here the system level designer will model the labour allocated to the physical act of creating the model (i.e. coding the model). This portion will be the most similar to COSYSMO or COCOMO II since both quantify person-hours. The system level designer will determine the variables to quantify this portion of his model through similar means such as Delphi exercises and expert knowledge and opinion. Through these Delphi exercises the system level designer will ask experts questions including: How many years of experience do they have? Are there additional drivers not considered? Do they agree with the selected drivers? The system level designer will also ask experts to rank potential drivers to determine their importance.
6. *Determining and Calibrate Computational Cost:* Through the study of complexity classes and complexity time the system level designer will formulate a means to quantify the computational time depending on the algorithms implemented in the models. Since this stage has the potential to be the most complicated the system level designer will need to formulate a means to simplify this step to insure that the cost model is efficient to use.
7. *Refine Model and Validate:* This step begins the iterative process to insure that the model is useful within the definition. Once the costs have been quantified for the cost model the system level designer must calibrate the variables to produce results that correspond with historical data and/or case studies. The system level designer will then refine his cost model to make it more accurate and repeat this process, returning to previous steps, until the cost model can be validated to a reasonable margin of error.

Though, the above steps can be applied to any generic cost model, in this algorithm I am looking at a very specific component of cost modeling *i.e.* cost modeling associated with reducing model structure uncertainty. Detailed understanding of the physical phenomena will also contribute to such cost modeling. Significant effort needs to be put in order to develop a domain independent cost modeling for mitigating model structure uncertainty in multiscale systems. An alternative approach is to develop cost models relevant to specific analysis of multiscale systems. Quantifying the value of information associated with refining the modeling assumptions will be

a rigorous task considering the large number of simulation software that assist modeling of various physical phenomena. We need to build a comprehensive list of all the simulation softwares and associated cost-benefit understanding for each of these softwares. An alternative method would be look at different physical phenomena like thermodynamics, structural dynamics etc. and common assumptions used in modeling these phenomena. However, in multiscale modeling, different physical laws will be used for modeling subsystems at different length and time scales. Considering the length and time scales can range from quantum or molecular domain to the macro domain of physical products or the nano second to entire product lifecycle which may be years, developing cost models will be a meticulous and challenging task. After having looked at the details of each of the algorithm and suggested improvement, I take it to a higher level of abstraction and justify the approaches from the standpoint of application.

With Respect to Microstructure Mediated Design

In MMD, my focus was on managing all the four kinds of uncertainty. A question from a material scientist maybe is what this approach offers that possibly the MSD or other material design techniques don't. My justification to this falls in the realm of multidisciplinary systems. The algorithm has been developed with the notion that material and its microstructure forms the building block for multidisciplinary applications. In age of rapidly developing scientific tools, there is an influx from various domains like electronics, aerospace, bioengineering etc. The common ground for advancement of each of these sciences is the material from which it stems from, i.e., the silicon material from which transistors are built, the low weight high strength composites from which airplanes are built, the materials in our natural environment used to mimic biology processes in nature inspired engineering. The MMD approach goes beyond the realms of UAV design. Current approaches focus on optimizing the performance of simulated microstructure using mathematical tools. Considering the simulation tools being developed are in its infancy and not well grounded like gravitation or other physical laws, proceeding to optimization without accounting for elements of uncertainty can only lead to erroneous results

and possibly loss of resources expecting the experimental results to yield the same results as predicted by the optimal solution. The idea is that every material is developed to produce a tangible product and hence it's the product characteristics that should drive the material microstructure and not the material properties. Bringing in product characteristics also has the additional advantage of allowing design freedom to the material designer, i.e., the product requirements may not dictate equal weights on say yield strength or crack propagation. It allows a designer to set weights on the material characteristics based on the desired product requirements instead of optimizing each material property. In terms of multidisciplinary analysis, a electronic application will lead to higher to higher weights being assigned to heat dissipation and hence thermal conductivity while a structural analysis will lead to higher weights being assigned to yield strength or bulk modulus. Also, the structure of IDEM allows different disciplines to formulate individual models and each of these can be linked based on the desired flow of information. At the macroscale, the different disciplines may lay down independent frameworks and the requirements are passed into the material domain which forms the interdependent parameter. The feasibility of macroscale product can be determined using the top-down approach and infeasibility leads to a system level designer relaxing some of the requirements in the macro domain. The HD-EMI metric also provides insight into the degree of infeasibility. A very small HD-EMI metric for a model in the macro scale leads one to conclude that it is bottle-neck for material design. Current approaches do not allow such conclusions based on mathematical constructs.

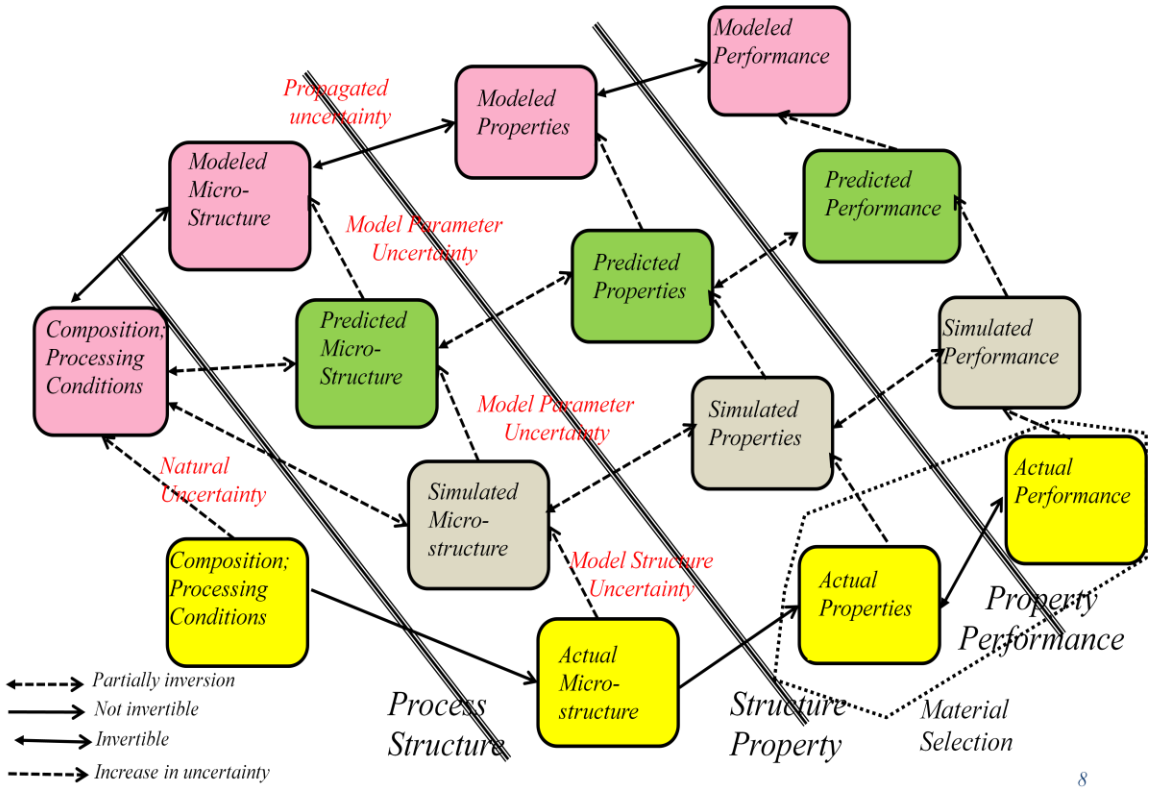

Figure 7.2: Microstructure Mediated Design (MMD)

I use Figure 7.2, to explain the flexibility of MMD. There are mappings between process-structure-property-performance relationships which I call horizontal mappings and there are lateral transformations reducing the order of modeling which I call vertical mappings as per the figure. Suppose, a designer has response surface models for all but the structure-property mappings, the structure of IDEM allows him/her to use experimental data (yellow box) instead of response model (pink box). Now a designer uses the experimental data to develop a response surface model instead of a simulation model. The components of MPU, MSU can be ignored in the modeling assuming accurate experimental set-up. Similarly, a designer can use the data (green box) directly instead of resorting to response modeling and develop constitutive mathematical models as mapping functions. Also, as IDEM is implemented in MATLAB, a subroutine can call a simulation model using some other software and hence the actual simulation model can be used to replace the response model. As uncertainty is systematically disseminated, depending on the kind of vertical mapping chosen (grey, green , yellow or pink

box) only the corresponding elements of uncertainty will need to be accounted for. Hence if experimental data is used, only noise factors need to accounted and natural uncertainty arises. If simulation model is used, model parameter uncertainty can be ignored and only model structure uncertainty needs to be managed in addition to natural uncertainty. If the green models are used, only the component of uncertainty that arises due to inaccurate data needs to be quantified in model parameter uncertainty along with model structure uncertainty and natural uncertainty; and the component arising due to insufficient data can be ignored. Such flexibility over the entire material and product design hierarchy is not offered by other approaches. Also MMD approach can be used in parallel with MSD approach as material models evolve. Only the mapping function needs to be changed without affecting the rest of the design, hence saving on resources and avoiding design iteration.

With Respect to Uncertainty Mitigation

One limitation of the current algorithm is that it is formulated on robust design principles without consideration of performance objectives. It is my belief that robust design and optimization of performance index should not be mixed. However the current algorithm gives the flexibility if the formulation is altered. I explain it briefly.

The HD-EM metric in Inductive Design Exploration Method needs to be reformulated in terms of desired target of performance values. The metric for calculation used in IDEM is Hyper Dimensional Error Margin Index (HD-EMI).

The HD-EMI by definition is:

$$EMI_1 = Min\left(\frac{mean_1 - b_1}{mean_1 - b_1^1}\right)$$

,i.e., the ratio of the distances of the mean from the constraints boundary and output boundary.

The further the mean is from the constraints boundary, higher the value of HD-EMI. HD-EMI is metric indicating the robustness against model structure uncertainty. However, HD-EMI metric

does not indicate performance attainment. Hence I define another metric of calculation which checks for the response values relative to the desired target values. This metric I call the fitness index (FI).

I define the target value as D and $D_1, D_2, D_3 \ldots$. This is vector of target values along different output directions. I define the FI as:

$$FI_1 = \left|\left(\frac{mean_1 - D_1}{mean_1 - b_1^1}\right)\right|$$

$$FI_2 = \left|\left(\frac{mean_2 - D_2}{mean_2 - b_2^1}\right)\right|$$

Contrary to several boundary points, we have only one target value and hence only one fitness value per output direction. A smaller value of FI indicates the mean output is close to the desired target value and hence is desired. Fitness indices are relevant only to performance parameters in the final stages of design. Fitness indices in the intermediate steps have little meaning. So the objective is to find the solution closest to the target values. For this we consider all response $means$ associated with finite positive HD-EMI values and small fitness values as close to zero as possible. For multiple performance objectives we can use compromise DSP to solve for fitness values.

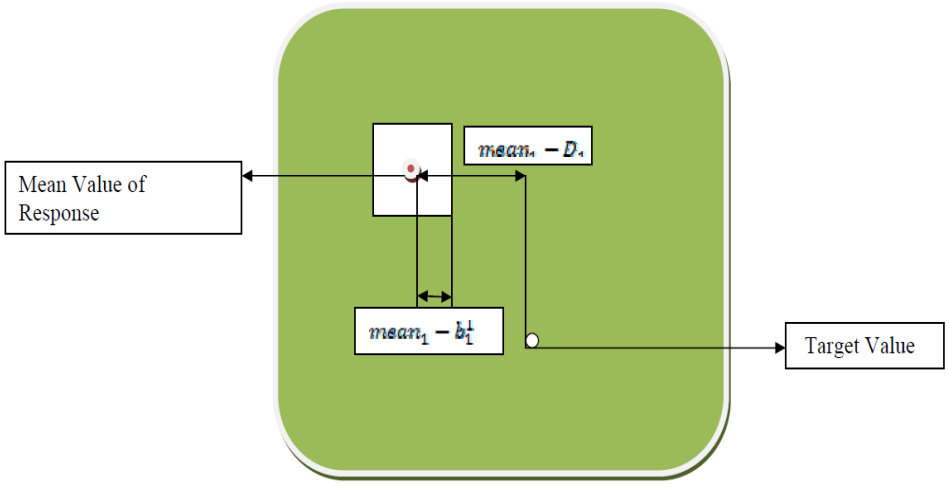

Figure 7.3 Evaluation of fitness index (FI)

So similar to HD-EMI's, every mean response is associated with a fitness values (FI).In IDEM we use the cDSP approach to trade-off the HD-EMI values at different levels of the problem to give us a final ranged set of feasible design space of the input variables. We can follow a similar approach for minimizing the fitness indices (FI) in different output directions of the performance variables. If HD-EMI calculation is used in conjunction with FI, it is possible to generate performance measures for ranged sets of solutions. The approach is similar to that of IDEM. We obtain initial ranged sets of feasible design space using IDEM based on HD-EMI metric. We evaluate the FI for each feasible input point. The cDSP can be reformulated to minimize the FI with targets being 0. In Figure 7.4, a preliminary approach is shown to reduce the initial feasible space based on FI metric by constraining the FI metric to be greater than 0 and less than 1 on the final output responses. We obtain a smaller subset of feasible design space based on the design metric.

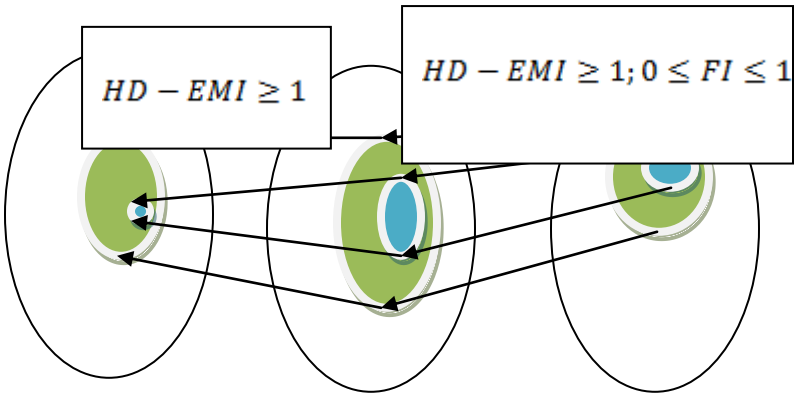

Figure 7.4 IDEM using fitness index (FI)

The Green region denotes feasible space where all HD-EMI's ≥ 1.The Blue region is a subset of the green region which denotes all feasible space with HD-EMI's$\geq$1 and 0$\leq$FI's≤ 1.Thus we see we get values which are closer to the desired performance targets. To evaluate the improvement potential metric, we use the blue subset of design space. Thus the improvement potential metric is determined in terms of performance attainment in addition to robust constraints.

The second concern is that of evaluating the improvement potential metric itself. As we are concerned with performance measures, the improvement potential needs to be defined in terms of optimization of performance measures and not uncertainty mitigation. Hence, the formulation of Panchal based on utility theory would be appropriate. Refer Panchal for additional details. However, the improvement potential metric defined by Panchal needs to be refined in order to account for cost considerations. The metric also develops upper and lower bounds for performance based on utility theory. A detailed understanding of utility theory can enable consideration of computational cost. An alternative approach would be to use previous trends of refinement to predict suggested improvement. Also, kriging metamodels have provision for optimization and have a statistical metric called the expected value of improvement (EVI) which may suit the problem at hand. These cases need to be investigated. The system level improvement potential determination and trade-off solution can follow the same formulation as the current algorithm.

Another concern is determining the order of response surface model suitable for simulation model. I lay the following guidelines for its determination:

- Higher order response surface should be chosen for non-linear phenomena. For a simple ordinary differential equation governing the simulation model, a linear or second order response surface may suffice. However for physical phenomena being governed by a set of partial differential equation, third order or fourth order response surfaces may be required. Deciding the order depends on the previous experience of a material designer. An alternative approach is to start off with say a high order response surface model and use backward elimination techniques in regression analysis to eliminate the unimportant regression coefficients. The order of the highest significant regression coefficient may be chosen as the degree of response surface model. However depending on the order of the initial degree of response model chosen for backward elimination, a large number of data points may be required, increasing the computational cost. This interrelationship needs to be investigated.

- While choosing the degree of the response surface model, it is also important to consider the computational cost of determining all the regression parameters of a response surface model. Though higher order response surface models will always lead to better fits, it comes at an increased computational expense. For example a second degree response surface model will have a total of 9 regression coefficients to calculate linear, quadratic and interaction effects for 2 input variables. Hence a minimum of 9 experiments will need to be run. However for a third order response surface model, the number of experiments increases to 16 and for a fourth order to 25. This increased computational expense needs to be justified while choosing the degree of the response surface.

- If a phenomenon follows an exponential behaviour, choosing a response surface model without exponential variables may lead to a bad fit. Hence it is crucial to analyze the data prior to choosing the order of response model and appropriate regression parameters need to be considered. Design of experiments knowledge needs to be coupled with response surface modelling constructs in order to determine the trend of the obtained data and plan future experiments. Though this has not been considered in the current algorithm, I propose it for future study.

Looking back at my thesis, I propose the following to whoever decides to work on uncertainty management in multiscale systems:

- Simple is better: In multiscale systems we deal with different disciplines. As all design teams need to work collaboratively, it is useful to keep the formulations as simple as possible.

- Avoid conflicting ideologies: Robust design and performance optimization are contradicting constructs. Hence a designer to stick to either one of the constructs while formulating the algorithm. I stuck to robust design constructs and performance objectives were considered independently in cDSP formulation. Robust design

constructs should be followed when there is presence of uncertainties within individual models, which are due to uncertain parameters, material properties, assumptions, etc or evolving simulation models, resulting in multiple fidelities of models at different points in a design process. This is especially relevant in the initial stages of design when the objective of a system level designer is to maintain design freedom. Significant model development and execution costs results in limited data and hence increased uncertainty component. However if the model development costs are low and sufficiently accurate, a system level designer can resort to performance optimization. However with material design in its infancy, I believe robust design constructs should be followed. The advantage of robust design is that it provides solutions in the presence of uncertainty. Performance optimization can lead to better results. However the optimal solution may be erroneous if uncertainty is not accounted for. Hence even in optimization solutions, a minimum level of robustness should be accounted for.

- Integrate constructs: The MMD was a culmination of IDEM and cDSP for robust design. The algorithm for uncertainty mitigation was reached by integrating robust design and information economics constructs. Integrating existing constructs serves as a good method to reach solutions of new research questions rather than starting from scratch.

- Maintain flexibility: In multiscale systems due to the evolutionary nature of modelling, it is crucial to maintain flexibility in the algorithm. The algorithm should not be rigid as it limits its applicability in case of evolving simulation models. It is also crucial to maintain this flexibility in the initial stages of design so as to avoid iterations and hence increase computational expense.

In conclusion, this thesis lays the framework for uncertainty management by developing a robust design algorithm against all four kinds of uncertainty in multiscale systems and

developing an algorithm or mitigating MPU. The algorithm and MMD construct is sufficiently general and hence can one can take the leap of faith to the fourth quadrant, i.e., theoretical performance validity. The next frontier of uncertainty management will be to develop an understanding to mitigate PU and model structure uncertainty and establish grounds for holistic uncertainty management. I end with a proposed one-page dissertation.

Table 7.5: Research questions and hypotheses

Research Question: How does one increase the efficiency in terms of maximizing performance or minimizing uncertainty in simulation-based multiscale systems design?
Hypothesis: Efficiency of multiscale systems can be increased by two approaches. One approach is to maximize the performance attainment. Another approach is to minimize the uncertainty component in multiscale systems. The two approaches should be independent of each other. A crucial component of efficiency is to evaluate performance or uncertainty metrics in terms of computational resources used. The objective is to minimize use of resources while either maximizing performance or minimizing uncertainty.
Research Question 1: How can one increase the performance of multiscale systems while minimizing use of computational resources?
Hypothesis: As we want to minimize the use of resources, a sequential approach should be followed rather than investing all resources all at once. Design of experiments technique should be used to develop accurate metamodels using minimum number of simulation runs. These metamodels should be used in IDEM to obtain feasible set of solutions while accounting for uncertainty and performance objectives. The fitness index approach described previously should be used to this end. Evaluation of improvement potential metric should be based on utility functions or the expected value of improvement construct in kriging. Cost models should be tied to the improvement potential metric and a designer should

Table 7.5 continued

proceed to trade-off to determine optimal resource allocation.
Research Question 2: How does the system level designer allocate resources for auxiliary simulation based model refinement while minimizing uncertainty?
Hypothesis: My algorithm focused on mitigating model parameter uncertainty. The formulation is to be extended to mitigate model structure uncertainty. The sensitivity of the response model coefficients is to be evaluated as a function of cost to understand the change of response surface model due to uncertainty model formulation. A holistic understanding of the assumptions involved in various model formulations is needed and it is to be tied to the impact on uncertainty. A cost model for reducing the error due to discretization resolution in IDEM is to be derived. A generic cost function coupling reduction of model parameter uncertainty, model structure uncertainty and propagated uncertainty is to be formulated and trade-off is to be performed to determine optimal resource allocation to mitigate each type of uncertainty.

REFERENCES

1. Choi, H., 2005, "A robust design method for model and propagated uncertainty," George W. Woodruff School of Mechanical Engineering, Georgia Institute of Technology, Atlanta.

2. Panchal, J. H., C. J. J. Paredis, J. K. Allen and F. Mistree, 2009, "Managing Design-Process Complexity: A Value-of-Information Based Approach for Scale and Decision Decoupling," *Journal of Computing and Information Science in Engineering,* Vol. 9, No. 2, 021015 .

3. Panchal, J. H., 2005, "A Framework for Simulation-Based Integrated Design of Multiscale Products and Design Processes ," *PhD Dissertation*, George W. Woodruff School of Mechanical Engineering, Georgia Institute of Technology, Atlanta.

4. Olson, G. B., 2000, "Designing a new material world," *Science,* Vol. 288, No. 5468, pp. 993-997.

5. McDowell, D. L., 2007, "Simulation-assisted materials design for the concurrent design of materials and products," *Jom,* Vol. 59, No. 9, pp. 21-25.

6. Kennedy, M. C. and A. O'Hagan, 2000, "Predicting the output from a complex computer code when fast approximations are available," *Biometrika,* Vol. 87, No. 1, pp. 1-13.

7. Simpson, T. W. and F. Mistree, 2001, "Kriging models for global approximation in simulation-based multidisciplinary design optimization," *AIAA Journal,* Vol. 39, No. 12, pp. 2233-2241.

8. Nair, V., 1992, "Taguchi Parameter Design: A Panel Discussion," *Technometircs,* Vol. 34, pp. 127-161.

9. Tsui, K.-L., 1992, "An Overview of Taguchi Method and Newly Developed Statistical Methods for Robust Design," *IIE Transactions,* Vol. 24, No. 5, pp. 44-57.

10. Chen, W., J. K. Allen, D. N. Mavris and F. Mistree, 1996, "A concept exploration method for determining robust top-level specifications," *Engineering Optimization,* Vol. 26, No. 2, pp. 137-158.

11. Chen, W., J. K. ALlen, K. L. Tsui and F. Mistree, 1996, "A procedure for robust design: Minimizing variations caused by noise factors and control factors," *Journal of Mechanical Design,* Vol. 118, No. 4, pp. 478-485.

12. Allen, J. K., C. Seepersad, H. J. Choi and F. Mistree, 2006, "Robust design for

multiscale and multidisciplinary applications," *Journal of Mechanical Design,* Vol. 128, No. 4, pp. 832-843.

13. Choi, H. J., D. L. McDowell, J. K. Allen and F. Mistree, 2008, "An inductive design exploration method for hierarchical systems design under uncertainty," *Engineering Optimization,* Vol. 40, No. 4, pp. 287-307.

14. Byrne, D. M. and S. Taguchi, 1986, "The Taguchi Approach to Parameter Design," *40th Annual Quality Congress Transactions*, pp. 370-376.

15. Taguchi, G. and D. Clausing, 1990, "Robust Quality," *Harvard Business Review,* Vol. Jan/Feb, pp. 65-75.

16. Choi, H.-J., 2005, "A Robust Design Method for Model and Propagated Uncertainty," *PhD Dissertation,* The George W. Woodruff School of Mechanical Engineering, Georgia Institute of Technology, Atlanta, GA, USA.

17. Taguchi, G., 1993, "Robust Technology Development," *Mechanical Engineering,* Vol. 115, No. 3, pp. 60-62.

18. Chen, W., J. K. Allen and F. Mistree, 1997, "A robust concept exploration method for enhancing productivity in concurrent systems design," *Concurrent Engineering-Research and Applications,* Vol. 5, No. 3, pp. 203-217.

19. Apley, D. W., J. Liu and W. Chen, 2006, "Understanding the effects of model uncertainty in robust design with computer experiments," *Journal of Mechanical Design,* Vol. 128, No. 4, pp. 945-958.

20. Isukapalli, S. S., A. Roy and P. G. Georgopoulos, 1998, "Stochastic Response Surface Methods (SRSMs) for uncertainty propagation: Application to environmental and biological systems," *Risk Analysis,* Vol. 18, No. 3, pp. 351-363.

21. Choi, H.-J., D. L. McDowell, J. K. Allen, D. Rosen and F. Mistree, 2008, "An inductive design exploration method for robust multiscale materials design," *Journal of Mechanical Design,* Vol. 130, No. 3, doi. 031402.

22. Booth, R. S., 1967, "Random Search for Zeroes," *Journal of Mathematical Analysis and Applications,* Vol. 20, No. 2, pp. 239-247.

23. Rippel, M., 2010, "Improved Robustness Formulations and a simulation-based robust concept exploration method," *MS Thesis* ,George W. Woodruff School of Mechanical Engineering, Georgia Institute of Technology, Atlanta.

24. Mistree, F., Smith and B. A. Bras, 1993, "A Decision Based Approach to Concurrent Engineering," *Handbook of Concurrent Engineering* (H. R. Paresai and W. Sullivan, Eds.), Chapman & Hall, New York**,** pp. 127-158.

25. Mistree, F., O. F. Hughes and B. A. Bras, 1992, "The Compromise Decision Support

Problem and the Adaptive Linear Programming Algorithm," *Structural Optimization: Status and Promise*, AIAA, Washington, D.C., Vol. 150**,** pp. 251-290.

26. Chen, W., 1995, "A Robust Concept Exploration Method for Configuring Complex Systems," *PhD Dissertation,*G. W. Woodruff School of Mechanical Engineering, Georgia Institute of Technology, Atlanta, GA, USA.

27. Seepersad, C. C., 2001, "The Utility-Based Compromise Decision Support Problem with Applications in Product Platform Design," *Master's Thesis,*G. W. Woodruff School of Mechanical Engineering, Georgia Institute of Technology, Atlanta.

28. Sinha, A., Allen, J. K. and Mistree, F. ,2010, *Game theoretic Protocols for Multilevel Design*. IDETC, Design Theory and Methodology Conference. Montreal, Quebec, Canada, ASME.

29. Sinha, A., A. Srivastava, S. Ghosh, J. H. Panchal, J. K. Allen, D. L. McDowell and F. Mistree, 2009, "Microstructure-Mediated Integration of Material and Product Design – Undersea Submersible," *ASME Design Automation Conference*, San Diego, CA. DETC2009/DAC-87276.

30. Sinha, A., 2009, "Robust Design of Underwater Submersible using Inductive Design Exploration Method," Mechanical Engineering, *B.Tech Thesis,* Indian Institute of Technology, Kharagpur.

31. Kumar, R. P., C. S. Kumar, D. Sen and A. Dasgupta, 2009, “Discrete time-delay control of an autonomous underwater vehicle: Theory and experimental results,” *Ocean Engineering,* Vol. 36, No. 1, pp. 74-81.

32. Rohatgi, P. and R. Asthana, 1991, “The Solidification of Metal-Matrix Particulate Composites,” *Jom-Journal of the Minerals Metals & Materials Society,* Vol. 43, No. 5, pp. 35-41.

33. Yang, B., Y. Q. Wang and B. L. Zhou, 1998, “The mechanism of formation of TiB2 particulates prepared by in situ reaction in molten aluminum,” *Metallurgical and Materials Transactions B-Process Metallurgy and Materials Processing Science,* Vol. 29, No. 3, pp. 635-640.

34. Anestiev, L., L. Froyen and L. van Vugt, 2000, “On the kinetics of diffusion controlled precipitation under microgravity,” *Journal of Applied Physics,* Vol. 88, No. 4, pp. 2130-2137.

35. Avrami, M., 1939, “Kinetics of phase change I - General theory,” *Journal of Chemical Physics,* Vol. 7, No. 12, pp. 1103-1112.

36. Johnson, W. A. and R. F. Mehl, 1939, “Reaction kinetics in processes of nucleation and growth,” *Transactions of the American Institute of Mining and Metallurgical Engineers,* Vol. 135, pp. 416-442.

37. Mirkovic, D., J. Grobner, R. Schmid-Fetzer, O. Fabrichnaya and H. L. Lukas, 2004, "Experimental study and thermodynamic re-assessment of the Al-B system," *Journal of Alloys and Compounds,* Vol. 384, No. 1-2, pp. 168-174.

38. Witusiewicz, V. T., A. A. Bondar, U. Hecht, S. Rex and T. Y. Velikanova, 2008, "The Al-B-Nb-Ti system I. Re-assessment of the constituent binary systems B-Nb and B-Ti on the basis of new experimental data," *Journal of Alloys and Compounds,* Vol. 448, No. 1-2, pp. 185-194.

39. Witusiewicz, V. T., A. A. Bondar, U. Hecht, S. Rex and T. Y. Velikanova, 2008, "The Al-B-Nb-Ti system III. Thermodynamic re-evaluation of the constituent binary system Al-Ti," *Journal of Alloys and Compounds,* Vol. 465, No. 1-2, pp. 64-77.

40. Herbert, M. A., R. Maiti, R. Mitra and M. Chakraborty, 2006, "Microstructural evolution and wear properties of in-situ Al-4.5Cu-5TiB(2) composite processed in mushy state," *Semi-Solid Processing of Alloys and Composites,* Vol. 116-117, pp. 217-220.

41. Herbert, M. A., C. Sarkar, R. Mitra and M. Chakraborty, 2007, "Microstructural evolution, hardness, and alligatoring in the mushy state rolled cast Al-4.5Cu alloy and in-situ Al4.5Cu-5TiB(2) composite," *Metallurgical and Materials Transactions a-Physical Metallurgy and Materials Science,* Vol. 38A, No. 9, pp. 2110-2126.

42. Das, A., S. Ji and Z. Fan, 2002, "Morphological development of solidification structures under forced fluid flow: a Monte-Carlo simulation," *Acta Materialia,* Vol. 50, No. 18, pp. 4571-4585.

43. Zhang, Z. and D. L. Chen, 2006, "Consideration of Orowan strengthening effect in particulate-reinforced metal matrix nanocomposites: A model for predicting their yield strength," *Scripta Materialia,* Vol. 54, No. 7, pp. 1321-1326.

44. Kumar, R. P., A. Dasgupta and C. S. Kumar, 2005, "Real-time optimal motion planning for autonomous underwater vehicles," *Ocean Engineering,* Vol. 32, No. 11-12, pp. 1431-1447.

45. Panchal, J. H., H. J. Choi, J. K. Allen, D. L. McDowell and F. Mistree, 2007, "A systems-based approach for integrated design of materials, products and design process chains," *Journal of Computer-Aided Materials Design,* Vol. 14, pp. 265-293.

46. Choi, H., D. L. McDowell, J. K. Allen, D. Rosen and F. Mistree, 2008, "An inductive design exploration method for robust multiscale materials design," *Journal of Mechanical Design,* Vol. 130, No. 3, doi.031402 .

47. Montgomery,D.C., 2008, "Design and Analysis of Experiments, 6th Edition", *Wiley, NY.*

48. McDowell, D. L. and G. B. Olson, 2008, "Concurrent design of hierarchical materials and structures," *Scientific Modeling and Simulations,* Vol. 15, No. 1-3, pp. 207-240.

49. Marston, M., "Game-Based Design: A Game Theory Based Approach to Engineering Design," *PhD Disseration,*The George W. Woodruff School of Mechanical Engineering, Georgia Institute of Technology, Atlanta.

50. Xiao, A. R., S. Zeng, J. K. Allen, D. W. Rosen and F. Mistree, 2005, "Collaborative multidisciplinary decision making using game theory and design capability indices," *Research in Engineering Design,* Vol. 16, No. 1-2, pp. 57-72.

51. Bras, B. and F. Mistree, 1995, "A Compromise Decision-Support Problem for Axiomatic and Robust Design," *Journal of Mechanical Design,* Vol. 117, No. 1, pp. 10-19.

52. Xiao, A., C. C. Seepersad, J. K. Allen, D. W. Rosen and F. Mistree, 2007, "Design for Manufacturing: Application of Collaborative Multidisciplinary Decision-making Methodology," *Engineering Optimization,* Vol. 39, No. 4, pp. 429-451.

53. Chen, W., T. W. Simpson, J. K. Allen and F. Mistree, 1999, "Satisfying Ranged Sets of Design Requirements using Design Capability Indices as Metrics," *Engineering Optimization,* Vol. 31, No. 5, pp. 615-639.

54. Hernandez, G., J. K. Allen and F. Mistree, 2001, "The Compromise Decision Support Problem: Modeling the Deviation Function as in Physical Programming," *Engineering Optimization,* Vol. 33, No. 4, pp. 445-471.

55. Vadde, S., J. K. Allen and F. Mistree, 1994, "Compromise Decision-Support Problems for Hierarchical Design Involving Uncertainty," *Computers & Structures,* Vol. 52, No. 4, pp. 645-658.

56. Lewis, K. and F. Mistree, 1997, "Modeling interactions in multidisciplinary design: A game theoretic approach," *AIAA Journal,* Vol. 35, No. 8, pp. 1387-1392.

57. Sobieski, I. P. and I. M. Kroo, 2000, "Collaborative optimization using response surface estimation," *AIAA Journal,* Vol. 38, No. 10, pp. 1931-1938.

58. Singh, M., 2010, "Structure-Property Correlation of Metal Matrix Composites," *B.Tech Thesis,*Metallurgical & Materials Engineering, Indian Institue of Technology, Kharagpur.

59. Montgomery, D. C., 2008, "Applications of design of experiments in engineering," *Quality and Reliability Engineering International,* Vol. 24, No. 5, pp. 501-502.

60. Myers, R. and D. Montgomery, 1995, *Response Surface Methodology: Product and Process Optimization Using Designed Experiments,* Wiley, New York.

61. Chen, W., J. K. Allen, K. L. Tsui and F. Mistree, 1996, "A Procedure for Robust Design: Minimizing Variations Caused by Noise Factors and Control Factors," *ASME Journal of Mechanical Design,* Vol. 118, pp. 478-485.

62. Wikipedia,*Central Composite Design*. http://en.wikipedia.org/wiki/Central_composite_design (March, 2011)

63. *Selecting the right central composite design for response surface methodology*, http://www.qualitydigest.com/june01/html/doe.html (February, 2011)

64. Engineering Statistics Handbook,*Central Composite Designs*, http://www.itl.nist.gov/div898/handbook/pri/section3/pri3361.htm (March, 2011)

65. Myers, R. H., D. C. Montgomery, G. G. Vining, C. M. Borror and S. M. Kowalski, 2004, "Response surface methodology: A retrospective and literature survey," *Journal of Quality Technology,* Vol. 36, No. 1, pp. 53-77.

66. Howard, R., 1966, "Information Value Theory," *IEEE Transactions on Systems Science and Cybernetics,* Vol. SSC-2, No. 1, pp. 779-783.

67. Reich, Y., 1995, "Measuring the Value of Knowledge," *International Journal of Human-Computer Studies,* Vol. 42, No. 1, pp. 3-30.

68. Lawrence, D. B., 1999, *The Economic Value of Information,* Springer, New York.

69. Panchal, J. H., C. J. J. Paredis, J. K. Allen and F. Mistree, 2008, "A Value-of-Information based approach to Simulation Model Refinement," *Engineering Optimization,* Vol. 40, No. 3, pp. 223-251.

70. Bradley, S. R. and A. M. Agogino, 1994, "An Intelligent Real Time Design Methodology for Component Selection: An Approach to Managing Uncertainty," *Journal of Mechanical Design,* Vol. 116, pp. 980-988.

71. Bradley, S. R., A. M. Agogino and W. H. Wood, 1994, "Intelligent Engineering Component Catalogs," *Artificial Intelligence in Design' 94*, Kluwer, Dordrecht, The Netherlands**,** pp. 641-658.

72. Panchal, J. H., J. K. Allen, C. J. J. Paredis and F. Mistree, 2006, "Simulation Model Refinement for Decision Making via a Value-of-Information Based Metric," *Design Automation Conference*, Philadelphia, PA.

73. Panchal, J. H., C. J. J. Paredis, J. K. Allen and F. Mistree, 2008, "A Value-of-Information Based Approach to Simulation Model Refinement," *Engineering Optimization,* Vol. 40, No. 3, pp. 223 - 251.

74. Sinha, A., Allen, J. K., Panchal, J.H. and Mistree, F. , 2011, "Microstructure Mediated Design," *Computer Aided Design,* Vol. (under Review).

75. Ashby, M. F. and D. Cebon, 1993, "Materials Selection in Mechanical Design," *Journal De Physique Iv,* Vol. 3, No. C7, pp. 1-9.

76. Fullwood, D. T., S. R. Niezgoda, B. L. Adams and S. R. Kalidindi, 2010, "Microstructure sensitive design for performance optimization," *Progress in Materials Science,* Vol. 55, No. 6, pp. 477-562.

77. Bendsoe, M. P., E. Lund, N. Olhoff and O. Sigmund, 2005, "Topology optimization - broadening the areas of application," *Control and Cybernetics,* Vol. 34, No. 1, pp. 7-35.

78. El-Mahallawy, N., M. A. Taha, A. E. W. Jarfors and H. Fredriksson, 1999, "On the reaction between aluminium, K2TiF6 and KBF4," *Journal of Alloys and Compounds,* Vol. 292, No. 1-2, pp. 221-229.

79. Lloyd, D. J., 1988, "Metal Matrix Composites - an Overview," *Cim Bulletin,* Vol. 81, No. 914, pp. 56-56.

80. Akhtar, F., 2008, "Microstructure evolution and wear properties of in situ synthesized TiB2 and TiC reinforced steel matrix composites," *Journal of Alloys and Compounds,* Vol. 459, No. 1-2, pp. 491-497.

81. Anestiev, L., 1994, "On the Solute Redistribution at Thermally Activated Phase-Transition Processes .1. Theory," *Journal of Crystal Growth,* Vol. 140, No. 1-2, pp. 167-174.

82. Patra, A., 2009, "Precipitation Modeling of in-situ aluminum-TiB2 Composite," *B.Tech Thesis,* Metallurgical and Materials Engineering, Indian Institute of Technology, Kharagpur.

83. Rappaz, M. and C. A. Gandin, 1994, "Stochastic Modeling of Grain-Structure Formation in Solidification Processes," *Mrs Bulletin,* Vol. 19, No. 1, pp. 20-24.

84. Rappaz, M. and C. A. Gandin, 1993, "Probabilistic Modeling of Microstructure Formation in Solidification Processes," *Acta Metallurgica Et Materialia,* Vol. 41, No. 2, pp. 345-360.

85. Kurz, W., B. Giovanola and R. Trivedi, 1986, "Theory of Microstructural Development during Rapid Solidification," *Acta Metallurgica,* Vol. 34, No. 5, pp. 823-830.

86. Lenka, S., 2010, "Modeling of Microstructural Evolution in Metal Matrix Composites and Correlation of Process Variables on Grain Size of Composite," *M.Tech Thesis,*Metallurgical And Materials Engineering, Indian Institute of Technology, Kharagpur.

87. Wu, J. F., M. S. Shephard, G. J. Dvorak and Y. A. Baheieldin, 1989, "A Material Model for the Finite-Element Analysis of Metal Matrix Composites," *Composites Science and Technology,* Vol. 35, No. 4, pp. 347-366.

88. Dvorak, G. J., T. Y. Chen and J. Teply, 1992, "Thermomechanical Stress-Fields in

High-Temperature Fibrous Composites .1. Unidirectional Laminates," *Composites Science and Technology,* Vol. 43, No. 4, pp. 347-358.

89. Mishra, D., 2010, "Structure-Property Correlation of Metal Matrix Composites," *B.Tech Thesis,* Metallurgical & Materials Engineering, Indian Institute of Technology, Kharagpur.

90. Maxwell, J. C., 1873, *Electricity and Magnetism,* Oxford, U.K.

91. Bera, N., 2010, "Microstructure Mapping and System Level design of the Underwater Vehicle," *B.Tech Thesis,*Mechanical Engineering, Indian Institute of Technology, Kharagpur.

92. Choi, H. J., R. Austin, J. K. Allen, D. L. McDowell, F. Mistree and D. J. Benson, 2005, "An approach for robust design of reactive power metal mixtures based on non-deterministic micro-scale shock simulation," *Journal of Computer-Aided Materials Design,* Vol. 12, No. 1, pp. 57-85.

93. Choi, H.-J., J. K. Allen, D. Rosen, D. L. McDowell and F. Mistree, 2005, "An Inductive Design Exploration Method for the Integrated Design of Multi-scale Materials and Products," *Design Engineering Technical Conferences - Design Automation Conference*, Long Beach, CA.

94. Montgomery, D. C., 1999, "Experimental design for product and process design and development," *Journal of the Royal Statistical Society Series D-the Statistician,* Vol. 48, pp. 159-173.

95. Olive, D. J., 2007, "Prediction intervals for regression models," *Computational Statistics & Data Analysis,* Vol. 51, No. 6, pp. 3115-3122.

96. Baik, J., B. Boehm and B. Steece, 2002, "Disaggregating and Calibrating the CASE Tool Variable in COCOMO II," *IEEE Transactions on Software Engineering,* Vol. 28, No. 11, pp. 1009-1022.

97. Valerdi, R., 2005, "The Constructive Systems Engineering Cost Model (COSYSMO)," *PhD Dissertation,*Industrial and Systems Engineering, University of Southern California, Los Angeles.

98. Fortune, J., 2009, "Estimating Systems Engineering Reuse with the Constructive Systems Engineering Cost Model (COSYSMO 2.0)," *Phd Dissertation,* Industrial and Systems Engineering, University of Southern California, Los Angeles.